Université de Montréal

Mitochondrial dysfunction in survivors of acute lymphoblastic leukemia

par Jade Leahy

Département de Nutrition
Faculté de Médicine

Mémoire présenté à la Faculté des études supérieures
en vue de l'obtention du grade de Maîtrise ès sciences (M.Sc.)
en Nutrition

Août 2017

Résumé

La leucémie aigüe lymphoblastique (LAL) est le cancer le plus commun chez l'enfant. Fort heureusement, les avancées thérapeutiques ont permis qu'environ 90% de patients diagnostiqués LAL survivent au moins 5 ans post traitements. Toutefois, deux tiers des survivants présentent au moins une complication secondaire à long terme suite au caractère de la maladie et surtout aux traitements agressifs. Le syndrome métabolique et ses composantes sont reconnus comme facteurs de risque de maladies cardiovasculaires et sont présents chez les survivants de LAL. De façon surprenante, très peu d'informations sont disponibles sur le statut mitochondrial chez les survivants de LAL. Pourtant, ces organelles cellulaires jouent un rôle central dans les voies métaboliques, et leurs dysfonctions sont associées à des complications cardiométaboliques. L'objectif de notre étude est donc de déterminer si l'émergence des complications cardiométaboliques chez les survivants pédiatriques LAL est associée à une altération de la composition des protéines clés de la mitochondrie menant à leur dysfonction. **Méthode.** Nous avons évalué le profile cardiométabolique de 52 survivants de LAL que nous avons repartis en deux groupes; l'un métaboliquement sain et l'autre muni de composantes du syndrome métabolique. Les mitochondries des globules blancs des survivants ont été isolées par ultracentrifugation, caractérisées dans certaines de leurs fonctions, et évaluées par l'approche protéomique. La peroxydation lipidique a été déterminée et l'expression de protéines fonctionnelles a été examinée par immunobuvardage et ELISA. **Résultats.** Les résultats ont montré des différences dans l'expression des protéines entre les contrôles et le groupe de survivants. Les survivants de la LAL expriment moins de protéines antioxydantes comme la superoxide dismutase et plus de stress oxydatif comme l'indique le marqueur malondialdehyde. L'augmentation de l'expression protéique du cytochrome c indique une élévation de l'apoptose alors que la diminution du facteur de transcription PGC1-α souligne un amoindrissement de la biogenèse mitochondriale. L'analyse protéomique a permis d'identifier 957 protéines mitochondriales chez nos survivants LAL et contrôles. Des altérations entre les groupes ont été observés dans la régulation des protéines liées aux voies de signalisation, l'inflammation, d'apoptose, de la production énergétique, de la β-oxydation, de l'oxydoréduction et transport et métabolisme de protéines. **Conclusions.** L'analyse protéomique et fonctionnelle chez les survivants LAL révèlent des différences dans la présence, concentration et fonction des protéines

mitochondriales, ce qui suggère des dysfonctions mitochondriales associées aux troubles cardiométaboliques. Des études plus approfondies seraient nécessaires pour confirmer si ces dysfonctions mitochondriales sont responsables du développement des complications cardiométaboliques dans cette population.

Mots-clés: leucémie aigüe lymphoblastique pédiatrique, mitochondrie, syndrome métabolique, désordres cardiométaboliques, survivant de cancer, obésité, résistance à l'insuline, hypertension et dyslipidémie.

Abstract

Background. Childhood acute lymphoblastic leukemia (cALL) is the most prevalent form of paediatric cancer. Fortunately, advances in treatment have allowed for approximately 90% of those diagnosed with cALL to survive at least 5 years post treatments. However, almost two thirds of cALL survivors present at least one considerable complication due to long-term secondary effects following aggressive treatments. The metabolic syndrome (metS) and its components are present among this group of paediatric cancer survivors and are risk factors of cardiovascular diseases. Surprisingly, little information is available on mitochondrial status in paediatric cancer survivors even if these organelles display central roles in metabolic processes and their dysfunction has been connected to the development of cardiometabolic complications. The objective of this study is to determine if the appearance of cardiometabolic complications in cALL survivors is associated with alterations in the composition and functions of key mitochondrial proteins leading to dysfunctional mitochondria. **Methods.** We evaluated the cardiometabolic profile of a group of 52 cALL survivors classing them as either metabolically healthy or metabolically unhealthy. Mitochondria from white blood cells were isolated, assessed in several of their characteristic functions, and analyzed by the proteomic approach. Lipid peroxidation was measured and the expression of functional proteins was examined by western blot analysis and commercial ELISA kits. **Results.** Our findings demonstrated differences in protein expression among controls and the cALL survivor group. cALL survivors expressed lower antioxidant superoxide dismutase along with increased oxidative stress as reflected by raised malondialdehyde levels. Increased cytochrome c indicated elevated apoptosis whereas decreased expression of PGC1-α transcription factor revealed mitochondrial biogenesis reduction. Proteomic analysis identified 957 proteins within our groups. Furthermore we could evidence alterations among groups in the regulation of mitochondrial proteins including those related to signalling pathways, inflammation, apoptosis, energy production, β-oxidation, oxidoreduction, and protein transport and metabolism. **Conclusion.** Our proteomic and functional analysis among cALL survivors reveal differences in the presence, concentration and function of mitochondrial proteins compared to controls. These results may indicate an association between dysfunctional mitochondria and cardiometabolic complications among cALL survivors. Further studies are necessary to confirm

whether mitochondrial dysfunctions are responsible for the development of cardiometabolic complications in this population.

Keywords: acute lymphoblastic leukemia, cancer survivors, paediatric, mitochondria, cardiometabolic, metabolic syndrome, obesity, dyslipidemia, insulin resistance, hypertension.

TABLE OF CONTENTS

LIST OF TABLES

LIST OF FIGURES

LIST OF ABBREVIATIONS

8-OHdG: 8-hydroxy-2'-deoxyguanosine

AA: Amino acids

ACO2: Aconitase 2

ADP: Adenosine diphosphate

ALL: Acute lymphoblastic leukemia

ALEs: Advanced lipoxidation end-products

AML: Acute myeloid leukemia

AMP: Adenosine monophosphate

AMPK: 5' adenosine monophosphate-activated protein kinase

AngIII: Angiotensin III

AOPPs: Advanced oxidized plasma protein

AP-1: Activating protein-1

APAF-1: Apoptotic protease activating factor 1

Apo-B: Apolipoprotein B

ATP: Adenosine triphosphate

ATP5B: ATP synthase, H+ transporting, mitochondrial F1 complex, beta subunit precursor.

BAX: Bcl-2-associated X protein

BAK: Bcl-2 homologous antagonist/killer

Bcl2: B-cell lymphoma 2

Bclx: B-cell lymphoma X

BH3: Interacting-domain death agonist

BID: BCL-2-homology domain 3 (BH3) interacting-domain death agonist

BMI: Body mass index

BP: Blood pressure

CAD: Coronary artery disease

cALL: Childhood acute lymphoblastic leukemia

cAMP: Cyclic adenosine 3,5'-monophosphate-activated protein kinase

CAT: carnitine translocase

CCSS: Canadian cancer survivor study

CE: Cholesteryl ester

CETP: Cholesterol ester transfer protein

CGL: Chronic granulocytic leukaemia

CHO: Carbohydrate

CHU: University hospital center

CNS: Central nervous system

CoA: Coenzyme A

COX-2: Cyclooxygenase-2

CPT1B: Carnitine palmitoyltransferase 1b

CPT1: Carnitine palmitoyltransferase I

CPT2: Carnitine palmitoyltransferase II

CREB: C-AMP Response Element-binding protein

CRP: C-creative protein

CRT: Cranial radiotherapy

CV: Cardiovascular

CYCS: Cytochrome c, somatic

DISC: Death-inducing signalling complex

eNOS: Endothelial nitric oxide synthase

ER: Endoplasmic reticulum

ERRα: Estrogen-related receptor-alpha

ETC: Electron transport chain

FA: Fatty acids

FACS: Fatty acyl-CoA synthase

FADD : Fas-associated death domain-containing protein

FasL: Fas ligand.

FFA: Free fatty acid

GPX: Glutathione peroxidase

GSH: Glutathione

GSH-Px: Glutathione peroxidase

HDL: High density lipoprotein

HDL-c: High density lipoprotein cholesterol

HFD: High fat diet

HIFs: Hypoxia inducible factors

HNE: 4-hydroxynonenal

HOMA-IR: Homeostasis model assessment

HT: Hypertension

ICAM: Intracellular adhesion molecule

IDH3A: Isocitrate dehydrogenase 3, alpha subunit

IGT: Impaired glucose tolerance

IFG: Impaired fasting glucose

IKK: I-κB kinase

IL-1: Interleukin 1

IL-6: Interleukin 6

IMM: Inner mitochondrial membrane

iNOS: Inducible nitric oxide synthase

IR: Insulin resistance

IRS: Insulin receptor substrates

IRS1: Insulin receptor substrate 1

JNK: c-jun N-terminal kinase

JNK1: jun-*N*-terminal kinase 1

LDL: Low density lipoprotein

LDL-c: Low density lipoprotein cholesterol

LPL: Lipoprotein lipase

MAPK: Mitogen activated protein kinases

MCAD: Medium-chain acyl-coA dehydrogenase

MCP-1: Monocyte chemoattractant protein 1

MDA: Malonyldialdehyde

metS: Metabolic syndrome

MFN2: Mitofusin-2

MMP: Mitochondrial membrane permeabilization

MnSOD: Manganese superoxide dismutase

mRNA: Messenger RNA

mROS: Mitochondrial ROS

mtDNA: Mitochondrial DNA

mTOR: Mammalian target of rapamycin

NAD: Nicotinamide adenine dinucleotide

NADH: Nicotinamide adenine dinucleotide + hydrogen

NADPH: Nicotinamide adenine dinucleotide phosphate

nDNA: Nuclear DNA

NF-kB: Nuclear factor-kappa B

NO: Nitric oxide

NRF-1: Nuclear respiratory factor 1

NRF2: Nuclear respiratory factor 2

O_2^-: Superoxide anion

OMM: Outer mitochondrial membrane

ONE: 4-oxy-2-nonenal

$ONOO^-$: Peroxynitrite

OxS: Oxidative stress

OXPHOS: Oxidative phosphorylation

PAI-1: Plasminogen activator inhibitor-1

PBMC: Peripheral blood mononuclear cells

PETALE: Prévenir les effets tardifs des traitements de la leucémie aigüe lymphoblastique chez l'enfant

PGC1-α: Proliferator-activated receptor gamma coactivator 1-alpha

PGC1-β: Peroxisome proliferator-activated receptor gamma coactivator 1-beta

Pi: Inorganic phosphate

PINK1: PTEN-induced kinase 1

PPAR: Peroxisome proliferator-activated receptors

PPARα: Peroxisome proliferator-activated receptors-alpha

PRDX3: peroxiredoxin 3

RNS: Reactive nitrogen species

ROS: Reactive oxygen species

RT: Radiotherapy

Rx: Medical treatment

Sd-LDL: Small dense LDL

SOD: Superoxide dismutase

SOD2: Superoxide dismutase 2

s-TG: Serum triglycerides

T2D: Type 2 diabetes

TAS: Total antioxidant status

TCA: Tricarboxylic acid

Tfam: Mitochondrial transcription factor A

TG: Triglycerides

TGF-β1: Transforming growth factor beta-1

TIMM13: Translocase of inner mitochondrial membrane 13

TNF: Tumour necrosis factor

TNF-α: Tumour necrosis factor alpha

TNFR-1: Tumour necrosis factor receptor 1

TNFR-2: Tumour necrosis factor receptor 2

TNFRs: Tumour necrosis factor receptors

TRAF: TNF receptor-associated factor

TRAF2: TNF receptor-associated factor 2

UPR: Unfolded protein response

VDAC: Voltage-dependent anion channel

VLDL: Very low density lipoprotein

WAT: White adipose tissue

I dedicate this master's thesis to my parents

Their motivation and encouragement has been essential throughout my studies

ACKNOWLEDGMENTS

I would first like to thank my research supervisor Dr. Emile Levy who included me in his team and allowed me to work on this research project. His encouragement to pursue my studies and his passion for science was inspirational.

Furthermore I would like to thank Schohraya Spahis (Zola) for her guidance in every step of my graduate studies. Her support was key in helping me complete this phase of my studies. Carole Garofalo was also fundamental in helping me complete my master's project. Her knowledge and help with lab work and love for science is admirable. Thank you to Alain Sainé for all the tips you gave me regarding lab experiments and helping me throughout all my western blotting.

Thank you to all the students who I've met, worked with and developed strong friendships during this process. You have all made this experience exceptional. Sophia Morel, who I worked with while doing my first stage increased my knowledge in the field of nutrition and her motivation and work ethic was something to look up to. Pantea, Maryse, Veronique whom I spent much of my time with and who helped me every step of the way.

Finally, I would like to thank my family for supporting me through this journey and encouraging me never to give up.

CHAPTER 1- INTRODUCTION

The survival rate for childhood cancer has increased due to the advances of cancer therapy [1]. Acute lymphoblastic leukemia (ALL) is the most common childhood cancer but luckily 90% of patients aged between 0-19 years at diagnosis will survive 5 years post treatment [2]. Although the prognosis for childhood ALL (cALL) is promising, the toxic treatments, the cancer itself or genetics can lead to late onset effects in some survivors [3]. For example, childhood cancer survivors can develop long term cardiovascular (CV) complications and/or diabetes due to the presence of components of the metabolic syndrome (metS) (i.e. obesity, insulin resistance, hypertension and dyslipidemia) [4]. Furthermore, they are significantly more likely than siblings to develop adverse cardiac outcomes [5]. Many studies have confirmed the presence of later complications among cancer survivors, however, the mechanisms of action in cALL survivors remains unclear. Recent evidence suggests that certain cancer therapies may lead to later onset cardiometabolic derangements by damaging mitochondrial functions [6]. Intriguingly, to our knowledge, this has never been studied in cALL survivors. Mitochondria are important organelles that play various cellular roles, namely in metabolic functions [7]. It is now understood that a wide range of metabolic diseases are associated with mitochondrial dysfunctions [8]. Furthermore, chemical medications are now known to be a major cause of mitochondrial damages [9]. In view of these literature observations, we have hypothesized that cALL survivors may present dysfunctional mitochondria. Therefore, the aim of this research project is to study important mitochondrial functions of cALL survivors and compare to a healthy control group. In addition, proteomic mitochondrial analyses were performed to more fully characterize the molecular changes and provide valuable insight into the underlying causes of metabolic disturbances in cALL. This may lead to biomarkers that could help us identify the risk of developing metabolic abnormalities among the cALL population and to eventually plan preventative interventions or closer follow up for those at risk.

1. Cancer

1.1 Definition

The Cancer Research Society defines cancer as a disease arising from a single normal cell that transforms into a tumour in multiple stages beginning as a pre-cancerous lesion. Cancer can be the result of genetic factors and/or external agents. The abnormal cells carrying different mutations evade apoptosis and divide uncontrollably leading to many mutated cells with the ability to invade other tissues [10].

Since 2005, cancer has been the leading cause of death in Canada and is expected to continue to increase [10, 11]. Fortunately the survival rates are gradually rising due to advancement of treatments. The 5-year survival rate of cancer is about 50% for adults and 80% for the younger population (i.e. children, adolescents and young adults) [12]. Survival rates depend on the type of cancer, the patient's characteristics, and medical care [13] [14].

1.2 Causes of cancer

The chance of developing cancer depends on the persons demographics, occurrence of risk factors and their life expectancy [14]. As displayed in figure 1 (page 3) development of cancer can be due to different cancer causing agents such as genetic and external factors that include physical, chemical and biological carcinogens [10]. Additionally, thirty percent of cancer mortality is due to avoidable behavioral and dietary risk factors (i.e. tobacco use, overweightness, lack of fruit and vegetable intake, sedentary behavior, alcohol consumption) [10, 15-17].

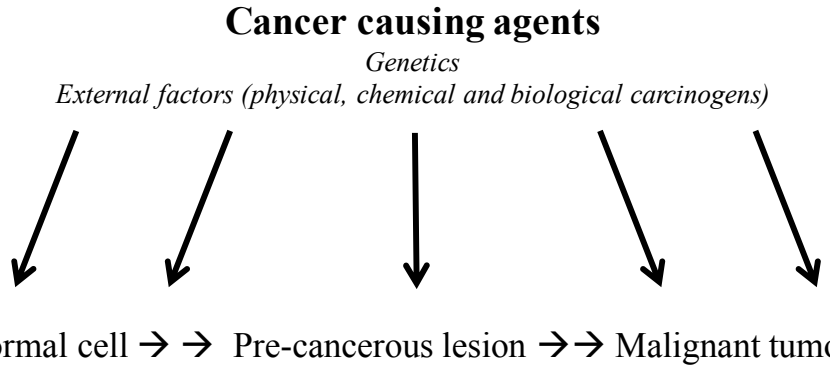

Figure 1. The various causes of cancer. Cancer causing agents can affect the many different steps involved in tumour development. Adapted from [10].

1.3 Treatments of cancer

There are two categories of available treatments (e.g. systemic and targeted) that vary depending on the type of cancer. Systemic treatments (e.g. conventional cytotoxic chemotherapy, hormonal therapy, immunotherapy) act in eliminating all actively dividing cells, which include cancer cells but also normal cells leading to side effects [18]. Targeted therapies (e.g. monoclonal antibodies, small-molecule drugs, surgery) are given in lower doses, have fewer side effects and are directed towards the cancer cells to eliminate the primary tumour and to avoid killing the normal cells [19, 20]. The most common treatments of cancer include surgery, chemotherapy and radiation therapy [20].

1.4 Complications after cancer and its treatments

Although cancer treatments save lives, we now recognize that many survivors present both physical and psychological long-term and late effects [12]. Late effects that have been studied in relation to cancer have included metabolic derangements, cardiac perturbations, neuropsychological system abnormalities, bone problems and quality of life outcomes.

The second most common cause of death in the paediatric population in developed countries is cancer [21]. Survivors of childhood cancer represent 1% of all new cancers diagnosed in the US [22], and despite the good prognosis, they are unfortunately at risk of developing long-term late effects. Survivors of cALL, the most common form of cancer in

children, are also at risk of developing complications after treatment.

1.5 Childhood Acute Lymphoblastic Leukemia

1.5.1 Definition and description of cALL

cALL is a malignant disease that begins primarily in the bone marrow and spreads to other parts of the body. However, it may arise from extramedullary sites (i.e. thymus or intestine) that invade the bone marrow [23]. It can originate from abnormal lymphoid stem cells that avoid apoptosis and undergo abnormal growth and activity, as shown in figure 2 (page 5). In other cases cALL is initiated from different genetic mutations in a single B or T-lymphoid progenitor that communicate the ability for unlimited self-renewal or that bring about the exact stage-specific halt in development [23]. Immunoglobin or T-cell receptor genes display clonal rearrangements in mutated cALL [23]. Their antigen-receptor molecules and differentiation-linked cell-surface glycoproteins are similar to the ones found on immature lymphoid progenitor cells at the early normal T and B lymphocyte development stages [23]. Furthermore the mutated cells are spread through white blood cells or immune cells that are crucial in fighting infections [24]. The outcome includes increased blast cell proliferation, maturation and survival, and eventually the accumulation of leukemic cells can be lethal, illustrated in figure 2 (page 5) [23]. Bone marrow can acquire too many immature white blood cells, making it harder for the body to fight infections, leaving the child with frequent infections, fever, bruises, weakness, etc. [24, 25]. Unfortunately the exact cause of cALL development is still unclear [23]. Only a small number of cases of cALL have been associated with inherited predisposing genetic syndromes (e.g. Down's syndrome, Bloom's syndrome, ataxia-telangiectasia, Nijmegan breakage syndrome) and ionizing radiation or exposure to chemotherapeutic drugs [23]. Moreover, it is believed that cALL aetiology can be provoked by prenatal influences [26], and many studies have associated the increased risk of development of cALL with high birth weight [26-28] as well as accelerated foetal growth [29]. The proposed rational behind this is that pregnancies generating higher birth weight babies have higher levels of circulating growth factors that may carry oncogenic properties to the developing immune system, which brings about an increased risk of cALL progression [26]. Other causes that have been studied but present conflicting data include parental occupation, maternal reproductive history, parental

tobacco and alcohol use, maternal diet, exposure to residual power-frequency magnetic fields, and several infection based assumptions [23].

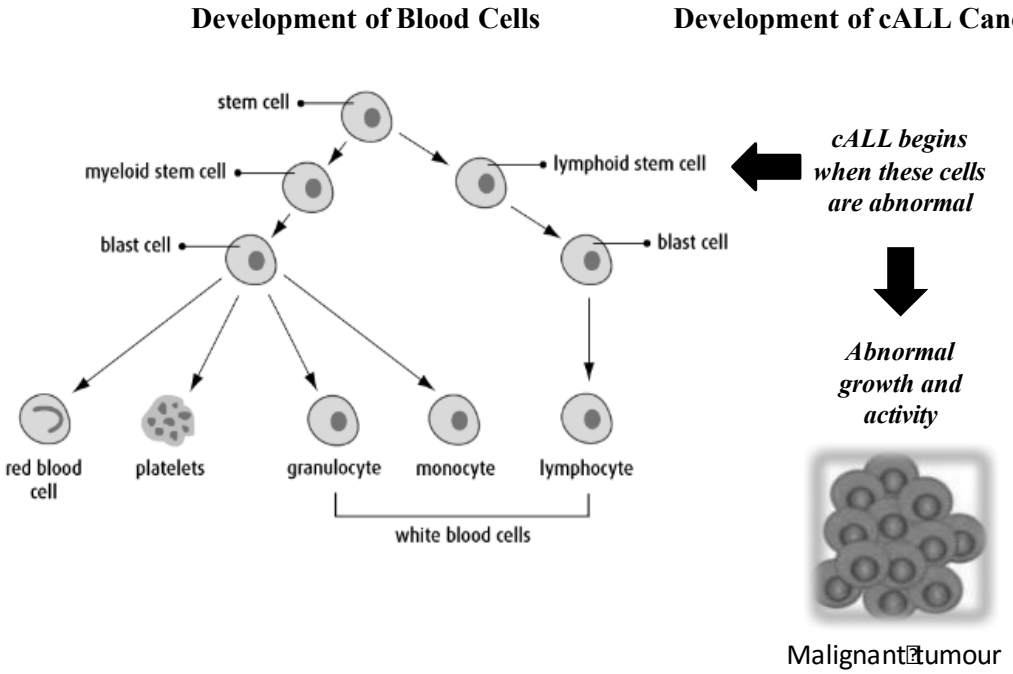

Figure 2. Process of development of cALL in blood cells. Adapted from Canadian Cancer Society [30]. Cancer initiates when abnormal lymphoid cells divide and develop into a malignant tumour. Cancer cells can escape the primary tumour and travel through the bloodstream leading the spread of cancer, otherwise known as metastasis.

1.5.2 Treatment of cALL

Treatment of cALL generally includes 4-6 weeks of induction chemotherapy initially administered in the hospital, followed by months of consolidation chemotherapy and finally 2-3 years of maintenance chemotherapy [18, 31]. Radiation therapy is a highly toxic treatment and is now only used on a small portion of patients with a high risk of CNS relapse [32]. Allogeneic bone marrow transplantation is recommended for some children with high-risk leukemia at diagnosis as well as those who develop a recurrence after their remission or when there is no remission after many courses of induction chemotherapy [31].

1.5.3 Prevalence and outcome statistics of cALL

Cancer in children is rare, nonetheless cALL is the common childhood cancer, accounting for 25% of all cases and has peak incidence between ages 2-5 years [31, 32]. Even though the overall incidence of cALL has increased from 1975-2010, the mortality rate has been in a steep decline [31]. The National Cancer institute found that 90% of children ages 0-19 years who are diagnosed with cALL will survive at least 5 years post treatment [31]. This number has increased from the 57% survival rate in the 1970s [31].

ALL is rare in adults and survival rates of cALL far exceed those of adult ALL [33]. Partial explanation for the difference in prognosis includes the more intensive regimens, decreased side effects, and higher compliance to the aggressive treatments in children. In adults, the toxic effects represent an important limit to the administration of the proper drug doses and timing of chemotherapy [33].

It must be noted that the elevated 5-year survival rate does not come without consequence. cALL survivors are at increased risk of developing other cancers, chronic diseases and/or functional impairments over time [31].

1.5.4 Long-term adverse health effects in cALL survivors

cALL survivors display long-term adverse health anomalies that include fertility problems, metabolic dysfunction, psychological issues, neurocognitive deficits [34], growth deficiencies and are at increased risk of a second cancer [31]. Many studies have focused on the development of the metS, or its components (i.e. obesity, insulin resistance, dyslipidemia, hypertension), as well as CV conditions (i.e. congestive heart failure, coronary artery disease, myocardial infarction, cardiac arrest and cerebrovascular accidents) and diabetes, which may arise as a consequence of metabolic anomalies in cALL survivors early into their remission period [1, 4-6, 35-38]. More specifically, studies have confirmed that there is a high prevalence of cALL survivors affected by the metS, its components and related complications [4, 12, 37-41].

The presence of adverse outcomes in this population of childhood cancer survivors may be due to a combination of factors related to the primary malignancy, demographics, underlying genetic predisposition and pre-morbid conditions, and health related behaviours may adjust the

risks associated with cancer treatment [40]. However, investigators suggest that the adverse late effects are determined by treatment-specific factors [40], especially when treatment involves total body irradiation (TBI) or abdominal radiotherapy (RT) [36].

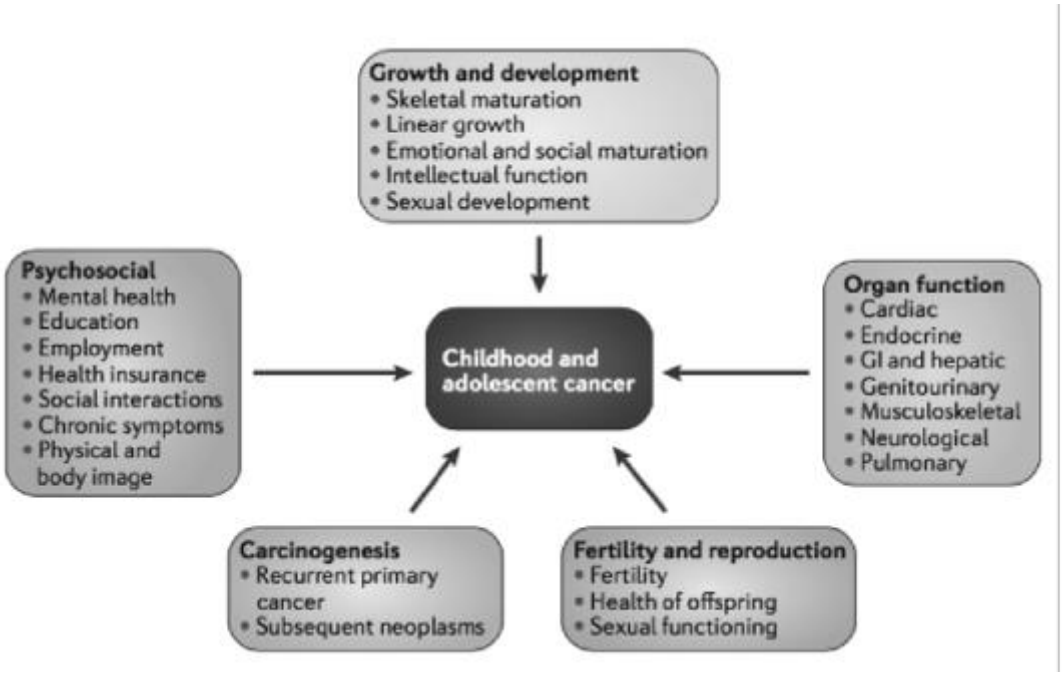

Figure 3. Health and quality-of-life related outcomes in survivors of childhood and adolescent cancers. Survivors of childhood and adolescent cancers may suffer from many adverse late effects including psychosocial problems, fertility and reproductive problems, organ dysfunction, altered growth and development and secondary carcinogenesis. Reproduced with permission [40].

Evidently, metabolic complications bear significant health consequences for cALL survivors even after they are treated and cured from their primary cancer. Late effects are expected to continue to increase as the person ages, signifying the importance of research to understand the aetiology of metabolic disease in cALL survivors, plan for earlier detection and establish prevention efforts to improve the long-term health of cALL survivors [36].

2. The metabolic syndrome

As mentioned previously, the metS and its components can emerge as adverse late effects in cALL survivors. Our research focused on metabolic complications in cALL survivors, therefore this section will describe the metS and its components in detail.

2.1 Definition of the metS

The metS is described as a cluster of metabolic abnormalities, including obesity, insulin resistance (IR), dyslipidemia and hypertension (HT) [42]. The interrelated risk factors have been independently associated with an increased risk for atherosclerotic CV disease and mortality [42, 43], type 2 diabetes (T2D), and their resulting complications [44]. The metS components share underlying mediators, mechanisms and pathways [43] and predominant risk factors include obesity and IR [44], which usually occur collectively. We must note that people with isolated components of the metS are still at risk for CV complications, however their risk remains lower than those diagnosed with the complete metS.

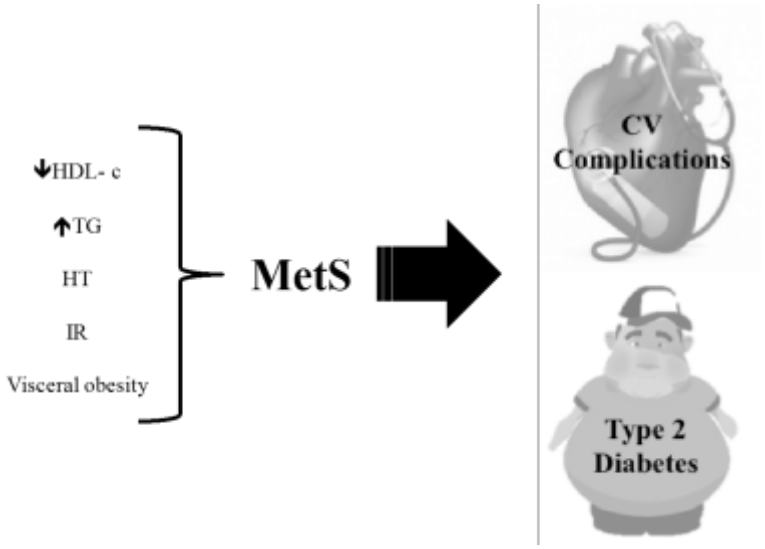

Figure 4. Risk factors and consequences of the metS. Altered lipoprotein levels, HT, IR and visceral obesity are the components involved in making up the metS. MetS development due to these risk factors may bring about further complications including CV complications and T2D. Abbreviations: HDL-c: high-density lipoprotein cholesterol, TG: triglycerides, HT: hypertension, IR: insulin resistance, MetS: metabolic syndrome, CV: cardiovascular.

Screening for diagnosis of the metS includes identifying at least 3 of 5 of the following: waist circumference (i.e. visceral obesity), high s-TG levels, low HDL-c levels, increased fasting glycaemia or IR, and increased blood pressure (BP) [44, 45]. Table I displayed below describes the criteria for these risk factors, however cut-off points may vary depending on the population of study.

Table I: The different metS screening tools displaying diagnosis criteria.

	NCEP ATP III (2005 revision)	WHO (1998)	EGIR (1999)	IDF (2005)
Absolutely required	None	Insulin resistance* (IGT, IFG, T2D or other evidence of IR)	Hyperinsulinemia‡ (plasma insulin >75th percentile)	Central obesity (waist circumference§): ≥94 cm (M), ≥80 cm (F)
Criteria	Any three of the five criteria below	Insulin resistance or diabetes, plus two of the five criteria below	Hyperinsulinemia, plus two of the four criteria below	Obesity, plus two of the four criteria below
Obesity	Waist circumference: >40 inches (M), >35 inches (F)	Waist/hip ratio: >0.90 (M), >0.85 (F); or BMI >30 kg/m^2	Waist circumference: ≥94 cm (M), ≥80cm (F)	Central obesity already required
Hyperglycemia	Fasting glucose ≥100 mg/dl or Rx	Insulin resistance already required	Insulin resistance already required	Fasting glucose ≥100 mg/dl
Dyslipidemia	TG ≥150 mg/dl or Rx	TG ≥150 mg/dl or HDL-C: <35 mg/dl (M), <39 mg/dl (F)	TG ≥177 mg/dl or HDL-C <39 mg/dl	TG ≥150 mg/dl or Rx
Dyslipidemia (second, separate criteria)	HDL cholesterol: <40 mg/dl (M), <50 mg/dl (F); or Rx			HDL cholesterol: <40 mg/dl (M), <50 mg/dl (F); or Rx
Hypertension	>130 mmHg systolic or >85 mmHg diastolic or Rx	≥140/90 mmHg	≥140/90 mmHg or Rx	>130 mmHg systolic or >85 mmHg diastolic or Rx
Other criteria		Microalbuminuria†		

This table describes the criteria of different screening tools used to diagnose the metS [43]. NCEP ATP III: National Cholesterol Education Program Adult Treatment Panel III, WHO: World Health Organization, EGIR: European Group for the Study of Insulin Resistance, IDF: International Diabetes Federation, IGT: impaired glucose tolerance, IFG: impaired fasting glucose, T2D: type 2 diabetes, IR: insulin resistance, BMI: body mass index, Rx: medical prescription, TG: triglycerides, HDL: high-density lipoprotein.

2.1.1 Abdominal obesity

Continued overweightness can eventually progress into obesity if not controlled or properly treated. The World Health Organization (WHO) describes obesity as a growing health and economic problem in Canadian society and its incidence is elevated and increasing in adults and unfortunately even in children. Statistics Canada found that approximately 20% of Canadian adults were classified as being obese [14]. Obesity is caused by an imbalance in intake of calories and energy expenditure, leading to an excess accumulation of body fat. The degree of adiposity is closely correlated with physiological parameters, including BP, systemic

insulin sensitivity, and circulating lipid levels [46]. In fact, obesity is directly related to the prognosis of the metS [46, 47]. Moreover, it can be an important precursor of the metS [41] thereby influencing CV risks and is actually an independent risk factor for cardiometabolic disorders (e.g. myocardial infarction, stroke, T2D) [46].

Weight reduction appears to improve certain features of the metS [43], hence its significance in this health disorder. Visceral adiposity rather than BMI is an especially important measure to consider because of its association with a number of pathologies (e.g. those associated with atherogenic and diabetogenic abnormalities) [45, 47].

2.1.2 Insulin resistance

Insulin is produced by the pancreas, an organ with endocrine and exocrine functionality. It is released when blood glucose levels are high stimulating the uptake of glucose by tissues, including the liver, skeletal muscle and adipose tissue. Insulin reduces circulating glucose by turning it into fat and glycogen, the two storage molecules. Under the manifestation of IR, the tissues are not able to respond to insulin and therefore cannot incorporate glucose leading to elevated blood glucose levels that can be pathological [43]. Noteworthy, IR is at the heart of the metS and can lead to metabolic complications. Additionally, the mechanism for which IR affects the body may advance into abnormalities in the vascular system (e.g. hyperglycaemia, advanced glycation products, toxicity from free fatty acids (FFAs), dyslipidemia and inflammatory agents) which consequently may incline T2D and atherosclerosis [43].

2.1.3 Dyslipidemia

Lipids, though physiologically essential, can contribute to disease if consumed in considerable amounts or if their metabolism is altered. Lipids include triglycerides (TG), phospholipids, FFAs, cholesterol and fat-soluble vitamins. TG are the main dietary lipid (95%), and along with cholesterol they are the primary contributors to disease. Lipoproteins are synthesized in the liver and transport endogenous TG and cholesterol through the blood until TG are taken up by peripheral tissues or until lipoproteins are cleared by the liver. TG and two types of lipoproteins are measured when determining the manifestation of dyslipidemia. These include LDL-c and HDL-c levels, or the bad and the good cholesterol, respectively. They are made up of different concentrations of TG, cholesteryl ester (CE) and phospholipids. LDL-c is

the most cholesterol rich lipoprotein and is associated with an increased risk of coronary artery disease [39] due to lipid accumulation on artery walls causing narrowing of the vessels. Furthermore, small dense LDL-c is atherogenic and linked to visceral adiposity, hypertriglyceridemia and IR [39]. HDL-c is synthesized by the liver and enterocytes and is important in collecting cholesterol from other lipoproteins and peripheral tissues to meet cell needs or for cholesterol clearance, a process known as the reverse cholesterol system. Due to its role in clearing cholesterol, HDL-c is an anti-atherogenic lipoprotein. It is not surprising then that TG, HDL-c and LDL-c are frequent components of the metS [48].

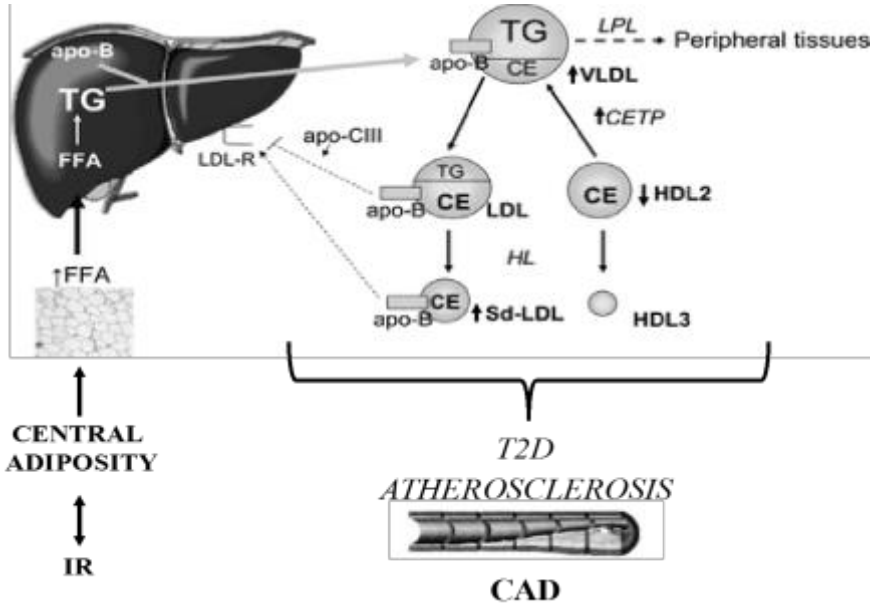

Figure 5. Development and consequences of dyslipidemia. Adapted from [49]. Dyslipidemia can include decreased concentrations of HDL-c and/or increased TG and LDL-c, which can consequently lead to progression of T2D and atherosclerosis, both risk factors for CAD. IR: insulin resistance, FFA: free fatty acids, TG: triglycerides, Apo-B: apolipoprotein B, LDL-R: low density lipoprotein receptor, apo-CIII: apolipoprotein CIII, CE: cholesteryl ester, LPL: lipoprotein lipase, VLDL: very low density lipoprotein, CETP: cholesterol ester transfer protein, LDL: low density lipoprotein, HDL2: high density lipoprotein 2, HDL3: high density lipoprotein 3, sd-LDL: small dense low density lipoprotein, T2D: type 2 diabetes mellitus, CAD: coronary artery disease.

2.1.4 Hypertension

Hypertension (HT) is defined as a state of abnormally high BP mostly due to modifiable lifestyle and dietary factors (e.g. tobacco, alcohol, physical inactivity, high sodium diet, low potassium and/or calcium diet, aging, obesity, IR) [50], consequently generating great physiological stress. Unfortunately, about 7.5 million people in Canada live with HT, which is a critical problem since it is the pivotal pathophysiological cause of CV morbidity and mortality [51]. HT is especially triggered by the interaction between genetics (e.g. epigenetic modifications in vessel wall smooth muscle cells) [52] and environmental factors [53] affecting smooth muscle cells of blood vessels, further playing a role in their dysfunction and leading to disease [54]. The association with vascular endothelial dysfunction is the final shared pathway concerning CV risk factors and is the central pathogenesis in atherosclerosis development [43, 55]. In the long run, HT can lead to a number of complications (e.g. CAD, CVD, heart failure, stroke, end-stage renal disease and death from the mentioned causes) [50] by the narrowing of blood vessels and is a key component in the diagnosis of the metS.

Mitochondria are organelles at the center of metabolic functions and their dysfunction has been associated with diseases related to components of the metS.

3. The mitochondrion

Discovered in the 1890s [56], the mitochondrion is a double membrane organelle otherwise known as the powerhouse of the cell due to its role in the production of energy in the form of adenosine triphosphate (ATP). This organelle is extremely dynamic and controls its morphology through the balance of fission and fusion, and has a unique structure that is crucial in the way mitochondria function. Furthermore, mitochondria exercise importance in maintaining normal structure, function and survival of tissues [57]. Aside from the nucleus, the mitochondrion is the only other subcellular organelle containing DNA, of which is maternally inherited [9].

Mitochondria are present in every human cell except mature erythrocytes and play major roles in metabolic processes (e.g. cellular respiration, FA β-oxidation, calcium metabolism, biosynthetic metabolism) due to their large quantity in the most metabolically active cells (e.g.

skeletal muscle, cardiac muscle, liver, brain) [9]. Other key functions include their role in apoptosis- and ROS-signalling pathways, and inflammatory processes. These functions make them important cellular stressors and supportive in the cell's adaptation to the environment [56].

3.1 Mitochondrial structure and dynamics

The Mitochondrion is made up of an outer mitochondrial membrane (OMM) surrounding its inner mitochondrial membrane (IMM). The IMM has a large surface area due to its ability to fold into large highly flexible tubular junctions called cristae [58]. In the case where the cell responds to a metabolic state and/or matrix volume, these junctions can endure morphological changes [58]. Furthermore, the shape and morphology of the mitochondrion's network in a cell depends on mitochondrial dynamics and its metabolic status [58] and the oxidative capacity of the cell depends on the number and size of mitochondria [57]. This underlines the importance of mitochondria structure in the cell.

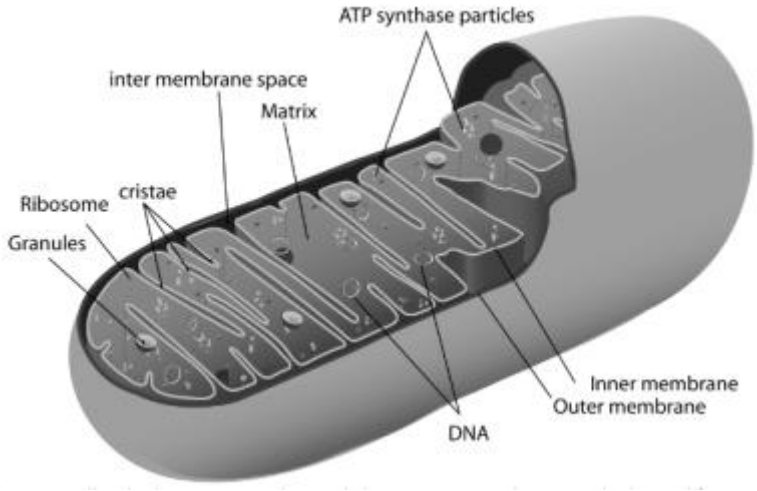

Figure 6. Shape, structure and components of the mitochondrion organelle [59]. The mitochondrion is a double membrane organelle consisting of an inner membrane, which has a large surface area and folds into cristae, and an outer membrane. The mitochondrial matrix is located within the inner membrane and holds mtDNA, ribosomes, and ATP synthase particles.

3.1.1 Fission and fusion dynamics

Mitochondria have a generally tubular external appearance. However, there is great variability in their shape depending on the organism and tissue, which may represent their different physiological and cellular states [60]. Mitochondria continually go through processes of fission and fusion, evidently changing their morphology, which is essential for the health and functioning of mitochondria and the cells [61]. Some mitochondrial shapes found inside the cell include small vesicles, short rods and reticular networks, and the main proteins responsible for this dynamic mitochondrial process are fission and fusion proteins such as the dynamin family of large GTPases [60].

Fusion and fission dynamics of mitochondria have been studied in relation to many pathological conditions. Some disorders related to metabolic and CV diseases have revealed dysfunctional mitochondria with alterations in their structure [60]. Therefore, dynamic processes have contributed to demonstrating the importance of mitochondria in human health.

3.1.2 Mitochondrial DNA

The IMM encloses a protein rich matrix where mtDNA is contained. The endosymbiotic theory explains that the mitochondrion began as a free living prokaryotic organism, thereby explaining the presence of mtDNA [62]. The human mitochondrion contains 16.6kb of circular maternally inherited mtDNA comprising 37 genes [63]. These genes code for 13 of the 90 proteins essential to the respiratory chain and for the 24 RNA (22tRNAs and 2 rRNAs) genes necessary for the synthesis of intra-mitochondrial proteins [64]. Proteins encoded by mtDNA are all subunits of the ETC complexes I, III, IV, and V, and are essential for ATP production by oxidative phosphorylation (OXPHOS). Thus, mtDNA is essential in cellular energy metabolism [65]. Moreover, the majority of mitochondrial proteins are encoded by nuclear DNA (nDNA) and synthesized on free ribosomes in the cytosol [66]. Additionally, they contain cytosolic precursors of mitochondrial proteins that hold information directing them towards the mitochondrion where they are imported by specialized systems [62, 66, 67]. The mitochondrion has receptors on its surface that recognize nuclear encoded proteins [66]. The transport process of nuclear encoded proteins into the mitochondrion is energy (i.e. ATP and membrane potential)

dependent and the import and intra-mitochondrial sorting of proteins is mediated by translocases on the OMM (TOM complex) and IMM (TIM23 complex) [66].

Mitochondria are able to maintain their genome and they have well-developed machinery for replication, transcription and translation [67]. However, unlike nDNA, mtDNA is not protected by histones and is therefore at risk of damage [9]. There is evidence that a number of inherited diseases are a result of mtDNA mutations and loss of mtDNA, giving rise to respiratory chain defects, modifying the synthesis of ATP and leading to organ dysfunction [64].

3.1.3 Mitochondrial biogenesis

Growth and division of existing mitochondria are defined as processes of mitochondrial biogenesis [63]. Proper mitochondrial biogenesis is dependent on the coordinated synthesis and import of proteins encoded by the nuclear genome in addition to the proper coordination of mitochondrial dynamics (i.e. fission and fusion) and mtDNA replication [63]. Biogenesis can be influenced by environmental stressors, including caloric restriction, exercise, low temperature, oxidative stress (OxS), cell renewal, cell differentiation and cell division [63]. Moreover, mitochondrial biogenesis is driven by its master regulator, the transcription factor peroxisome proliferator-activated receptor gamma coactivator 1-alpha (PGC1-α) [68] in the nucleus. Expression of PGC1-α can be controlled by signalling cascades including endothelial nitric oxide synthase (eNOS), cyclic adenosine 3,5'-monophosphate (cAMP) and 5' adenosine monophosphate-activated protein kinase (AMPK) signalling [57, 69] among others, illustrated in figure 7 (page 16). Mechanisms of PGC1-α regulation by eNOS are not well established, however high levels of NO results in cGMP-dependent signalling inducing PGC1-α, mitochondrial transcription factor A (Tfam) and nuclear respiratory factor 1 (NRF-1), and this has been correlated with increased mitochondrial biogenesis in some cell lines [69]. Under moments of energy deprivation (e.g. during exercise), AMPK induces PGC1-α transcription and enhances PGC1-α co-transcriptional activity by phosphorylating threonine-177 and serine-538, all leading to increased mitochondrial biogenesis [70]. Additionally under cold or fasting, the thermogenic signalling cascade increases cyclase activity and increases cAMP production who's elevated levels phosphorylate CREB, activating it and further inducing PGC1-α [69].

Furthermore, PGC1-α implements its functions by binding to and regulating the activity of many transcription factors including peroxisome proliferator-activated receptors (PPAR)γ and α, nuclear respiratory factor (NRF) 1 and 2 and estrogen-related receptor-alpha (ERRα), provoking the expression of their target genes shown in figure 7 (page 16) [57, 70]. The regulation of these proteins by PGC1-α modifies genes involved in metabolic pathways (e.g. FA oxidation, OXPHOS, gluconeogenesis, etc.) [70]. For example, NRF-1 regulates the expression of mitochondrial genes (e.g. OXPHOS genes & Tfam) needed for mitochondrial gene expression and mitochondrial genome replication [57].

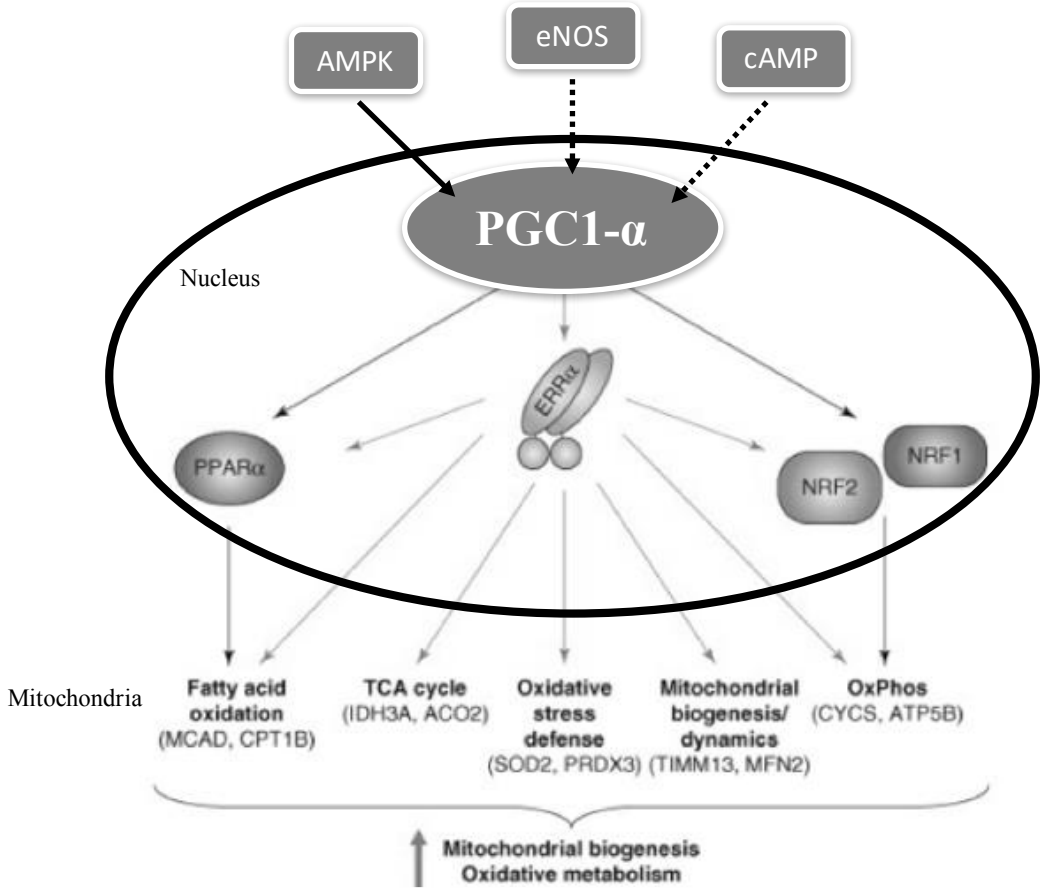

Figure 7. Regulation of expression of PPARα, ERRα, NRF1 and NRF2 by transcription factor PGC1-α driving biogenesis and oxidative metabolism. Adapted with permission from [71]. Abbreviations: eNOS: endothelial nitric oxide synthase, cAMP: cyclic adenosine 3,5'-monophosphate, AMPK: 5' adenosine monophosphate-activated protein kinase, PGC1-α:

peroxisome proliferator-activated receptor gamma coactivator 1-alpha, PGC1-β: peroxisome proliferator-activated receptor gamma coactivator 1-beta, PPARα: peroxisome proliferator-activated receptor-alpha, ERRα: estrogen-related receptor-alpha, NRF1: nuclear respiratory factor 1, NRF2: nuclear respiratory factor 2, TCA: tricarboxylic acid, MCAD: medium-chain acyl-CoA dehydrogenase, CPT1B: carnitine palmitoyltransferase 1b, IDH3A: isocitrate dehydrogenase 3 alpha subunit, ACO2: aconitase 2, SOD2: superoxide dismutase 2, PRDX3: peroxiredoxin 3, TIMM13: translocase of inner mitochondrial membrane 13, MFN2: mitofusin-2, CYCS: cytochrome c somatic, ATP5B: ATP synthase, H+ transporting, mitochondrial F1 complex, beta subunit precursor.

Biogenesis of mitochondria is significant in the way they function and a decreased number of mitochondria may cause decreased mitochondrial function [57]. Consequently a decline in the mitochondrion's electron transport activity is partly due to decreased mitochondrial content or number, which may induce an interruption in normal cell metabolic functions.

3.2 Mitochondrial functions

3.2.1 Metabolic functions of the mitochondrion

The mitochondrion's abundant metabolic pathways are important in the metabolism of carbohydrates (CHO), lipids and amino acids (AA). The production of metabolic energy in eukaryotic cells is a critical role implemented by the mitochondrion and is achieved by its oxidative respiration and metabolism of nutrients [57], especially from the breakdown of CHO and fatty acids (FA) [72]. Cellular respiration is a catabolic process in which glucose molecules from food fuels, are broken down releasing energy that can be captured to form ATP [56]. Mitochondria, with the help of oxygen, completes the breakdown of food by producing CO_2, water and large amounts of ATP for cellular use [56].

Production of ATP involves anaerobic and aerobic processes. Firstly, glycolysis comprises the breakdown of glucose to pyruvate coupled with the anaerobic synthesis of ATP in the cytosol [73]. However, most of the ATP is harvested through the aerobic processes that initiate when pyruvate enters the mitochondrion producing acetyl-CoA and on setting the

tricarboxylic acid (TCA) cycle [73]. The TCA cycle produces intermediates that donate electrons to the OXPHOS pathway generating energy in the form of ATP. Most of the energy produced (~95%) [74] in the cells comes from the OXPHOS pathway and the remainder arises through glycolysis [57]. The three mitochondrial pathways of energy production, i.e. TCA cycle, OXPHOS and FA β-oxidation, will be further discussed.

A) *TCA cycle*

The TCA cycle is the central metabolic pathway of the cell, taking place inside the mitochondrial matrix. It involves a series of oxidation-reduction reactions resulting in two molecules of carbon dioxide from the oxidation of an acetyl group. In addition, this is the final common pathway where fuel molecules, including AA, FA and CHO, are oxidized. Any molecule that can be transformed into an acetyl group or dicarboxylic acid can enter into aerobic metabolism. Carbon fuels, that mostly enter the cycle as acetyl CoA, are oxidized and act as a precursor source for biosynthetic processes, as well as for storage forms of fuels, and for building blocks of AA, cholesterol, porphyrin and nucleotide bases [73]. However, the primary function of this cycle is to use carbon fuels to yield high-energy electrons. The TCA cycle is important in the production of energy. However, this process alone doesn't produce a significant amount of ATP but it forms NADH and $FADH_2$ that carry electrons to the OXPHOS pathway (i.e. ETC and chemiosmosis) where most of the energy is produced.

B) *Fatty acid β-oxidation*

In moments of fasting or stress, the human body uses metabolic fuels to function. FA are essential metabolic fuels [75] that are activated in the cytosol, however oxidation of FA occurs largely in the mitochondrion. This process includes a series of enzymatic steps generating acetyl-CoA. First, fatty acyl-coA must cross the impermeable IMM and achieves this with the help of carnitine palmitoyltransferase I (CPT1), carnitine translocase (CAT) and carnitine palmitoyltransferase II (CPT2) enzymes, shown in figure 8 (page 19). Once inside the matrix the process of β-oxidation oxidizes short chained fatty acyl-CoA ester until it becomes acetyl-CoA [75]. As discussed previously, acetyl-coA initiates the TCA cycle leading to energy production. Thus FA oxidation fuels the TCA cycle and yields important amounts of NADH and $FADH_2$, which are needed in the OXPHOS pathway [67].

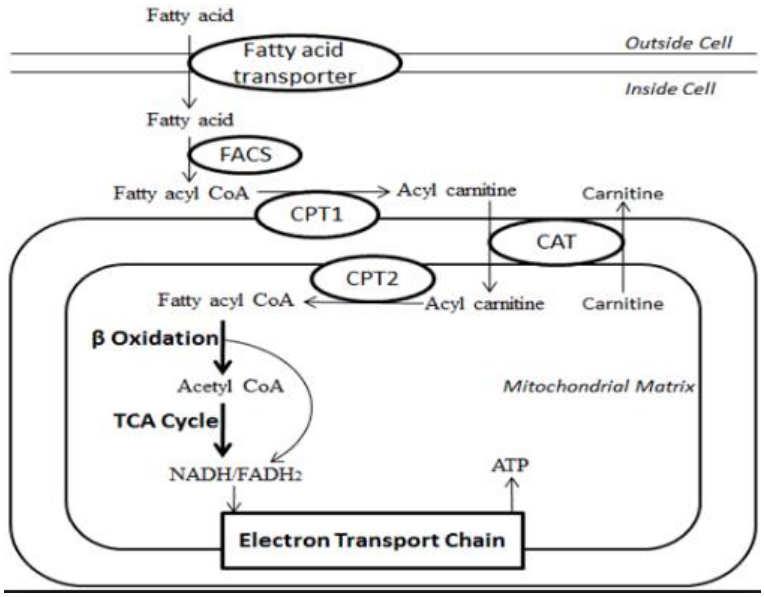

Figure 8. ATP production by the FA β-oxidation pathway [76]. This image shows the different enzymes and transporters involved in carrying FA from outside the cell into the mitochondrial matrix for ATP production. Abbreviations: FACS: fatty acyl-CoA synthase, CPT1: carnitine palmitoyl transferase 1, CPT2: carnitine palmitoyl transferase 2, CAT: carnitine translocase, TCA: tricarboxylic acid, NADH: nicotinamide adenine dinucleotide + hydrogen, $FADH_2$: flavin adenine dinucleotide, ATP: adenosine triphosphate.

C) *Oxidative phosphorylation*

High-energy intermediates in the mitochondrial matrix, including NADH, NADPH and $FADH_2$ produced by the mitochondrion from the TCA cycle and FA β-oxidation metabolic pathways, are electron donors involved in the production of energy [67, 77, 78]. They are used to fuel the ETC complexes and ATP synthase in the IMM in a process called OXPHOS or cellular respiration [56, 57, 78]. This process yields the highest amount of energy in the form of ATP [78].

OXPHOS consists of a system of five multisubunit complexes- NADH: ubiquinone oxidoreductase (complex I), succinate: ubiquinone oxidoreductase (complex II), ubiquinol: cytochrome c oxidoreductase (complex III), cytochrome c oxidase (complex IV), and F_0 F_1-ATP-synthase (complex V), depicted in figure 9 (page 20) [67]. This pathway can be separated into two different functional parts: complexes I-IV make up the ETC whereas complex V is

responsible for the synthesis of ATP through a process known as chemiosmosis [67]. The ETC consists of passing electrons from one molecule to another, using enzymes to oxidize nutrients releasing ATP. When electrons are transported along the ETC, protons are released. Some of the energy collected during this process is then used to pump protons out of the matrix resulting in a pH gradient and charge gradient across the IMM [78]. The proton motive force produced by disruption in gradients pumps protons into the mitochondrial matrix where it couples with ATP synthase and energy is produced [78].

OXPHOS has been demonstrated as having critical control over metabolic pathways [79]. In addition, the number and size of mitochondria is related to the mitochondrial oxidative capacity. For example, decreased mitochondrial oxidative capacity is joined by decreased expression of mitochondrial proteins [e.g. encoded by mtDNA (e.g. cyt c oxidase 1) and nDNA (e.g. succinate dehydrogenase & pyruvate dehydrogenase)] [57].

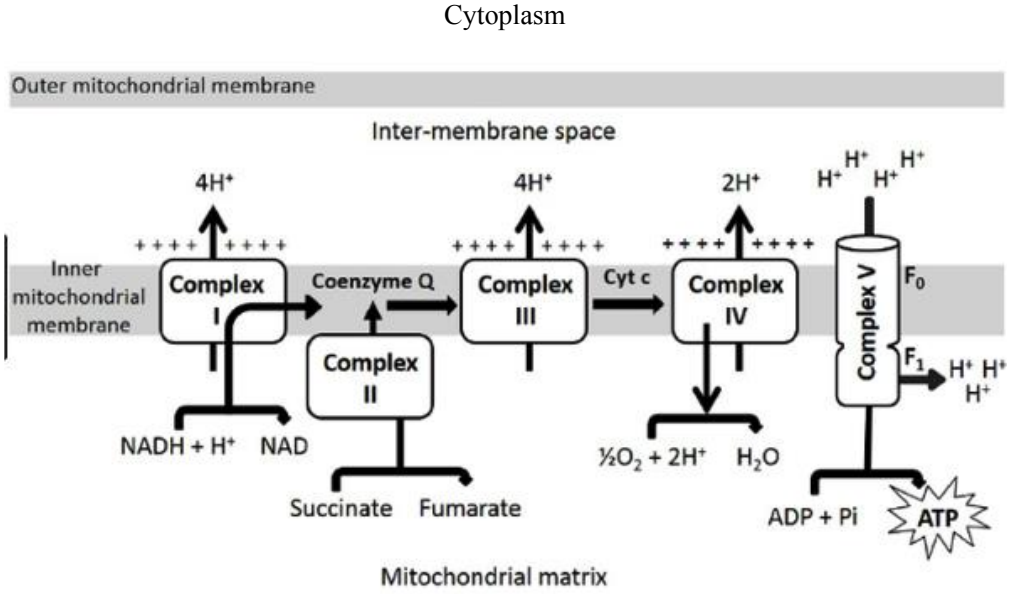

Figure 9. Enzymes and complexes involved in the OXPHOS pathway [80]. The OXPHOS pathway can be separated into 2 parts, the ETC and chemiosmosis, utilizing and producing many enzymes leading to the production of ATP in the final step (complex V). Abbreviations: NAD: nicotinamide adenine dinucleotide, NADH: nicotinamide adenine dinucleotide + hydrogen, ADP: adenosine diphosphate, ATP: adenosine triphosphate, Pi: inorganic phosphate.

3.2.2 Mitochondrial signalling pathways

Aside from metabolic functions, it is understood that mitochondria possess signalling pathways allowing them to communicate their bioenergetic and biosynthetic states with other parts of the cell [7, 81]. Mitochondria are established in the cytosol and evidently communicate with this part of the cell through the release of proteins, ROS, or metabolites, by interacting with other organelles, and by acting as a framework in the arrangement of signalling molecules [7]. Signalling processes ensure that the mitochondrial fitness is adequate in order to carry out its many functions and ensures that mitochondria have the capacity to meet their functional demands [7].

A) Calcium signalling

The transport of calcium into the mitochondrion is a highly regulated system that is vital for the cell. Calcium from the cytosol crosses the outer membrane into the intermembrane space through the voltage-dependent anion channel (VDAC) situated on the OMM [82]. The main role of calcium in the mitochondrion is the stimulation of OXPHOS occurring at many levels, more specifically by activating the enzymes involved in the OXPHOS machinery [82]. When mitochondrial calcium is increased, the entire OXPHOS machinery is upregulated causing rapid respiratory chain activity and increased output of energy [82]. So, depending on cellular demand, ATP output can be controlled by calcium.

Under normal circumstances, calcium positively influences mitochondrial function, though any disturbance in mitochondrial or cytosolic calcium homeostasis can have consequences on cell function, as displayed in figure 10 (page 22). In addition, pathologies where calcium concentration is high can alter mitochondrial function.

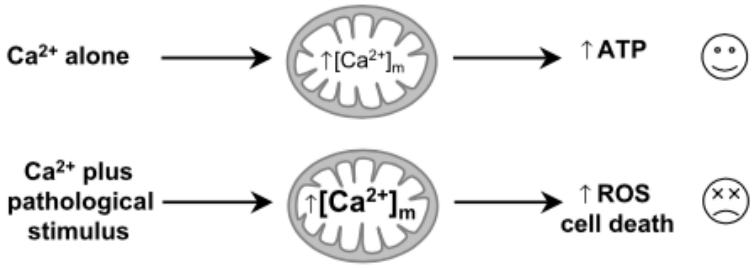

Figure 10. **Hypothesized mechanisms of the effect of calcium on the mitochondrion** [82]. Calcium positively affects mitochondrial function under physiological conditions, however under pathological stimulus, increased calcium can harm mitochondrial function. Abbreviations: ATP: adenosine triphosphate, ROS: reactive oxygen species.

B) Apoptosis signalling

Another essential physiological process of the mitochondrion used by multicellular organisms in development and morphogenesis is controlling the regulation of cell death. This process is known as apoptosis and regulates the number of cells in tissues [67]. Apoptosis is characterized by distinct morphological characteristics and its biochemical reactions are energy-dependent [83]. In addition, when cells are damaged, apoptosis acts as a defense mechanism to eliminate damaged cells [83]. For example, during a stress response, it is important that mitochondria are under a normal physiological state for cellular homeostasis and cell death [84].

Cell death by apoptosis depends on mitochondrial membrane permeabilization (MMP), this may include the inner or outer MMP [84]. Apoptosis involves mitochondrial signalling by releasing cytochrome c from the mitochondrion into the cytosol. Cytochrome c release is an all or nothing process of apoptosis [85] where the cell is ultimately broken down by proteins called caspases.

Caspases can be activated via 2 different pathways; the intrinsic (i.e. mitochondrial pathway) and extrinsic (i.e. death receptor pathways) pathways displayed in figure 11 (page 23). During the intrinsic pathway, caspases are activated from signals within the cell, for example from DNA damage beyond repair or severe stress. This pathway depends on the balance of 2 sets of mitochondrial membrane proteins, anti-apoptotic (Bcl2, Bclx) and pro-apoptotic (BAX, BAK) proteins [84]. In a healthy cell, the anti-apoptotic proteins bind to the pro-apoptotic

proteins blocking their actions. If a cell is damaged or stops receiving survival signals, these stimuli will alter the inner mitochondrial membrane resulting in the opening of the mitochondrial permeability pore and loss of mitochondrial transmembrane potential [83]. By locking Bcl2 and Bclx, Bax and Bak are free to pierce a series of punctures in the mitochondrion membrane allowing cytochrome c to leak out into the cytoplasm. Cytochrome c binds to the APAF-1 and procaspase-9 protein creating a compound (i.e. apoptosome) that activates the caspase cascade, leading to cell death [83]. The extrinsic apoptotic pathway is triggered by external signals from outside the cell. For example, T-lymphocytes have a surface molecule (i.e. Fas-ligand) that recognizes receptors on the surface of target cells (i.e. Fas receptor), leading to a chain of events resulting in apoptosis. This is mediated by the Fas associated domain protein (FADD) triggering caspases, which then activate each other in a self-amplifying process called the caspase cascade. The activation of caspase initiates the phase of apoptosis breaking down the cellular material, resulting in cell death. Once the cells have undergone apoptosis, their debris are cleared by macrophages.

Altered apoptosis homeostasis has been implicated in many human conditions involving excessive or deficient apoptosis activity [86].

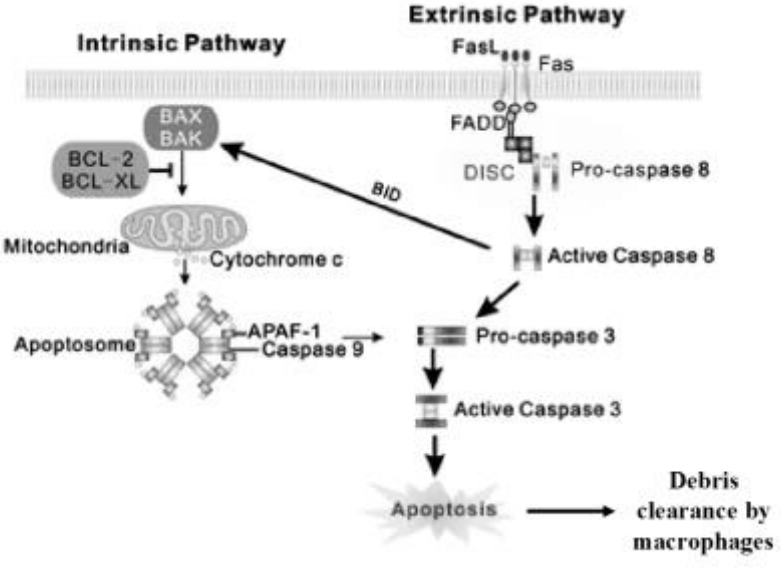

Figure 11. Mechanisms of the intrinsic and extrinsic pathways of apoptosis. Apoptosis can occur through 2 different cellular pathways which lead to cell death and clearance by macrophages. Abbreviations: FADD: Fas-associated death domain-containing protein, DISC:

death-inducing signalling complex, BID: BCL-2-homology domain 3 (BH3) interacting-domain death agonist, APAF-1: apoptotic protease activating factor 1, FasL: fas ligand. Reproduced with permission [87].

C) ROS signalling

ROS are ubiquitous, highly reactive, short lived oxygen metabolites with functions such as the striping of electrons from other molecules (i.e. oxidizing), donating electrons to other molecules (i.e. reducing), or reacting with parts of molecules (i.e. oxidative modification) [88]. ROS, when isolated, are very unstable molecules with powerful oxidative effects on the cells proteins, lipids and DNA, consequently impairing cellular functions [89]. Under normal conditions mitochondria are responsible for 90% of free radical production. Furthermore, the ETC is an essential cellular process, however when it is inhibited it creates the superoxide anion radical, a toxic reactive by-product [55]. ROS accumulation can damage cell structure and function [90] while causing inflammation and cell death [91]. Furthermore, mitochondria and mtDNA are vulnerable to the ROS they produce. There are several reasons for this vulnerability, including: 1. mtDNA is located near the inner mitochondrial membrane where the ETC forms free radicals; 2. mtDNA is not protected by histones; and 3. mitochondria have limited DNA repair ability. Since ETC components are encoded by mtDNA, mutations induced by ROS can damage OXPHOS, leading to more mitochondria and cellular damage because of the additional ROS production [9, 55, 57]. Once mitochondria are damaged, cellular energy requirements are increased in order to repair it, and direct damage to mitochondria reduces their affinity for coenzymes or substrates [9].

ROS have had a negative image due to the previous thought that they were the respiratory processes damaging by-products responsible for aging and oxidative damage [82]. However, the ROS/RNS systems of the mitochondrion have crucial signalling roles [86], that under physiological conditions, are able to communicate with the rest of the cell [7, 81]. These systems are important in normal cell functions, including growth, migration, apoptosis, and remodelling [88], making them fundamental for life [92]. Under hypoxic conditions (i.e. low oxygen) mitochondria release ROS stabilizing hypoxia inducible factors (HIFs) and inducing genes responsible for the metabolic adaption to low oxygen conditions, summarized in figure 12

(page 25) [7]. Moreover, low levels of mitochondrial ROS (mROS) are essential in maintaining homeostatic biological processes, and slightly higher levels of mROS can stimulate adaption to stress pathways [7].

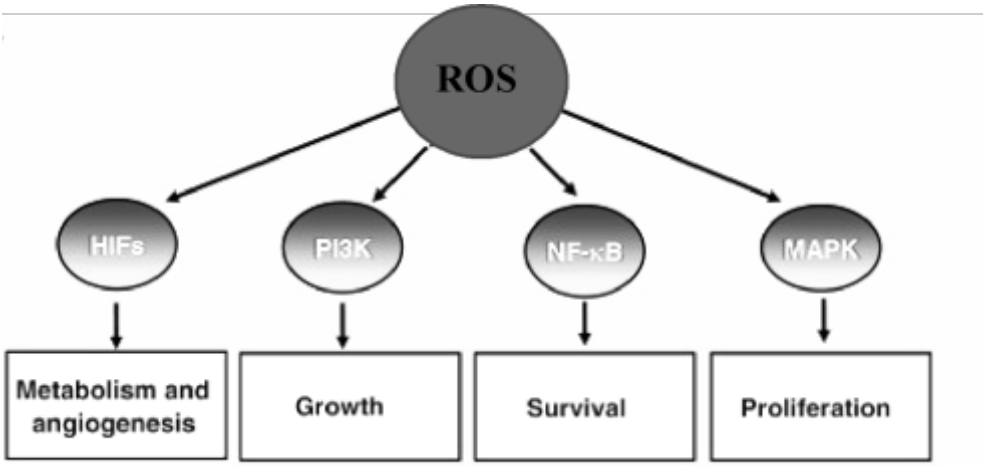

Figure 12. Normal functions of ROS and the factors involved in these processes. Abbreviations: ROS: reactive oxygen species, HIFs: hypoxia inducible factors, PI3K: phosphoinositide 3-kinase, NF-κB: nuclear factor kappa-light-chain-enhancer of activated B cells, MAPK: mitogen activated protein kinases. Adapted with permission [93].

Superoxide (O_2), the primary source of ROS produced by the mitochondrion, is converted to H_2O_2 by spontaneous dismutation or by the superoxide dismutase (SOD) enzyme [82], an important antioxidant. Antioxidant enzymes (e.g. Cu/Zn-superoxide dismutase (SOD), MnSOD, endothelial cell SOD, glutathione peroxidase (GPX), and catalase) as well as other substances with antioxidant activity (e.g. vitamin C, vitamin E, glutathione (GSH)) protect against ROS [89]. OxS depends on the balance of ROS and antioxidant. When the antioxidant system is overwhelmed due to too much ROS, this results in OxS [89] and may lead to pathological conditions.

D) Inflammation

Inflammation is a normal biological process supporting the repair or prevention of damage to tissues or cells in response to pathogens [94]. Furthermore, inflammation is involved in the aging process by changing OxS-induced inflammatory responses and redox status [94, 95]. Mitochondria can be released from the cell to promote inflammation by stimulating pro-inflammatory signalling processes [96]. Hence, they have an important role in pro-inflammatory

processes yet their function may also be affected by pro-inflammatory mediators [94]. Additionally, altered mitochondrial function has been associated with diseases involving acute and chronic inflammation [94].

There is indication that mitochondrial ROS are fundamental signalling activators of the innate immune response [91]. Under physiological conditions antioxidant systems can repress OxS in the mitochondrion but under pathological conditions excess O_2^- ions are produced and redox-sensitive transcription factors are activated (e.g. NF-κB, cytokines, iNOS, etc.) [94]. NF-κB, is a transcription factor involved in the activation of genes implicated in inflammation [97], OxS and endothelial dysfunction. It is activated by the proinflammatory cytokine tumour necrosis factor alpha (TNF-α) [98], IL-1, bacterial products and physical stress forms [97]. Cellular I-κB proteins interact with NF-κB in an uninduced state masking its nuclear location sequence so it remains in the cytoplasm [97]. The TNF-α mediated inflammatory event begins with the binding of its heterotrimeric ligand to either TNFR-1 or TNFR-2 surface receptors [99], where TNFR-1 seems to be the main mediator [97]. TNFRs can activate gene expression by recruitment TNF receptor-associated factor (TRAF) family members [97]. This binding then allows TNF to activate the I-κB kinase (IKK) complex leading to the proteolytic degradation of I-κB by phosphorylation and ubiquitination [98]. This liberates NF-κB where it can be further phosphorylated and translocated into the nucleus [97] thereby inducing the transcription of NF-κB responsive genes leading to inflammation [100]. To note, the IL-6 proinflammatory cytokine uses a similar transduction mechanism to activate IKK and NF-κB [101].

Additionally, research throughout the last decade has proposed that TNF-α is connected to mitochondrial damage, by functionally damaging certain components of the mitochondrial ETC and causing structural changes to its morphology [102]. Some cell types actually have protection against TNF, for example, overexpression of the mitochondrial enzyme manganese SOD shows increased resistance against TNF implying that the overexpressed superoxide radicals or other ROS may play a role in TNF-mediated cytotoxic pathway [102]. In addition, TNF cytotoxic activity can either be increased or blocked by certain electron transport inhibitors [102]. Furthermore, TNF alters the mitochondrial ultrastructure by a degenerative clumping of mitochondrial cristae, inhibits the electron transport chain by early functional damage to electron flow thereby decreasing the mitochondrion's ability to oxidize succinate and NADH-linked substrates therefore decreasing synthesis of ATP, and by mediating mitochondrial

oxygen radical production especially at the ubiquinone site [91, 102]. Damage to the mitochondrial ETC results in increased production of free radicals inside the mitochondrion, leading to further damage [102]. For example, if mitochondria are damaged and are not cleared this can induce an inflammatory response [91], which could develop into various diseases or disorders.

Now that we have described the mitochondrion and demonstrated its important roles in metabolic process, we will review its functions in metabolic complications. The next section is the basis of our hypothesis and key in understanding how mitochondria dysfunction can influence metS aetiology in cALL survivors.

3.3 Mitochondrial dysfunctions and cardiometabolic complications

In the last decade, there has been an eruption in mitochondrial research due to the discovery of its many essential functions within the organism. The relationship between metabolic disorders and the mitochondrion have been and are being explored thoroughly. This has led to the discovery of mitochondrial implication in more or less all diseases, including neurodegenerative diseases, muscular dystrophy, CV disorders, liver pathologies, diabetes and cancer [79] as a primary site of pathology or as a site of cellular signalling with major impact on disease pathogenesis [103].

Mitochondrial dysfunction can include any abnormality in the mitochondrion's main physiological functions, including but not limited to ATP production, ROS detoxification and ROS-related damage, apoptosis signalling, cytosolic calcium regulation, and synthesis and catabolism of metabolites [104]. Dysfunction can be due to a lack of oxygen for ETC function, or through genetic alterations that damage mitochondrial proteins. It is described as the inability to produce energy or metabolites, as well as proteins involved in import/export systems [81]. Cells can contain a mix of functional and dysfunctional mitochondria, where dysfunctional mitochondria send signals to begin a stress response until mitophagy removes them. When there is a deficiency in mitophagy, dysfunctional mitochondria accumulate leading to a disruption in its functions [81]. Since the mitochondrion is crucial in metabolic function, mitochondrial dysfunction can impact cellular metabolic processes.

Cardiometabolic complications present in cALL survivors years into their remission period are marked by several factors that can be controlled by mitochondria or due to altered mitochondrial function, especially OxS and inflammation [89]. Additionally, continued OxS can lead to inflammation as explained previously, contributing in the development of components of the metS and its complications [90, 105]. OxS is fundamental in the pathogenesis of metS complications. Furthermore, inflammatory and OxS processes both play important roles in the characterization of atherosclerosis [106], a consequence of the metS.

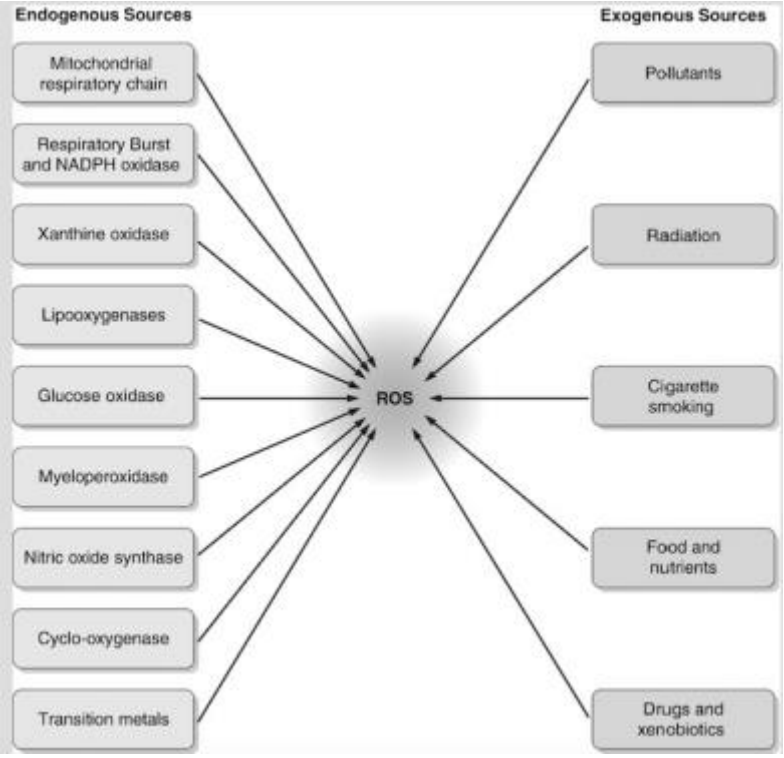

Figure 13. **Endogenous and exogenous sources of ROS production** [107]. Many endogenous sources of reactive oxygen species (ROS) production are linked to mitochondrial function, demonstrating the mitochondrion's crucial role in ROS production.

3.3.1 Oxidative stress and metabolic complications

The pathogenesis of many diseases depends highly on the state of OxS [108]. For instance, the metS and its related components involve increased OxS [109]. Moreover, it is suggested that the presence of OxS actually occurs early in metS pathology and is not simply a consequence [109].

Once again, OxS is an imbalance between production of free radicals and reactive oxidants (e.g. ROS) and their elimination by antioxidants [109], processes largely controlled by the mitochondrion. This can lead to biomolecule and cell damages by ROS that can impact the organism [90] by impairing normal cell functions [89]. In consequence, this may bring about metabolic deregulation, changes in cell signalling and in other functions of the cell [109]. Individuals living with the metS and its risk factors have altered oxidative/antioxidant status and present subclinical inflammation which can have causal roles in the development of atherosclerosis [105]. Studies have associated the presence of OxS with the Adult Treatment Panel (ATP) III criteria of metS diagnosis, and ROS are the major influences in the metS. In addition, there was an increase in peroxides and other OxS markers proportionate to the number of metS risk factors in patients [105]. Since mitochondria are the main sources of ROS/antioxidant in the cell, it is believed that they may play a part in metS pathogenesis. Figure 14 (page 30) demonstrates how each component of the metS (i.e. obesity, dyslipidemia, IR, HT) can affect oxidative/antioxidant status leading to CHO, lipid and protein oxidation [105]. Additionally, atherosclerosis and inflammation have been consequences of the above changes [109] and ROS play an important role in vascular biology. Therefore, balancing the oxidative/antioxidant status is one of the first steps in reaching a metabolically healthy status [105] in order to prevent the appearance of CV complications.

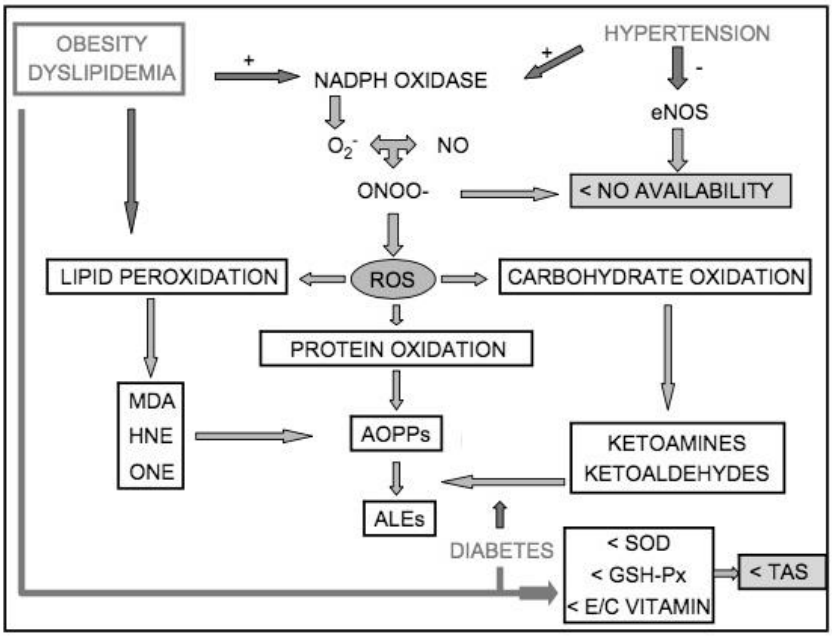

Figure 14. **Involvement of oxidative stress pathways with components of the MetS.** OxS pathways are involved in all components of the metS. Abbreviations: NADPH: nicotinamide adenine dinucleotide phosphate, O_2^-: superoxide anion, NO: nitric oxide, $ONOO^-$: peroxinitrite, ROS: reactive oxygen species, eNOS: endothelial NO synthase, MDA: malonyldialdehyde, HNE: 4-hydroxynonenal, ONE: 4-oxy-2-nonenal, AOPPs: advanced oxidized plasma protein, ALEs: advanced lipoxidation end-products, SOD: superoxide dismutase, GSH-Px: glutathione peroxidase, TAS: total antioxidant status. Reproduced with permission [105].

A) Oxidative stress and obesity

Obesity has been linked to the pathogenesis of a number of diseases including the metS and its components, as well as T2D, atherosclerosis and some cancers [89, 110]. Obesity is a central and causal component of the metS and ROS are increased in obesity [111]. In addition, the Framingham study reported that systemic OxS is closely associated with BMI [108], and OxS of visceral adipose tissue is an early marker of the metS in humans and animals [105] and is key in the pathogenesis of obesity-related metS [108].

Glucose is metabolized in the mitochondrion by the TCA cycle, forming electron donors (e.g. NADH and $FADH_2$). An excess in glucose can generate superoxide by increasing electron donors in the mitochondrion ETC easing the transfer of electrons to molecular oxygen [89].

Furthermore excess FFAs can enhance mitochondrial FFA oxidation creating electron donors (NADH and $FADH_2$), as does the oxidation of acetyl CoA derived from FFAs that can enter the TCA cycle. Both processes described result in ROS overproduction by mitochondria, or provoke OxS in the tissue or cell. FFAs resulting from the increased release of over accumulated FA from over nutrition or obesity activate NADPH oxidase in adipose cells or in other cells provoking the production of ROS, illustrated in figure 15 (page 31) [89]. Furthermore, expression of antioxidant enzymes in adipose tissue are decreased in obese individuals [89, 108]. The increased oxidative status in adipose tissue further impairs the regulation of local adipocytokines (e.g. TNF-α) [108]. Increased OxS in the blood caused by the increased production of OxS in accumulated fat is able to direct towards other organs (e.g. aorta, liver, skeletal muscle) consequently disturbing them [108]. Moreover, ROS production by the NADPH oxidase pathway in accumulated fat may play a key role in obesity-associated metS pathogenesis [89, 108]

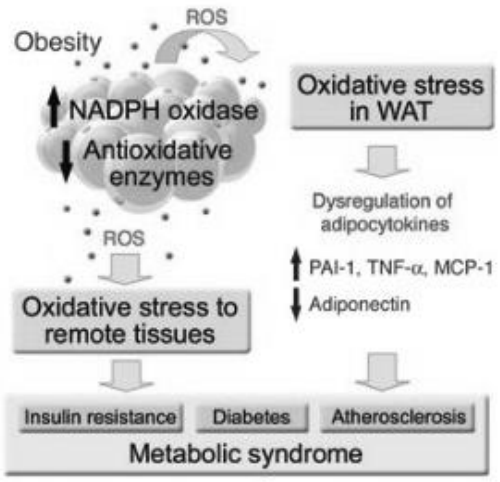

Figure 15. **ROS production in adipocytes and its contribution and pathogenesis in the metS** [108]. Abbreviations: PAI-1: plasminogen activator inhibitor-1, TNF-α: tumour necrosis factor alpha, MCP-1: monocyte chemoattractant protein 1, NADPH: nicotinamide adenine dinucleotide phosphate, ROS: reactive oxygen species, WAT: white adipose tissue.

High OxS and decreased antioxidant production may damage cellular structures bringing about the different complications associated with obesity [110]. Mice fed a HFD presented mitochondrial dysfunction, shown by their decreased ATP levels and antioxidant proteins, and

increased OxS that are involved in the development of IR [65]. Similarly, another study found that obese mice had increased ROS production in fat tissue, along with decreased expression of antioxidant enzymes and increased expression of NADPH oxidase enzyme, which plays a major role in atherosclerosis [108]. Moreover, increased FA in cultured adipocytes displayed increased systemic OxS levels by activating NADPH oxidase [89].

Increased ROS act as local messengers between endoplasmic reticulum (ER) stress and mitochondria, displayed in figure 16 (page 33), and ER stress is known to cause mitochondrial dysfunction [65]. Furthermore, there is evidence that mitochondrial dysfunction heightens ER stress markers in adipocytes [65]. The ER is the major cellular site responsible for folding, trafficking and quality control of proteins making it important for many functions of the cell [112]. The collection of newly synthesized unfolded proteins leads to ER stress, thereby activating the unfolded protein response (UPR) [112]. In the case of failed adaptive capacity of the ER, e.g. under obese conditions, there is an activation of the UPR, which meets different signalling pathways involved in inflammation and stress that are crucial in chronic diseases of metabolic systems (e.g. obesity, IR, T2D) [112].

Research has proposed that a new therapeutic target for metS could involve the oxidative status of adipose tissues [105]. Studies have also found that OxS is a central player in endothelial dysfunction in obese individuals [105, 113, 114], and it is suggested that local vascular OxS is the primary factor responsible for early obesity related endothelial dysfunction [105].

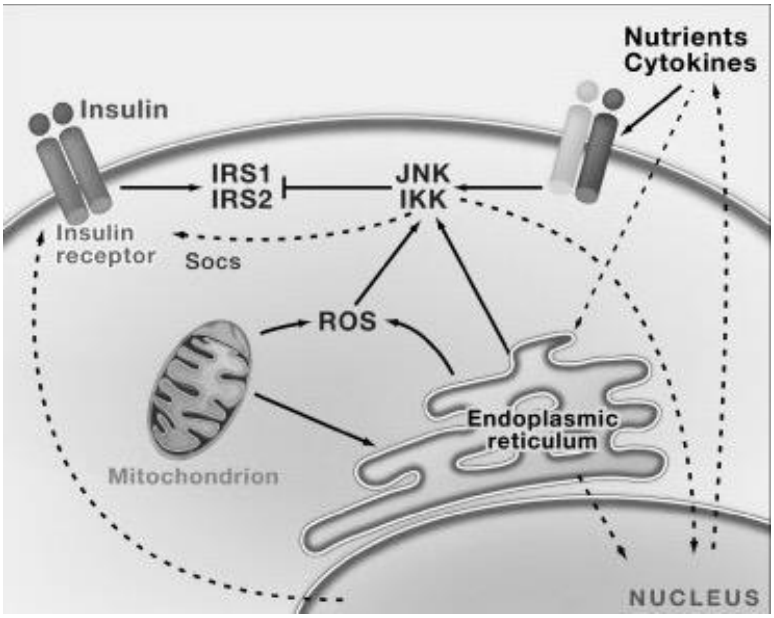

Figure 16: Obesity mediated inflammation and ROS production in the cell involving ER and mitochondrion organelles. Abbreviations: IRS: insulin receptor substrates, JNK: c-jun N-terminal kinase, IKK: I-κB kinase, ROS: reactive oxygen species. Reproduced with permission [112].

Additionally, adipose tissue is an endocrine organ that releases adipocytokines and adipokines, including proinflammatory molecules, namely IL-6 and TNF-α, primarily through macrophage infiltration [45]. This can occur due to ROS presence in adipose cells or increased generation of ROS that increases mRNA expression of proinflammatory cytokines or high macrophage infiltration and inflammatory changes. The release of FFAs from adipocytes facilitates the production of TNF-α in macrophages consequently leading to inflammation and lipolysis in adipose tissue [89]. These altered levels of proinflammatory molecules are possibly linked to obesity-associated disease pathogenesis. Therefore OxS in obesity can trigger increased inflammation in adipose tissue leading to a vicious cycle [89]. Furthermore, ER function has also been linked to inflammatory signalling. For example, under ER stress UPRs are activated causing the release of NF-κB from its inhibitor I-κB, allowing NF-κB to move towards the nucleus where it enables the expression of different inflammatory genes like the ones encoding for cytokines (e.g. IL-1 and TNF-α) [112]. TRAF2 complex can also be recruited from UPRs activating the inflammatory kinases JNK (c-jun N-terminal kinase) and IKK which

then phosphorylate and activate succeeding inflammatory mediators [112]. Fat tissue of obese individuals, especially the abdominally obese [45], compared to that of lean people have more proinflammatory proteins including TNF-α, IL-6, iNOS, TGF-β1, C-reactive protein (CRP), soluble ICAM and MCP-1, and procoagulant proteins (i.e. PAI-1, tissue factor, and factor VII) [46]. Additionally, adiponectin levels, a protective adipokine, are lowered in obesity, T2D and metS [43]. Consequently pro-inflammatory molecules in obese individuals have direct effects on cellular metabolism [46]. For example, TNF-α has been correlated with severe obesity and can directly decrease insulin sensitivity mediating IR [115] and vascular dysfunction in visceral obesity [43], as well as increase lipolysis and adipocytes. Furthermore, IL-6 leads to hypertriglyceridemia by stimulating lipolysis and hepatic TG secretion [46]. It was also found that patients with visceral adiposity have increased plasma levels of CRP, an inflammatory marker that can predict the risk of myocardial infarction and is thought to contribute to IR and altered glucose homeostasis [45]. Moreover, FFAs are significant in the connection of IR and chronic adipose inflammation [116].

Thus, obesity can involve a permanently increased state of OxS and low-grade chronic systemic inflammation by the interplay of ER and mitochondria ROS in adipose tissue and may be critical in the pathogenesis of IR seen in obesity [89].

B) Oxidative stress and insulin resistance

As mentioned above, IR can be a consequence of obesity and its pathogenesis has been associated with OxS. Furthermore, it is thought that excess ROS may cause IR [111] possibly by the activation of stress signalling pathways including the NF-κB pathway [105], which could negatively alter insulin signalling and participate in the development of IR, β-cell dysfunction and mitochondria dysfunction [117]. For example, impaired mitochondrial function, measured by oxidative capacity, was associated with greater IR in patients without T2D, therefore these individuals have a higher chance of developing pre-diabetes [118]. It must be noted that IR development occurred after mitochondrial impairment [118]. Another study infused rats with Angiotensin II (AngII) causing ROS overproduction and found this group to be insulin resistant [111]. Furthermore, OxS impaired the uptake of glucose in fat and muscle and reduced the secretion of insulin from pancreatic beta cells [108]. The integrity of mtDNA is also crucial in mitochondrial dysfunction and IR. This was demonstrated by mitochondrial dysfunction and the

increased production of mitochondrial ROS by palmitate-induced mtDNA damage causing impaired insulin signalling [65].

Although mechanisms of IR are not completely clear, Hotamisligil et al [112] were the first to discover that inflammation may drive IR. The increased concentrations of the pro-inflammatory cytokine TNF-α causing acute inflammation inhibits the phosphorylation of serine residues on insulin receptor substrate 1 (IRS1) leading to IR [119]. Studies also suggest that defects in insulin signalling could be linked to serine phosphorylation of IRS1 at serine-307 residue by activation of jun-*N*-terminal kinase 1 (JNK1), which is the first explanation of how inflammation and IR might be linked [120]. Furthermore, there is increasing evidence of causative relationship between inflammation and IR/T2D [116].

C) Oxidative stress and Hypertension

The pathogenesis of HT involves OxS in all layers of the vascular walls [88, 108] as well as decreased antioxidant enzyme activity [105]. Production of ROS in CV organs involves NADPH oxidases (i.e. the major ROS source in vessels), the mitochondrion, xanthine oxidase and sometimes nitric oxide synthases, which were shown to be activated in HT [88]. In pulmonary arterial HT, SOD, an important antioxidant that can be localized in the mitochondrion, was seen to be deficient due to hypermethylation and gene silencing leading to the increased production of ROS in the form of H_2O_2 [52]. Therefore, OxS may play a role in HT pathogenesis by changing methylation patterns in genes important in antioxidant action [52]. In view of this, OxS is crucial in HT and endothelial dysfunction development [105].

Additionally, pro-inflammatory molecules increased by ROS production accumulate in the vessels leading to an increase in plasma markers of inflammation in hypertensive individuals [88]. Obesity related HT is associated with pro-inflammatory pathways where increased Ang II, a peptide hormone that increases BP, can lead to endothelial damage through promotion of inflammatory processes [121]. For example, AngII can activate COX-2, a mitochondrial respiratory chain protein, promoting ROS and vasoactive prostaglandins, it can also trigger specific cytokine/chemokine production by the recruitment of infiltrating inflammatory cells into tissues [121].

D) Oxidative stress and dyslipidemia

OxS and inflammation have been associated with high LDL-c and/or TG and/or low levels of HDL-c, as seen in dyslipidemia [105]. Patients with familial combined hyperlipidemia, especially those with IR, exhibited high levels of OxS (i.e. oxidized GSH and 8-OHdG) compared to a control group [106]. It is therefore suggested that the increased prevalence of CHO metabolic disorders and CV disease incidence in hyperlipidemic patients may be due to increased oxidative damage [106]. Another study found that the presence of ROS production positively correlates with TGs in VLDLs or LDLs, in subjects with hyperlipidemia and these subjects displayed lower antioxidant activity [122]. 8-OHdG, a major product of DNA oxidation and a measure of OxS within the cell, was positively correlated with insulin and TG, whereas it was negatively correlated with HDL-c [123]. Therefore, evidence suggests that 2 pathways in which the mitochondrion plays a role, i.e. OxS and the inflammatory process, are involved in dyslipidemia.

Thus, the components of the metS have been associated with mitochondrial dysfunctions, particularly relating to elevated OxS and inflammatory processes.

4. cALL and metabolic complications

As mentioned previously, the interrelated risk factors that make up the metS are all atherogenic factors [124] and can all lead to vascular endothelial dysfunction, altered lipid profile and vascular inflammation [42]. Childhood cancer survivors, including cALL survivors, are known to be at elevated risk of developing the metS or its components that can further lead to premature CV outcomes if not treated [38, 125].

Kourti et al [126] studied a population of cALL survivors and found that only 6% of them had the metS, however 56% were affected by at least one of its components. Furthermore, the risk of development of these complications occurs early (i.e. average of 6 years since completion of cancer treatment) into their remission period [124]. The form of treatment can impact the manifestation of the metS. For example, studies found that those treated with cranial radiotherapy are especially at risk of developing components of the metS [124, 127]. The Childhood Cancer Survivor Study (CCSS), the largest cohort of childhood and adolescent

cancer survivors in the world, found that adult cancer survivors, including cALL survivors, displayed significant incidences of CV complications years after they were treated. Moreover, they had a seven-fold excess risk of chronic cardiac conditions compared to sibling controls [128], likely as a consequence of metS development. Furthermore, US survivors of cALL who make it to adulthood unfortunately have a 4-fold higher risk of CV disease mortality [38].

It should be noted that the average age of participants in these studies is young regarding the development of cardiometabolic complications. Therefore, timely recognition of metabolic risk factors in cALL survivors is crucial in preventing the development of CV disease in this population [126].

4.1 Obesity in cALL survivors

There is an increased frequency of overweightness (48%) even in the younger population (i.e. children and adolescent) of survivors of cALL [126]. In clinical cohorts where BMI was taken by objective measures rather than self-reports, obesity rates ranged from 31 to 43% for median ages of 22 and 32 years, respectively, which is higher than the general population for this age range [129]. cALL survivors having undergone CRT treatment have been associated with an accumulation of abdominal fat, especially visceral fat, and increased metabolic risk [41]. Moreover, a pattern of abdominal obesity was discovered, especially in women cALL survivors and those treated with chemotherapy [127].

4.2 Insulin resistance in cALL survivors

A study by Oeffinger et al [130] found that a population of young adult cALL survivors were significantly more likely to present IR compared to healthy individuals 10 years older than them regardless of gender and cancer therapy. Another study found that 31.4% of cALL survivors had a manifestation of fasting hyperglycaemia or were being treated for it and 49.9% had an abnormal HOMA-IR, predicting IR in an important portion of this population [38].

4.3 Dyslipidemia in cALL survivors

Dyslipidemia has been detected in adult survivors of cALL and as mentioned is another significant component of the metS. A pattern of dyslipidemia exists especially in women cALL

survivors and those treated with chemotherapy [127]. Small dense LDL-c (sd-LDL) are the more atherogenic subfraction and one study found that 36% of cALL survivors had at least 50% of sd-LDL [36]. These specific survivors were more likely to have the metS, low HDL-c and high TG levels [36]. Another study found that regardless of treatment therapy, visceral adiposity in cALL survivors was associated with sd-LDL [39]. Similarly, cALL survivors from another cohort presented risk factors of dyslipidemia, demonstrated by their high levels of LDL-c or TG (31.8%), low HDL-c (28.2%), or treatment of any of these (44.6%) [38]. A recent study that we performed at the Sainte-Justine UHC on a French-Canadian population of cALL, determined that 50% of survivors had dyslipidemia and 16% were borderline dyslipidemic. Overall, this was explained especially by low HDL-c levels, followed by high LDL-c and high TG [35].

4.4 Hypertension in cALL survivors

A large proportion of survivors of cALL are hypertensive compared to the National Healthy and Nutrition Examination Study (NHANES) of population norms [38]. Moreover, being a male and older in the cALL survivor group was predictive of HT and identified in 46.4% of survivors [38]. Gurney et al [127] studied a population of cALL survivors and found a significant increase in prevalence of HT in male cALL survivor subjects (29.7%) compared to males from the NHANES (23.9%). Another study observed an increased number of hypertensive children after completion of cALL treatment, compared to a normal population [131]. Similarly, the St Jude Lifetime Cohort Study (SJLIFE) of cALL survivors uncovered that survivors had increased odds of HT that were nearly doubled in those who received cranial radiotherapy (CRT) [132].

4.5 Cardiometabolic complications in connection to genetics, cancer and cancer treatments

It is important to understand the aetiology of the metS in cancer survivors, which may be different than the general population metS, to establish preventative and therapeutic actions. cALL treatments are toxic and can damage or interfere with organ systems bringing about changes in endocrine and metabolic functions that may develop into metS [12]. Endocrine disturbances can be due to damage to the hypothalamus-pituitary axis leading to deficiencies in

different hormones (e.g. growth hormone, thyroid hormone) that have been associated with the metS or its components [12]. cALL survivors treated with cranial, total body or abdominal radiation are at higher risk of late effects, including metS and its components, diabetes and hyperglycaemia, all precursors of CV diseases [12, 36]. Furthermore, treatments like anthracyclines, which are primarily responsible for cardiac-related outcomes can damage the myocardium and vascular structures or organ systems leading to cardiac complications (e.g. myocardial infarction, congestive cardiac insufficiency, pericarditis) in long term survivors of cALL [12, 31, 133]. Cardiac myocytes are damaged by the oxygen free radicals produced by anthracyclines, and left ventricle walls become thinner eventually increasing the stress in these walls and decreasing contractile function of the myocardium [133]. Anthracyclines induce cardiac stress in the form of OxS, that can trigger apoptosis and necrosis by mitochondrial pathways [134]. The risk of late adverse outcomes also depends on the source, dose, volume and fractionation of radiation, as well as gender and age of the patient at the time of treatment [40]. Studies on genetics have found associations between genes involved in lipoprotein metabolism, adipokines and inflammatory genes with metS development. Furthermore, genes linked to inflammation were implicated in the development of cardiometabolic complications [135].

Management of cardiometabolic complications includes lifestyle therapies such as weight reduction, increased physical activity and an antiatherogenic diet. Management can also include drug therapy to treat individual risk factors [44] in order to improve or evade the metS and therefore prevent CV complications and T2D development in this young population. Finding the cause or the mechanism of development of the metS or its components in this population would help identify those at risk and support the development of better management or treatment of complications.

Aside from the mitochondrion's involvement in the metS and its components, it also plays a key role in cancer itself. Therefore regardless of treatment-related mitochondrial dysfunctions, we cannot leave out the possibility that alterations in mitochondrial functions could possibly occur due to the cancer development.

5. Mitochondrial dysfunction in cancer

The discovery of aerobic glycolysis of cancer cells by Warburg, brought attention to the mitochondrion in tumour growth. However, he believed that this was due to damaged or dysfunctional mitochondria but we now know that many cancer cells depend on functional mitochondria to survive [56]. Furthermore, mitochondria are key players in tumourigenesis, expressing altered mitochondrial functions compared to normal cells. It has become evident that cancer pathogenesis arises through the resulting altered metabolism [67]. Cancer has been strongly associated with defects in the mitochondrial system, demonstrated in figure 17 (page 41), involving mtDNA mutations and deletions, and changes in nuclear-coded proteins having crucial roles in mitochondrial function [84].

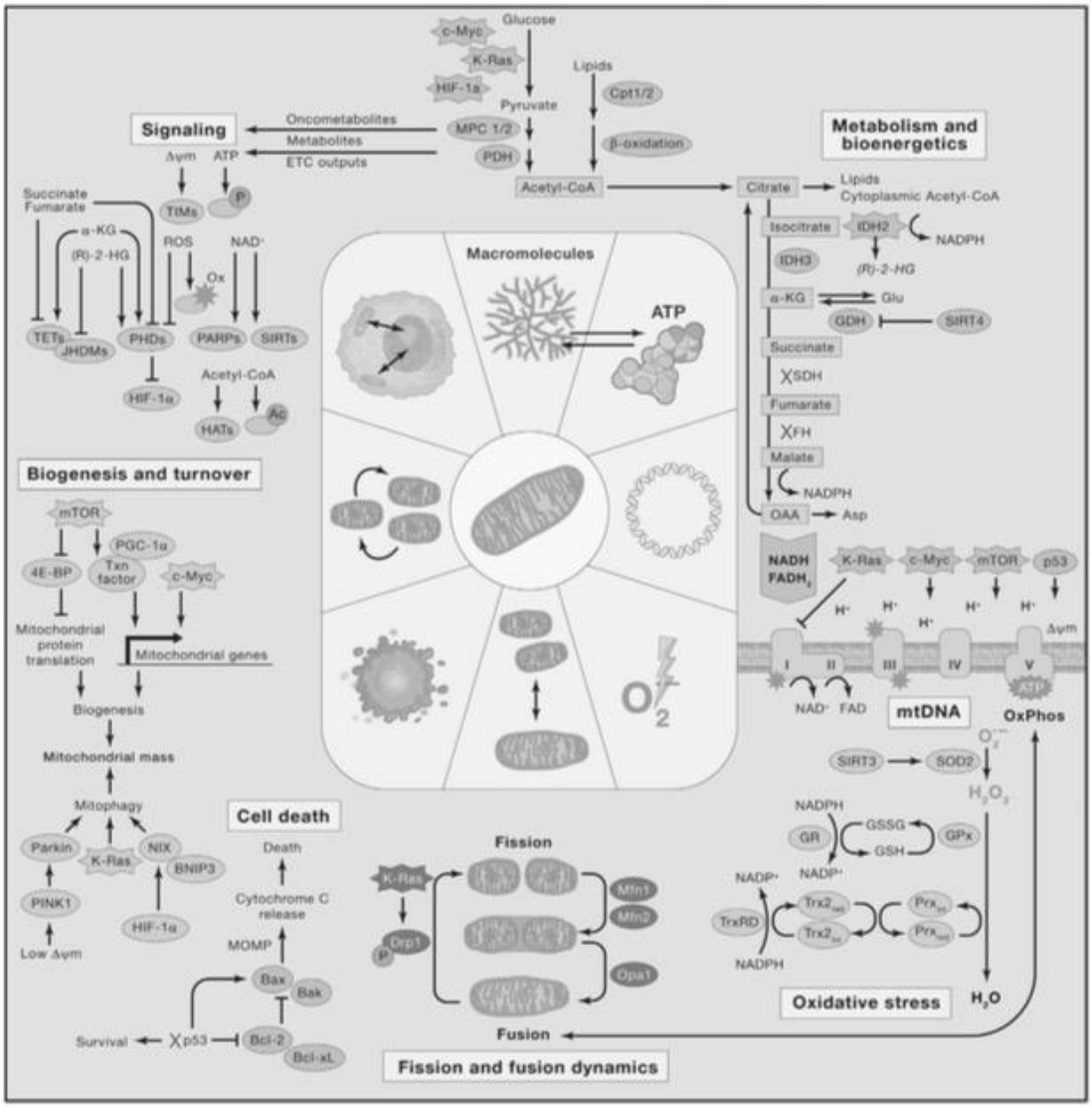

Figure 17. **Functions of mitochondria biology contributing to tumourigenesis.** These functions include fission and fusion dynamics, mitochondrial biogenesis and turnover, cell death, metabolism and bioenergetics, OxS regulation, signalling and mtDNA. Reproduced with permission [56].

5.1 Mitochondrial biogenesis and turnover in cancer

Mitochondrial biogenesis and turnover are essential in maintaining a healthy mitochondrial population and appear to be positive and negative regulators of tumourigenesis

[56]. In cancer, mitochondrial biogenesis can be controlled by its metabolic state, tumour heterogeneity, microenvironment, tissue type and tumour stage, whereas mitochondrial turnover requires mitophagy [56].

As previously mentioned, PGC1-α is the key regulator of mitochondrial biogenesis and does so by interacting with a number of transcription factors. PGC1-α has recently been shown to be important in the control of cancer development [136]. Some tumour cells increase PGC1-α expression leading to increased mitochondrial respiration, whereas other cancer cells use this protein as a tumour suppressor, initiating apoptosis [136]. Another protein involved in mitochondrial biogenesis is c-Myc, a transcription factor that globally regulates cell cycle, cell growth, metabolism and apoptosis pathways. Cancer cells can advantageously increase c-Myc causing amplified mitochondrial biogenesis, resulting in increased cellular biosynthetic and respiratory capacity [56]. In addition, mammalian target of rapamycin (mTOR), another mitochondrial protein involved in biogenesis, was found misregulated in cancer [56].

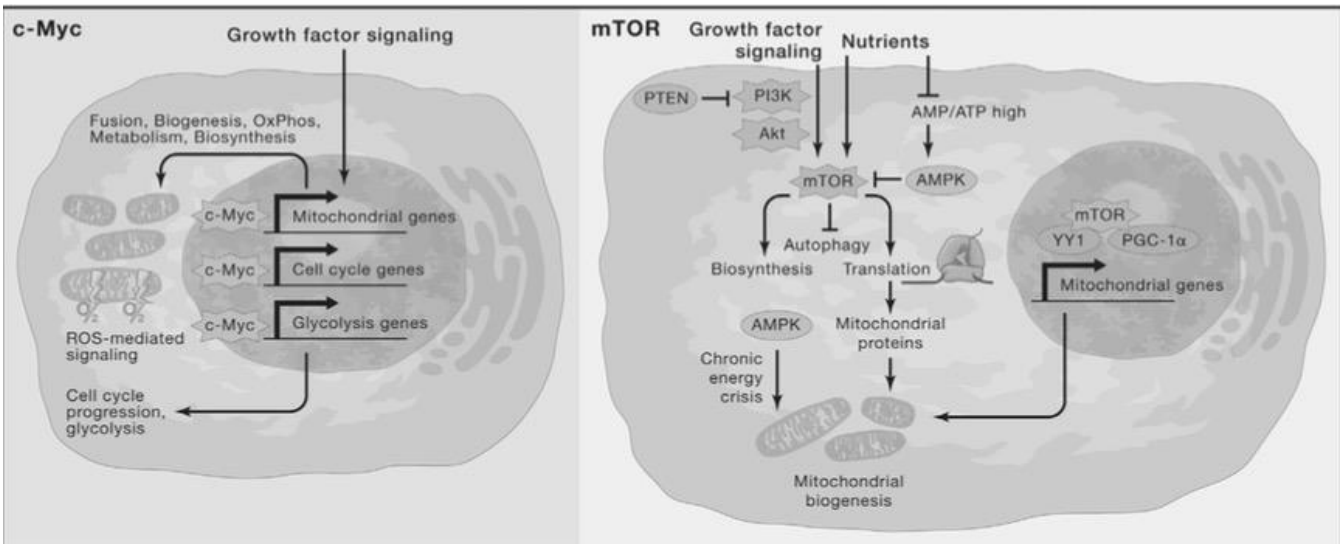

Figure 18. Mitochondrial biogenesis proteins c-Myc and mTOR in their oncogenic forms supporting rapid cell growth. Abbreviations: mTOR: mammalian target of rapamycin, PGC1-α: peroxisome proliferator-activated receptor gamma coactivator-1 alpha, YY1: Yin Yang 1, PTEN: phosphatase and tensin homolog, PI3K: phophoinositide 3-kinase, Akt: protein kinase

B, AMPK: 5'adenosine monophosphate-activated protein kinase, AMP: adenosine monophosphate, ATP: adenosine triphosphate. Reproduced with permission [56].

Unfortunately, regulators of mitochondrial biogenesis fundamental in normal cellular state are able to adapt to cancer treatments and tumour microenvironment, thereby giving cancer cells metabolic flexibility. This has a prominent impact on therapeutic outcomes [56].

Mitochondrial mitophagy, its selective autophagic pathway, is the process of clearing damaged mitochondria that could otherwise cause mitochondrial dysfunction. This process is important in maintaining a healthy mitochondrial population. When there is a lack of reducing equivalents (e.g. NADH, $FADH_2$), hypoxia or an impaired electron transport system, mitochondria are dysfunctional. This leads to mitochondrial membrane depolarization and activation of PTEN-induced kinase 1 (PINK1), which plays a role in mitophagy in cancer cells [56]. Additionally, mitophagy or mitochondrial turnover depends on the stage of the tumour and may allow for a threshold of mitochondrial dysfunction to persist resulting in increased tumour promotion, ROS generation, and other tumorigenic mitochondrial signals [56]. Therefore, cancer cells demonstrate reliability on mitochondrial function and respiration for survival and can adapt mitochondria functions to their advantage according to the present stress [56].

5.2 Mitochondria fission and fusion dynamics in cancer

Mitochondria have a close relationship between their structure and function and the balance of fission and fusion directs their morphology. In normal morphology, fission and fusion are balanced, on the other hand fragmentation or tubulation caused by their imbalance can result in pathological consequences [85]. In cancer studies, an imbalance of fission and fusion has been demonstrated, for example increased fission activity and/or decreased fusion results in a fragmented mitochondrial network [137]. Cancer cells therefore change their mitochondrial dynamics to resist apoptosis. In addition, they have the ability to adjust their bioenergetic needs to support the instalment of the tumour and properties related to transformation (e.g. proliferation, migration, therapeutic resistance) [137]. Hence, tumourigenesis places great importance on mitochondrial network remodelling [56].

5.3 Control of cell death in cancer

Recently, it has been indicated that cell proliferation, apoptosis and metabolism are interconnected and mitochondria are central to where these signals interconnect [67]. Defects in the apoptosis system can lead to the development of different human pathologies [138] and is one of the first cellular malfunctions seen in tumour growth and progression [84].

Apoptosis plays a key role in growth, immune surveillance, and neoplastic development. Evidently, the survival of cancer cells is due to their ability of escaping cell death by bypassing apoptotic signals [67]. Furthermore, they down-regulate pro-apoptotic Bcl2 genes and/or up-regulate anti-apoptotic Bcl2 genes to evade apoptosis [56]. Additionally, cancer cells exhibit a hyperactive glycolytic pathway, which can inhibit the OXPHOS pathway, thereby blocking energy production. This is linked to the resistance of apoptosis and therefore greater survival of cells [84]. In acute myeloid leukemia (AML), identified mutations and fusion proteins were seen to generate the progression of the disease and were implicated in anti-apoptotic signalling [138].

5.4 Oxidative stress in cancer

As discussed previously, the mitochondrion is a major contributor and production site of OxS in the form of ROS [67] and has antioxidant pathways to balance out ROS. Moreover, ROS production or the imbalance in ROS and antioxidants has been a cause of cancerous transformations [67, 139]. In cancer, antioxidant production is upregulated due to ROS production and is essential for the tumour to prevent ROS mediated cytotoxicity, thereby enhancing survival of the tumour [56]. The success of a tumour depends on its ability to create ROS and maintain them within a window to stimulate proliferation without causing cytotoxicity. Furthermore, ROS can damage DNA and the collection of DNA damage through incomplete repair or mispair can bring about mutagenesis and transformation especially when lacking a sufficient apoptotic pathway [139]. Oncogenes further produce ROS adding to the transformation of these cells and ROS levels quickly activate or modulate transcription factors such as Activating protein-1 (AP-1), a protein that has demonstrated importance in tumour progression and cellular transformation [139]. Additionally, the elevation of cell proliferation, survival and migration displayed increased levels of mitochondrial ROS [139].

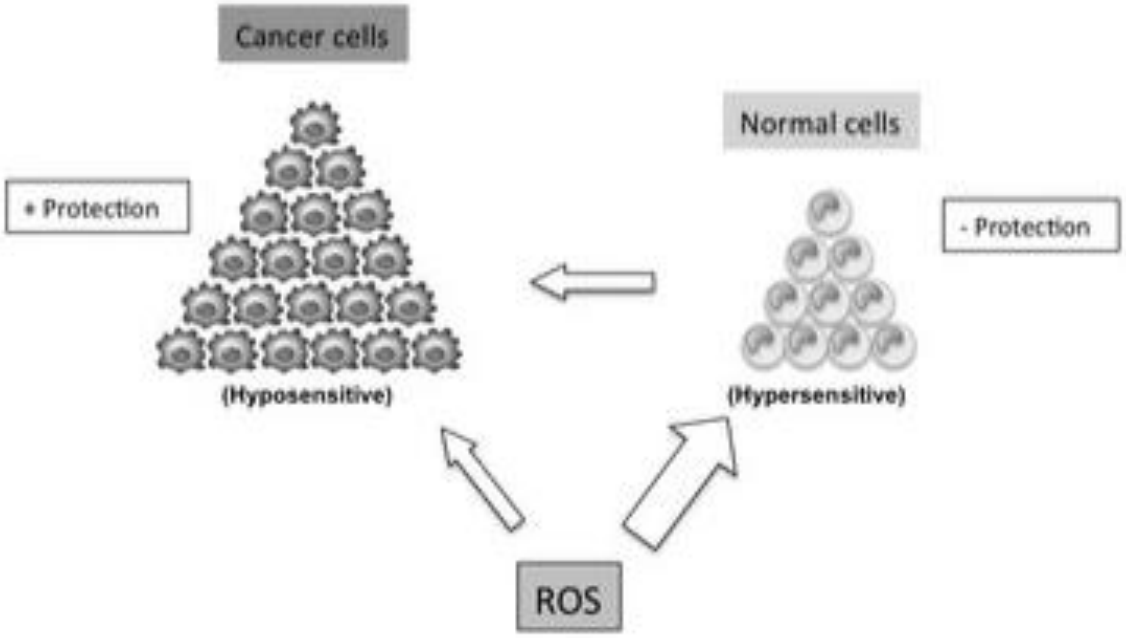

Figure 19. The sensitivity of normal cells compared to cancer cells in response to ROS. The upregulated antioxidant mechanisms (e.g. glutathione, SOD, catalase) in cancer cells protect them from reactive oxygen species (ROS), whereas normal cells are sensitive to ROS. Reproduced with permission [90].

5.5 Metabolic processes in cancer

One of the primary mechanisms of mitochondrial dysfunction leading to disease is the dysfunctional OXPHOS system [79]. A key survival mechanism of tumours is their proficiency to metabolically reprogram themselves subsequently supporting bioenergetic demand, synthesis of macromolecules and cell survival. Mitochondria are central to metabolic reactions and use different mechanisms to drive the reprogramming of tumour cells [56]. For example, the progress of AML is dependent on the mitochondrion's OXPHOS regulation, glutamine metabolism and FA metabolism [67]. In addition, cancer progression has been associated with mutations in isocitrate dehydrogenase (i.e. an enzyme involved in mitochondrial localized pathways) in AML cells [67]. Therefore, the interaction of signalling pathways, mitochondrial metabolism and communication with other parts of the cell are suspected to be significant for regulation of the development, maintenance and progression of this form of leukemia [67].

5.6 mtDNA mutations in cancer

mtDNA is in close proximity of ROS sources making it more susceptible to ROS-mediated oxidative damage, which can consequently lead to mtDNA mutations [140]. In addition, mtDNA mutations could be a result of defective replication and less efficient repair machinery [140]. Since mtDNA is essential in OXPHOS [79], the type and number of mtDNA mutations can impact different levels of the cells bioenergetics systems, for example cellular respiration, which is considered to be a trademark in cancer [140, 141]. Tumour cells use adaptation mechanisms to change mtDNA copy number, which has been correlated with different cancers, and mtDNA copy number can be altered during evolution of the tumour or as a response to cancer treatments [140]. Mutations in mtDNA alters the bioenergetics and metabolic state of the cell rather than inactivating mitochondrial energy metabolism [67] and may contribute to the tumourigenic phenotype of human malignancy [140]. Whatever the source of mtDNA mutations, an increased mutation rate can lead to the appearance of certain variants possibly resulting in a clonal advantage in the progression of cancer [140] because of changes in mitochondrial function and physiology.

A study looked at the blast cells of AML and found mtDNA to be amplified, a feature of the transformation of chronic granulocytic leukaemia (CGL) to acute leukaemia [142]. Furthermore, electron microscopy has confirmed the presence of circular dimers and catenated forms of mtDNA in acute leukemia [142] and previous studies on AML noted a presence of mtDNA with abnormal morphology [143]. Another study discovered disparity in the number of point mutations and deleted mtDNA between a group post cancer treatment compared to a control group [144]. Cancer treatments can produce high levels of ROS in the cell damaging mitochondrial proteins, DNA and components of the lipid membrane [125]. In consequence, this leads to a decreased number and smaller mitochondria with decreased oxidative capacity, revealing mitochondrial dysfunction [125].

6. Rational behind this study

Although cALL is the most prevalent childhood cancer, the 5-year survival is high for these patients because of the advances in treatments. However, this does not come without consequence, since an elevated proportion of cALL survivors present chronic health problems

later into their remission, either due to the cancer itself, treatments and/or the person's genetics. Health problems in the cALL population include components of the metS, including obesity, IR, HT and dyslipidemia. Question remains regarding what mechanisms are involved or responsible for the generation of metabolic complications after cancer and cancer treatment.

Advances in mitochondrial research has associated mitochondrial alterations with many diseases such as neurodegenerative, muscular, CV, malignant and metabolic diseases [61]. Moreover, treatment of cancer and cancer per se has been linked to changes in mitochondria and demonstrated mitochondrial dysfunction. For example, cancer and cancer treatment cause systemic inflammation, leading to metabolic disturbances that can persist even after exposure to treatment. In addition, a disruption in the balance of inflammatory signalling can promote pro-atherosclerotic signalling pathways [125]. Finally mitochondrial dysfunction involving increased ROS and inflammation has been associated with components of the metS, namely obesity, dyslipidemia, HT, and IR. To date, no research has examined mitochondrial dysfunction in association with cardiometabolic complications in the paediatric cancer survivor population.

7. Aim of this study

The main objective of this study is to identify factors implicated in cardiometabolic complications of cALL survivors by testing key mitochondrial functions in this population and by further analyzing their mitochondrial proteome. The aim of our study is to determine whether metabolic complications presented in childhood acute lymphoblastic leukemia survivors, who have all undergone cancer treatment, could be linked to mitochondrial changes or dysfunctions.

CHAPTER 2- ARTICLE

INSIGHT FROM MITOCHONDRIAL FUNCTIONS AND PROTEOMICS TO UNDERSTAND CARDIOMETABOLIC DISORDERS IN SURVIVORS OF ACUTE LYMPHOBLASTIC LEUKEMIA

Jade Leahy[1,2], Schohraya Spahis[1,2], Eric Bonneil[3], Carole Garofalo[1], Guy Grimard[4], Sophia Morel[1,2], Caroline Laverdière[1,4], Maja Krajinovic PhD[1,4], Simon Drouin[1], Edgard Delvin[1], Daniel Sinnett [1,4], Valérie Marcil [1,2], and Emile Levy[1,2*]

[1]Research Centre, CHU-Sainte-Justine, Departments of [2]Nutrition and [3]Paediatrics, Université de Montréal, Montreal, Quebec, Canada

[3]Proteomic Platform, IRIC Université de Montréal, Montreal, QC, Canada

Running Title: Mitochondrial impairment in childhood cancer survivors

Address for correspondence:
*Dr. Emile Levy
GI-Nutrition Unit
CHU Sainte-Justine
3175 Ste-Catherine Road, #4.17.005
Montreal, Quebec, Canada, H3T 1C5
Tel.:(514) 345-7783
E-mail: emile.levy@recherche-ste-Justine.qc.ca

ABBREVIATION LIST

Apo	Apolipoprotein
cALL	Childhood acute lymphoblastic leukemia
BMI	Body mass index
CRP	C-reactive protein
HDL-c	High-density lipoprotein-cholesterol
IR	Insulin resistance
LDL-c	Low-density lipoprotein-cholesterol
MDA	Malondialdehyde
MetS	Metabolic syndrome
SOD2	Superoxide dismutase 2
OxS	Oxidative stress
ROS	Reactive oxygen species
PBMC	Peripheral blood mononuclear cell
TC	Total cholesterol
TG	Triglycerides

Keywords: mitochondria, metabolic syndrome, proteomic, acute lymphoblastic leukemia, cancer, survivors.

ABSTRACT

Childhood acute lymphoblastic leukemia (cALL) is the most prevalent form of cancer in children. Due to advances in treatment and therapy, young cALL subjects now achieve a 90% survival rate. However, this tremendous advance does not come without consequence since ~2/3 of cALL survivors are affected by long-term and late, severe complications. Although the metabolic syndrome is a very serious sequel of cALL, the mechanisms remain undefined. It is also surprising to note that the mitochondrion, a central organelle in metabolic functions and the main cellular energy generator, has not been explored so far. Therefore, the primary objective of the present study was to determine whether cALL survivors exhibit impairments in their mitochondrial functions and proteomic profiling in relationship with metabolic disorders in cALL survivors compared to Controls. To this end, anthropometric measures, metabolic characteristics and lipid profiles were assessed, mitochondria isolated from peripheral blood mononuclear cells, and proteomic analyzed. Our data demonstrated that Unhealthy survivors exhibited several metabolic syndrome components (e.g. overweight, insulin resistance, dyslipidemia, inflammation) whereas Healthy cALL survivors resemble the Controls. In line with these abnormalities, functional experiments in these subjects revealed a significant decrease in the protein expression of mitochondrial antioxidant superoxide dismutase, PGC1-α transcription factor (a key modulator of mitochondrion biogenesis), and an increase in pro-apoptotic cytochrome c. Proteomic analysis of mitochondria by mass spectrometry revealed changes in the regulation of proteins related to inflammation, apoptosis, energy production, redox and antioxidant activity, fatty acid β-oxidation, protein transport and metabolism, and signalling pathways between groups. In summary, through the use of proteomic analysis, our work demonstrated a number of significant alterations in protein expression in mitochondria of cALL survivors, especially the Unhealthy group. Further investigation of these proteins may help delineate the mechanisms by which mitochondrial dysfunctions exert cardiometabolic derangements in cALL survivors.

INTRODUCTION

Childhood cancer accounts for less than 1% of all types of cancers diagnosed every year in Canada and remains the primary cause of death in the paediatric population [1]. Fortunately, the 5-year survival rate for childhood cancer is almost 85% as a result of cancer therapy advances [1]. Acute lymphoblastic leukemia (ALL) is the most prevalent childhood cancer, accounting for 26% of all cases of cancers in children aged 0-14 years [2]. Nonetheless, childhood ALL (cALL) has a promising 5-year survival rate of ~90% [1]. Despite this comforting prognosis, various factors such as toxic treatments, the cancer illness per se, and genetics may lead to late onset effects in some survivors [3]. Accordingly, The Childhood Cancer Survivor Study recognized that only ~37% of survivors had no chronic health conditions at least 5 years after diagnosis [4], which substantially increases the economic burden of the health care system. Childhood cancer survivors can develop severe life-threatening complications such as long-term cardiometabolic disorders, including diabetes due to the presence of the metabolic syndrome (MetS) components [i.e. obesity, insulin resistance (IR), hypertension and dyslipidemia] [5-11]. Although various studies confirmed the presence of late-onset metabolic derangements in the cALL survivor population, the mechanisms of action remain unclear, which makes it difficult to identify important molecular targets for secondary preventive measures and appropriate treatments. Surprisingly, even if abnormalities are reported in the MetS [12], no information is available about the mitochondrion status of cALL survivors. Nevertheless, these important organelles are central to metabolic functions as they represent the powerhouse and main energy generator of the cell [13]. Furthermore, the mitochondrion plays a significant role in cellular signalling pathways, including regulation of cell death by apoptosis, stress responses and inflammatory processes [13]. Moreover, chemical medications are known to be a major cause of mitochondrial damage [14] without omitting to underline that certain cancer therapies may conduct to late onset cardiometabolic derangements by harming mitochondrial functions [15]. To our knowledge, the mitochondrion has not been studied in cALL survivors in attempt to explain the appearance of cardiometabolic complications.

Proteomics is a large-scale analysis of the proteins in the organism allowing to globally determine their expressions, interactions and localizations [16]. Proteomic methods using mass spectrometry have become more sensitive, faster and more precise, which has shed important

light on the pathogenesis and pathophysiology of many complex disorders, and contributed to mitochondrial medicine advances [17]. The protein makeup of the mitochondrion is dynamic and crucial for their many functions [18]. The current estimate of the number of proteins is 1,100-1,900 in the mitochondrion [19], which are mostly encoded by nuclear genes and must be imported into the organelle by specialized systems [20]. As no previous studies focused on the relationship between metabolic perturbations and mitochondrial dysfunction in paediatric cancer survivors, the major aim of the present work was to determine whether cALL survivors exhibit impairments in their mitochondrial functions and alterations in their protein profile using proteomics analysis.

MATERIALS AND METHODS

STUDY POPULATION

The ALL survivors included in this study were enrolled between January 2012 and September 2014 as part of the PETALE program at the Sainte-Justine University Hospital Center (SJUHC) in Montreal. This cohort aims at determining biomarkers for the identification of the risks of developing late complications in cALL survivors. Eligible participants in this study were all of European-descent from the province of Quebec, over 19 years, and with at least 5 years remission. The cohort comprises participants who were event-free, had not suffered from refractory ALL, relapse or hematopoietic stem cell transplant ≥5 years since diagnosis [21]. This study was evaluated and approved by the SJUHC Institutional Ethic Committee Board and the interventions respected the Declaration of Helsinki. All participants and/or guardians gave written informed consent prior to participation.

Our study included 2 groups of survivors as either the most metabolically healthy (Healthy cALL survivors) or the most metabolically unhealthy (Unhealthy cALL survivors). Their clinical, anthropometric and biochemical data were collected. An age- and gender-matched healthy Control group was recruited for the reference values. Blood samples were collected in the morning from cALL survivors and the healthy Control group after an overnight fast.

CLINICAL, BIOCHEMICAL AND ANTHROPOMETRIC DATA

Each participant was measured for height, weight and waist circumference and Body mass index (BMI) was calculated. Systolic and diastolic blood pressure was determined using Hypertension Canada's guidelines [22]. Date of diagnosis was recorded in the patients' chart. Insulin, glucose, HOMA-IR, HOMA-beta, lipids-triglycerides (TG), total cholesterol (TC), high-density lipoprotein cholesterol (HDL-C), non-HDL-C, low-density lipoprotein cholesterol (LDL-C), and apolipoproteins (Apo) [B-100, AI, E, C2, and C3] concentrations were assessed as previously described [21]. C-reactive protein (CRP) was measured as a marker of inflammation by a commercial ELISA kit. This specific study evaluated the participants as being either Healthy or Unhealthy cALL survivors. Healthy cALL survivors did not present any metS components/risk factors (i.e. hypertension, obesity, dyslipidemia, glucose intolerance or IR) whereas Unhealthy cALL had at least one risk factor.

MITOCHONDRIAL ISOLATION

Peripheral blood mononuclear cell (PBMC) separation

Following blood collection in EDTA buffered collection tubes (1g EDTA/L), PBMCs were immediately isolated by differential centrifugation. Firstly, whole blood was centrifuged to separate plasma using low-speed J2-21M/E centrifuge (Beckman Coulter, Brea, California, USA) at 2,200 rpm at 4°C for 20 minutes. Plasma was removed and D-PBS 1X (Dulbecco's phosphate buffered saline 1X) (Wisent bioproducts, St-Bruno, Quebec, Canada) was mixed with leftover blood in a 3:1 ratio. PBMCs were isolated from whole blood by Ficoll-Hypaque density gradient centrifugation. Fifteen milliliters (ml) of Ficoll-Paque PLUS (GE Healthcare Life Sciences, Mississauga, Ontario, Canada) separating solution was added in 50 ml Sepmate-50 tube (Stemcell technologies, Vancouver, BC, Canada) and leftover blood in ice cold D-PBS was gently layered above Ficoll-hypaque. The Sepmate-50 tube was centrifuged in low-speed centrifuge at 2,500 rpm at 4°C for 10 minutes. Buffy coat was collected and resuspended in D-PBS 1X in a 50-ml tube, and contents were centrifuged at 2,200 rpm at 4° C for 10 minutes. The isolated PBMCs were washed once with 1ml of D-PBS and centrifuged (Quickspin centrifuge 5415C, Eppendorf) at 12,000 rpm at 4° C for 5 minutes. Supernatant was removed, precipitated and resuspended in 1 ml of sucrose EDTA. Contents were homogenized on ice 10 times up and down. A sample of 100µl of homogenized PBMC was frozen at -80°C and the remaining was used for mitochondrial isolation.

Mitochondrial isolation

Homogenate was transferred into 10.4 ml polycarbonate centrifuge bottle (Beckman, Palo Alto, CA, USA) and ultracentrifuged (LE-80 ultracentrifuge, Beckman) in a 70.1ti rotor at 3,300 rpm (750g) at 4 °C for 10 minutes. Precipitate (nucleus) was resuspended in 500µl of sucrose, homogenized and immediately stored at -80° C. Supernatant was transferred into 10.4 ml polycarbonate centrifuge bottle and ultracentrifuged at 10,500 rpm (7600g) at 4° C for 10 minutes. Supernatant (cytosol, microsome) was removed, and pelleted (purified) mitochondria were resuspended in 100cµl of ice cold D-PBS. All samples were immediately frozen at -80° C.

Sample preparation for proteomics

For mitochondrial proteomic analysis, 5 age- and gender-matched participants were selected from each group (i.e. Controls, Healthy and Unhealthy cALL survivors). Protein concentration of mitochondria was determined by the Bradford method using the Biorad protein assay dye reagent (USA), and 4 µg of each mitochondria sample was sent to the Institute for Research in

Immunology and Cancer proteomic platform (Université de Montréal, Canada) for proteomic analysis.

MASS SPECTROMETRY ANALYSIS AND PROTEIN QUANTITATION

Mass spectrometry analysis was carried out on 4 µg of purified mitochondria from chosen cALL survivor samples and Controls. Sample reduction was performed by adding 50 µl of 5mM TCEP in 100 mM ammonium bicarbonate to the dry sample. Alkylation was performed by adding 50 µl of chloroacetamide 20 mM with ammonium bicarbonate 100 mM. 1 µg of trypsin was added and the digestion was performed for 8 hours at 37°C. Samples were loaded and separated on a home-made C_{18} analytical column (15cm * 150µm i.d.) with a 116-min gradient from 0–30% acetonitrile (0.2% FA) and a 600 Nl/minute flow rate on an Easy nLC (Dionex) connected to a Q-Exactive HF (Thermo Fisher Scientific). Each full MS spectrum acquired with a 60,000-resolution was followed by up to 20 MS/MS spectra, where the 20 most abundant multiply charged ions were selected for MS/MS sequencing. Peptides were identified using Peaks 8.0 (Bioinformatics Solution Inc.) and peptide sequences were blasted against the Human Uniprot database. Tolerance was set at 10 ppm for precursor and 0.01 Da for fragment ions for protein identification and 7 ppm and 2 min for peptide alignment and profiling. For the post-translational modification of proteins, occurrence of carbamidomethylation (C), oxidation (M), deamidation (NQ) was considered. Volcano plots were made with Perseus 1.5.0.30.

WESTERN BLOTTING

Protein mass analysis was performed to compare expression of different proteins among cALL survivor groups and Controls. The protein concentrations of biological specimens (e.g. PBMC homogenate, nucleus and cytosol) were determined by the Bradford method using the Biorad protein assay dye reagent (USA), as mentioned above. The cell lysates of PBMC and samples of nucleus and cytosol were run on prepared SDS-PAGE gel (4-12%) and transferred to nitrocellulose membranes (GE Healthcare Life Sciences, Mississauga, Ontario, Canada) for standard western blotting. Non-specific binding sites were blocked with 0.75g of skimmed milk powder in 15 ml Tris-buffered saline-Tween (TBS-T) buffer for 1hour at room temperature. Immunoblotting of membranes was performed overnight at 4°C, incubating with primary antibodies in 2% milk. Specific primary antibodies included anti-Bcl2 (1:1000; Abcam, Cambridge, MA, USA), anti-cytochrome c (1:1000; Novus Biologicals, Littleton, CO,

USA), anti-NF-κB (1:1000; Santa Cruz, Dallas, TX, USA), anti-I-κB (1:1000; Cell Signaling Technology, Danvers, MA, USA), anti-Nrf2 (1:1000; Abcam, Cambridge, MA, USA), anti-Ogg1 (1:1000; Novus Biologicals, Littleton, CO, USA), anti-SOD2 (1:1000; Novus Biologicals, Littleton, CO, USA), anti-PGC1-α (1:1000; Abcam, Cambridge, MA, USA), anti-TNF-α (1:1000; R&D Systems, Minneapolis, MN, USA), and anti-Cox2 (1:1000; Novus Biologicals, Littleton, CO, USA). For the whole cell lysate, the expression of β-actin or GAPDH protein was determined to confirm equal loading using antibodies of β-actin (1:10000; Santa Cruz, Dallas, TX, USA) or GAPDH (1:10000; Abcam, Cambridge MA, USA). The membranes were then washed with TBS-T buffer and incubated with secondary antibodies: anti-rabbit (1:5000; BD Bioscience, Mississauga, ON, Canada), anti-goat (1:5000; Calbiochem, San Diego, CA, USA), and anti-mouse (1:4000; BD Bioscience, Mississauga, ON, Canada). Immunoreactive proteins were detected using Clarity Western ECL substrate & Clarity Max Western ECL substrate (Biorad, Hercules, CA, USA) on the ChemiDoc MP imaging system (Biorad, Hercules, CA, USA).

ATP ANALYSIS

Commercial enzyme linked immunosorbent assay (ELISA) kits were used to measure ATP and ADP/ATP expression (Bioluminescent Assay, BioAssay Systems, Hayward, CA, USA) and 8-hydroxydeoxyguanosine (8-OHdG) using the highly sensitive 8-OHdG kit (JaICA, Fukurol, Shi3zuoka, Japan) in isolated mitochondria of cALL survivor groups and Controls.

LIPID PEROXYDATION

Malondialdehyde (MDA) was measured in plasma samples as a marker of lipid peroxidation/oxidative stress (OxS). Briefly, proteins from plasma were precipitated with 8% sodium tungstate (Na_2WO_4). The protein-free supernatants were reacted with an equivalent volume of 0.5% (wt/vol) thiobarbituric acid solution at 95°C for 60 minutes. After cooling to room temperature, the pink chromagene [MDA-$(TBA)_2$] was extracted twice with 1-butanol and dried over a stream of nitrogen at 50°C for 3 hours. The dry extract was then resuspended in water before MDA determination using high performance liquid chromatography with UV/VIS detector at 535 nm. 25µL of purified sample were injected on a 4.6 mm i.d. x 150 mm Poroshell 2.7µm EC18 column using an Agilent 1260 Infinity HPLC system. The column was maintained at 25°C and eluted with a flow rate of 0.5 mL/minute. The mobile phase consisted of 98% solvent A (H_2O + 2 mM ammonium acetate) with linear increase of solvent

B (MeOH + 2 mM ammonium acetate) to 60% at 6 minutes and increasing up to 90% over the next minute before returning to initial composition.

STATISTICAL ANALYSIS

Continuous variables are expressed as means ± SEM, unless otherwise specified. Normality of the distributions was systematically tested before applying the appropriate tests. Differences in mitochondrial proteins between cALL survivor groups and Controls were assessed using unpaired Student's *t*-test or Mann-Whitney U tests depending on the normality of the distribution. A *P* value <0.05 was considered statistically significant. Statistical analysis was performed using GraphPad Prism Version 6.0.

RESULTS

A total of 78 participants were included in this study (42% male) with the following distribution: 26 Controls, 23 Healthy and 29 Unhealthy cALL survivors (**Table 1**). No differences were noted in the average age of all participants. Similarly, the average age at diagnosis was not significantly different between Healthy and Unhealthy cALL survivors. On the other hand, BMI and waist circumference were significantly higher in Unhealthy survivors compared to Controls and Healthy survivors, which influenced the combined data of the whole group of cALL survivors (**Table 1**). Unlike systolic BP, diastolic BP was statistically increased in Unhealthy compared to Healthy survivors (**Table 2**). Likewise, fasting insulin concentrations, HOMA-IR and HOMA-beta were significantly higher in Unhealthy survivors compared to Controls and Healthy survivors. Importantly, Unhealthy survivors exhibited low-grade inflammation given the elevated value of CRP, the clinically most relevant inflammatory marker (**Table 2**).

When plasma lipid components were analyzed, increased values of TG, TC and LDL-C characterized mostly the Unhealthy survivors (**Table 3**). The latter also displayed reduced values of HDL-C and TC/HDL-C ratio, a robust cardiovascular risk biomarker.

Overall, the anthropometric measures, metabolic characteristics and lipid profiles demonstrate that Unhealthy survivors had several MetS components whereas Healthy cALL survivors resemble the Controls.

ANALYSIS OF MITOCHONDRIAL FUNCTIONS

Energy production in cALL survivors

As mitochondria are energy-producing organelles (e.g. the ‘’powerhouse’’ center of the host cell) and given their direct link with cardiometabolic disorders, efforts were invested to isolate mitochondria from PBMC of cALL survivors and determine their ATP production. No significant differences were observed in ATP content or in the ADP/ATP ratio in Controls as well as Healthy and Unhealthy survivors (**Figure 1**).

Oxidative stress and antioxidant status of cALL survivors

In another series of experiments, we assessed lipid peroxidation since mitochondria constitute the principal source of OxS. The level of MDA, a robust marker of lipid peroxidation, was markedly raised in the entire group of cALL survivors compared to Controls (**Figure 2A**), without significant differences between Healthy and Unhealthy survivors (**Figure 2B**). We

also assessed 8-OHdG that results from OxS-mediated DNA damage. However, no variations were seen in 8-OHdG levels between Controls and cALL survivors (**Figure 2C**). Only a trend of 8-OHdG increase was shown in Unhealthy cALL survivors (**Figure 2D**). Accordingly, measurement of the protein expression of 8-oxoguanine DNA glycosylase (OGG1), the enzyme repairing oxidative DNA damage, did not differ among groups (**Figures 2E and 2F**). To explain the exaggerated MDA elevation in cALL survivors, we examined the protein expression of superoxide dismutase (SOD)2, one of the most powerful antioxidant enzymes located in mitochondria. The protein expression of this enzyme was significantly down regulated in mitochondria of cALL survivors (**Figure 2G**), without differences between Healthy and Unhealthy survivors (**Figure 2H**). To understand the mechanisms for SOD2 down regulation, we analyzed the protein expression of two strong transcription factors: Nrf2, a master regulator of antioxidant response, and PGC1-α, a key modulator of mitochondrion biogenesis and OxS. While there was no divergence in Nrf2 between Controls and cALL survivors (**Figure 2I**), a noticeable drop of PGC1-α expression was apparent in cALL survivors (**Figure 2K**).

Apoptosis in cALL survivors

Mitochondria play a crucial cellular role by functioning in the release of apoptotic proteins located in the inter-membrane space. The apoptotic process was stimulated in cALL survivors compared to Controls in view of the significant increase in the pro-apoptotic protein cytochrome c (**Figure 3A**) and the trend of decrease in the anti-apoptotic protein Bcl2 (**Figure 3C**). Comparison of Healthy and Unhealthy cALL survivors also showed a trend of increase in cytochrome c in Unhealthy cALL survivors (**Figure 3B**).

Inflammation in cALL survivors

Mitochondria are increasingly recognized as key regulators of immunity. To determine whether mitochondrial dysfunction is related to inflammation, we assessed the protein expression of inflammatory mediators. For example, COX-2 protein mass was not different among groups (**Figures 4A, 4B**). Similar results were obtained for TNF-α (**Figures 4C, 4D**) although a trend of increase characterized Unhealthy compared to Healthy cALL survivors (**Figure 4D**). Analysis of NF-κB by Western blot did not disclose any difference between cALL survivors and Controls, but surprisingly, the protein expression of this transcription factor was significantly reduced in Unhealthy compared to Healthy cALL survivors (Figure

4F) along with a trend of decrease noted in I-κB (**Figure 4G, 4H**) or even the NF-κB/I-κB ratio (**Figure 4I, 4J**) between groups.

MITOCHONDRIAL PROTEOME ANALYSIS

To further our understanding in the functions of mitochondria of cALL survivors, we performed proteomic analysis to unravel the protein variations between cALL survivors and Controls, and between Healthy and Unhealthy cALL survivors. Analysis of the total protein extract of mitochondria by SDS-PAGE revealed the presence of several bands that were consistently visible when stained with Coomassie Blue (**Figure 5**). A total of 957 proteins from these bands were identified using trypsin digestion followed by LC-MS/MS analysis and subsequent database searching (**Supplemental Table I**). Controls displayed a total of 722 mitochondrial proteins and cALL survivors exhibited a total of 859 (666 in the Healthy and 771 in the Unhealthy survivor group) with at least 2 peptides for each protein identified in each sample. Identification was done at a 95% confidence with FDR<1%.

Of the mitochondrial proteins identified overall, the majority originated from the cytoplasm (29%), followed by the nucleus (22%), plasma membrane (19%) and mitochondria (12%), whereas the remainder originated from other cell localizations (endoplasmic reticulum 4%, Golgi 5%, cytoskeleton 4%, lysosome 2%, vesicles 2%) as illustrated in **Figure 6A**. When the different groups were separated, slight differences were observed in the protein distribution with respect to specific localizations between the Controls and the whole cALL survivor group (**Figure 6B, 6C**). Similarly, small differences appeared in the distribution of proteins in accordance with localization between Healthy and Unhealthy cALL survivors (**Figure 6D, 6E**). However, these two survivor groups exhibited noticeable differences in the quantity of proteins originating from the nucleus: 160 and 41 proteins, respectively.

The identified proteins were then grouped together based on their functions/biological processes (**Figure 7A**) according to the Gene Ontology terms from the Uniprot KnowledgeBase. The majority of these proteins referred to structure development (17%), cell differentiation (13%), protein metabolism regulation (12%), signalling-regulation (12%), defense response (8%), oxidation-reduction (8%) and protein transport (7%), while the remaining (23%) are involved in other processes (i.e. oxoacid, carboxylic acid and coenzyme metabolism, metabolic response to lipid and nucleotide, protein localization to organelle). The

comparison of the distribution of functions between Controls (**Figure 7B)** and the whole group of cALL survivors (**Figure 7C**) or Healthy (**Figure 7D**) and Unhealthy cALL survivors (**Figure 7E**) did not reveal extensive differences. However, it should be noted that hundreds of mitochondrial proteins were identified and small % differences could actually account for many proteins.

Therefore, to better appreciate protein differences among the groups, the chromatogram precursor ion was quantified by area under the curve, a label-free technique, since the quantity of a protein in a sample is known to correlate well with the area under the curve of its peptide [23]. **Figure 8** illustrates the volcano plots representing the magnitude of change (log_2 fold change) on the x-axis, as well as the statistical significance (-log10(*p*-value)) on the y-axis, indicating the observation reproducibility. If the protein expression was at least half or double the Control group, thereby corresponding to the values <-1 or >1 on the x-axis, it was considered to have a potential clinical significance. Noteworthy, a value >1 on the y-axis represents a significant p-value of <0.05. In **Figure 8**, the proteins labelled with numbers represent proteins that were significantly, differentially expressed between the 2 groups of interest, e.g. Controls and the whole group of cALL survivors. The plot unravelled numerous changes in protein expression, whether up- or down-regulated, between the two groups. **Figure 8 A-D** displays each volcano plot with its associated summary list of the significant changes in protein expression organized by the related functions of these identified proteins. Additionally, to clearly highlight the differential proteins indicated by the volcano plots among the groups, they were summarized in **Supplemental Table II,** according to the category of protein function. These functions include inflammation, apoptosis and cell cycle, ATP, redox and antioxidant activity, FA beta-oxidation, protein transport and metabolism, and signalling pathways.

To point out, Healthy cALL survivors compared to Unhealthy cALL survivors had significantly decreased expression of 2 proteins involved in inflammatory processes, *Alpha-1-acid glycoprotein 1* and *Leukotriene A-4 hydrolase*. Another interesting finding was the differences in the expression of proteins involved in apoptosis between Controls and cALL survivors. We identified significantly increased expression of the anti-apoptotic protein *Serine/threonine-protein kinase PAK2* in Controls compared to the whole survivor group. This significance was mainly a result of the significant increase in expression of this protein in

Controls compared to the Unhealthy cALL survivor group. Four pro-apoptotic proteins (*Galectin-1, L-lactate dehydrogenase A chain, GDGSH iron-sulfur domain-containing protein 2, Isoform 5 of unconventional myosin-XVIIIa*) were down regulated in Controls compared to cALL survivors, where *Galectin-1* was also significantly down regulated in Controls compared to the Unhealthy cALL survivor group. In addition, proteins involved in energy processes have been identified with significantly different expressions between groups. The protein *ATPase inhibitor* was significantly up regulated in Controls compared to cALL survivors. Similarly, *ATP synthase subunit epsilon* was significantly up regulated in Controls compared to survivors, while the expression of *ATP synthase subunit delta* was significantly increased in both Control and Healthy cALL survivor groups compared to the Unhealthy cALL survivor group. Two stress related proteins, *Stress-induced-phosphoprotein 1* and *Amine oxidase [flavin-containing] B,* were down regulated in Controls compared cALL survivors and Unhealthy cALL survivors, respectively. Finally, the expression of the antioxidant protein *Catalase* was significantly different between Controls and cALL survivors.

DISCUSSION

Since mitochondria are crucial in metabolic functioning, our study was designed in attempt to determine whether they are implicated in the development of cardiometabolic complications in a population of paediatric cancer survivors. Our study has confirmed the assumption that a large number of cALL survivors had an increased risk of metabolic and cardiovascular diseases given their high levels of BMI, IR, low-grade inflammation, dyslipidemia and hypertension, all known as components of the MetS. When mitochondria were isolated from PBMC of cALL survivors, they exhibited raised lipid peroxidation, weak antioxidant defense, reduced expression of the PGC1-α transcription factor, a robust modulator of mitochondrion biogenesis and OxS, and increased protein expression of the pro-apoptotic cytochrome c. In addition, proteomics analysis revealed differences in mitochondrial protein content and subcellular profiling. Moreover, this state-of-the-art technique identified 69 differentially expressed proteins between Controls, Unhealthy cALL survivors and/or Healthy cALL survivors, indicating changes in the regulation of mitochondrial processes such as inflammation, apoptosis and cell cycle, energy metabolism, oxidoreduction, fatty acid β-oxidation, protein transport and metabolism, and signalling pathways.

The first step of this interesting work was to identify late cardiometabolic risk factors in cALL survivors selected from a unique cohort given its homogeneous French Canadian origin and its established genetic founder effect. A large proportion of subjects presented MetS components, including overweightness, IR, dyslipidemia and hypertension. This is consistent with our study that highlighted the relationship between metabolic abnormalities and lipid/lipoprotein disorders, factors predisposing to the development of atherosclerosis [11]. So far, there have been no clinical trials done in the cALL population to treat the MetS or its components, which is likely due to the limited knowledge of the etiology.

In a second step, we examined whether significantly functional derangements were present in mitochondria isolated from PBMC of Healthy and Unhealthy cALL survivors compared to Controls. Mitochondria are essential in maintaining normal structure, function and survival of organ tissues, and there is considerable evidence that their dysfunction leads to severe metabolic complications (e.g. IR, obesity, diabetes, MetS) [16, 24, 25]. Mitochondria are not only considered as the cellular powerhouse, but also as the key regulators of metabolic pathways [14] in view of their multiple functions, including apoptosis, antioxidant and

reactive oxygen species (ROS) signalling, calcium homeostasis, cell differentiation and inflammatory processes [13]. They are both the primary source and target of ROS within the cell, and their dysfunction is emerging as an important determinant of human metabolic health [12, 26]. Although many investigators depicted the association of mitochondrial dysfunction and oxidative damage with the MetS, diabetes and cardiovascular diseases [26-30], as well as in the progression of cancers [31, 32], rare are the studies that focused on specific mitochondrion perturbations in cardiometabolic disorders characterizing cancer survivors. Our findings underlined that PBMC mitochondria of cALL survivors generate lipid peroxidation marked by their increase in MDA and are equipped with weak antioxidant defense in view of the substantial decline of SOD2, which is central for mitochondrial signalling [33]. SOD2 is highly effective in eliminating superoxide and to counteract apoptosis via the tight control of H2O2, the primary ROS signalling [33]. In fact, our experiments revealed elevated levels of the pro-apoptotic factor cytochrome c. To delineate the mechanisms, we analyzed the protein expression of crucial transcription factors and found reduced level of PGC1α mass in cALL survivors. Noteworthy, PGC1α is known to be the primary regulator of the mitochondrial biogenesis pathway, as well as mitochondrial antioxidant defense and function [34]. Even if alterations were noted in other mitochondrial functions, the tiny mitochondrial amounts isolated from limited blood sampling did not allow us to repeat the experiments, validate the trends and to confirm the results by attaining statistical significance.

The third step called for a more strategic and sophisticated experimental approach, and we therefore undertook a thorough mass spectrometry-based proteomics analysis, which generally enables the identification and quantification of thousands of proteins in biological samples while facilitating the development of biomarkers for early diagnosis, thereby contributing to a more effective patient management. It is also worth mentioning that previous studies showed that the proteomics technique is a very convenient and efficient tool for examining the complexity and dynamics of mitochondria under pathological states [18]. Hence, our hypothesis was alterations in mitochondrial proteomic profiling may be indicative of mitochondrial dysfunction in association with cardiometabolic complications in cALL survivors. Even if a few investigations reported mitochondrial dysfunction in cancer development and progression, we are to our knowledge the first group to study mitochondrial

proteomics in relation to metabolic complications in paediatric cancer, and especially, ALL survivors.

Using LC-MS/MS, we identified a total of 957 proteins with 247 (26%) proteins only identified in one sample. A total number of 722 (75%) of all identified proteins characterized the Control group, whereas 859 (90%) were present in cALL survivors. With a focus on cALL, we could identify 666 (70%) proteins in Healthy and 771 (81%) in Unhealthy survivors. Although mitochondrial protein content varies depending on cell type and state [19], all our mitochondrial samples were isolated from the same cell type, e.g. PBMC. Therefore, variations in mitochondrial protein content in our studies may be due to the trafficking of proteins from mitochondria and subcellular organelles or because the subject conditions.

Of the proteins identified, 69 were found to be differentially and significantly expressed among our different groups as shown in **Supplemental Table II.** These proteins are involved in key mitochondrial processes such as inflammation, apoptosis and cell cycle, energy metabolism, oxidoreduction, fatty acid β-oxidation, protein transport and metabolism, and signalling. Interestingly, we identified 2 inflammatory proteins, *Alpha-1-acid glycoprotein 1* and *Leukotriene A-4 hydrolase*, with significantly down-regulated expression in Healthy survivors compared to Unhealthy survivors. Accordingly, the Unhealthy cALL survivors had an increased inflammatory profile marked by their higher serum CRP levels compared to healthy survivors (P=0.0004).

When mitochondria are dysfunctional or damaged, the apoptosis process is able to eliminate the host cells by inducing pro-apoptotic proteins [35]. Accordingly, *Serine/threonine-protein kinase PAK 2,* a protein suppressing apoptosis was up regulated in Controls versus Survivors. Furthermore 4 proteins (*Galectin-1, Isoform 5 of Unconventional myosin-XVIIIa, L-lactate dehydrogenase A chain, CDGSH iron-sulfur domain-containing protein 2*) with pro-apoptotic functions were significantly down regulated in Controls compared to cALL survivors, thereby indicating high apoptosis potency in cALL survivors. In line with these data, our functional experiments demonstrated elevated apoptosis in cALL survivors compared to Controls, as reflected by the marked increase in the pro-apoptotic cytochrome c expression. Interestingly, *Galectin-1* expression was increased in cALL survivors compared to Controls. Previous

studies reported an increase in *Galectin-1* levels in the left ventricle and plasma during early ischemic periods in a mouse model within 4 hours of myocardial infarction [36].

Proteomic analysis allowed us to further explore energy production capacity contrary to our functional experiments that required a lot of mitochondrial material in which we were limited. We were able to identify 3 proteins (*ATPase inhibitor mitochondrial, ATP synthase subunit epsilon mitochondrial*, *ATP synthase subunit delta mitochondrial)* involved in ATP synthesis and metabolism, which were up regulated in the Controls compared to the cALL survivor group. Furthermore, *ATP synthase subunit delta mitochondrial* was also up regulated in Healthy compared to Unhealthy cALL survivors. Therefore, these interesting data suggest a decrease in the expression of proteins involved in energy metabolism in cALL survivors, especially in the Unhealthy group. This is in agreement with diabetes and IR studies, which reported a decline in ATP synthase subunits in the pathological groups compared to Controls [37, 38]. Another study on contractile dysfunction discovered decreased ATP synthase D chain in the hearts of diabetic mice [39].

OxS plays a fundamental role in the pathogenesis and development of cardiometabolic complications [40-44]. In our proteomic experiments, *Stress-induced-phosphoprotein 1* and *Amine oxidase [flavin-containing] B*, which represent proteins able to initiate a stress response, were down-regulated in the Control group compared to Unhealthy cALL survivors. These findings are in line with the MDA data and indicate that mitochondria from Unhealthy survivors may elicit ROS production.

CONCLUSION

In conclusion, we have detected significant differences in the metabolic profile of cALL survivors, which allowed the distinction between metabolically Healthy and Unhealthy cALL survivors. In the light of our functional and proteomic studies, it appears that mitochondria of cALL survivors, especially the Unhealthy group, display various abnormalities in various pathways, which may be accountable for their metabolic disorders in this population. More studies are certainly needed to confirm and extend these findings in order to delineate the mechanisms and establish therapeutic strategies targeting mitochondria. Identification of potential biomarkers may help designate cALL survivors at risk of developing metabolic complications as a consequence of the nature of their illness or cancer treatments.

GRANT SUPPORT

This work was supported by a grant from the Institute of Cancer Research of the Canadian Institutes of Health Research, in collaboration with C17 Council, Canadian Cancer Society, Cancer Research Society, Garron Family Cancer Centre at the Hospital for Sick Children, Ontario Institute for Cancer Research, and the J.A. DeSeve Research Chair in Nutrition.

Table 1: Anthropometric data of Controls and cALL participants

	CONTROLS	ALL SURVIVORS		
		Whole group	Healthy survivors	Unhealthy survivors
Total	*n=26*	*n=52*	*n=23*	*n=29*
Gender (male)	8	25	11	14
Age (y)	23.73 ±0.96	24.16 ±0.84	22.59 ±1.30	25.40 ±1.06
Age at diagnosis (y)	ND	6.90±0.68	6.04±1.06	7.58±0.88
Weight (kg)	65.98 ±2.38	68.92 ±2.26	59.97 ±2.35	76.01 ±3.04$^{*, c}$
Height (m)	1.72 ±0.02	1.66 ±0.01*	1.65 ±0.02*	1.67 ±0.02
BMI (kg/m^2)	22.25 ±0.47	24.85 ±0.65**	21.98 ±0.70	27.13 ±0.81$^{***, c}$
WC (cm)	77.72 ±1.71	87.17 ±1.95**	78.50 ±2.00	94.24 ±2.40$^{***, c}$

Anthropometric characteristics were collected from cALL survivors (n=52) and Controls (n=26). Data are expressed as mean ±SEM. BMI: body mass index, WC: waist circumference, ND: not determined. *P<0.05, **P<0.01, ***P<0.001 vs Controls. ^{c}P<0.001 vs Healthy survivors.

Table 2: Biochemical and clinical characterization of Controls and cALL participants

	CONTROLS	ALL SURVIVORS		
		Whole group	Healthy survivors	Unhealthy survivors
Systolic BP (mmHg)	ND	116.90 ±1.86	114.00 ±2.79	119.10 ±2.46
Diastolic BP (mmHg)	ND	70.29 ±1.29	67.09 ±1.98	72.72 ±1.58[b]
Glucose (mmol/L)	4.98 ±0.07	5.00 ±0.11	4.91 ±0.12	5.08 ±0.18
Insulin (pmol/L)	45.22 ±3.70	77.57 ±15.32[*]	48.38 ±5.10	100.50 ±26.47[**, b]
HOMA-IR	1.82±0.15	2.88 ±0.79	1.54 ±0.17	3.93 ±1.38[b]
HOMA-beta	ND	157.30 ±35.84	171.80 ±79.22	145.90 ±17.79[a]
CRP (pmol/ml)	ND	2.74 ±0.58	1.37 ±0.56	3.73 ±0.87[c]

Biochemical and clinical variables of cALL survivor subgroups and Controls were determined. HOMA-IR was calculated using the formula: [fasting insulin (mU/mL) × fasting glucose (mmol/L)]/22.5. Data are expressed as mean ±SEM.
BP: blood pressure, HOMA-IR: Homeostatic model assessment - insulin resistance, HOMA-beta: Homeostatic model assessment- beta cell function, CRP: C-reactive protein, ND: not determined. [*]P<0.05, [**]P<0.01 vs Controls. [a]P<0.05, [b]P<0.01, [c]P<0.001 vs Healthy survivors.

Table 3: Lipid profile of study participants

	CONTROLS	ALL SURVIVORS		
		Whole group	Healthy survivors	Unhealthy survivors
TG (mmol/L)	1.00 ± 0.06	1.02 ± 0.08	0.83 ± 0.11**	1.18 ± 0.11^{b}
TC (mmol/L)	4.45 ± 0.10	4.55 ± 0.13	4.15 ± 0.19	4.87 ± 0.15$^{*, b}$
LDL-C (mmol/L)	2.51 ± 0.10	2.78 ± 0.11	2.42 ± 0.10	3.06 ± 0.15$^{***, c}$
HDL-C (mmol/L)	1.50 ± 0.05	1.32 ± 0.05**	1.46 ± 0.08	1.20 ± 0.04$^{***, c}$
TC/HDL-C	3.05 ± 0.12	3.65 ± 0.13**	3.00 ± 0.14	4.16 ± 0.16$^{***, c}$
Non-HDL-C (mmol/L)	2.96 ± 0.10	3.28 ± 0.11	2.80 ± 0.12	3.67 ± 0.14$^{***, c}$
Apo-AI (mg/ml)	2.62 ± 0.09	2.40 ± 0.10	2.42 ± 0.11	2.38 ± 0.20
Apo B-100 (g/L)	0.70 ± 0.02	0.89 ± 0.04**	0.92 ± 0.05**	0.84 ± 0.07
Apo E (ug/ml)	35.19 ± 0.94	33.18 ± 1.69	30.07 ± 1.53	37.40 ± 3.04
Apo C2 (ug/ml)	126.37 ± 14.83	127.79 ± 7.46	125.15 ± 8.74	131.39 ± 13.43
Apo C3 (ug/ml)	77.96 ± 3.47	84.68 ± 17.66	89.27 ± 28.91	77.80 ± 10.92
Apo B 100/TG	0.81 ± 0.05	1.09 ± 0.15	1.40 ± 0.22*	0.69 ± 0.13^{a}
Apo B 100/Apo AI	0.28 ± 0.01	0.38 ± 0.02**	0.39 ± 0.02*	0.38 ± 0.05*
Apo C2/Apo C3	1.64 ± 0.18	2.52 ± 0.47	3.01 ± 0.76	1.78 ± 0.20

The lipid profile of cALL survivor subgroups and Controls were characterized. Data are expressed as mean ±SEM. TG: triglycerides, TC: total cholesterol, LDL-C: low-density lipoprotein cholesterol, HDL-C: high-density lipoprotein cholesterol, Apo: apolipoprotein. *P<0.05, **P<0.01, ***P<0.001 vs Controls. ^{a}P<0.05, ^{b}P<0.01, ^{c}P<0.001 vs Healthy survivors.

REFERENCES

1. Statistics, C.C.S.s.A.C.o.C., *Canadian Cancer Statistics 2017* 2017, Canadian Cancer Society Toronto, ON.
2. Ward, E., et al., *Childhood and adolescent cancer statistics, 2014.* CA Cancer J Clin, 2014. **64**(2): p. 83-103.
3. Apostolidou, E., et al., *Treatment of acute lymphoblastic leukaemia : a new era.* Drugs, 2007. **67**(15): p. 2153-71.
4. Oeffinger, K.C., et al., *Chronic health conditions in adult survivors of childhood cancer.* N Engl J Med, 2006. **355**(15): p. 1572-82.
5. Meacham, L.R., et al., *Cardiovascular risk factors in adult survivors of pediatric cancer--a report from the childhood cancer survivor study.* Cancer Epidemiol Biomarkers Prev, 2010. **19**(1): p. 170-81.
6. Gurney, J.G., et al., *Metabolic syndrome and growth hormone deficiency in adult survivors of childhood acute lymphoblastic leukemia.* Cancer, 2006. **107**(6): p. 1303-12.
7. Oeffinger, K.C., et al., *Cardiovascular risk factors in young adult survivors of childhood acute lymphoblastic leukemia.* J Pediatr Hematol Oncol, 2001. **23**(7): p. 424-30.
8. Oeffinger, K.C., et al., *Insulin resistance and risk factors for cardiovascular disease in young adult survivors of childhood acute lymphoblastic leukemia.* J Clin Oncol, 2009. **27**(22): p. 3698-704.
9. Janiszewski, P.M., et al., *Abdominal obesity, liver fat, and muscle composition in survivors of childhood acute lymphoblastic leukemia.* J Clin Endocrinol Metab, 2007. **92**(10): p. 3816-21.
10. Malhotra, J., et al., *Atherogenic low density lipoprotein phenotype in long-term survivors of childhood acute lymphoblastic leukemia.* J Lipid Res, 2012. **53**(12): p. 2747-54.
11. Morel, S., et al., *Lipid and lipoprotein abnormalities in acute lymphoblastic leukemia survivors.* J Lipid Res, 2017. **58**(5): p. 982-993.
12. Lyakhovich, A., et al., *Mitochondrial dysfunction in DDR-related cancer predisposition syndromes.* Biochim Biophys Acta, 2016. **1865**(2): p. 184-9.
13. Chandel, N.S., *Mitochondria as signaling organelles.* BMC Biol, 2014. **12**: p. 34.
14. Neustadt, J. and S.R. Pieczenik, *Medication-induced mitochondrial damage and disease.* Mol Nutr Food Res, 2008. **52**(7): p. 780-8.
15. Aleman, B.M., et al., *Cardiovascular disease after cancer therapy.* EJC Suppl, 2014. **12**(1): p. 18-28.
16. Jiang, Y. and X. Wang, *Comparative mitochondrial proteomics: perspective in human diseases.* J Hematol Oncol, 2012. **5**: p. 11.
17. Calvo, S.E. and V.K. Mootha, *The mitochondrial proteome and human disease.* Annu Rev Genomics Hum Genet, 2010. **11**: p. 25-44.
18. Eremina, L., et al., *Proteomics of mammalian mitochondria in health and malignancy: From protein identification to function.* Anal Biochem, 2017.
19. Palmfeldt, J. and P. Bross, *Proteomics of human mitochondria.* Mitochondrion, 2016.

20. Neupert, W. and J.M. Herrmann, *Translocation of proteins into mitochondria.* Annu Rev Biochem, 2007. **76**: p. 723-49.
21. Marcoux, S., et al., *The PETALE study: Late adverse effects and biomarkers in childhood acute lymphoblastic leukemia survivors.* Pediatr Blood Cancer, 2017. **64**(6).
22. Leung, A.A., et al., *Hypertension Canada's 2016 Canadian Hypertension Education Program Guidelines for Blood Pressure Measurement, Diagnosis, Assessment of Risk, Prevention, and Treatment of Hypertension.* Can J Cardiol, 2016. **32**(5): p. 569-88.
23. Zhang, G., et al., *Protein quantitation using mass spectrometry.* Methods Mol Biol, 2010. **673**: p. 211-22.
24. Aroor, A.R., et al., *Mitochondria and Oxidative Stress in the Cardiorenal Metabolic Syndrome.* Cardiorenal Medicine, 2012. **2**(2): p. 87-109.
25. Pieczenik, S.R. and J. Neustadt, *Mitochondrial dysfunction and molecular pathways of disease.* Exp Mol Pathol, 2007. **83**(1): p. 84-92.
26. Green, K., M.D. Brand, and M.P. Murphy, *Prevention of mitochondrial oxidative damage as a therapeutic strategy in diabetes.* Diabetes, 2004. **53 Suppl 1**: p. S110-8.
27. Fosslien, E., *Mitochondrial medicine--molecular pathology of defective oxidative phosphorylation.* Ann Clin Lab Sci, 2001. **31**(1): p. 25-67.
28. Bunkar, N., et al., *Mitochondrial anomalies: driver to age associated degenerative human ailments.* Front Biosci (Landmark Ed), 2016. **21**: p. 769-93.
29. Schrauwen, P. and M.K. Hesselink, *Oxidative capacity, lipotoxicity, and mitochondrial damage in type 2 diabetes.* Diabetes, 2004. **53**(6): p. 1412-7.
30. Abdul-Ghani, M.A. and R.A. DeFronzo, *Mitochondrial dysfunction, insulin resistance, and type 2 diabetes mellitus.* Curr Diab Rep, 2008. **8**(3): p. 173-8.
31. Basak, N.P. and S. Banerjee, *Mitochondrial dependency in progression of acute myeloid leukemia.* Mitochondrion, 2015. **21**: p. 41-8.
32. Vyas, S., E. Zaganjor, and M.C. Haigis, *Mitochondria and Cancer.* Cell, 2016. **166**(3): p. 555-66.
33. Schieber, M. and N.S. Chandel, *ROS function in redox signaling and oxidative stress.* Curr Biol, 2014. **24**(10): p. R453-62.
34. Jornayvaz, F.R. and G.I. Shulman, *Regulation of mitochondrial biogenesis.* Essays Biochem, 2010. **47**: p. 69-84.
35. Gregersen, N., J. Hansen, and J. Palmfeldt, *Mitochondrial proteomics--a tool for the study of metabolic disorders.* J Inherit Metab Dis, 2012. **35**(4): p. 715-26.
36. Al-Salam, S. and S. Hashmi, *Galectin-1 in early acute myocardial infarction.* PLoS One, 2014. **9**(1): p. e86994.
37. Patti, M.E., et al., *Coordinated reduction of genes of oxidative metabolism in humans with insulin resistance and diabetes: Potential role of PGC1 and NRF1.* Proc Natl Acad Sci U S A, 2003. **100**(14): p. 8466-71.
38. Peinado, J.R., et al., *Mitochondria in metabolic disease: getting clues from proteomic studies.* Proteomics, 2014. **14**(4-5): p. 452-66.
39. Essop, M.F., W.A. Chan, and S. Hattingh, *Proteomic analysis of mitochondrial proteins in a mouse model of type 2 diabetes.* Cardiovasc J Afr, 2011. **22**(4): p. 175-8.
40. Roberts, C.K. and K.K. Sindhu, *Oxidative stress and metabolic syndrome.* Life Sci, 2009. **84**(21-22): p. 705-12.

41. Matsuda, M. and I. Shimomura, *Increased oxidative stress in obesity: implications for metabolic syndrome, diabetes, hypertension, dyslipidemia, atherosclerosis, and cancer.* Obes Res Clin Pract, 2013. **7**(5): p. e330-41.
42. Furukawa, S., et al., *Increased oxidative stress in obesity and its impact on metabolic syndrome.* J Clin Invest, 2004. **114**(12): p. 1752-61.
43. Hopps, E., et al., *A novel component of the metabolic syndrome: the oxidative stress.* Nutr Metab Cardiovasc Dis, 2010. **20**(1): p. 72-7.
44. Marseglia, L., et al., *Oxidative stress in obesity: a critical component in human diseases.* Int J Mol Sci, 2014. **16**(1): p. 378-400.

FIGURE LEGENDS

Figure 1. Analysis of mitochondrial ATP and ADP/ATP ratio in cALL survivors and Controls. The energy variables were measured in mitochondria isolated from PBMCs by a commercial ELISA kit. (A, B) panels are for ATP and (C,D) for ADP/ATP ratio. Results represent means ± SEM.

Figure 2. Oxidative stress and antioxidant status among cALL survivors and Controls. PBMCs were used to evaluate oxidative stress markers: (A, B) MDA; (C, D) 8-OHdG; (E, F) OGG1; (G, H) antioxidant enzyme SOD2; (I, J) Nrf2 transcription factor; and (K, L) PGC1-α transcription factor. Commercial ELISA kit was used for the measurement of 8-OHdG, HPLC for MDA, and western blot for OGG1, SOD2, Nrf2 and PGC1- α. Values are expressed as means ± SEM. **P*<0.05, ****P*<0.001 vs Controls.

Figure 3. Apoptotic factors measurement in cALL survivors and Controls. PBMCs were evaluated for the pro-apoptotic proteins by western blot: (A, B) cytochrome c and (C, D) Bcl2 anti-apoptotic proteinResults are represented as % of control group or % healthy cALL group and values are expressed as means ± SEM. **P*<0.05 vs Controls.

Figure 4. Inflammatory factors in cALL survivors and Controls. PBMCs were evaluated for inflammatory markers by western blot. (A, B) Cox-2, (C, D) TNF-α, (E, F) NF-κB, (G, H) I-κB and (I, J) NF-κB/I-κB. Results are represented as % of Control group or % of healthy cALL survivors and values are expressed as means ± SEM. ^{b}P<0.01 vs healthy cALL survivors.

Figure 5. Representative SDS-PAGE of mitochondrial proteins. Gels of mitochondrial lysate from a Control and a cALL survivor samples (in duplicate) are illustrated. Slices from this gel were subjected to in-gel digestion by trypsin and then by the nano-capillary LC-MS/MS analysis. This allowed the identification of 957 proteins containing ≥2 peptides at 95% confidence and FDR <1%.

Figure 6. Localization of the different proteins found in mitochondria. Localization of proteins identified in mitochondria was defined from the Gene Ontology terms from the UniProt Knowledgebase (n=957 proteins). All localizations that applied for a single protein were considered. (A) All groups combined; (B) Controls; (C) cALL survivors combined; (D) Healthy cALL survivors; and (E) Unhealthy cALL survivors. Results are expressed as:

localization; number of proteins involved in this localization; and % of proteins involved in this localization. Localizations are colour coded and described in the affiliated legend.

Figure 7. Functions of the different proteins found in mitochondria. Classification of proteins identified in mitochondria in each study group by their related functions. Functions of proteins identified in mitochondria were defined from the Gene Ontology terms from the UniProt Knowledgebase (n=957 proteins). All the functions that applied for a single protein were considered. (A) All groups combined; (B) Controls; (C) cALL survivors combined; (D) Healthy cALL survivors; and (E) Unhealthy cALL survivors. Results are expressed as: function; number of proteins involved in this function; and % of proteins involved in this function. Functions are colour coded and described in the affiliated legend.

Figure 8. Volcano plot representations of statistically different proteins expressed between groups. (A) Controls vs cALL survivors; (B) Controls vs Healthy cALL survivors; (C) Controls vs Unhealthy cALL survivors; and (D) Healthy vs Unhealthy cALL survivors. X-axis represents the variation in expression [$\log_2$(fold change)], y-axis represents the statistical significance [-log10(p-value)]. Proteins with coordinates (x,y) where x is <-1 or > 1 and y is > 1 are statistically reproducibly halved or doubled in a group of samples. Statistically reproducible proteins have been numbered. Proteins on the left of x=0 are down regulated whereas those on the right of x=0 are up regulated. Abbreviations: C: Controls, S: cALL survivors, H: healthy cALL survivors, UH: unhealthy cALL survivors. The affiliated summary tables beside each graph separate each protein with significantly altered expression between groups by their related function. # in the table represents the protein number on the affiliated graph.

Supplemental Table I. Identification and distribution of proteins present in the mitochondria of cALL survivor groups and controls

	Accession #	Protein name	Number of peptide	% Sequence coverage	Presence	
					Control	*Survivor*
1	1433B_HUMAN	14-3-3 protein beta/alpha	114	36	5	7 (3H, 4UH)
2	1433E_HUMAN	14-3-3 protein epsilon	91	38	4	8 (4H, 4UH)
3	1433F_HUMAN	14-3-3 protein eta	82	36	5	9 (5H, 4UH)
4	1433G_HUMAN	14-3-3 protein gamma	86	38	5	7 (3H, 4UH)
5	1433S_HUMAN	14-3-3 protein sigma	4	19	0	1 (H)
6	1433T_HUMAN	14-3-3 protein theta	60	33	3	4 (2H, 2UH)
7	1433Z_HUMAN	14-3-3 protein zeta/delta	523	58	5	10
8	1A02_HUMAN	HLA class I histocompatibility antigen, A-2 alpha chain	48	40	2	2 (H)
9	1A03_HUMAN	HLA class I histocompatibility antigen, A-3 alpha chain	25	28	1	2 (H,UH)
10	1A11_HUMAN	Isoform 2 of HLA class I histocompatibility antigen, A-11 alpha chain	157	24	4	5 (3H, 2UH)
11	1A23_HUMAN	HLA class I histocompatibility antigen, A-23 alpha chain	13		0	1 (H)
12	1A34_HUMAN	HLA class I histocompatibility antigen, A-34 alpha chain	27	25	0	2 (H, UH)
13	1A68 _HUMAN	HLA class I histocompatibility antigen, A-68 alpha chain	9	39	1	0
14	1B15_HUMAN	HLA class I histocompatibility antigen, B-15 alpha chain	13	18	0	1 (H)
15	1B18_HUMAN	HLA class I histocompatibility antigen, B-18 alpha chain	17	27	0	1 (UH)
16	1B27_HUMAN	HLA class I histocompatibility antigen, B-27 alpha chain	20	23	0	2 (UH)
17	1B37_HUMAN	HLA class I histocompatibility antigen, B-37 alpha chain	32	10	2	2 (H, UH)
18	1B41_HUMAN	HLA class I histocompatibility antigen, B-41 alpha chain	22	23	1	1 (UH)
19	1B44_HUMAN	HLA class I histocompatibility antigen, B-44 alpha chain	17	23	1	1 (UH)
20	1B47_HUMAN	HLA class I histocompatibility antigen, B-47 alpha chain	29	29	0	2 (H, UH)
21	1B59_HUMAN	HLA class I histocompatibility antigen, B-59 alpha chain	45	23	3	2 (UH)
22	1B78_HUMAN	HLA class I histocompatibility antigen, B-78 alpha chain	11	16	1	0
23	1C12_HUMAN	HLA class I histocompatibility antigen, Cw-12 alpha chain	44	25	2	3 (1H, 2UH)
24	2AAA_HUMAN	Serine/threonine-protein phosphatase 2A 65 kDa regulatory subunit A alpha isoform	10	5	1	3 (1H, 2UH)
25	41_HUMAN	Isoform 2 of Protein 4.1	10	4	1	3 (1H, 2UH)
26	6PGD_HUMAN	6-phosphogluconate dehydrogenase,	43	19	2	4

	Accession #	Protein name	Number of peptide	% Sequence coverage	Presence	
					Control	*Survivor*
		decarboxylating				(2H, 2UH)
27	6PGL_HUMAN	6-phosphogluconolactonase	4	11	1	1 (H)
28	A1AG1_HUMAN	Alpha-1-acid glycoprotein 1	6	10	1	1 (UH)
29	sp|P05067-8|A4_HUMAN	Isoform APP751 of Amyloid beta A4 protein	60	11	3	6 (2H, 4UH)
30	sp|Q96IU4|ABHEB_HUMAN	Alpha/beta hydrolase domain-containing protein 14B	4	12	1	1 (UH)
31	sp|O95870-2|ABHGA_HUMAN	Isoform 2 of Abhydrolase domain-containing protein 16A	4	5	1	1 (UH)
32	Q8IZP0-10|ABI1_HUMAN	Isoform 10 of Abl interactor 1	9	7	1	3 (1H, 2UH)
33	sp|P11310-2|ACADM_HUMAN	Isoform 2 of Medium-chain specific acyl-CoA dehydrogenase, mitochondrial	34	14	3	5 (2H, 3UH)
34	sp|P49748-2|ACADV_HUMAN	Isoform 2 of Very long-chain specific acyl-CoA dehydrogenase, mitochondrial	15	6	2	3 (H, 2UH)
35	Q99798|ACON_HUMAN	Aconitate hydratase, mitochondrial	59	18	4	3 (1H, 2UH)
36	sp|Q15067-2|ACOX1_HUMAN	Isoform 2 of Peroxisomal acyl-coenzyme A oxidase 1	3	6	1	0
37	sp|Q9ULC5-3|ACSL5_HUMAN	Isoform 2 of Long-chain-fatty-acid--CoA ligase 5	2	4	0	1 (UH)
38	P60709|ACTB_HUMAN	Actin, cytoplasmic 1	1935	84	5	10
39	ACTBL_HUMAN	Beta-actin-like protein 2	2192	87	5	10
40	P68032|ACTC_HUMAN	Actin, alpha cardiac muscle 1	971	56	5	10
41	ACTG_HUMAN	Actin, cytoplasmic 2	1064	89	3	4 (2H, 2UH)
42	ACTH_HUMAN	Actin, gamma-enteric smooth muscle	86	69	1	0
43	sp|P12814|ACTN1_HUMAN	Alpha-actinin-1	960	52	5	10
44	ACTN2_HUMAN	Alpha-actinin-2	13	15	1	0
45	ACTN3_HUMAN	Alpha-actinin-3	11	17	1	0
46	ACTN4_HUMAN	Alpha-actinin-4	357	34	5	7 (3H, 4UH)
47	ACTS_HUMAN	Actin, alpha skeletal muscle	341	59	1	3 (2H, 1UH)
48	ACTZ_HUMAN	Alpha-centractin	5	8	1	1 (H)
49	ADA10_HUMAN	Disintegrin and metalloproteinase domain-containing protein 10	26	13	2	3 (1H, 1UH)
50	ADDG_HUMAN	Isoform 1 of Gamma-adducin	4	4	0	2 (H, UH)
51	ADHX_HUMAN	Alcohol dehydrogenase class-3	14	11	3	2 (UH)
52	ADSV_HUMAN	Isoform 2 of Adseverin	2	2	0	1 (UH)
53	ADT2_HUMAN	ADP/ATP translocase 2	13	11	3	3 (2H, UH)
54	ADT3_HUMAN	ADP/ATP translocase 3	39	18	3	3 (1H, 2UH)
55	ANHK_HUMAN	Neuroblast differentiation-associated protein AHNAK	90	4	3	4 (2H, 2UH)
56	AIFM1_HUMAN	Isoform 3 of Apoptosis-inducing factor 1, mitochondrial	2	4	0	1 (H)
57	AK1A1_HUMAN	Alcohol dehydrogenase [NADP(+)]	3	4	0	1 (UH)

	Accession #	Protein name	Number of peptide	% Sequence coverage	Presence	
					Control	*Survivor*
58	AL4A1_HUMAN	Isoform 2 of Delta-1-pyrroline-5-carboxylate dehydrogenase, mitochondrial	5	8	0	2 (H)
59	ALBU_HUMAN	Serum albumin	427	72	5	10
60	ALDOA_HUMAN	Fructose-bisphosphate aldolase A	359	74	5	10
61	ALDOC_HUMAN	Fructose-bisphosphate aldolase C	47	15	5	5 (2H, 3UH)
62	sp|Q01433-2|AMPD2_HUMAN	Isoform Ex1A-2-3 of AMP deaminase 2	6	5	1	2 (H, UH)
63	sp|P28838-2|AMPL_HUMAN	Isoform 2 of Cytosol aminopeptidase	7	3	2	1 (UH)
64	P39687|AN32A_HUMAN	Acidic leucine-rich nuclear phosphoprotein 32 family member A	4	13	0	2 (UH)
65	ANGP1_HUMAN	Angiopoietin-1	2	5	0	1 (UH)
66	sp|P16157-10|ANK1_HUMAN	Isoform Er9 of Ankyrin-1	2	1	0	1 (UH)
67	sp|Q4KMQ2-2|ANO6_HUMAN	Isoform 2 of Anoctamin-6	7	3	1	2 (H, UH)
68	ANX11_HUMAN	Annexin A11	11	10	1	2 (H, UH)
69	P04083|ANXA1_HUMAN	Annexin A1	45	15	5	6 (3H, 3UH)
70	sp|P07355-2|ANXA2_HUMAN	Isoform 2 of Annexin A2	50	19	4	5 (3H, 2UH)
71	ANXA4_HUMAN	Annexin A4	4	8	1	1 (H)
72	ANXA5_HUMAN	Annexin A5	12	8	1	3 (2H, 1UH)
73	P08133|ANXA6_HUMAN	Annexin A6	58	10	4	8 (4H, 4UH)
74	sp|P20073-2|ANXA7_HUMAN	Isoform 2 of Annexin A7	7	12	1	1 (UH)
75	AOFB_HUMAN	Amine oxidase [flavin-containing] B	4	4	0	2 (H)
76	sp|O95782-2|AP2A1_HUMAN	Isoform B of AP-2 complex subunit alpha-1	2	2	0	1 (UH)
77	APEX1_HUMAN	DNA-(apurinic or apyrimidinic site) lyase	7	12	2	0
78	sp|Q06481-2|APLP2_HUMAN	Isoform 2 of Amyloid-like protein 2	4	3	1	1 (UH)
79	APOA1_HUMAN	Apolipoprotein A-I	7	14	0	2 (H, UH)
80	O15143|ARC1B_HUMAN	Actin-related protein 2/3 complex subunit 1B	80	23	3	7 (3H, 4UH)
81	ARF1_HUMAN	ADP-ribosylation factor 1	29	27	3	4 (2H, 2UH)
82	ARF3_HUMAN	ADP-ribosylation factor 3	5	15	0	1 (H)
83	ARF4_HUMAN	ADP-ribosylation factor 4	5	22	1	1 (H)
84	ARF5_HUMAN	ADP-ribosylation factor 5	2	11	0	1 (UH)
85	ARK72_HUMAN	Aflatoxin B1 aldehyde reductase member 2	9	7	1	2 (H, UH)
86	ARL8B_HUMAN	ADP-ribosylation factor-like protein 8B	4	12	0	2 (1H, 1UH)
87	P61160|ARP2_HUMAN	Actin-related protein 2	82	22	5	9 (4H, 5UH)

	Accession #	Protein name	Number of peptide	% Sequence coverage	Presence	
					Control	*Survivor*
88	ARP3_HUMAN	Actin-related protein 3	99	32	5	4 (2H, 2UH)
89	ARP3B_HUMAN	Actin-related protein 3B	7		0	1 (H)
90	ARPC2_HUMAN	Actin-related protein 2/3 complex subunit 2	56	30	2	4 (2H, 2UH)
91	ARPC3_HUMAN	Actin-related protein 2/3 complex subunit 3	28	18	2	6 (4H, 2UH)
92	P59998|ARPC4_HUMAN	Actin-related protein 2/3 complex subunit 4	31	21	3	6 (3H, 3UH)
93	sp|O15511-2|ARPC5_HUMAN	Isoform 2 of Actin-related protein 2/3 complex subunit 5	43	53	3	6 (3H, 3UH)
94	sp|P49407-2|ARRB1_HUMAN	Isoform 1B of Beta-arrestin-1	14	9	1	3 (2H, 1UH)
95	sp|Q13510-2|ASAH1_HUMAN	Isoform 2 of Acid ceramidase	2	4	1	0
96	O43150|ASAP2_HUMAN	Arf-GAP with SH3 domain, ANK repeat and PH domain-containing protein 2	7	4	0	3 (2H, UH)
97	sp|P05023|AT1A1_HUMAN	Sodium/potassium-transporting ATPase subunit alpha-1	6	3	0	2 (H, UH)
98	sp|P16615-2|AT2A2_HUMAN	Isoform 2 of Sarcoplasmic/endoplasmic reticulum calcium ATPase 2	91	16	3	4 (2H, 2UH)
99	Q93084-2|AT2A3_HUMAN	Isoform SERCA3A of Sarcoplasmic/endoplasmic reticulum calcium ATPase 3	197	21	5	7 (3H, 4UH)
100	AT5EL_HUMAN	ATP synthase subunit epsilon-like protein, mitochondrial	2	45	1	0
101	AT5F1_HUMAN	ATP synthase subunit b, mitochondrial	23	15	2	3 (1H, 2UH)
102	sp|Q9Y2Q0-2|AT8A1_HUMAN	Isoform 2 of Probable phospholipid-transporting ATPase IA	2	2	0	1 (H)
103	sp|Q9UII2|ATIF1_HUMAN	ATPase inhibitor, mitochondrial	25	34	2	3 (H, 2UH)
104	ATLA3_HUMAN	Atlastin-3	3	7	0	1 (UH)
105	sp|O75947|ATP5H_HUMAN	ATP synthase subunit d, mitochondrial	18	23	2	3 (1H, 2UH)
106	ATP5I_HUMAN	ATP synthase subunit e, mitochondrial	3	22	0	1 (UH)
107	P18859|ATP5J_HUMAN	ATP synthase-coupling factor 6, mitochondrial	11	28	1	3 (1H, 2H)
108	P25705|ATPA_HUMAN	ATP synthase subunit alpha, mitochondrial	180	28	4	9 (5H, 4UH)
109	P06576|ATPB_HUMAN	ATP synthase subunit beta, mitochondrial	219	33	5	9 (5H, 4UH)
110	P30049|ATPD_HUMAN	ATP synthase subunit delta, mitochondrial	8	15	1	2 (H, UH)
111	sp|P36542-2|ATPG_HUMAN	ATP synthase subunit gamma, mitochondrial	26	16	2	5 (3H, 2UH)
112	sp|P56134-2|ATPK_HUMAN	Isoform 2 of ATP synthase subunit f, mitochondrial	2	27	1	0
113	ATPO_HUMAN	ATP synthase subunit O, mitochondrial	27	24	2	3 (2H, 1UH)
114	B2MG_HUMAN	Beta-2-microglobulin	47	36	4	7 (4H, 3UH)
115	P02730|B3AT_HUMAN	Band 3 anion transport protein	28	6	1	6 (4H, 2UH)

	Accession #	Protein name	Number of peptide	% Sequence coverage	Presence	
					Control	*Survivor*
116	sp|P51572-2|BAP31_HUMAN	Isoform 2 of B-cell receptor-associated protein 31	19	15	2	3 (2H, 1UH)
117	BASI_HUMAN	Isoform 2 of Basigin	15	12	3	3 (2H, 1UH)
118	P80723|BASP1_HUMAN	Brain acid soluble protein 1	10	30	1	3 (H, 2UH)
119	sp|Q07812-2|BAX_HUMAN	Isoform Beta of Apoptosis regulator BAX	2	9	0	1 (UH)
120	sp|P16278-3|BGAL_HUMAN	Isoform 3 of Beta-galactosidase	4	4	0	2 (H, UH)
121	sp|P55957-2|BID_HUMAN (+1)	Isoform 2 of BH3-interacting domain death agonist	4	11	0	2 (H, UH)
122	BIN2_HUMAN	Bridging integrator 2	205	37	5	10
123	BOP1_HUMAN	Ribosome biogenesis protein BOP1	2	2	1	0
124	BTK_HUMAN	Tyrosine-protein kinase BTK	2	3	0	1 (UH)
125	Q07021|C1QBP_HUMAN	Complement component 1 Q subcomponent-binding protein, mitochondrial	37	25	4	5 (2H, 3UH)
126	P43155-2|CACP_HUMAN	Isoform 2 of Carnitine O-acetyltransferase	9	9	0	3 (1H, 2UH)
127	sp|Q9P1Z2-2|CACO1_HUMAN (+3)	Isoform 2 of Calcium-binding and coiled-coil domain-containing protein 1	3	4	0	1 (H)
128	P00918|CAH2_HUMAN	Carbonic anhydrase 2	29	26	2	3 (H, 2UH)
129	Q05682-4|CALD1_HUMAN	Isoform 4 of Caldesmon	345	42	5	10
130	P62158|CALM_HUMAN	Calmodulin	103	43	5	10
131	P27797|CALR_HUMAN	Calreticulin	283	54	5	10
132	O43852-3|CALU_HUMAN	Isoform 3 of Calumenin	59	27	5	8 (5H, 3UH)
133	P27824|CALX_HUMAN	Calnexin	139	23	4	8 (4H, 4UH)
134	CAMP_HUMAN	Cathelicidin antimicrobial peptide	7	28	0	1 (UH)
135	P07384|CAN1_HUMAN	Calpain-1 catalytic subunit	88	12	5	7 (3H, 4UH)
136	Q01518-2|CAP1_HUMAN	Isoform 2 of Adenylyl cyclase-associated protein 1	246	37	5	10
137	CAP7_HUMNA	Azurocidin	3	7	0	1 (UH)
138	P47756-2|CAPZB_HUMAN	Cluster of Isoform 2 of F-actin-capping protein subunit beta	101	43	2	7 (3H, 4UH)
139	P42574|CASP3_HUMAN	Caspase-3	8	8	1	2 (2UH)
140	Q9NQ75-2|CASS4_HUMAN	Isoform 2 of Cas scaffolding protein family member 4	7	4	1	2 (H, UH)
141	P04040|CATA_HUMAN	Catalase	16	14	0	4 (2H, 2UH)
142	CATB_HUMAN	Cathepsin B	9	8	1	3 (2H, 1UH)
143	CATC_HUMAN	Dipeptidyl peptidase 1	11	5	3	2 (1H, 1UH)

	Accession #	Protein name	Number of peptide	% Sequence coverage	Presence	
					Control	*Survivor*
144	CATD_HUMAN	Cathepsin D	23	16	2	3 (2H, 1UH)
145	P08311|CATG_HUMAN	Cathepsin G	19	20	2	5 (2H, 3UH)
146	CATL1_HUMAN	Cathepsin L1	2	9	0	1 (H)
147	P25774-2|CATS_HUMAN	Isoform 2 of Cathepsin	12	11	1	4 (2H, 2UH)
148	P52907|CAZA1_HUMAN	F-actin-capping protein subunit alpha-1	74	29	5	10
149	CAZA2_HUMAN	F-actin-capping protein subunit alpha-2	49	23	5	10
150	CCL5_HUMAN	C-C motif chemokine 5	35	32	3	5 (3H, 2UH)
151	CCS_HUMAN	Copper chaperone for superoxide dismutase	9	12	2	1 (H)
152	CD14_HUMAN	Monocyte differentiation antigen CD14	4	9	0	1 (UH)
153	CD226_HUMAN	CD226 antigen	17	11	4	3 (2H, 1UH)
154	P16671|CD36_HUMAN	Platelet glycoprotein 4	54	15	4	5 (3H, 2UH)
155	sp|P16070-10|CD44_HUMAN	Isoform 10 of CD44 antigen	3	5	0	1 (H)
156	sp|Q08722-2|CD47_HUMAN	Isoform OA3-293 of Leukocyte surface antigen CD47	3	6	0	1 (H)
157	sp|P34810-2|CD68_HUMAN	Isoform Short of Macrosialin	2	4	0	1 (H)
158	CD9_HUMAN	CD9 antigen	22	14	4	2 (1H, 1UH)
159	CDC37_HUMAN	Hsp90 co-chaperone Cdc37	12	8	2	3 (1H, 2UH)
160	P60953-1|CDC42_HUMAN	Isoform 1 of Cell division control protein 42 homolog	49	30	3	5 (2H, 3UH)
161	Q9UKY7-2|CDV3_HUMAN	Isoform 2 of Protein CDV3	14	24	2	3 (1H, 2UH)
162	Q9NZK5|CECR1_HUMAN	Adenosine deaminase CECR1	3		0	1 (UH)
163	CFAH_HUMAN	Complement factor H	4	4	0	1 (UH)
164	CG073_HUMAN	Uncharacterized protein C7orf73	2	47	1	0
165	P61604|CH10_HUMAN	Cluster of 10 kDa heat shock protein, mitochondrial	32	45	2	5 (3H, 2UH)
166	P10809|CH60_HUMAN	60 kDa heat shock protein, mitochondrial	178	29	4	10
167	CHCH3_HUMAN	Coiled-coil-helix-coiled-coil-helix domain-containing protein 3, mitochondrial	6	17	1	1 (UH)
168	O75390|CISY_HUMAN	Citrate synthase, mitochondrial	154	28	5	10
169	sp|Q96DZ9-2|CKLF5_HUMAN	Isoform 2 of CKLF-like MARVEL transmembrane domain-containing protein 5	2	12	0	1 (H)
170	P09496-2|CLCA_HUMAN	Isoform Non-brain of Clathrin light chain A	26	18	4	5 (2H, 3UH)
171	Q00610-2|CLH1_HUMAN	Isoform 2 of Clathrin heavy chain 1	96	8	4	5 (3H, 2UH)
172	CLH2_HUMAN	Clathrin heavy chain 2	2	2	0	1 (UH)

	Accession #	Protein name	Number of peptide	% Sequence coverage	Presence	
					Control	*Survivor*
173	CLIC1_HUMAN	Chloride intracellular channel protein 1	127	51	5	5 (2H, 3UH)
174	CLIC4_HUMAN	Chloride intracellular channel protein 4	14	23	2	2 (1H, 1UH)
175	sp|Q9UDT6-2|CLIP2_HUMAN	Isoform 2 of CAP-Gly domain-containing linker protein 2	4	4	1	1 (UH)
176	CLPP_HUMAN	Putative ATP-dependent Clp protease proteolytic subunit, mitochondrial	2	8	1	0
177	P10909-2|CLUS_HUMAN	Isoform 2 of Clusterin	108	21	4	8 (4H, 4UH)
178	Q96KP4|CNDP2_HUMAN	Cytosolic non-specific dipeptidase	16	9	2	4 (2H, 2UH)
179	Q99439|CNN2_HUMAN	Calponin-2	115	37	5	10
180	CNPY2_HUMAN	Protein canopy homolog 2	4	13	1	1 (UH)
181	CNST_HUMAN	Consortin	17	11	1	3 (1H, 2UH)
182	CO3_HUMAN	Complement C3	2	1	1	0
183	COF1_HUMAN	Cofilin-1	306	73	5	10
184	sp|P53621-2|COPA_HUMAN	Isoform 2 of Coatomer subunit alpha	4	2	0	2 (H)
185	P31146|COR1A_HUMAN	Coronin-1A	133	25	5	10
186	Q9BR76|COR1B_HUMAN	Coronin-1B	14	9	2	5 (3H, 2UH)
187	COR1C_HUMAN	Coronin-1C	143	24	5	9 (5H, 4UH)
188	COTL1_HUMAN	Cluster of Coactosin-like protein	57	49	4	5 (3H, 2UH)
189	COX41_HUMAN	Cytochrome c oxidase subunit 4 isoform 1, mitochondrial	8	17	2	1 UH
190	COX5A_HUMAN	Cytochrome c oxidase subunit 5A, mitochondrial	36	32	4	3 (1H, 2UH)
191	P10606|COX5B_HUMAN	Cytochrome c oxidase subunit 5B, mitochondrial	13	31	2	3 (1H, 2UH)
192	CPNS1_HUMAN	Calpain small subunit 1	22	17	2	3 (2H, 1UH)
193	sp|P50416-2|CPT1A_HUMAN	Isoform 2 of Carnitine O-palmitoyltransferase 1, liver isoform	6	3	1	2 (H, UH)
194	CRIP1_HUMAN	Cysteine-rich protein 1	2	25	1	0
195	sp|P54108-2|CRIS3_HUMAN	Isoform 2 of Cysteine-rich secretory protein 3	2	8	0	1 (UH)
196	P46109|CRKL_HUMAN	Cluster of Crk-like protein	22	16	3	4 (2H, 2UH)
197	Q9Y2S2-2|CRYL1_HUMAN	Isoform 2 of Lambda-crystallin homolog	2	6	0	1 (H)
198	Q969H8|CS010_HUMAN	UPF0556 protein C19orf10	6	11	2	1 (1UH)
199	CSK_HUMAN	Tyrosine-protein kinase CSK	7	9	1	1 (UH)
200	P21291|CSRP1_HUMAN	Cysteine and glycine-rich protein 1	120	49	5	10

	Accession #	Protein name	Number of peptide	% Sequence coverage	Presence	
					Control	*Survivor*
201	sp|O60888-2|CUTA_HUMAN (+2)	Isoform A of Protein CutA	2	10	1	0
202	P14854|CX6B1_HUMAN	Cytochrome c oxidase subunit 6B1	6	21	1	2 (2UH)
203	CX7A2_HUMAN	Cytochrome c oxidase subunit 7A2, mitochondrial	4	19	1	1 (H)
204	P02775|CXCL7_HUMAN	Platelet basic protein	359	61	5	10
205	CY1_HUMAN	Cytochrome c1, heme protein, mitochondrial	2	4	1	0
206	CY24A_HUMAN	Cytochrome b-245 light chain	2	24	1	0
207	CY24B_HUMAN	Cytochrome b-245 heavy chain	2	3	0	1 (H)
208	P99999|CYC_HUMAN	Cytochrome c	4	27	1	3 (2UH, 1H)
209	CYFP1_HUMAN	Cytoplasmic FMR1-interacting protein 1	2	2	0	1 (UH)
210	sp|Q5M775-2|CYTSB_HUMAN	Isoform 2 of Cytospin-B	2	3	0	1 (UH)
211	sp|Q9Y4D1|DAAM1_HUMAN	Disheveled-associated activator of morphogenesis 1	13	4	2	2 (1H, 1UH)
212	DAP1_HUMAN	Death-associated protein 1	2	35	1	0
213	DAPP1_HUMAN	Dual adapter for phosphotyrosine and 3-phosphotyrosine and 3-phosphoinositide	2	10	0	1 (UH)
214	Q9UJU6-2|DBNL_HUMAN (+2)	Isoform 2 of Drebrin-like protein	97	25	5	9 (5H, 4UH)
215	sp|P81605|DCD_HUMAN	Dermcidin	4	40	0	2 (UH)
216	sp|Q14203|DCTN1_HUMAN	Dynactin subunit 1	10	3	0	3 (2H, 1UH)
217	sp|Q13561-3|DCTN2_HUMAN	Isoform 3 of Dynactin subunit 2	27	15	2	3 (2H, 1UH)
218	DDAH2_HUMAN	N(G),N(G)-dimethylarginine dimethylaminohydrolase 2	2	7	0	1 (H)
219	DECR_HUMAN	2,4-dienoyl-CoA reductase, mitochondrial	24	15	2	4 (2H, 2UH)
220	P59665|DEF1_HUMAN	Neutrophil defensin 1	11	42	0	3 (2H, 1UH)
221	DEF3_HUMAN	Neutrophil defensin 3	28	21	2	6 (2H, 4UH)
222	Q08495|DEMA_HUMAN	Dematin	43	20	2	4 (2H, 2UH)
223	sp|P60981|DEST_HUMAN	Destrin	21	23	2	4 (2H, 2UH)
224	DHAK_HUMAN	Bifunctional ATP-dependent dihydroxyacetone kinase/FAD-AMP lyase (cyclizing)	2	4	1	0
225	DHB12_HUMAN	Estradiol 17-beta-dehydrogenase 12	2	6	0	1 (UH)
226	DHB4_HUMAN	Peroxisomal multifunctional enzyme type 2	35	13	3	3 (2H, 1UH)

	Accession #	Protein name	Number of peptide	% Sequence coverage	Presence	
					Control	*Survivor*
227	P00367|DHE3_HUMAN	Glutamate dehydrogenase 1, mitochondrial	152	30	5	10
228	DHE4_HUMAN	Glutamate dehydrogenase 2, mitochondrial	8	13	1	1 (UH)
229	DHPR_HUMAN	Dihydropteridine reductase	2	9	0	1 (UH)
230	DHSA_HUMAN	Succinate dehydrogenase [ubiquinone] flavoprotein subunit, mitochondrial	10	9	2	1 (UH)
231	O60610-2|DIAP1_HUMAN	Isoform 2 of Protein diaphanous homolog 1	30	5	2	5 (2H, 3UH)
232	DLDH_HUMAN	Dihydrolipoyl dehydrogenase, mitochondrial	2	3	0	1 (H)
233	DNJC3_HUMAN	DnaJ homolog subfamily C member 3	3	7	0	1 (UH)
234	O00429-6|DNM1L_HUMAN	Isoform 6 of Dynamin-1-like protein	45	11	2	5 (2H, 3UH)
235	Q99704-3|DOK1_HUMAN	Isoform 3 of Docking protein 1	7	11	2	2 (UH)
236	Q7L591|DOK3_HUMAN	Docking protein 3	4	6	0	2 (H, UH)
237	DP13B_HUMAN	DCC-interacting protein 13-beta	3	4	0	1 (H)
238	Q9UHL4|DPP2_HUMAN	Dipeptidyl peptidase 2	17	8	2	4 (2H, 2UH)
239	DPYL2_HUMAN	Dihydropyrimidinase-related protein 2	21	11	2	2 (1H, 1UH)
240	Q16643-2|DREB_HUMAN	Isoform 2 of Drebrin	96	19	5	7 (4H, 3UH)
241	DUS3_HUMAN	Dual specificity protein phosphatase 3	16	22	2	3 (2H, 1UH)
242	DYHC1_HUMAN	Cytoplasmic dynein 1 heavy chain 1	2	1	0	1 (UH)
243	DYL1_HUMAN	Dynein light chain 1, cytoplasmic	4	25	0	2 (H)
244	sp|P42892-2|ECE1_HUMAN	Isoform A of Endothelin-converting enzyme 1	3	6	0	1 (UH)
245	ECH1_HUMAN	Delta(3,5)-Delta(2,4)-dienoyl-CoA isomerase, mitochondrial	46	26	2	4 (2H, 2UH)
246	ECHA_HUMAN	Trifunctional enzyme subunit alpha, mitochondrial	36	7	2	4 (2H, 2UH)
247	ECHB_HUMAN	Trifunctional enzyme subunit beta, mitochondrial	13	6	2	3 (1H, 2UH)
248	ECHM_HUMAN	Enoyl-CoA hydratase, mitochondrial	11	17	2	1 (UH)
249	P68104|EF1A1_HUMAN	Elongation factor 1-alpha 1	97	22	5	10

	Accession #	Protein name	Number of peptide	% Sequence coverage	Presence	
					Control	*Survivor*
250	EF1A2_HUMAN	Elongation factor 1-alpha 2	3	10	0	1 (UH)
251	EF1A3_HUMAN	Putative elongation factor 1-alpha-like 3	26	19	3	2 (1H, 1UH)
252	P24534|EF1B_HUMAN	Elongation factor 1-beta	32	23	4	5 (2H, 3UH)
253	P29692-2|EF1D_HUMAN	Isoform 2 of Elongation factor 1-delta	5	5	0	2 (1H, 1UH)
254	EF1G_HUMAN	Elongation factor 1-gamma	24	14	2	4 (2H, 2UH)
255	EF2_HUMAN	Elongation factor 2	8	2	3	1 (UH)
256	EFHD2_HUMAN	EF-hand domain-containing protein D2	3	24	1	0
257	EFTU_HUMAN	Elongation factor Tu, mitochondrial	34	12	4	4 (1H, 2UH)
258	Q9H4M9|EHD1_HUMAN	EH domain-containing protein 1	55	18	3	6 (3H, 3UH)
259	EHD3_HUMAN	EH domain-containing protein 3	118	26	5	9 (5H, 4UH)
260	EHD4_HUMAN	EH domain-containing protein 4	2	6	0	1 (UH)
261	EIF3J_HUMAN	Eukaryotic translation initiation factor 3 subunit J	2	12	1	0
262	ELNE_HUMAN	Neutrophil elastase	25	14	2	4 (1H, 3UH)
263	sp|Q00013-3|EM55_HUMAN	Isoform 3 of 55 kDa erythrocyte membrane protein	6	10	0	2 (H, UH)
264	P50402|EMD_HUMAN	Emerin	11	9	0	4 (2H, 2UH)
265	EMIL1_HUMAN	EMILIN-1	60	12	3	3 (2H, 1UH)
266	O94919|ENDD1_HUMAN	Endonuclease domain-containing 1 protein	9	10	1	2 (H, UH)
267	P06733|ENOA_HUMAN	Alpha-enolase	567	69	5	10
268	ENOB_HUMAN	Beta-enolase	14	20	0	3 (2H, 1UH)
269	ENOG_HUMAN	Gamma-enolase	58	27	5	9 (5H, 4UH)
270	P14625|ENPL_HUMAN	Endoplasmin	166	23	5	10
271	Q9UBC2-2|EP15R_HUMAN	Isoform 2 of Epidermal growth factor receptor substrate 15-like 1	9	4	1	3 (2H, 1UH)
272	EPN4_HUMAN	Clathrin interactor 1	21	10	2	3 (2UH, 1H)
273	P42566-2|EPS15_HUMAN	Isoform 2 of Epidermal growth factor receptor substrate 15	2		0	1 (UH)
274	sp|Q9NZ08-2|ERAP1_HUMAN	Isoform 2 of Endoplasmic reticulum aminopeptidase 1	13	7	2	1 (UH)
275	P15170-2|ERF3A_HUMAN	Isoform 2 of Eukaryotic peptide chain release factor GTP-binding subunit ERF3A	2	5	0	1 (UH)
276	ERP29_HUMAN	Endoplasmic reticulum resident protein 29	13	12	1	3 (2H, 1UH)

	Accession #	Protein name	Number of peptide	% Sequence coverage	Presence	
					Control	*Survivor*
277	ERP44_HUMAN	Endoplasmic reticulum resident protein 44	6	5	1	2 (1H, 1UH)
278	sp|P30042|ES1_HUMAN	ES1 protein homolog, mitochondrial	11	27	2	1 (UH)
279	ESAM_HUMAN	Endothelial cell-selective adhesion molecule	24	16	2	6 (3H, 3UH)
280	P10768|ESTD_HUMAN	S-formylglutathione hydrolase	44	24	2	9 (4H, 5UH)
281	sp|Q9BSJ8-2|ESYT1_HUMAN	Isoform 2 of Extended synaptotagmin-1	40	7	3	4 (2H, 2UH)
282	sp|A0FGR8-2|ESYT2_HUMAN	Isoform 2 of Extended synaptotagmin-2	2	2	0	1 (UH)
283	sp|P13804-2|ETFA_HUMAN (+1)	Electron transfer flavoprotein subunit alpha, mitochondrial	32	16	4	3 (H, 2UH)
284	sp|P38117|ETFB_HUMAN	Electron transfer flavoprotein subunit beta	17	17	2	2 (1H, 1UH)
285	sp|Q9UI08-2|EVL_HUMAN	Isoform 1 of Ena/VASP-like protein	4	13	1	0
286	P15311|EZRI_HUMAN	Ezrin	109	22	3	5 (2H, 3UH)
287	P50502|F10A1_HUMAN (+1)	Hsc70-interacting protein	24	12	2	4 (2H, 2UH)
288	F13A_HUMAN	Coagulation factor XIII A chain	524	46	5	10
289	P12259|FA5_HUMAN	Coagulation factor V	109	7	4	6 (3H, 3UH)
290	FA63A_HUMAN	Ubiquitin carboxyl-terminal hydrolase MINDY-1	2	11	0	1 (UH)
291	FACE1_HUMAN	CAAX prenyl protease 1 homolog	2	5	0	1 (UH)
292	FCERG_HUMAN	High affinity immunoglobulin epsilon receptor subunit gamma	3	19	0	1 (UH)
293	sp|Q9NVK5-2|FGOP2_HUMAN	Isoform 2 of FGFR1 oncogene partner 2	6	17	1	1 (UH)
294	Q13642-1|FHL1_HUMAN	Isoform 1 of Four and a half LIM domains protein 1	66	26	5	9 (5H, 4UH)
295	Q9Y613|FHOD1_HUMAN	FH1/FH2 domain-containing protein 1	22	5	1	4 (2H, 2UH)
296	P02671-2|FIBA_HUMAN	Isoform 2 of Fibrinogen alpha chain	1077	70	5	10
297	P02675|FIBB_HUMAN	Fibrinogen beta chain	1050	74	5	10
298	P02679-2|FIBG_HUMAN	Isoform Gamma-A of Fibrinogen gamma chain	636	64	5	10
299	sp|P02751-10|FINC_HUMAN	Isoform 10 of Fibronectin	8	3	0	3 (2H, 1UH)
300	FKBP2_HUMAN	Peptidyl-prolyl cis-trans isomerase FKBP2	3	13	0	1 (UH)
301	sp|Q13045|FLII_HUMAN	Protein flightless-1 homolog	6	2	0	2 (H, UH)
302	P21333-2|FLNA_HUMAN	Isoform 2 of Filamin-A	2772	60	5	10
303	FLNB_HUMAN	Filamin-B	30	6	0	2 (2UH)
304	Q14315-2|FLNC_HUMAN	Isoform 2 of Filamin-C	31	6	0	2

	Accession #	Protein name	Number of peptide	% Sequence coverage	Presence	
					Control	*Survivor*
						(1H, 1UH)
305	FLOT1_HUMAN	Flotillin-1	4	5	1	1 (UH)
306	FLOT2_HUMAN	Flotillin-2	2	8	0	1 (UH)
307	sp|Q9Y2L6-2|FRM4B_HUMAN	Isoform 2 of FERM domain-containing protein 4B	2	3	0	1 (UH)
308	P07954-2|FUMH_HUMAN	Isoform Cytoplasmic of Fumarate hydratase, mitochondrial	15	10	3	2 (1H, 1UH)
309	O15117-2|FYB_HUMAN	Isoform FYB-130 of FYN-binding protein	138	21	4	10
310	FYN_HUMAN	Isoform 2 of Tyrosine-protein kinase Fyn	8	4	1	2 (1H, 1UH)
311	P04406|G3P_HUMAN	Glyceraldehyde-3-phosphate dehydrogenase	840	84	5	10
312	G3PT_HUMAN	Glyceraldehyde-3-phosphate dehydrogenase, testis-specific	6	7	2	1 (UH)
313	O95866-2|G6B_HUMAN	Isoform A of Protein G6b	70	33	5	5 (2H, 3UH)
314	P11413-2|G6PD_HUMAN	Isoform Long of Glucose-6-phosphate 1-dehydrogenase	41	13	2	5 (2H, 3UH)
315	sp|P06744-2|G6PI_HUMAN	Isoform 2 of Glucose-6-phosphate isomerase	28	10	3	4 (2H, 2UH)
316	Q14697|GANAB_HUMAN	Neutral alpha-glucosidase AB	100	13	4	7 (5H, 2UH)
317	GAPR1_HUMAN	Golgi-associated plant pathogenesis-related protein 1	4	24	1	1 (H)
318	GBB1_HUMAN	Guanine nucleotide-binding protein G(I)/G(S)/G(T) subunit beta-1	57	20	3	4 (2H, 2UH)
319	GBB2_HUMAN	Guanine nucleotide-binding protein G(I)/G(S)/G(T) subunit beta-2	24	13	1	4 (2H, 2UH)
320	GBB4_HUMAN	Guanine nucleotide-binding protein subunit beta-4	9	10	0	2 (UH)
321	GBG11_HUMAN	Guanine nucleotide-binding protein G(I)/G(S)/G(O) subunit gamma-11	17	48	2	3 (2H, 1UH)
322	GBG5_HUMAN	Guanine nucleotide-binding protein G(I)/G(S)/G(O) subunit gamma-5	8	16	2	2 (1H, 1UH)
323	P63244|GBLP_HUMAN	Guanine nucleotide-binding protein subunit beta-2-like 1	20	27	1	5 (2H, 3UH)
324	P31150|GDIA_HUMAN	Rab GDP dissociation inhibitor alpha	47	19	4	7 (3H, 4UH)
325	P50395|GDIB_HUMAN	Rab GDP dissociation inhibitor beta	21	10	2	4 (3H, 1UH)
326	GDIR1_HUMAN	Rho GDP-dissociation inhibitor 1	54	27	5	6 (3H, 3UH)
327	P52566|GDIR2_HUMAN	Rho GDP-dissociation inhibitor 2	144	55	5	10
328	sp|P07093-2|GDN_HUMAN	Isoform 2 of Glia-derived nexin	2	7	0	1 (UH)
329	P06396-2|GELS_HUMAN	Isoform 2 of Gelsolin	482	48	4	8 (4H, 4UH)
330	GI24_HUMAN	Platelet receptor Gi24	4	5	0	2 (2H)

	Accession #	Protein name	Number of peptide	% Sequence coverage	Presence	
					Control	*Survivor*
331	GILT_HUMAN	Gamma-interferon-inducible lysosomal thiol reductase	6	9	2	1 (H)
332	GIMA4_HUMAN	GTPase IMAP family member 4	2	6	1	0
333	sp|Q9HC38-2|GLOD4_HUMAN	Isoform 2 of Glyoxalase domain-containing protein 4	6	10	2	0
334	P14314-2|GLU2B_HUMAN	Isoform 2 of Glucosidase 2 subunit beta	47	14	2	5 (2H, 3UH)
335	GMFG_HUMAN	Glia maturation factor gamma	9	14	3	1 (UH)
336	GMPR1_HUMAN	GMP reductase 1	15	13	2	2 (1H, 1UH)
337	GMPR2_HUMAN	GMP reductase 2	4	7	1	1 (UH)
338	GNA13_HUMAN	Guanine nucleotide-binding protein subunit alpha-13	3	9	0	1 (UH)
339	sp|P04899-2|GNAI2_HUMAN	Isoform 2 of Guanine nucleotide-binding protein G(i) subunit alpha-2	80	28	3	4 (2H, 2UH)
340	GNAQ_HUMAN	Guanine nucleotide-binding protein G(q) subunit alpha	29	14	3	4 (2H, 2UH)
341	GNAS2_HUMAN	Guanine nucleotide-binding protein G(s) subunit alpha isoforms short	2	7	0	1 (UH)
342	GNAZ_HUMAN	Guanine nucleotide-binding protein G(z) subunit alpha	3	8	0	1 (UH)
343	P07359|GP1BA_HUMAN	Platelet glycoprotein Ib alpha chain	201	19	5	10
344	P13224-2|GP1BB_HUMAN	Isoform 2 of Platelet glycoprotein Ib beta chain	139	17	5	10
345	sp|P43304|GPDM_HUMAN	Glycerol-3-phosphate dehydrogenase, mitochondrial	22	10	3	3 (1H, 2UH)
346	GPIX_HUMAN	Platelet glycoprotein IX	67	30	5	10
347	P40197|GPV_HUMAN	Platelet glycoprotein V	120	23	4	9 (5H, 4UH)
348	P07203|GPX1_HUMAN	Glutathione peroxidase 1	48	30	4	5 (2H, 3UH)
349	GRAP2_HUMAN	GRB2-related adapter protein 2	3	5	1	0
350	P62993|GRB2_HUMAN	Growth factor receptor-bound protein 2	26	20	2	5 (2H, 3UH)
351	GRHPR_HUMAN	Glyoxylate reductase/hydroxypyruvate reductase	9	13	2	2 (1H, 1UH)
352	sp|Q7LDG7-2|GRP2_HUMAN	Isoform 2 of RAS guanyl-releasing protein 2	16	7	2	3 (2H, 1UH)
353	GRP75_HUMAN	Stress-70 protein, mitochondrial	73	23	2	4 (2H, 2UH)
354	P11021|GRP78_HUMAN	78 kDa glucose-regulated protein	334	41	5	10
355	sp|Q9Y2Q3|GSTK1_HUMAN	Glutathione S-transferase kappa 1	22	24	2	3 (2H, 1UH)
356	sp|P09488-2|GSTM1_HUMAN	Isoform 2 of Glutathione S-transferase Mu 1	3	12	1	0
357	GSTO1_HUMAN	Glutathione S-transferase omega-1	68	26	3	6 (3H, 3UH)
358	P09211|GSTP1_HUMAN	Glutathione S-transferase P	108	47	5	10
359	P11169|GTR3_HUMAN	Solute carrier family 2, facilitated glucose transporter member 3	53	14	3	7 (3H, 4UH)

	Accession #	Protein name	Number of peptide	% Sequence coverage	Presence	
					Control	*Survivor*
360	H12_HUMAN	Histone H1.2	77	18	1	9 (4H, 5UH)
361	H13_HUMAN	Histone H1.3	108	21	2	9 (4H, 5UH)
362	P10412|H14_HUMAN	Histone H1.4	75	28	2	9 (4H, 5UH)
363	H15_HUMAN	Histone H1.5	41	24	2	5 (3H, 2UH)
364	P0C0S8|H2A1_HUMAN (+6)	Histone H2A type 1	52	44	0	5 (5H, 2UH)
365	H2A1C_HUMAN	Histone H2A type 1-C	158	45	5	10
366	H2A1D_HUMAN	Histone H2A type 1-D	46	43	4	4 (1H, 2UH)
367	H2A2A_HUMAN	Histone H2A type 2-A	78	50	5	5 (2H, 3UH)
368	H2A2B_HUMAN	Histone H2A type 2-B	4	45	0	1 (UH)
369	P16104|H2AX_HUMAN	Histone H2A.x	23	43	2	2 (H)
370	O75367-2|H2AY_HUMAN (+2)	Isoform 1 of Core histone macro-H2A.1	8	9	0	3 (H)
371	P0C0S5|H2AZ_HUMAN	Histone H2A.Z	5	20	0	2 (H)
372	H2B1B_HUMAN	Histone H2B type 1-B	78	48	5	5 (2H, 3UH)
373	H2BFS_HUMAN	Histone H2B type F-S	52	55	5	2 (1H, 1UH)
374	H31_HUMAN [3]	Cluster of Histone H3.1	6	24	0	3 (2H, 1UH)
375	H33_HUMAN	Histone H3.3	17	33	3	4 (2H, 2UH)
376	P62805|H4_HUMAN	Histone H4	93	44	5	10
377	H90B3_HUMAN	Putative heat shock protein HSP 90-beta-3	5		0	1 (H)
378	HAP28_HUMAN	28 kDa heat- and acid-stable phosphoprotein	4	15	1	1 (UH)
379	P69905|HBA_HUMAN	Hemoglobin subunit alpha	452	84	5	10
380	P68871|HBB_HUMAN	Hemoglobin subunit beta	618	93	5	10
381	P02042|HBD_HUMAN	Hemoglobin subunit delta	275	70	4	8 (5H, 3UH)
382	HBE_HUMAN	Hemoglobin subunit epsilon	1	18	0	1 (UH)
383	P69891|HBG1_HUMAN	Hemoglobin subunit gamma-1	5	21	1	1 (UH)
384	Q99714-2|HCD2_HUMAN (+1)	Isoform 2 of 3-hydroxyacyl-CoA dehydrogenase type-2	20	23	2	3 (1H, 2UH)
385	sp|Q16836|HCDH_HUMAN	Hydroxyacyl-coenzyme A dehydrogenase, mitochondrial	22	17	2	4 (2H, 2UH)
386	P14317|HCLS1_HUMAN	Hematopoietic lineage cell-specific protein	33	12	2	5 (2H, 3UH)
387	HDGF_HUMAN	Hepatoma-derived growth factor	5	14	1	1 (UH)

	Accession #	Protein name	Number of peptide	% Sequence coverage	Presence	
					Control	*Survivor*
388	Q9H0R4|HDHD2_HUMAN	Haloacid dehalogenase-like hydrolase domain-containing protein 2	10	25	0	3 (1H, 2UH)
389	P06865|HEXA_HUMAN	Beta-hexosaminidase subunit alpha	8	6	0	3 (2H, 1UH)
390	P07686|HEXB_HUMAN	Beta-hexosaminidase subunit beta	36	10	2	6 (3H, 3UH)
391	HIBCH_HUMAN	3-hydroxyisobutyryl-CoA hydrolase, mitochondrial	2	8	1	0
392	HINT1_HUMAN	Histidine triad nucleotide-binding protein 1	15	51	2	2 (1H, 1UH)
393	HINT2_HUMAN (+1)	Histidine triad nucleotide-binding protein 2, mitochondrial	9	21	3	1 (UH)
394	HLAE_HUMAN	HLA class I histocompatibility antigen, alpha chain E	12	16	0	2 (1H, 1UH)
395	HLAH_HUMAN	Putative HLA class I histocompatibility antigen, alpha chain H	8	12	0	1 (H)
396	P09429|HMGB1_HUMAN	High mobility group protein B1	29	19	2	3 (2H, 1UH)
397	HMGB2_HUMAN	High mobility group protein B2	21	36	1	2 (1H, 1UH)
398	HMGN2_HUMAN	Non-histone chromosomal protein HMG-17	14	60	2	2 (1H, 1UH)
399	HMGN4_HUMAN	High mobility group nucleosome-binding domain-containing protein 4	2	28	1	0
400	Q92619-2|HMHA1_HUMAN (+1)	Isoform 2 of Minor histocompatibility protein HA-1	21	5	1	4 (2H, 2UH)
401	sp|P07910-2|HNRPC_HUMAN	Isoform C1 of Heterogeneous nuclear ribonucleoproteins C1/C2	12	14	2	1 (H)
402	Q14103-2|HNRPD_HUMAN (+3)	Isoform 2 of Heterogeneous nuclear ribonucleoprotein D0	4	7	1	0
403	sp|P61978-2|HNRPK_HUMAN	Isoform 2 of Heterogeneous nuclear ribonucleoprotein K	30	12	3	4 (2H, 2UH)
404	sp|Q00839|HNRPU_HUMAN	Cluster of Heterogeneous nuclear ribonucleoprotein U	4	8	1	0
405	HPRT_HUMAN	Hypoxanthine-guanine phosphoribosyltransferase	2	7	0	1 (UH)
406	sp|Q9Y251-2|HPSE_HUMAN	Isoform 2 of Heparanase	66	15	3	5 (3H, 2UH)
407	HPRT_HUMAN	Hypoxanthine-guanine phosphoribosyltransferase	2	7	0	1 (UH)
408	sp|Q9Y251|HPSE_HUMAN	Heparanase	63	15	3	5 (3H, 2UH)
409	P00738|HPT_HUMAN	Haptoglobin	4	15	0	1 (UH)
410	HRG_HUMAN	Histidine-rich glycoprotein	2	4	0	1 (UH)
411	HS71L_HUMAN	Heat shock 70 kDa protein 1-like	17	24	3	0
412	HS90_HUMAN	Heat shock protein HSP 90-beta	2		0	1 (UH)
413	P07900-2|HS90A_HUMAN	Isoform 2 of Heat shock protein HSP 90-alpha	171	18	3	7 (3H, 4UH)
414	P08238|HS90B_HUMAN	Heat shock protein HSP 90-beta	102	20	3	6 (2H, 4UH)
415	HSP71_HUMAN	Heat shock 70 kDa protein 1A	93	17	5	8 (3H, 5UH)
416	HSP72_HUMAN	Heat shock-related 70 kDa protein 2	6		0	1 (H)

	Accession #	Protein name	Number of peptide	% Sequence coverage	Presence	
					Control	*Survivor*
417	HSP74_HUMAN	Heat shock 70 kDa protein 4	3	3	0	1 (UH)
418	HSP76_HUMAN	Heat shock 70 kDa protein 6	14	11	2	1 (UH)
419	P11142|HSP7C_HUMAN	Heat shock cognate 71 kDa protein	270	34	5	10
420	HSPB1_HUMAN	Heat shock protein beta-1	100	41	5	10
421	P19367-2|HXK1_HUMAN	Isoform 2 of Hexokinase-1	124	14	5	9 (5H, 4UH)
422	HXK2_HUMAN	Hexokinase-2	3	5	0	1 (H)
423	HYOU1_HUMAN	Hypoxia up-regulated protein 1	19	5	2	3 (2H, 1UH)
424	sp|P20810-2|ICAL_HUMAN	Isoform 2 of Calpastatin	3	4	1	0
425	ICAM2_HUMAN	Intercellular adhesion molecule 2	2	7	1	0
426	IDHC_HUMAN	Isocitrate dehydrogenase [NADP] cytoplasmic	11	8	2	2 (1H, 1UH)
427	IDHP_HUMAN	Isocitrate dehydrogenase [NADP], mitochondrial	160	31	4	9 (5H, 4UH)
428	IF1AX_HUMAN (+1)	Eukaryotic translation initiation factor 1A, X-chromosomal	2	15	1	0
429	IF2A_HUMAN	Eukaryotic translation initiation factor 2 subunit 1	2	6	0	1 (UH)
430	IF4A1_HUMAN	Eukaryotic initiation factor 4A-I	10	6	2	3 (1H, 2UH)
431	IF4B_HUMAN	Eukaryotic translation initiation factor 4B	8	8	1	1 (UH)
432	sp|Q15056-2|IF4H_HUMAN	Isoform Short of Eukaryotic translation initiation factor 4H	9	18	1	2 (H)
433	P63241-2|IF5A1_HUMAN	Isoform 2 of Eukaryotic translation initiation factor 5A-1	47	29	4	5 (3H, 2UH)
434	P01857|IGHG1_HUMAN	Ig gamma-1 chain C region	27	13	3	7 (3H, 4UH)
435	P01859|IGHG2_HUMAN (+1)	Ig gamma-2 chain C region	2	6	0	1 (UH)
436	IGHG3_HUMAN	Ig gamma-3 chain C region	3	10	0	1 (UH)
437	sp|P01871-2|IGHM_HUMAN	Isoform 2 of Ig mu chain C region	11	7	1	3 (2H, 1UH)
438	ILEU_HUMAN	Leukocyte elastase inhibitor	3	9	1	0
439	Q13418|ILK_HUMAN	Integrin-linked protein kinase	224	38	5	10
440	sp|Q16891|IMMT_HUMAN	Mitochondrial inner membrane protein	40	12	2	4 (2H, 2UH)
441	sp|Q9GZP8-2|IMUP_HUMAN	Isoform 2 of Immortalization up-regulated protein	3	23	0	1 (UH)
442	Q27J81-2|INF2_HUMAN	Isoform 2 of Inverted formin-2	57	9	3	5 (3H, 2UH)
443	IPYR_HUMAN	Inorganic pyrophosphatase	2	18	1	0
444	sp|Q9H2U2|IPYR2_HUMAN	Inorganic pyrophosphatase 2, mitochondrial	18	15	2	3 (1H, 2UH)
445	IQGA1_HUMAN	Ras GTPase-activating-like protein IQGAP1	2	1	0	1 (UH)

	Accession #	Protein name	Number of peptide	% Sequence coverage	Presence	
					Control	*Survivor*
446	IQGA2_HUMAN	Ras GTPase-activating-like protein IQGAP2	27	4	2	4 (2H, 2UH)
447	ITA2_HUMAN	Integrin alpha-2	23	6	1	2 (1H, 1UH)
448	P08514|ITA2B_HUMAN	Integrin alpha-IIb	162	15	3	6 (3H, 3UH)
449	ITA5_HUMAN	Integrin alpha-5	2	3	0	1 (UH)
450	sp|P23229-2|ITA6_HUMAN (+6)	Isoform Alpha-6X1A of Integrin alpha-6	67	12	3	4 (2H, 2UH)
451	ITB1_HUMAN	Integrin beta-1	110	23	4	4 (2H, 2UH)
452	ITB2_HUMAN	Integrin beta-2	25	8	2	3 (2H, 1UH)
453	sp|P05106|ITB3_HUMAN	Integrin beta-3	578	37	5	10
454	sp|Q14643-2|ITPR1_HUMAN	Isoform 2 of Inositol 1,4,5-trisphosphate receptor type 1	2	1	0	1 (UH)
455	IVD_HUMAN	Isovaleryl-CoA dehydrogenase, mitochondrial	6	7	2	1 (UH)
456	JAM1_HUMAN	Junctional adhesion molecule A	12	13	1	3 (2H, 1UH)
457	sp|Q9BX67-2|JAM3_HUMAN	Isoform 2 of Junctional adhesion molecule C	4	7	1	1 (H)
458	P13645|K1C10_HUMAN	Keratin, type I cytoskeletal 10	41	13	1	5 (3H, 2UH)
459	K1C14_HUMAN	Keratin, type I cytoskeletal 14	5	12	1	0
460	K1C19_HUMAN	Keratin, type I cytoskeletal 19	2	6	1	0
461	P35527|K1C9_HUMAN	Keratin, type I cytoskeletal 9	63	20	2	7 (4H, 3UH)
462	P35908|K22E_HUMAN	Keratin, type II cytoskeletal 2 epidermal	51	24	0	6 (3H, 3UH)
463	P04264|K2C1_HUMAN	Keratin, type II cytoskeletal 1	93	19	3	7 (4H, 3UH)
464	K2C1B_HUMAN	Keratin, type II cytoskeletal 1b	3	5	0	1
465	P13647|K2C5_HUMAN	Keratin, type II cytoskeletal 5	7	4	0	1 (H)
466	K2C6A_HUMAN	Keratin, type II cytoskeletal 6A	9	6	2	0
467	K2C6C_HUMAN	Keratin, type II cytoskeletal 6C	6	14	1	0
468	K2C75_HUMAN	Keratin, type II cytoskeletal 75	4		0	1 (H)
469	K6PL_HUMAN	6-phosphofructokinase, liver type	2	5	1	0
470	K6PP_HUMAN	6-phosphofructokinase type C	19	8	3	3 (2H, 1UH)
471	KAD1_HUMAN	Adenylate kinase isoenzyme 1	9	14	2	1 (UH)
472	sp|P54819-2|KAD2_HUMAN	Isoform 2 of Adenylate kinase 2, mitochondrial	46	24	3	6 (3H, 3UH)
473	sp|Q9UIJ7|KAD3_HUMAN	GTP:AMP phosphotransferase, mitochondrial	5	21	1	1 (UH)
474	O60229-4|KALRN_HUMAN	Isoform 4 of Kalirin	7	0	0	3 (1H, 2UH)
475	KAP0_HUMAN	cAMP-dependent protein kinase type I-alpha regulatory subunit	29	14	2	4 (2H, 2UH)

	Accession #	Protein name	Number of peptide	% Sequence coverage	Presence	
					Control	*Survivor*
476	sp|P22694-2|KAPCB_HUMAN	Isoform 2 of cAMP-dependent protein kinase catalytic subunit beta	3	7	0	1 (UH)
477	KCC1A_HUMAN	Calcium/calmodulin-dependent protein kinase type 1	2	7	0	1 (H)
478	KCY_HUMAN	UMP-CMP kinase	17	29	2	2 (IH, IUH)
479	KGP1_HUMAN	Isoform Beta of cGMP-dependent protein kinase 1	2	2	0	1 (UH)
480	O00139-1|KIF2A_HUMAN	Isoform 1 of Kinesin-like protein KIF2A	26	9	2	3 (1H, 2UH)
481	KINH_HUMAN	Kinesin-1 heavy chain	2	1	1	0
482	sp|P01042-2|KNG1_HUMAN	Isoform LMW of Kininogen-1	2	5	0	1 (UH)
483	sp|P05771-2|KPCB_HUMAN	Isoform Beta-II of Protein kinase C beta type	14	5	2	3 (2H, 1UH)
484	sp|Q05655|KPCD_HUMAN	Protein kinase C delta type	6	3	2	1 (H)
485	P14618|KPYM_HUMAN	Pyruvate kinase isozymes M1/M2	498	57	5	10
486	P43405-2|KSYK_HUMAN (+1)	Isoform Short of Tyrosine-protein kinase SYK	15	6	1	4 (2H, 2UH)
487	sp|Q86UP2|KTN1_HUMAN	Kinectin OS=Homo sapiens	7	3	0	2 (1H, 1UH)
488	LAMC1_HUMAN	Laminin subunit gamma-1	2	2	0	1 (H)
489	LAMP1_HUMAN	Lysosome-associated membrane glycoprotein 1	12	8	2	1 (UH)
490	Q14847|LASP1_HUMAN	LIM and SH3 domain protein 1	124	39	5	10
491	O43561|LAT_HUMAN	Linker for activation of T-cells family member 1	11	16	1	3 (1H, 2UH)
492	Q13094|LCP2_HUMAN	Lymphocyte cytosolic protein 2	15	7	2	4 (2H, 2UH)
493	P00338-3|LDHA_HUMAN	Isoform 3 of L-lactate dehydrogenase A chain	41	15	2	8 (4H, 4UH)
494	P07195|LDHB_HUMAN	L-lactate dehydrogenase B chain	81	22	2	9 (4H, 5UH)
495	P09382|LEG1_HUMAN	Galectin-1	8	23	1	2 (UH)
496	Q3ZCW2|LEGL_HUMAN	Galectin-related protein	29	29	3	4 (3H, 1UH)
497	LETM1_HUMAN	LETM1 and EF-hand domain-containing protein 1, mitochondrial	2	4	1	0
498	LGUL_HUMAN	Lactoylglutathione lyase	2	20	1	0
499	sp|P48059-2|LIMS1_HUMAN	Isoform 2 of LIM and senescent cell antigen-like-containing domain protein 1	120	31	4	9 (4H, 5UH)
500	sp|Q7Z4I7-2|LIMS2_HUMAN	Isoform 2 of LIM and senescent cell antigen-like-containing domain protein 2	2	11	0	1 (H)
501	P09960|LKHA4_HUMAN	Leukotriene A-4 hydrolase	13	9	1	3 (UH)
502	LMAN2_HUMAN	Vesicular integral-membrane protein VIP36	9	7	2	2 (1H, 1UH)
503	LMNB1_HUMAN	Lamin-B1	9	4	1	2 (H)

	Accession #	Protein name	Number of peptide	% Sequence coverage	Presence	
					Control	*Survivor*
504	LOX12_HUMAN	Arachidonate 12-lipoxygenase, 12S-type	6	4	1	1 (UH)
505	P50851-2|LRBA_HUMAN	Isoform 2 of Lipopolysaccharide-responsive and beige-like anchor protein	5	1	1	1 (UH)
506	LRC59_HUMAN	Leucine-rich repeat-containing protein 59	13	12	2	2 (H, UH)
507	Q32MZ4|LRRF1_HUMAN	Leucine-rich repeat flightless-interacting protein 1	22	6	2	3 (1H, 2UH)
508	Q9Y608-2|LRRF2_HUMAN	Isoform 2 of Leucine-rich repeat flightless-interacting protein 2	28	14	3	4 (2H, 2UH)
509	P33241|LSP1_HUMAN	Lymphocyte-specific protein 1	21	22	3	2 (2UH)
510	Q14766-3|LTBP1_HUMAN	Latent-transforming growth factor beta-binding protein 1	473	27	5	10
511	LTOR5_HUMAN	Ragulator complex protein LAMTOR5	6	35	1	2 (1H, 1UH)
512	LY66F_HUMAN	Lymphocyte antigen 6 complex locus protein G6f	13	22	1	1 (UH)
513	P16109|LYAM3_HUMAN	P-selectin	137	19	4	6 (3H, 3UH)
514	sp|P07948-2|LYN_HUMAN	Isoform 2 of Tyrosine-protein kinase Lyn	28	11	3	4 (2H, 2UH)
515	sp|O75608-2|LYPA1_HUMAN	Isoform 2 of Acyl-protein thioesterase 1	2	6	1	0
516	Q86UE4|LYRIC_HUMAN	Protein LYRIC	6	9	1	1 (UH)
517	P61626|LYSC_HUMAN	Lysozyme C	164	57	5	10
518	Q9UNF1-2|MAGD2_HUMAN	Isoform 2 of Melanoma-associated antigen D2	2		0	1 (UH)
519	P55145|MANF_HUMAN	Mesencephalic astrocyte-derived neurotrophic factor	56	29	3	6 (3H, 3UH)
520	sp|P23368-2|MAOM_HUMAN	Isoform 2 of NAD-dependent malic enzyme, mitochondrial	20	10	3	3 (1H, 2UH)
521	sp|P27816-6|MAP4_HUMAN	Isoform 6 of Microtubule-associated protein 4	2	1	1	0
522	Q15691|MARE1_HUMAN	Microtubule-associated protein RP/EB family member 1	28	21	3	4 (2H, 2UH)
523	Q15555|MARE2_HUMAN	Microtubule-associated protein RP/EB family member 2	62	30	3	8 (4H, 4UH)
524	Q7Z434|MAVS_HUMAN	Mitochondrial antiviral-signaling protein	29	17	2	6 (3H, 3UH)
525	sp|P15529-16|MCP_HUMAN	Isoform 3 of Membrane cofactor protein	2	8	0	1 (UH)
526	sp|Q8NE86-3|MCU_HUMAN	Isoform 3 of Calcium uniporter protein, mitochondrial	3	9	0	1 (H)
527	sp|P40925-2|MDHC_HUMAN	Malate dehydrogenase, mitochondrial	11	13	2	2 (2H)
528	MDHM_HUMAN	Malate dehydrogenase, mitochondrial	91	28	5	9 (5H, 4UH)
529	MESD_HUMAN	LDLR chaperone MESD	5	18	0	2 (1H, 1UH)
530	MIF_HUMAN	Macrophage migration inhibitory factor	7	29	2	0
531	MK14_HUMAN	Mitogen-activated protein kinase 14	2	4	1	0
532	P19105|ML12A_HUMAN	Myosin regulatory light chain 12A	160	68	5	10

	Accession #	Protein name	Number of peptide	% Sequence coverage	Presence	
					Control	*Survivor*
533	ML12B_HUMAN	Myosin regulatory light chain 12B	118	63	4	4 (H, 3UH)
534	MLEC_HUMAN	Malectin	8	16	0	3 (2H, 1UH)
535	MMP8_HUMAN	Neutrophil collagenase	3	6	0	1 (UH)
536	MMP9_HUMAN	Matrix metalloproteinase-9	3	4	0	1 (UH)
537	Q13201|MMRN1_HUMAN	Multimerin-1	397	23	5	10
538	P26038|MOES_HUMAN	Moesin	537	47	5	10
539	MPCP_HUMAN	Isoform B of Phosphate carrier protein, mitochondrial	14	10	3	2 (1H, 1UH)
540	MPRD_HUMAN	Cation-dependent mannose-6-phosphate receptor	5	10	0	1 (1H, 1UH)
541	Q9Y6F6-2|MRVI1_HUMAN	Isoform 2 of Protein MRVI1	19	7	2	4 (2H, 2UH)
542	MST4_HUMAN	Serine/threonine-protein kinase 26	2	17	0	1 (H)
543	P58546|MTPN_HUMAN	Myotrophin	52	43	5	9 (5H, 4UH)
544	Q92614-2|MY18A_HUMAN	Isoform 2 of Unconventional myosin-XVIIIa	9	2	1	3 (2H, 1UH)
545	sp|P35580-2|MYH10_HUMAN	Isoform 2 of Myosin-10	196	83	4	3 (1H, 2UH)
546	sp|P35749-2|MYH11_HUMAN	Isoform 2 of Myosin-11	65	10	1	4 (2H, 2UH)
547	MYH13_HUMAN	Myosin-13	2	2	0	1 (H)
548	MYH14_HUMAN	Myosin-14	94	7	3	3 (1H, 2UH)
549	MYH2_HUMAN	Myosin-2	6	2	0	3 (1H, 2UH)
550	MYH3_HUMAN	Myosin-3	2		0	1 (H)
551	MYH4_HUMAN	Myosin-4	2	2	0	1 (UH)
552	P35579|MYH9_HUMAN	Myosin-9	2793	59	5	10
553	Q9BUA6|MYL10_HUMAN	Myosin regulatory light chain 10	3		0	1 (UH)
554	P60660-2|MYL6_HUMAN	Isoform Smooth muscle of Myosin light polypeptide 6	218	78	5	10
555	P24844|MYL9_HUMAN	Myosin regulatory light polypeptide 9	324	64	5	10
556	Q15746-3|MYLK_HUMAN	Isoform 3A of Myosin light chain kinase, smooth muscle	45	4	2	5 (3H, 2UH)
557	sp|O14974-4|MYPT1_HUMAN	Isoform 4 of Protein phosphatase 1 regulatory subunit 12A	22	6	2	3 (2H, 1UH)
558	NB5R1_HUMAN	NADH-cytochrome b5 reductase 1	5	8	0	2 (H, UH)
559	sp|P00387-2|NB5R3_HUMAN	Isoform 2 of NADH-cytochrome b5 reductase 3	41	24	3	4 (2H, 2UH)
560	NCK2_HUMAN	Cytoplasmic protein NCK2	2	8	0	1 (UH)

	Accession #	Protein name	Number of peptide	% Sequence coverage	Presence	
					Control	*Survivor*
561	P15531-2|NDKA_HUMAN	Isoform 2 of Nucleoside diphosphate kinase A	8		0	1 (UH)
562	sp|P22392-2|NDKB_HUMAN	Isoform 3 of Nucleoside diphosphate kinase B	24	9	2	2 (1H, 1UH)
563	NDUA5_HUMAN	NADH dehydrogenase [ubiquinone] 1 alpha subcomplex subunit 5	2	14	0	1 (H)
564	NDUS6_HUMAN	NADH dehydrogenase [ubiquinone] iron-sulfur protein 6, mitochondrial	4	25	1	1 (H)
565	NDUV2_HUMAN	NADH dehydrogenase [ubiquinone] flavoprotein 2, mitochondrial	2	13	0	1 (UH)
566	NEB2_HUMAN	Neurabin-2	4	3	1	1 (H)
567	NEDD8_HUMAN	NEDD8	2	24	0	1 (H)
568	NENF_HUMAN	Neudesin	5	16	0	2 (H, UH)
569	NEUG_HUMAN	Neurogranin	16	32	2	2 (1H, 1UH)
570	Q0ZGT2-4|NEXN_HUMAN	Isoform 4 of Nexilin	112	22	4	6 (3H, 3UH)
571	sp|P80188-2|NGAL_HUMAN	Isoform 2 of Neutrophil gelatinase-associated lipocalin	5	24	0	1 (UH)
572	O14745|NHRF1_HUMAN	Na(+)/H(+) exchange regulatory cofactor NHE-RF1	48	19	2	5 (2H, 3UH)
573	P14543|NID1_HUMAN	Nidogen-1	38	5	2	5 (3H, 1UH)
574	NID2_HUMAN	Nidogen-2	6	5	0	1 (H)
575	sp|O75323-2|NIPS2_HUMAN	Isoform 2 of Protein NipSnap homolog 2	2	7	1	0
576	sp|P22307|NLTP_HUMAN	Non-specific lipid-transfer protein	4	4	1	1 (H)
577	NMT1_HUMAN	Glycylpeptide N-tetradecanoyltransferase 1	2	5	0	1 (UH)
578	NNTM_HUMAN	NAD(P) transhydrogenase, mitochondrial	45	7	3	4 (2H, 2UH)
579	NP1L1_HUMAN	Nucleosome assembly protein 1-like 1	56	15	5	6 (3H, 3UH)
580	NP1L4_HUMAN	Nucleosome assembly protein 1-like 4	10	6	1	3 (1H, 1UH)
581	NPM_HUMAN	Nucleophosmin	8	17	2	0
582	NUCB1_HUMAN	Nucleobindin-1	2	6	1	0
583	P19338|NUCL_HUMAN	Nucleolin	27	6	3	6 (4H, 2UH)
584	OCAD1_HUMAN	OCIA domain-containing protein 1	2	16	1	0
585	sp|Q02218-2|ODO1_HUMAN	Isoform 2 of 2-oxoglutarate dehydrogenase, mitochondrial	2	3	0	1 (UH)
586	ODO2_HUMAN	Dihydrolipoyllysine-residue succinyltransferase component of 2-oxoglutarate dehydrogenase complex, mitochondrial	13	7	2	2 (H)
587	sp|P11177-2|ODPB_HUMAN (+1)	Isoform 2 of Pyruvate dehydrogenase E1 component subunit beta, mitochondrial	9	9	2	1 (UH)
588	sp|Q9NTK5-2|OLA1_HUMAN	Isoform 2 of Obg-like ATPase 1	2	9	0	1 (UH)
589	OLFM4_HUMAN	Olfactomedin-4	2	9	0	1 (UH)

	Accession #	Protein name	Number of peptide	% Sequence coverage	Presence	
					Control	*Survivor*
590	OST48_HUMAN	Dolichyl-diphosphooligosaccharide--protein glycosyltransferase 48 kDa subunit	4	5	2	0
591	PA2G4_HUMAN	Proliferation-associated protein 2G4	18	16	2	2 (H, UH)
592	PABP1_HUMAN	Polyadenylate-binding protein 1	5	5	1	1 (UH)
593	Q9UNF0-2|PACN2_HUMAN	Isoform 2 of Protein kinase C and casein kinase substrate in neurons protein 2	24	8	2	8 (4H, 4UH)
594	PAI1_HUMAN	Plasminogen activator inhibitor 1	2	4	0	1 (H)
595	sp|Q8NC51-2|PAIRB_HUMAN (+3)	Isoform 2 of Plasminogen activator inhibitor 1 RNA-binding protein	2	10	1	0
596	PAK2_HUMAN	Serine/threonine-protein kinase PAK 2	5	8	1	1 (H)
597	Q99497|PARK7_HUMAN	Protein DJ-1	129	57	5	10
598	sp|Q9HBI1-2|PARVB_HUMAN (+1)	Isoform 2 of Beta-parvin	94	18	5	9 (5H, 4UH)
599	Q15365|PCBP1_HUMAN	Poly(rC)-binding protein 1	55	28	2	5 (3H, 2UH)
600	sp|Q15366-2|PCBP2_HUMAN	Isoform 2 of Poly(rC)-binding protein 2	18	18	2	2 (H, UH)
601	sp|P29122-2|PCSK6_HUMAN	Isoform PACE4A-II of Proprotein convertase subtilisin/kexin type 6	2	4	0	1 (UH)
602	PDC10_HUMAN	Programmed cell death protein 10	2	8	0	1 (UH)
603	PDC6I_HUMAN	Programmed cell death 6-interacting protein	14	4	1	2 (H, UH)
604	sp|O76074-2|PDE5A_HUMAN	cGMP-specific 3',5'-cyclic phosphodiesterase	12	6	2	1 (UH)
605	P07237|PDIA1_HUMAN	Protein disulfide-isomerase	193	33	5	10
606	P30101|PDIA3_HUMAN	Protein disulfide-isomerase A3	351	47	5	10
607	PDIA4_HUMAN	Protein disulfide-isomerase A4	58	14	3	3 (2H, 1UH)
608	PDIA5_HUMAN	Protein disulfide-isomerase A5	35	14	2	3 (1H, 2UH)
609	Q15084-2|PDIA6_HUMAN	Isoform 2 of Protein disulfide-isomerase A6	96	19	5	9 (5H, 4UH)
610	PDLI1_HUMAN	PDZ and LIM domain protein 1	412	73	5	10
611	Q96HC4-2|PDLI5_HUMAN	Isoform 2 of PDZ and LIM domain protein 5	10	11	0	3 (1H, 2UH)
612	Q9NR12-2|PDLI7_HUMAN	PDZ and LIM domain protein 7	49	20	3	7 (3H, 4UH)
613	Q5VY43|PEAR1_HUMAN	Platelet endothelial aggregation receptor 1	3	1	0	1 (UH)
614	P30086|PEBP1_HUMAN	Phosphatidylethanolamine-binding protein 1	39	52	3	6 (3H, 3UH)
615	P16284-2|PECA1_HUMAN	Isoform Delta12 of Platelet endothelial cell adhesion molecule	90	21	3	5 (2H, 3UH)
616	PEPD_HUMAN	Xaa-Pro dipeptidase	3	13	1	0
617	PERE_HUMAN	Eosinophil peroxidase	7	11	0	1 (UH)

	Accession #	Protein name	Number of peptide	% Sequence coverage	Presence	
					Control	*Survivor*
618	P05164-2|PERM_HUMAN (+2)	Isoform H14 of Myeloperoxidase	170	21	5	10
619	P10720|PF4V_HUMAN	Platelet factor 4 variant	300	64	5	10
620	PFD2_HUMAN	Prefoldin subunit 2	3	16	1	0
621	PGAM1_HUMAN	Phosphoglycerate mutase 1	37	23	3	4 (2H, 2UH)
622	PGAM2_HUMAN	Phosphoglycerate mutase 2	3	18	1	0
623	sp|P23219-2|PGH1_HUMAN	Isoform Short of Prostaglandin G/H synthase 1	32	10	4	4 (2H, 2UH)
624	P00558|PGK1_HUMAN	Phosphoglycerate kinase 1	283	52	5	10
625	PGK2_HUMAN	Phosphoglycerate kinase 2	15		2	1 (H)
626	sp|P36871|PGM1_HUMAN	Phosphoglucomutase-1	5	7	0	2 (H, UH)
627	PGM2_HUMAN	Phosphoglucomutase-2	4	4	1	1 (H)
628	PGRC1_HUMAN	Membrane-associated progesterone receptor component 1	20	18	2	4 (2H, 2UH)
629	PGRP1_HUMAN	Peptidoglycan recognition protein 1	5	30	0	1 (UH)
630	PHB_HUMAN	Prohibitin	22	12	3	5 (3H, 2UH)
631	PHB2_HUMAN	Prohibitin-2	18	12	3	3 (1H, 2UH)
632	PI42A_HUMAN	Phosphatidylinositol 5-phosphate 4-kinase type-2 alpha	31	13	2	4 (2H, 2UH)
633	sp|P22061-2|PIMT_HUMAN	Isoform 2 of Protein-L-isoaspartate(D-aspartate) O-methyltransferase	13	18	2	2 (H, UH)
634	PIN1_HUMAN	Peptidyl-prolyl cis-trans isomerase NIMA-interacting 1	2	16	0	1 (UH)
635	Q8TD55-2|PKHO2_HUMAN	Isoform 2 of Pleckstrin homology domain-containing family O member 2	7	6	0	2 (H, UH)
636	sp|Q15149-3|PLEC_HUMAN	Isoform 3 of Plectin	96	3	1	6 (2H, 4UH)
637	P08567|PLEK_HUMAN	Pleckstrin	390	48	5	10
638	P02776|PLF4_HUMAN	Platelet factor 4	279	63	5	10
639	sp|O60664-3|PLIN3_HUMAN (+1)	Isoform 3 of Perilipin-3	2	4	0	1 (UH)
640	PLIN3_HUMAN	Perilipin-3	2	5	0	1 (UH)
641	PLMN_HUMAN	Plasminogen	7	6	1	1 (UH)
642	P13796|PLSL_HUMAN	Plastin-2	93	21	4	6 (2H, 4UH)
643	PLST_HUMAN	Plastin-3	3	6	0	1 (UH)
644	Q6XQN6-2|PNCB_HUMAN	Isoform 2 of Nicotinate phosphoribosyltransferase	3	5	0	1 (UH)
645	sp|Q8N490-3|PNKD_HUMAN	Isoform 3 of Probable hydrolase PNKD	2	9	0	1 (H)

	Accession #	Protein name	Number of peptide	% Sequence coverage	Presence	
					Control	*Survivor*
646	P00491|PNPH_HUMAN	Purine nucleoside phosphorylase	23	16	3	3 (2H, 1UH)
647	POTEE_HUMAN	POTE ankyrin domain family member E	586	19	5	4 (2H, 2UH)
648	POTEI_HUMAN	POTE ankyrin domain family member I	165	18	1	2 (1H, 1UH)
649	POTEJ_HUMAN	POTE ankyrin domain family member J	237	17	3	3 (2H, 1UH)
650	PP1A_HUMAN	Serine/threonine-protein phosphatase PP1-alpha catalytic subunit	11	6	0	3 (2H, 1UH)
651	PP1B_HUMAN	Serine/threonine-protein phosphatase PP1-beta catalytic subunit	5	6	0	2 (1H, 1UH)
652	sp|Q96A00-2|PP14A_HUMAN	Serine/threonine-protein phosphatase PP1-alpha catalytic subunit	11	8	0	3 (2H, UH)
653	**PP1G_HUMAN**	Serine/threonine-protein phosphatase PP1-gamma catalytic subunit			0	1 (H)
654	TPP2_HUMAN	Tripeptidyl-peptidase 2	2	2	0	1 (H)
655	P24666|PPAC_HUMAN	Low molecular weight phosphotyrosine protein phosphatase	19	19	3	4 (2H, 2UH)
656	P48147|PPCE_HUMAN	Prolyl endopeptidase	5	4	1	1 (UH)
657	PPGB_HUMAN	Lysosomal protective protein	17	10	3	2 (1H, 1UH)
658	P62937|PPIA_HUMAN	Peptidyl-prolyl cis-trans isomerase A	251	78	5	10
659	P23284|PPIB_HUMAN	Peptidyl-prolyl cis-trans isomerase B	56	32	4	8 (4H, 4UH)
660	P30405|PPIF_HUMAN	Peptidyl-prolyl cis-trans isomerase F, mitochondrial	135	64	5	10
661	Q9H939|PPIP2_HUMAN	Proline-serine-threonine phosphatase-interacting protein 2	41	29	2	4 (2H, 2UH)
662	sp|P35813-2|PPM1A_HUMAN	Isoform Alpha-2 of Protein phosphatase 1A	7	11	1	2 (H, UH)
663	PRAF3_HUMAN	PRA1 family protein 3	12	15	1	3 (2H, 1UH)
664	Q06830|PRDX1_HUMAN	Peroxiredoxin-1	47	33	2	4 (2H, 2UH)
665	P32119|PRDX2_HUMAN	Peroxiredoxin-2	17	24	3	2 (2UH)
666	P30048|PRDX3_HUMAN	Thioredoxin-dependent peroxide reductase, mitochondrial	63	31	4	6 (4H, 2UH)
667	Q13162|PRDX4_HUMAN	Peroxiredoxin-4	14	14	2	3 (H, 2UH)
668	P30044-2|PRDX5_HUMAN	Isoform Cytoplasmic+peroxisomal of Peroxiredoxin-5, mitochondrial	53	39	4	9 (5H, 4UH)
669	P30041|PRDX6_HUMAN	Peroxiredoxin-6	129	43	5	10
670	P07737|PROF1_HUMAN	Profilin-1	347	75	5	10
671	PROS_HUMAN	Vitamin K-dependent protein S	23	8	2	3 (2H, 1UH)
672	PRS10_HUMAN	26S protease regulatory subunit 10B	2	7	1	0

	Accession #	Protein name	Number of peptide	% Sequence coverage	Presence	
					Control	*Survivor*
673	P24158|PRTN3_HUMAN	Myeloblastin	10	14	1	2 (UH)
674	P55786|PSA_HUMAN	Puromycin-sensitive aminopeptidase	11	3	2	3 (1H, 2UH)
675	Q06323|PSME1_HUMAN	Proteasome activator complex subunit 1	11	20	2	1 (UH)
676	sp|P06454-2|PTMA_HUMAN	Isoform 2 of Prothymosin alpha	12	20	2	2 (2UH)
677	sp|Q06124-2|PTN11_HUMAN	Isoform 2 of Tyrosine-protein phosphatase non-receptor type 11	2	5	0	1 (UH)
678	Q05209|PTN12_HUMAN	Tyrosine-protein phosphatase non-receptor type 12	16	5	1	3 (1H, 2UH)
679	sp|Q99952-2|PTN18_HUMAN	Isoform 2 of Tyrosine-protein phosphatase non-receptor type 18	22	18	2	4 (2H, 2UH)
680	sp|P29350-4|PTN6_HUMAN	Isoform 4 of Tyrosine-protein phosphatase non-receptor type 6	14	3	1	4 (1H, 3UH)
681	P08575-2|PTPRC_HUMAN	Isoform 2 of Receptor-type tyrosine-protein phosphatase C	41	6	2	4 (2H, 2UH)
682	PTPRJ_HUMAN	Receptor-type tyrosine-protein phosphatase eta	15	3	2	3 (2H, 1UH)
683	sp|P22234-2|PUR6_HUMAN	Isoform 2 of Multifunctional protein ADE2	2	5	1	0
684	P31939|PUR9_HUMAN	Bifunctional purine biosynthesis protein PURH	51	13	3	7 (4H, 3UH)
685	PYGB_HUMAN	Glycogen phosphorylase, brain form	25	5	4	3 (2H, 1UH)
686	PYGL_HUMAN	Glycogen phosphorylase, liver form	7	5	1	2 (1H, 1UH)
687	QCR1_HUMAN	Cytochrome b-c1 complex subunit 1, mitochondrial	14	11	2	2 (1H, 1UH)
688	QCR2_HUMAN	Cytochrome b-c1 complex subunit 2, mitochondrial	11	9	2	2 (1H, 1UH)
689	P07919|QCR6_HUMAN	Cytochrome b-c1 complex subunit 6, mitochondrial	9	47	1	2 (1H, 1UH)
690	RAB10_HUMAN	Ras-related protein Rab-10	44	32	2	4 (2H, 2UH)
691	RAB14_HUMAN	Ras-related protein Rab-14	52	19	3	4 (2H, 2UH)
692	sp|P62820|RAB1A_HUMAN	Ras-related protein Rab-1A	60	39	4	4 (2H, 2UH)
693	Q9H0U4|RAB1B_HUMAN	Ras-related protein Rab-1B	94	22	4	7 (4H, 3UH)
694	RAB21_HUMAN	Ras-related protein Rab-21	11	11	1	3 (1H, 2UH)
695	sp|P61019-2|RAB2A_HUMAN	Isoform 2 of Ras-related protein Rab-2A	6	18	0	2 (1H, 1UH)
696	RAB32_HUMAN	Ras-related protein Rab-32	4	15	0	1 (UH)
697	RAB35_HUMAN	Ras-related protein Rab-35	2	21	1	0
698	RAB37_HUMAN	Ras-related protein Rab-37	4	9	0	1 (UH)
699	RAB43_HUMAN	Ras-related protein Rab-43	5	8	1	1 (UH)
700	RAB44_HUMAN	Ras-related protein Rab-44	2	3	0	1 (UH)
701	RAB4B_HUMAN	Ras-related protein Rab-4B	4		0	1 (H)
702	RAB5A_HUMAN	Ras-related protein Rab-5A	10	15	1	2

	Accession #	Protein name	Number of peptide	% Sequence coverage	Presence	
					Control	*Survivor*
						(1H, 1UH)
703	RAB5C_HUMAN	Cluster of Ras-related protein Rab-5C	15	12	1	3 (1H, 2UH)
704	sp|P20340-2|RAB6A_HUMAN	Isoform 2 of Ras-related protein Rab-6A	37	32	2	4 (2H, 2UH)
705	RAB6B_HUMAN	Ras-related protein Rab-6B	27	32	2	2 (1H, 1UH)
706	P51149|RAB7A_HUMAN	Ras-related protein Rab-7a	78	45	5	8 (4H, 4UH)
707	RAB8A_HUMAN	Ras-related protein Rab-8A	64	16	3	9 (5H, 4UH)
708	RAB8B_HUMAN	Ras-related protein Rab-8B	22	27	1	2 (H, UH)
709	RAB9B_HUMAN	Ras-related protein Rab-9B	3		0	1 (H)
710	P63000-2|RAC1_HUMAN	Isoform B of Ras-related C3 botulinum toxin substrate 1	68	40	2	5 (2H, 3UH)
711	P15153|RAC2_HUMAN	Ras-related C3 botulinum toxin substrate 2	83	33	2	6 (2H, 4UH)
712	RADI_HUMAN	Radixin	67	20	2	3 (1H, 2UH)
713	RALB_HUMAN	Ras-related protein Ral-B	15	14	2	2 (UH)
714	RAN_HUMAN	GTP-binding nuclear protein Ran	11	10	2	3 (1H, 2UH)
715	P43487|RANG_HUMAN	Ran-specific GTPase-activating protein	2	8	0	2 (1H, 1UH)
716	RAP1A_HUMAN	Ras-related protein Rap-1A	62	74	1	1 (UH)
717	P61224|RAP1B_HUMAN	Ras-related protein Rap-1b	381	76	5	10
718	RAP2B_HUMAN	Cluster of Ras-related protein Rap-2b	6	22	0	2 (UH)
719	RAP2C_HUMAN	Ras-related protein Rap-2c	5	18	0	2 (UH)
720	RARR2_HUMAN	Retinoic acid receptor responder protein 2	2	11	1	0
721	RASA3_HUMAN	Ras GTPase-activating protein 3	23	6	3	3 (2UH, 1H)
722	RASK_HUMAN	GTPase KRas	8	16	1	2 (1H, 1UH)
723	RASN_HUMAN	GTPase NRas	2		0	1 (H)
724	RB11A_HUMAN	Ras-related protein Rab-11A	9	11	0	1 (H)
725	RB11B_HUMAN	Ras-related protein Rab-11B	343	37	5	10
726	RB27B_HUMAN	Ras-related protein Rab-27B	128	29	4	10
727	RB33B_HUMAN	Ras-related protein Rab-33B	2	7	0	1 (UH)
728	RB39B_HUMAN	Ras-related protein Rab-39B	4		0	1 (UH)
729	sp|Q8TC12|RDH11_HUMAN	Retinol dehydrogenase 11 OS=Homo sapiens GN=RDH11 PE=1 SV=2	11	10	2	2 (1H, 1UH)
730	Q9H4X1-2|RGCC_HUMAN	Isoform 2 of Regulator of cell cycle RGCC	19	35	2	5 (2H, 3UH)

	Accession #	Protein name	Number of peptide	% Sequence coverage	Presence	
					Control	*Survivor*
731	sp|O43665-3|RGS10_HUMAN	Isoform 3 of Regulator of G-protein signaling 10	19	32	2	2 (1H, 1UH)
732	RHG01_HUMAN	Rho GTPase-activating protein 1	6	6	1	1 (H)
733	O43182-4|RHG06_HUMAN	Isoform 4 of Rho GTPase-activating protein 6	15	4	1	4 (2H, 2UH)
734	sp|Q8N392-2|RHG18_HUMAN	Isoform 2 of Rho GTPase-activating protein 18	16	7	2	3 (2H, 1UH)
735	P61586|RHOA_HUMAN	Transforming protein RhoA	84	45	4	7 (2H, 5UH)
736	RHOC_HUMAN	Rho-related GTP-binding protein RhoC	19	22	2	2 (1H, 1UH)
737	RHOG_HUMAN	Rho-related GTP-binding protein RhoG	13	25	2	2 (UH)
738	RINI_HUMAN	Ribonuclease inhibitor	12	7	2	3 (1H, 2UH)
739	P62906|RL10A_HUMAN	60S ribosomal protein L10a	2	8	0	1 (UH)
740	sp|P30050|RL12_HUMAN	60S ribosomal protein L12	3	19	1	0
741	RL18_HUMAN	60S ribosomal protein L18	2	10	1	0
742	RL26L_HUMAN	60S ribosomal protein L26-like 1	2	17	1	0
743	RL38_HUMAN	60S ribosomal protein L38	2	28	1	0
744	RL4_HUMAN	60S ribosomal protein L4	3	6	0	1 (H)
745	RL40_HUMAN	Ubiquitin-60S ribosomal protein L40	25	20	2	7 (4H, 3UH)
746	RL6_HUMAN	60S ribosomal protein L6	2	6	1	0
747	RL7_HUMAN	60S ribosomal protein L7	4	8	2	0
748	RL8_HUMAN	60S ribosomal protein L8	2	7	1	0
749	RLA1_HUMAN	60S acidic ribosomal protein P1	7	27	2	1 (UH)
750	RLA2_HUMAN	60S acidic ribosomal protein P2	16	27	5	1 (H)
751	sp|P09651-2|ROA1_HUMAN	Isoform A1-A of Heterogeneous nuclear ribonucleoprotein A1	13	11	1	3 (1H, 2UH)
752	P22626-2|ROA2_HUMAN	Isoform A2 of Heterogeneous nuclear ribonucleoproteins A2/B1	35	16	2	5 (2H, 3UH)
753	sp|P51991|ROA3_HUMAN	Heterogeneous nuclear ribonucleoprotein A3	5	9	1	1 (H)
754	ROCK1_HUMAN	Rho-associated protein kinase 1	16	5	2	2 (1H, 1UH)
755	O75116|ROCK2_HUMAN	Rho-associated protein kinase 2	82	9	4	5 (2H, 3UH)
756	RPN1_HUMAN	Dolichyl-diphosphooligosaccharide--protein glycosyltransferase subunit 1	32	10	3	4 (2H, 2UH)
757	sp|P04844-2|RPN2_HUMAN	Isoform 2 of Dolichyl-diphosphooligosaccharide--protein glycosyltransferase subunit 2	2	8	1	0
758	RS12_HUMAN	40S ribosomal protein S12	6	19	2	0
759	RS21_HUMAN	40S ribosomal protein S21	4	29	2	0
760	RS27_HUMAN	40S ribosomal protein S27	2	22	1	0

	Accession #	Protein name	Number of peptide	% Sequence coverage	Presence	
					Control	*Survivor*
761	RS28_HUMAN	40S ribosomal protein S28	3	28	1	0
762	RS3A_HUMAN	40S ribosomal protein S3a	2	9	1	0
763	RSSA_HUMAN	40S ribosomal protein SA	4	8	2	0
764	Q15404-2|RSU1_HUMAN	Isoform 2 of Ras suppressor protein 1	129	36	5	9 (5H, 4UH)
765	Q16799|RTN1_HUMAN	Reticulon-1 OS=Homo sapiens	4	3	0	2 (1H, 1UH)
766	Q9NQC3-2|RTN4_HUMAN	Isoform 2 of Reticulon-4	84	14	5	10
767	RUFY1_HUMAN	RUN and FYVE domain-containing protein 1	3	11	0	1 (H)
768	S100P_HUMAN	Protein S100-P	2	26	0	1 (UH)
769	P26447|S10A4_HUMAN	Protein S100-A4	78	62	4	9 (4H, 5UH)
770	S10A6_HUMAN	Protein S100-A6	2	14	0	1 (H)
771	P05109|S10A8_HUMAN	Protein S100-A8	33	43	2	5 (1H, 4UH)
772	P06702|S10A9_HUMAN	Protein S100-A9	89	59	4	7 (3H, 4UH)
773	S10AA_HUMAN	Protein S100-A10	7	39	1	1 (UH)
774	S10AB_HUMAN	Protein S100-A11	3	31	1	0
775	S10AC_HUMAN	Protein S100-A12	5	33	1	1 (UH)
776	SAC1_HUMAN	Phosphatidylinositide phosphatase SAC1	38	10	2	4 (2H, 2UH)
777	SAHH_HUMAN	Adenosylhomocysteinase	4	5	1	1 (UH)
778	P07602-2|SAP_HUMAN	Isoform Sap-mu-6 of Proactivator polypeptide	40	8	3	5 (2H, 3UH)
779	SARG_HUMAN	Specifically androgen-regulated gene protein	2	4	1	0
780	SC22B_HUMAN	Vesicle-trafficking protein SEC22b	4	10	0	2 (1H, 1UH)
781	SCAM2_HUMAN	Secretory carrier-associated membrane protein 2	6	7	1	2 (1H, 1UH)
782	SCMC1_HUMAN	Calcium-binding mitochondrial carrier protein SCaMC-1	2	5	0	1 (UH)
783	P55809|SCOT1_HUMAN	Succinyl-CoA:3-ketoacid coenzyme A transferase 1, mitochondrial	18	6	2	2 (1H, 1UH)
784	O95810|SDPR_HUMAN	Serum deprivation-response protein	404	55	5	10
785	sp|Q9NVA2-2|SEP11_HUMAN	Isoform 2 of Septin-11	88	14	5	7 (4H, 3UH)
786	Q15019-2|SEPT2_HUMAN	Isoform 2 of Septin-2	61	22	3	9 (5H, 4UH)
787	sp|Q99719|SEPT5_HUMAN	Septin-5 OS=Homo sapiens	9	8	2	1 (UH)
788	Q14141-2|SEPT6_HUMAN	Isoform I of Septin-6	67	22	4	8 (4H, 4UH)
789	Q16181-2|SEPT7_HUMAN	Isoform 2 of Septin-7	88	23	3	8

	Accession #	Protein name	Number of peptide	% Sequence coverage	Presence	
					Control	*Survivor*
						(4H, 4UH)
790	sp|Q9UHD8-2|SEPT9_HUMAN	Isoform 2 of Septin-9	4	7	0	1 (UH)
791	sp|Q01105-2|SET_HUMAN	Isoform 2 of Protein SET	6	13	1	1 (UH)
792	sp|P23246-2|SFPQ_HUMAN	Isoform Short of Splicing factor, proline- and glutamine-rich	2	3	1	0
793	SFXN1_HUMAN	Sideroflexin-1	2	5	1	0
794	SFXN3_HUMAN	Sideroflexin-3	2	5	1	0
795	SH3G1_HUMAN	Endophilin-A2	2	7	0	1 (H)
796	SH3L1_HUMAN	SH3 domain-binding glutamic acid-rich-like protein	37	44	3	8 (5H, 3UH)
797	Q9H299|SH3L3_HUMAN	SH3 domain-binding glutamic acid-rich-like protein 3	84	59	5	10
798	SKAP2_HUMAN	Src kinase-associated phosphoprotein 2	14	17	0	3 (2H, 1UH)
799	Q9UIB8-2|SLAF5_HUMAN	Isoform 2 of SLAM family member 5	11	19	1	2 (UH)
800	SLK_HUMAN	Isoform 2 of STE20-like serine/threonine-protein kinase	4	2	0	2 (1H, 1UH)
801	sp|Q14BN4-2|SLMAP_HUMAN	Isoform 2 of Sarcolemmal membrane-associated protein	6	4	1	1 (UH)
802	SMIM1_HUMAN	Small integral membrane protein 1	2	21	0	1 (UH)
803	SNAA_HUMAN	Alpha-soluble NSF attachment protein	9	13	1	2 (H, UH)
804	SND1_HUMAN	Staphylococcal nuclease domain-containing protein 1	16	6	1	2 (UH)
805	O00161|SNP23_HUMAN	Synaptosomal-associated protein 23	88	45	3	9 (5H, 4UH)
806	SNTB1_HUMAN	Beta-1-syntrophin	2	4	1	0
807	SNX2_HUMAN	Sorting nexin-2	4	5	1	1 (H)
808	SODC_HUMAN	Superoxide dismutase [Cu-Zn]	103	71	5	10
809	P04179-2|SODM_HUMAN	Isoform 2 of Superoxide dismutase [Mn], mitochondrial	9	31	0	3 (2H, 1UH)
810	SORCN_HUMAN	Sorcin	5	12	2	0
811	P09486|SPRC_HUMAN	SPARC	200	51	5	10
812	sp|P02549|SPTA1_HUMAN	Spectrin alpha chain, erythrocytic 1	14	2	1	4 (2H, 2UH)
813	P11277-2|SPTB1_HUMAN	Isoform 2 of Spectrin beta chain, erythrocytic	48	5	1	6 (3H, 3UH)
814	Q01082|SPTB2_HUMAN	Spectrin beta chain, non-erythrocytic 1	32	3	2	5 (2H, 3UH)
815	sp|Q13813-2|SPTN1_HUMAN	Isoform 2 of Spectrin alpha chain, non-erythrocytic 1	3	0	1	0
816	SQRD_HUMAN	Sulfide:quinone oxidoreductase, mitochondrial	3	5	1	0
817	P12931-2|SRC_HUMAN	Isoform 2 of Proto-oncogene tyrosine-protein kinase Src	62	18	3	4 (2H, 2UH)
818	Q14247-3|SRC8_HUMAN	Isoform 3 of Src substrate cortactin	181	31	5	10
819	P10124|SRGN_HUMAN	Serglycin	166	49	5	10

	Accession #	Protein name	Number of peptide	% Sequence coverage	Presence	
					Control	*Survivor*
820	SRSF1_HUMAN	Serine/arginine-rich splicing factor 1	4	8	2	0
821	SRSF3_HUMAN	Serine/arginine-rich splicing factor 3	2	20	1	0
822	ST1A3_HUMAN	Sulfotransferase 1A3/1A4	3	12	0	1 (UH)
823	STA5A_HUMAN (+1)	Signal transducer and activator of transcription 5A	2	3	0	1 (H)
824	STIM1_HUMAN	Stromal interaction molecule 1	62	22	3	3 (2H, 1UH)
825	P31948|STIP1_HUMAN	Stress-induced-phosphoprotein 1	37	11	3	5 (2H, 3UH)
826	STK10_HUMAN	Serine/threonine-protein kinase 10	2	3	0	1 (UH)
827	sp|Q9Y6E0-2|STK24_HUMAN	Cluster of Isoform A of Serine/threonine-protein kinase 24	4	10	0	1 (H)
828	STML2_HUMAN	Stomatin-like protein 2	2	6	1	0
829	STMN1_HUMAN	Stathmin	3	17	1	0
830	sp|P27105|STOM_HUMAN	Erythrocyte band 7 integral membrane protein	112	41	4	5 (2H, 3UH)
831	STRAP_HUMAN	Serine-threonine kinase receptor-associated protein	5	10	1	1 (UH)
832	sp|O43815-2|STRN_HUMAN	Isoform 2 of Striatin	2	3	0	1 (UH)
833	STX11_HUMAN	Syntaxin-11	32	30	2	2 (1H, 1UH)
834	O15400-2|STX7_HUMAN	Isoform 2 of Syntaxin-7	23	20	3	3 (1H, 2UH)
835	sp|Q15833|STXB2_HUMAN	Syntaxin-binding protein 2	70	16	3	5 (3H, 2UH)
836	sp|Q96I99|SUCB2_HUMAN	Succinyl-CoA ligase [GDP-forming] subunit beta, mitochondrial	2	4	1	0
837	SUMO3_HUMAN	Small ubiquitin-related modifier 3	2	12	0	1 (H)
838	SYAC_HUMAN	Alanine--tRNA ligase, cytoplasmic	5	3	1	1 (UH)
839	SYSC_HUMAN	Serine--tRNA ligase, cytoplasmic	16	7	2	3 (3UH)
840	sp|Q96C24|SYTL4_HUMAN	Synaptotagmin-like protein 4	91	22	4	8 (4H, 4UH)
841	sp|P37840|SYUA_HUMAN	Alpha-synuclein	33	53	2	3 (2H, 1UH)
842	sp|P23381|SYWC_HUMAN	Tryptophan--tRNA ligase, cytoplasmic	2	4	0	1 (UH)
843	SYYC_HUMAN	Tyrosine--tRNA ligase, cytoplasmic	12	10	0	3 (2H, 1UH)
844	P37802|TAGL2_HUMAN	Transgelin-2	264	67	5	10
845	P37837|TALDO_HUMAN	Transaldolase	45	16	3	5 (2H, 3UH)
846	TAOK3_HUMAN	Serine/threonine-protein kinase TAO3	6	3	1	1 (UH)
847	TAP1_HUMAN	Antigen peptide transporter 1	2	3	0	1 (UH)
848	sp|Q03519-2|TAP2_HUMAN	Isoform 2 of Antigen peptide transporter 2	3	6	0	1 (UH)

	Accession #	Protein name	Number of peptide	% Sequence coverage	Presence	
					Control	*Survivor*
849	Q71U36|TBA1A_HUMAN	Tubulin alpha-1A chain	121	61	0	3 (3H, 1UH)
850	P68363|TBA1B_HUMAN	Tubulin alpha-1B chain	543	60	5	9 (4H, 5UH)
851	Q9BQE3|TBA1C_HUMAN	Tubulin alpha-1C chain	491	60	5	6 (4H, 2UH)
852	TBA3C_HUMAN	Tubulin alpha-3C/D chain	169	60	2	2 (1H, 1UH)
853	P68366|TBA4A_HUMAN	Tubulin alpha-4A chain	707	61	5	10
854	Q9NY65|TBA8_HUMAN	Tubulin alpha-8 chain	303	36	5	8 (4H, 4UH)
855	TBAL3_HUMAN	Isoform 2 of Tubulin alpha chain-like 3	17	17	1	2 (1H, 1UH)
856	Q9H4B7|TBB1_HUMAN	Tubulin beta-1 chain	522	60	5	10
857	TBB3_HUMAN	Tubulin beta-3 chain	96	35	0	4 (2H, 2UH)
858	TBB4A_HUMAN	Tubulin beta-4A chain	34	63	1	0
859	P68371|TBB4B_HUMAN	Tubulin beta-4B chain	574	60	5	10
860	P07437|TBB5_HUMAN	Tubulin beta chain	461	58	5	10
861	TBCA_HUMAN	Tubulin-specific chaperone A	7	30	2	1 (UH)
862	TBCB_HUMAN	Tubulin-folding cofactor B	2	9	1	0
863	TCPA_HUMAN	T-complex protein 1 subunit alpha	19	8	2	3 (2H, 1UH)
864	sp|P78371|TCPB_HUMAN	T-complex protein 1 subunit beta	24	13	2	3 (2H, 1UH)
865	TCPD_HUMAN	T-complex protein 1 subunit delta	14	11	2	2 (1H, 1UH)
866	TCPE_HUMAN	T-complex protein 1 subunit epsilon	14	6	1	4 (2H, 2UH)
867	sp|P49368|TCPG_HUMAN	T-complex protein 1 subunit gamma	28	13	2	2 (1H, 1UH)
868	sp|Q99832|TCPH_HUMAN	T-complex protein 1 subunit eta	12	7	2	2 (1H, 1UH)
869	TCPQ_HUMAN	T-complex protein 1 subunit theta	21	10	2	3 (2H, 1UH)
870	TCPZ_HUMAN	T-complex protein 1 subunit zeta	7	7	1	1 (UH)
871	TCTP_HUMAN	Translationally-controlled tumor protein	8	27	2	1 (UH)
872	TEBP_HUMAN	Prostaglandin E synthase 3	2	17	0	1 (UH)
873	P55072|TERA_HUMAN	Transitional endoplasmic reticulum ATPase	122	19	5	8 (4H, 4UH)
874	TGFB1_HUMAN	Transforming growth factor beta-1	45	17	3	5 (3H, 2UH)
875	O43294-2|TGFI1_HUMAN	Isoform 2 of Transforming growth factor beta-1-induced transcript 1 protein	6	11	0	2 (1H, 1UH)
876	THAS_HUMAN	Thromboxane-A synthase	23	14	1	3 (2H, 1UH)
877	P42765|THIM_HUMAN	3-ketoacyl-CoA thiolase,	11	12	0	4

	Accession #	Protein name	Number of peptide	% Sequence coverage	Presence	
					Control	*Survivor*
		mitochondrial				(2H, 2UH)
878	THIO_HUMAN	Thioredoxin	47	31	4	8 (4H, 4UH)
879	THTM_HUMAN	3-mercaptopyruvate sulfurtransferase	2	5	1	0
880	Q16762|THTR_HUMAN	Thiosulfate sulfurtransferase	30	15	4	5 (1H, 4UH)
881	TIMP1_HUMAN	Metalloproteinase inhibitor 1	9	23	1	1 (UH)
882	TIMP3_HUMAN	Metalloproteinase inhibitor 3	2	17	0	1 (H)
883	P29401|TKT_HUMAN	Transketolase	40	12	2	5 (3H, 2UH)
884	Q9Y490|TLN1_HUMAN	Talin-1	2760	61	5	10
885	Q9Y4G6|TLN2_HUMAN	Talin-2	110	9	1	3 (1H, 2UH)
886	sp|Q5BJD5-2|TM41B_HUMAN	Isoform 2 of Transmembrane protein 41B	2	12	0	1 (UH)
887	TMA7_HUMAN	Translation machinery-associated protein 7	2	38	1	0
888	TMED7_HUMAN	Transmembrane emp24 domain-containing protein 7	2	10	0	1 (H)
889	TMEDA_HUMAN	Transmembrane emp24 domain-containing protein 10	12	19	2	2 (1H, 1UH)
890	Q8WWA1-2|TMM40_HUMAN	Isoform 2 of Transmembrane protein 40	16	18	2	2 (1H, 1UH)
891	Q9NYL9|TMOD3_HUMAN	Tropomodulin-3	81	25	5	7 (4H, 3UH)
892	TMX1_HUMAN	Thioredoxin-related transmembrane protein 1	7	10	1	2 (1H, 1UH)
893	TOR4A_HUMAN	Torsin-4A	2	3	0	1 (H)
894	O43399-2|TPD54_HUMAN	Isoform 2 of Tumor protein D54	11	17	2	2 (1H, 1UH)
895	P60174-1|TPIS_HUMAN	Isoform 2 of Triosephosphate isomerase	191	59	5	10
896	P09493-3|TPM1_HUMAN	Isoform 3 of Tropomyosin alpha-1 chain	1406	83	5	10
897	P07951-2|TPM2_HUMAN	Isoform 2 of Tropomyosin beta chain	294	44	4	10
898	P06753-2|TPM3_HUMAN	Isoform 2 of Tropomyosin alpha-3 chain	533	87	5	10
899	TPM3L_HUMAN	Putative tropomyosin alpha-3 chain-like protein	5	30	1	0
900	P67936-2|TPM4_HUMAN	Isoform 2 of Tropomyosin alpha-4 chain	740	86	4	10
901	O14773-2|TPP1_HUMAN	Isoform 2 of Tripeptidyl-peptidase 1	33	10	4	6 (3H, 3UH)
902	sp|O15533-2|TPSN_HUMAN	Isoform 2 of Tapasin	2	7	0	1 (UH)
903	TRFE_HUMAN	Serotransferrin	59	10	4	4 (2H, 2UH)
904	P02788-2|TRFL_HUMAN	Isoform DeltaLf of Lactotransferrin	77	16	1	5 (2H, 3UH)
905	Q86YW5|TRML1_HUMAN	Trem-like transcript 1 protein	128	36	5	10
906	P07477|TRY1_HUMAN	Trypsin-1	31	27	3	7

	Accession #	Protein name	Number of peptide	% Sequence coverage	Presence	
					Control	*Survivor*
						(3H, 4UH)
907	P07478|TRY2_HUMAN	Trypsin-2	13	22	0	5 (3H, 2UH)
908	P35030-2|TRY3_HUMAN	Isoform B of Trypsin-3	18	11	2	6 (1H, 5UH)
909	Q8NHM4|TRY6_HUMAN	Putative trypsin-6	11	15	3	6 (2H, 4UH)
910	P07996|TSP1_HUMAN	Thrombospondin-1	1568	66	5	10
911	TTHY_HUMAN	Transthyretin	4	17	0	2 (H, UH)
912	TWF2_HUMAN	Twinfilin-2	12	13	1	3 (2H, 1UH)
913	O95881|TXD12_HUMAN	Thioredoxin domain-containing protein 12	11	18	0	4 (1H, 3UH)
914	Q9BRA2|TXD17_HUMAN	Thioredoxin domain-containing protein 17	5	31	0	2 (1H, 1UH)
915	TXND5_HUMAN	Thioredoxin domain-containing protein 5	11	8	1	3 (2H, 1UH)
916	P63313|TYB10_HUMAN	Thymosin beta-10	16	42	2	2 (UH)
917	P62328|TYB4_HUMAN	Thymosin beta-4	221	69	5	10
918	TYPH_HUMAN	Thymidine phosphorylase	20	10	2	3 (2H, 1UH)
919	UBA1_HUMAN	Ubiquitin-like modifier-activating enzyme 1	27	6	2	4 (2H, 2UH)
920	UBA7_HUMAN	Ubiquitin-like modifier-activating enzyme 7	5	3	1	1 (UH)
921	P0CG47|UBB_HUMAN	Polyubiquitin-B	12	14	0	4 (2H, 2UH)
922	UBE2N_HUMAN	Ubiquitin-conjugating enzyme E2 N	2	12	0	1 (UH)
923	sp|P45974-2|UBP5_HUMAN	Isoform Short of Ubiquitin carboxyl-terminal hydrolase 5	2	4	0	1 (UH)
924	UBS3B_HUMAN	Ubiquitin-associated and SH3 domain-containing protein B	2	2	0	1 (H)
925	UCRI_HUMAN	Cytochrome b-c1 complex subunit Rieske, mitochondrial	7	17	1	1 (UH)
926	sp|Q9NYU2-2|UGGG1_HUMAN	Isoform 2 of UDP-glucose:glycoprotein glucosyltransferase 1	9	2	2	2 (1H, 1UH)
927	sp|Q16851-2|UGPA_HUMAN	Isoform 2 of UTP--glucose-1-phosphate uridylyltransferase	8	5	2	1 (UH)
928	Q70J99-3|UN13D_HUMAN	Isoform 3 of Protein unc-13 homolog D	26	4	3	4 (2H, 2UH)
929	Q86UX7-2|URP2_HUMAN	Isoform 2 of Fermitin family homolog 3	433	44	5	10
930	sp|O60763-2|USO1_HUMAN	Isoform 2 of General vesicular transport factor p115	3	4	0	1 (UH)
931	Q15836|VAMP3_HUMAN	Vesicle-associated membrane protein 3	10	26	3	2 (UH)
932	VAMP8_HUMAN	Vesicle-associated membrane protein 8	13	36	2	2 (1H, 1UH)
933	sp|Q9P0L0-2|VAPA_HUMAN	Isoform 2 of Vesicle-associated membrane protein-associated protein A	18	9	2	2 (1H, 1UH)
934	VAPB_HUMAN	Vesicle-associated membrane protein-associated protein B/C	11	13	1	2 (1H, 1UH)
935	P50552|VASP_HUMAN	Vasodilator-stimulated phosphoprotein	182	38	5	10
936	VATA_HUMAN	V-type proton ATPase catalytic	2	4	0	1

	Accession #	Protein name	Number of peptide	% Sequence coverage	Presence	
					Control	*Survivor*
		subunit A				(H)
937	VATB2_HUMAN	V-type proton ATPase subunit B, brain isoform	2	4	1	0
938	VATG1_HUMAN	V-type proton ATPase subunit G 1	4	17	0	2 (1H, 1UH)
939	VDAC1_HUMAN	Voltage-dependent anion-selective channel protein 1	22	17	3	3 (1H, 2UH)
940	sp|P45880-1|VDAC2_HUMAN	Isoform 1 of Voltage-dependent anion-selective channel protein 2	16	11	2	3 (1H, 2UH)
941	sp|Q9Y277-2|VDAC3_HUMAN	Isoform 2 of Voltage-dependent anion-selective channel protein 3	42	19	3	6 (4H, 2UH)
942	P08670|VIME_HUMAN	Vimentin	160	30	5	10
943	P18206-2|VINC_HUMAN	Isoform 1 of Vinculin	720	42	5	10
944	sp|P02774-3|VTDB_HUMAN	Isoform 3 of Vitamin D-binding protein	6	9	1	1 (UH)
945	P04004|VTNC_HUMAN	Vitronectin	13	8	3	2 (1H, 1UH)
946	P04275|VWF_HUMAN	von Willebrand factor	256	12	4	8 (4H, 4UH)
947	WASF2_HUMAN	Wiskott-Aldrich syndrome protein family member 2	9	6	1	2 (1H, 1UH)
948	WASP_HUMAN	Wiskott-Aldrich syndrome protein	14	8	2	3 (2H, 1UH)
949	O75083|WDR1_HUMAN	WD repeat-containing protein 1	556	68	5	10
950	Q5JSH3-2|WDR44_HUMAN	Isoform 2 of WD repeat-containing protein 44	31	6	2	4 (2H, 2UH)
951	O43516-2|WIPF1_HUMAN	Isoform 2 of WAS/WASL-interacting protein family member 1	24	11	2	4 (2H, 2UH)
952	sp|Q9NQW7-2|XPP1_HUMAN	Isoform 2 of Xaa-Pro aminopeptidase 1	2	5	1	0
953	XRCC6_HUMAN	X-ray repair cross-complementing protein 6	2	4	1	0
954	sp|Q7Z2W4-2|ZCCHV_HUMAN	Isoform 2 of Zinc finger CCCH-type antiviral protein 1	2	2	0	1 (H)
955	sp|O15231-3|ZN185_HUMAN (+2)	Isoform 3 of Zinc finger protein 185	4	4	1	1 (UH)
956	Q9UDY2|ZO2_HUMAN	Tight junction protein ZO-2	28	5	2	4 (2H, 2UH)
957	Q15942|ZYX_HUMAN	Zyxin	429	54	5	10

Identification of proteins from purified mitochondria was performed using liquid chromatography-tandem mass spectrometry. Thresholds for identification were: FDR<1%, minimum of 2 peptides per sample. Results are presented as Mean ± SEM. Controls (n=5), Healthy survivors (H, n=5), Unhealthy survivors (UH, n=5).

Supplemental Table II: Proteins displaying regulatory alterations among the different groups

RELATED FUNCTION	PROTEIN NAME	ACCESSION NUMBER	C vs S	C vs H	C vs UH	H vs UH
INFLAMMATION	Alpha-1-acid glycoprotein 1	P02763|A1AG1_HUMAN	↑	↑	↑	↓
	Neutrophil defensin 1	P59665|DEF1_HUMAN	↑	↑		
	Disintegrin and metalloproteinase domain-containing protein 10	O14672|ADA10_HUMAN		↑		
	Ig lambda-2 chain C regions	P0CG05|LAC2_HUMAN			↑	
	Leukotriene A-4 hydrolase	P09960|LKHA4_HUMAN				↓
APOPTOSIS & CELL CYCLE	Serine/threonine-protein kinase PAK 2	Q13177|PAK2_HUMAN	↑		↑	
	Isoform 2 of Prothymosin alpha	P06454-2|PTMA_HUMAN	↑			
	Serine/arginine-rich splicing factor 3	P84103|SRSF3_HUMAN	↑			
	Eukaryotic initiation factor 4A-I	P60842|IF4A1_HUMAN	↑			
	Isoform 5 of Unconventional myosin-XVIIIa	Q926145|MY18A_HUMAN	↓	↓		
	Isoform 2 of Putative ribosomal RNA methyltransferase NOP2	P46087-2|NOP2_HUMAN	↓			
	Galectin-1	P09382|LEG1_HUMAN	↓		↓	
	L-lactate dehydrogenase A chain	P00338|LDHA_HUMAN	↓			
	CDGSH iron-sulfur domain-containing protein 2	Q8N5K1|CISD2_HUMAN	↓			
	Guanine nucleotide-binding protein G(i) subunit alpha-2	P04899|GNAI2_HUMAN		↓		↑
	Laminin subunit gamma-1	P11047|LAMC1_HUMAN		↓		
	14-3-3 protein theta 14-3-3 protein eta	P27348|1433T_HUMAN Q04917|1433F_HUMAN			↑	↓
	Isoform 1 of Four and a half LIM domains protein 1	Q13642-1|FHL1_HUMAN				↓
	Vacuolar protein sorting-associated protein 35	Q96QK1|VPS35_HUMAN				↓

ATP	ATPase inhibitor, mitochondrial	Q9UII2|ATIF1_HUMAN	↑	↑	↑	
	ATP synthase subunit epsilon, mitochondrial ATP synthase subunit delta, mitochondrial	P56381|ATP5E_HUMAN P30049|ATPD_HUMAN	↑		↑	↑
REDOX	Isoform 2 of Malate dehydrogenase, cytoplasmic	P40925-2|MDHC_HUMAN	↓	↓	↓	
	NADH-cytochrome b5 reductase 1	Q9UHQ9|NB5R1_HUMAN	↓			
	Stress-induced-phosphoprotein 1	P31948|STIP1_HUMAN	↓			
	GMP reductase 2	Q9P2T1|GMPR2_HUMAN	↓		↓	
	Glyoxylate reductase/hydroxypyruvate reductase	Q9UBQ7|GRHPR_HUMAN		↑		
	Amine oxidase [flavin-containing] B	P27338|AOFB_HUMAN			↓	
ANTIOXIDANT	Catalase	P04040|CATA_HUMAN	↓			
BETA-OXIDATION	Peroxisomal multifunctional enzyme type 2	P51659|DHB4_HUMAN				↓
	Isoform 2 of Peroxisomal acyl-coenzyme A oxidase 1	Q150672|ACOX1_HUMAN	↑	↑		
	Isoform 3 of Carnitine O-acetyltransferase	P43155-3|CACP_HUMAN	↓			
	Medium-chain specific acyl-CoA dehydrogenase, mitochondrial	P11310|ACADM_HUMAN			↓	
PROTEIN TRANSPORT & METABOLISM	Serotransferrin	P02787|TRFE_HUMAN	↓		↓	↓
	Isoform 1 of Gamma-adducin	Q9UEY8-2|ADDG_HUMAN	↓	↓		↑
	60S ribosomal protein L10a 60S ribosomal protein L12 60S acidic ribosomal protein P2 60S ribosomal protein L7	P62906|RL10A_HUMAN P30050|RL12_HUMAN P05387|RLA2_HUMAN P18124|RL7_HUMAN	↓ ↑ ↑	↓	↑	↓
	Hsc70-interacting protein	P50502|F10A1_HUMAN	↓			
	F-actin-capping protein subunit alpha-1	P52907|CAZA1_HUMAN	↓			
	Rho GTPase-activating protein 1	Q07960|RHG01_HUMAN	↓			
	V-type proton ATPase subunit G 1	O75348|VATG1_HUMAN	↑			
	Endonuclease domain-containing 1 protein	O94919|ENDD1_HUMAN	↑	↑		
	Isoform 2 of Filamin-A	P21333-2|FLNA_HUMAN		↓		

	Ras-related protein Rab-6A Ras-related protein Rab-6B	P20340|RAB6A_HUMAN Q9NRW1|RAB6B_HUMAN			↓ ↓	↓
	Dynactin subunit 1	Q14203|DCTN1_HUMAN			↓	↓
	Elongation factor 1-beta	P24534|EF1B_HUMAN			↓	
	Isoform 2 of Syntaxin-7	O15400-2|STX7_HUMAN			↓	
	Alpha-actinin-4	O43707|ACTN4_HUMAN				↑
	Vesicle-associated membrane protein 3	Q15836|VAMP3_HUMAN				↓
SIGNALLING	Isoform 4 of Otoferlin	Q9HC10-4|OTOF_HUMAN	↑	↑		
	Protein S100-A11	P31949|S10AB_HUMAN	↑			
	Isoform 2 of Sarcoplasmic/endoplasmic reticulum calcium ATPase 2	P16615-2|AT2A2_HUMAN	↓			
	Ras-related C3 botulinum toxin substrate 1	P63000|RAC1_HUMAN	↓			
	Isoform 2 of Minor histocompatibility protein HA-1	Q92619-2|HMHA1_HUMAN	↓			
	Guanine nucleotide-binding protein G(q) subunit alpha	P50148|GNAQ_HUMAN			↑	
	Tyrosine-protein phosphatase non-receptor type 18	Q99952|PTN18_HUMAN			↑	
	Isoform 3 of 55 kDa erythrocyte membrane protein	Q00013-3|EM55_HUMAN				↑
OTHER	Isoform C of Endothelin-converting enzyme 1	P42892-3|ECE1_HUMAN	↓			
	Ankyrin repeat domain-containing protein 13B	Q86YJ7|AN13B_HUMAN	↑	↑		
	Coagulation factor V	P12259|FA5_HUMAN			↓	
	Isoform 4 of Girdin	Q3V6T2-4|GRDN_HUMAN			↓	
	Ribonuclease T2	O00584|RNT2_HUMAN			↓	
	Isoform 2 of Disheveled-associated activator of morphogenesis 1	Q9Y4D12|DAAM1_HUMAN				↑
	Beta-hexosaminidase subunit alpha	P06865|HEXA_HUMAN				↓

The results from Volcano plots (Figure 8:A-D) were organized according to their related functions. Only the proteins with significant up regulation (↑) and down regulation (↓) between two different groups (i.e. control vs survivors, control vs healthy cALL survivors, control vs unhealthy cALL survivors, healthy cALL survivors vs unhealthy cALL survivors) are represented. The arrow relates to the expression of the first group in comparison with (vs) the second group. Abbreviations: C: controls, S: cALL survivors, H: healthy cALL survivors, UH: unhealthy cALL survivors.

Figure 1

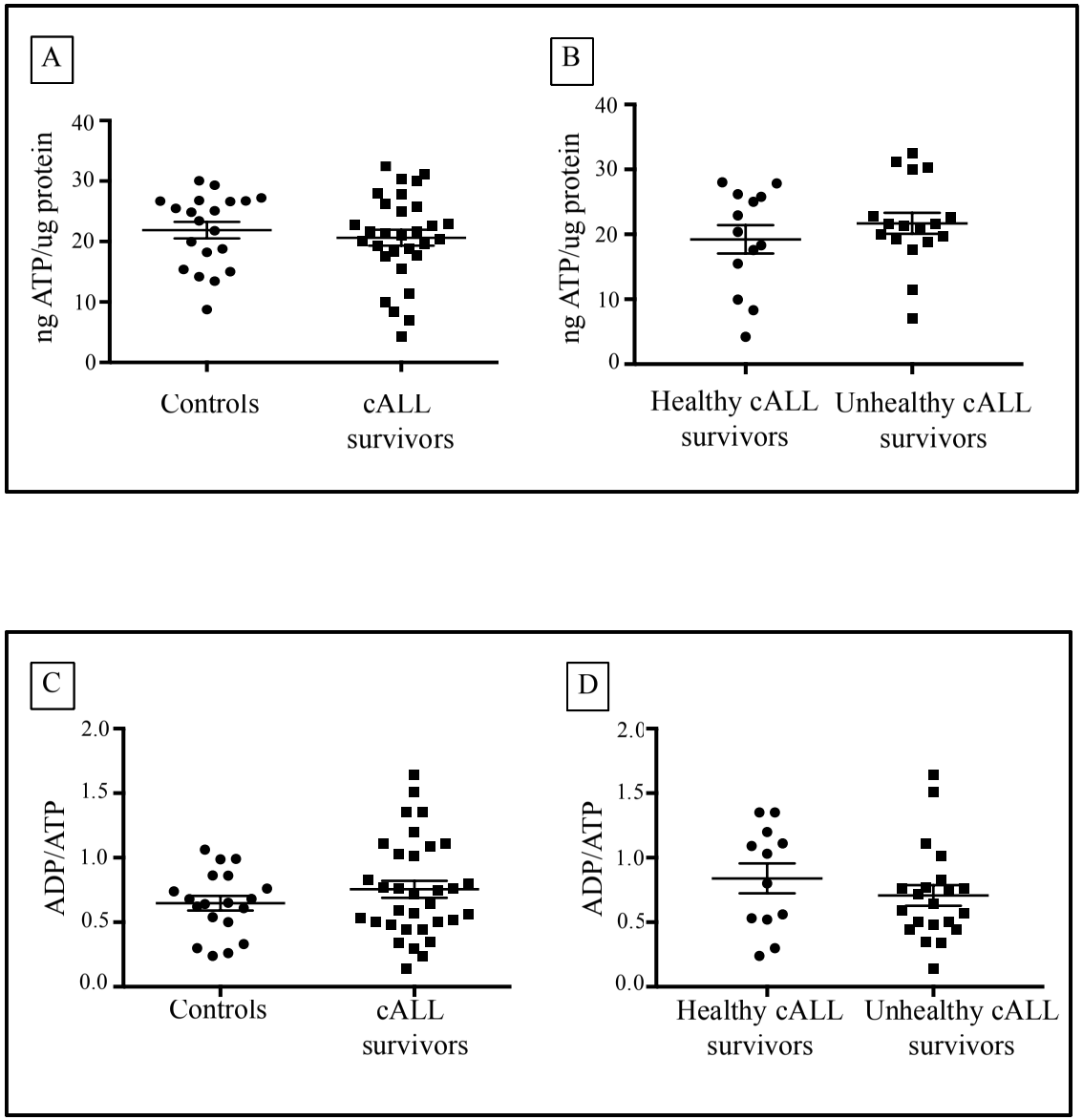
A
ng ATP/ug protein
40
30
20
10
0
Controls
cALL survivors
B
ng ATP/ug protein
40
30
20
10
0
Healthy cALL survivors
Unhealthy cALL survivors
C
ADP/ATP
2.0
1.5
1.0
0.5
0.0
Controls
cALL survivors
D
ADP/ATP
2.0
1.5
1.0
0.5
0.0
Healthy cALL survivors
Unhealthy cALL survivors

Figure 2

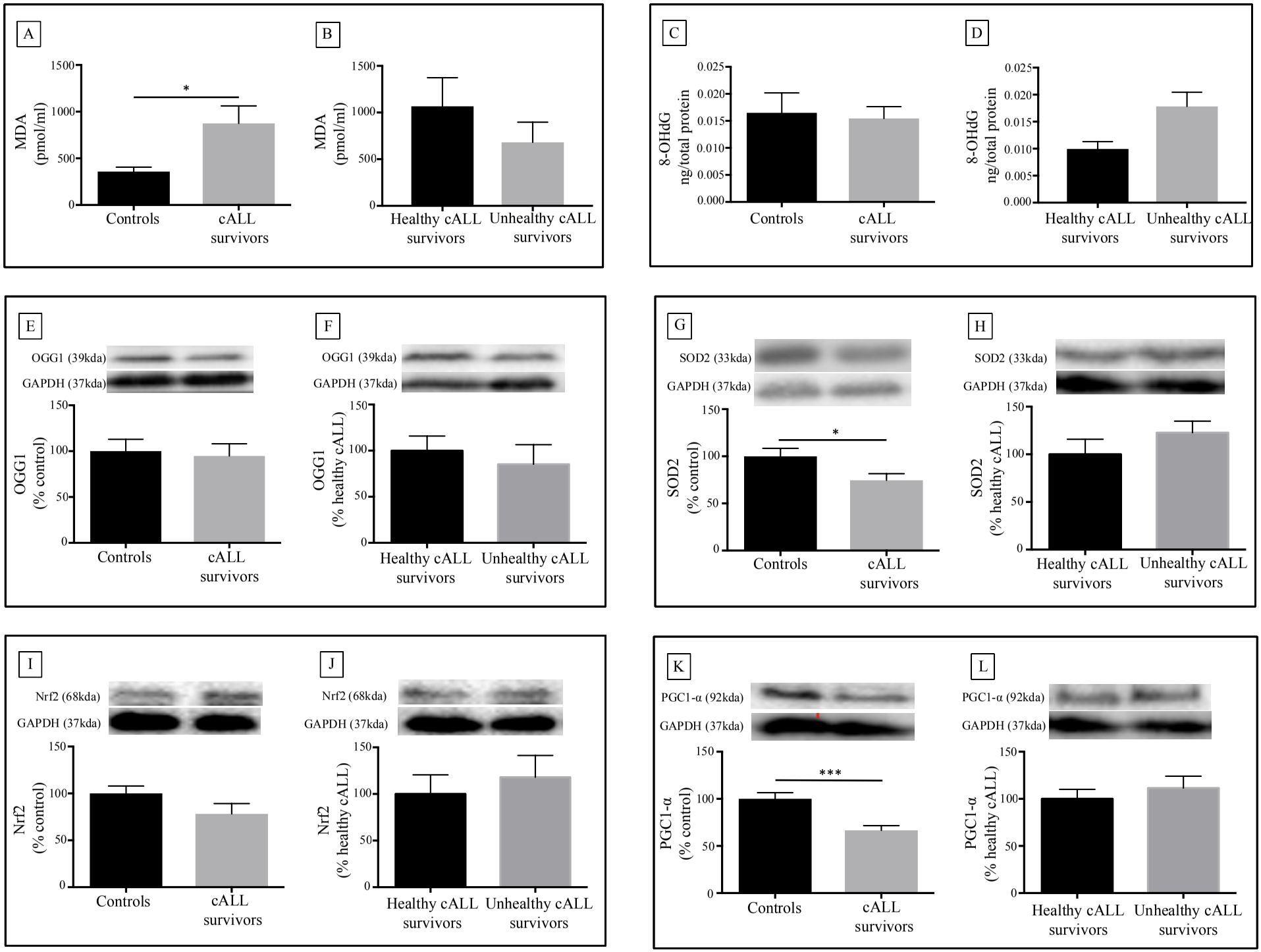
A
MDA (pmol/ml)
1500
1000
500
0
*
Controls
cALL survivors
B
MDA (pmol/ml)
1500
1000
500
0
Healthy cALL survivors
Unhealthy cALL survivors
C
8-OHdG ng/total protein
0.025
0.020
0.015
0.010
0.005
0.000
Controls
cALL survivors
D
8-OHdG ng/total protein
0.025
0.020
0.015
0.010
0.005
0.000
Healthy cALL survivors
Unhealthy cALL survivors
E
OGG1 (39kda)
GAPDH (37kda)
OGG1 (% control)
150
100
50
0
Controls
cALL survivors
F
OGG1 (39kda)
GAPDH (37kda)
OGG1 (% healthy cALL)
150
100
50
0
Healthy cALL survivors
Unhealthy cALL survivors
G
SOD2 (33kda)
GAPDH (37kda)
SOD2 (% control)
150
100
50
0
*
Controls
cALL survivors
H
SOD2 (33kda)
GAPDH (37kda)
SOD2 (% healthy cALL)
150
100
50
0
Healthy cALL survivors
Unhealthy cALL survivors
I
Nrf2 (68kda)
GAPDH (37kda)
Nrf2 (% control)
150
100
50
0
Controls
cALL survivors
J
Nrf2 (68kda)
GAPDH (37kda)
Nrf2 (% healthy cALL)
150
100
50
0
Healthy cALL survivors
Unhealthy cALL survivors
K
PGC1-α (92kda)
GAPDH (37kda)
PGC1-α (% control)
150
100
50
0
***
Controls
cALL survivors
L
PGC1-α (92kda)
GAPDH (37kda)
PGC1-α (% healthy cALL)
150
100
50
0
Healthy cALL survivors
Unhealthy cALL survivors

Figure 3

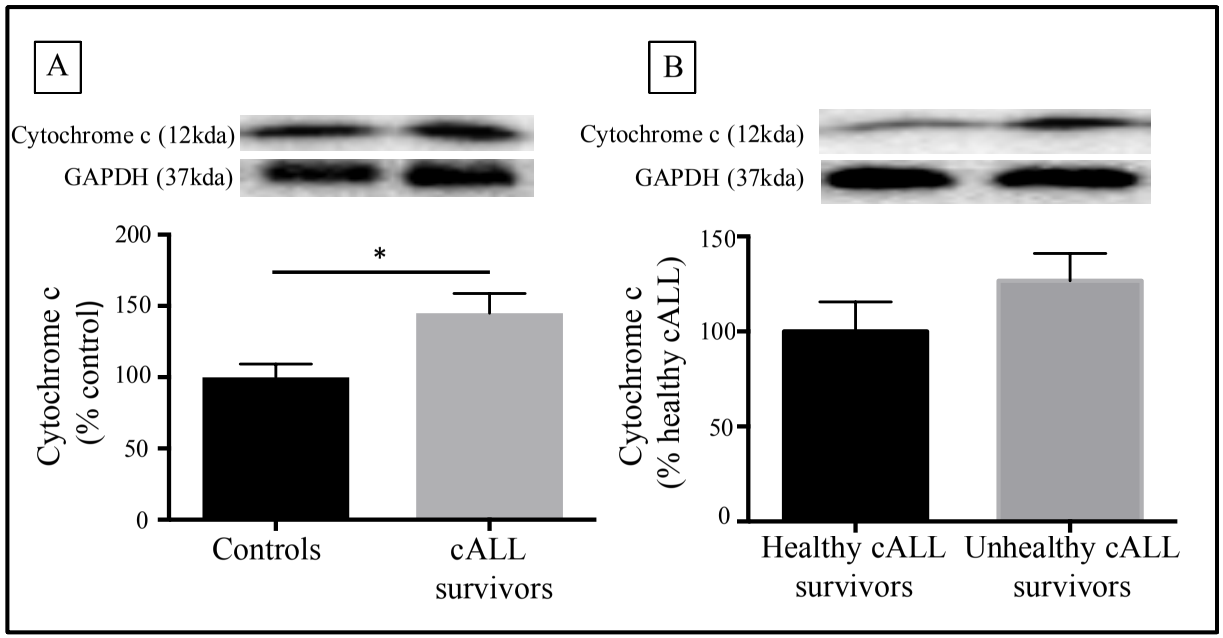
A
Cytochrome c (12kda)
GAPDH (37kda)
Cytochrome c (% control)
200
150
100
50
0
*
Controls
cALL survivors
B
Cytochrome c (12kda)
GAPDH (37kda)
Cytochrome c (% healthy cALL)
150
100
50
0
Healthy cALL survivors
Unhealthy cALL survivors

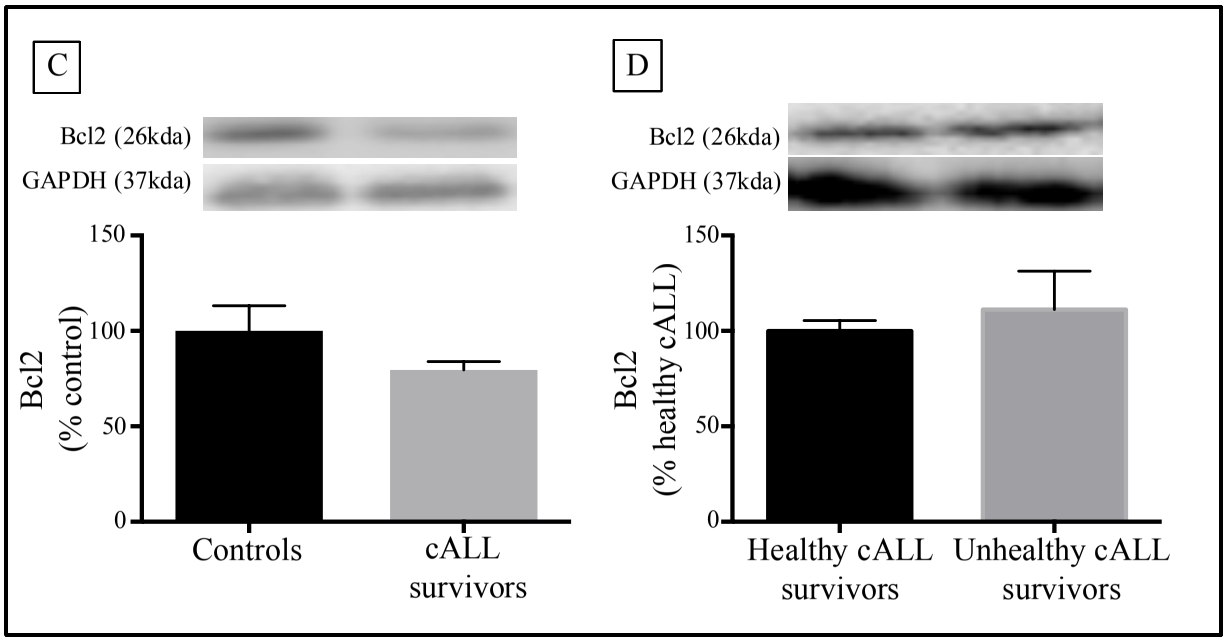
C
Bcl2 (26kda)
GAPDH (37kda)
Bcl2 (% control)
150
100
50
0
Controls
cALL survivors
D
Bcl2 (26kda)
GAPDH (37kda)
Bcl2 (% healthy cALL)
150
100
50
0
Healthy cALL survivors
Unhealthy cALL survivors

Figure 4

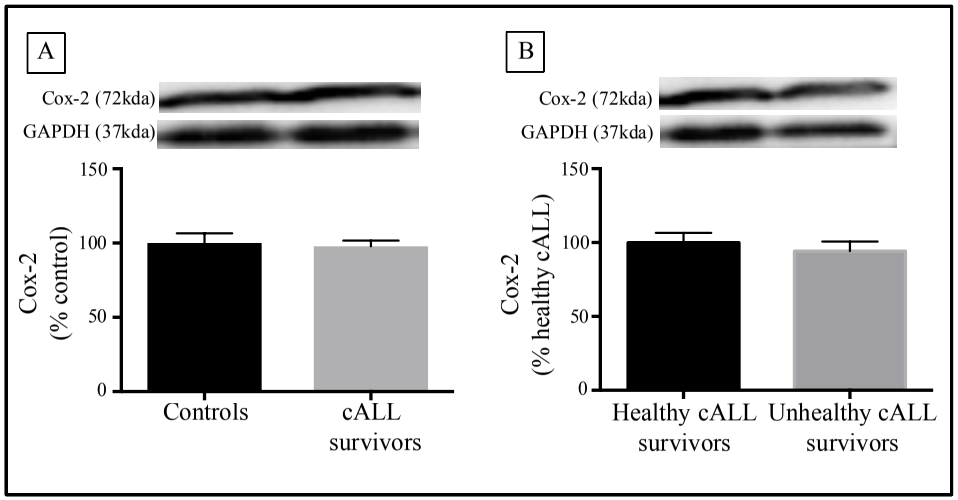
A
Cox-2 (72kda)
GAPDH (37kda)
Cox-2 (% control)
150
100
50
0
Controls
cALL survivors
B
Cox-2 (72kda)
GAPDH (37kda)
Cox-2 (% healthy cALL)
150
100
50
0
Healthy cALL survivors
Unhealthy cALL survivors

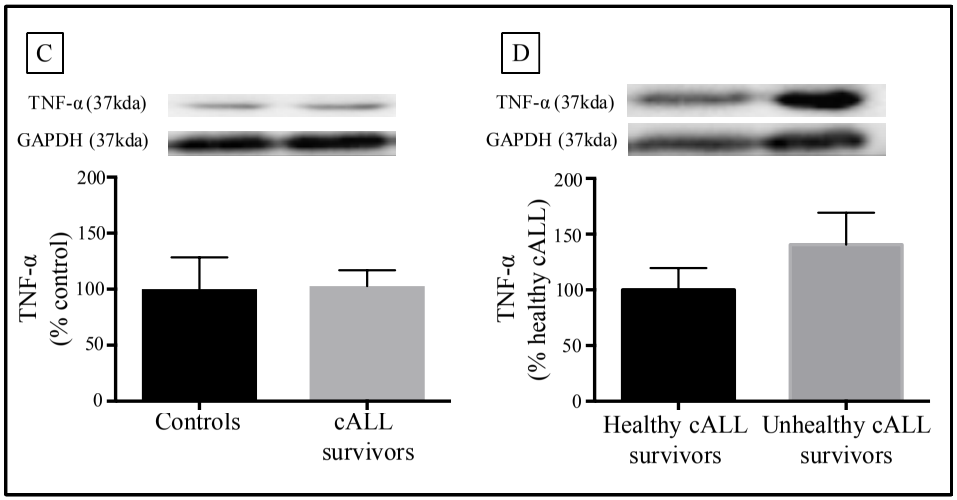
C
TNF-α (37kda)
GAPDH (37kda)
TNF-α (% control)
200
150
100
50
0
Controls
cALL survivors
D
TNF-α (37kda)
GAPDH (37kda)
TNF-α (% healthy cALL)
200
150
100
50
0
Healthy cALL survivors
Unhealthy cALL survivors

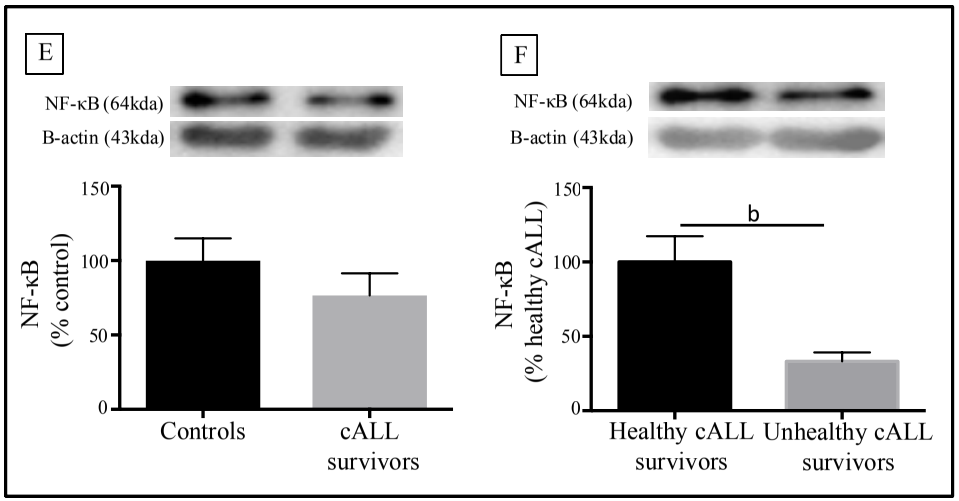
E
NF-κB (64kda)
B-actin (43kda)
NF-κB (% control)
150
100
50
0
Controls
cALL survivors
F
NF-κB (64kda)
B-actin (43kda)
NF-κB (% healthy cALL)
b
150
100
50
0
Healthy cALL survivors
Unhealthy cALL survivors

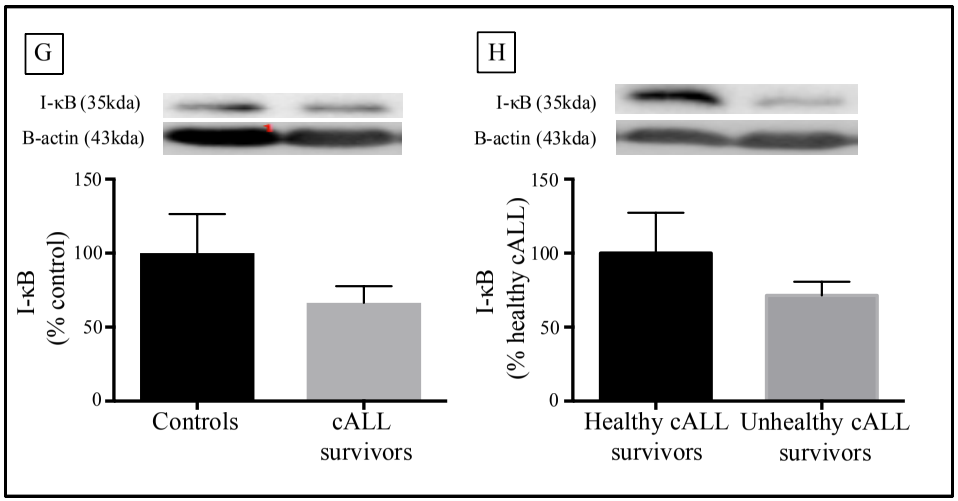
G
I-κB (35kda)
B-actin (43kda)
I-κB (% control)
150
100
50
0
Controls
cALL survivors
H
I-κB (35kda)
B-actin (43kda)
I-κB (% healthy cALL)
150
100
50
0
Healthy cALL survivors
Unhealthy cALL survivors

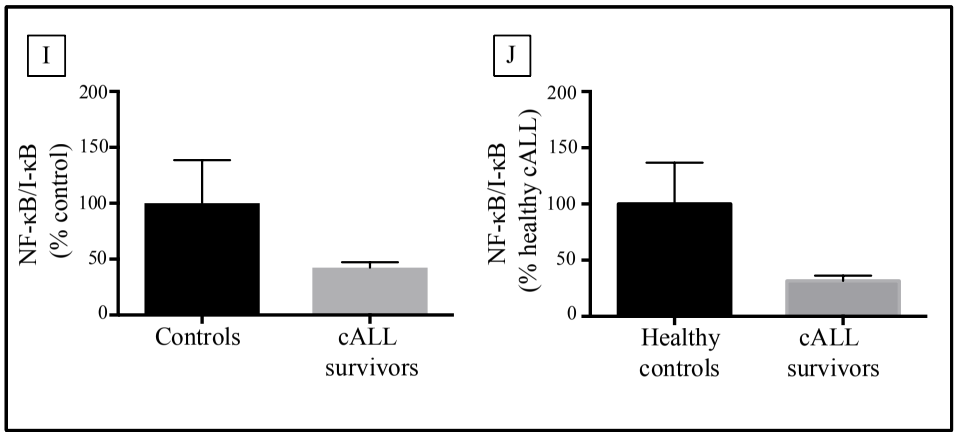
I
NF-κB/I-κB (% control)
200
150
100
50
0
Controls
cALL survivors
J
NF-κB/I-κB (% healthy cALL)
200
150
100
50
0
Healthy controls
cALL survivors

Figure 5

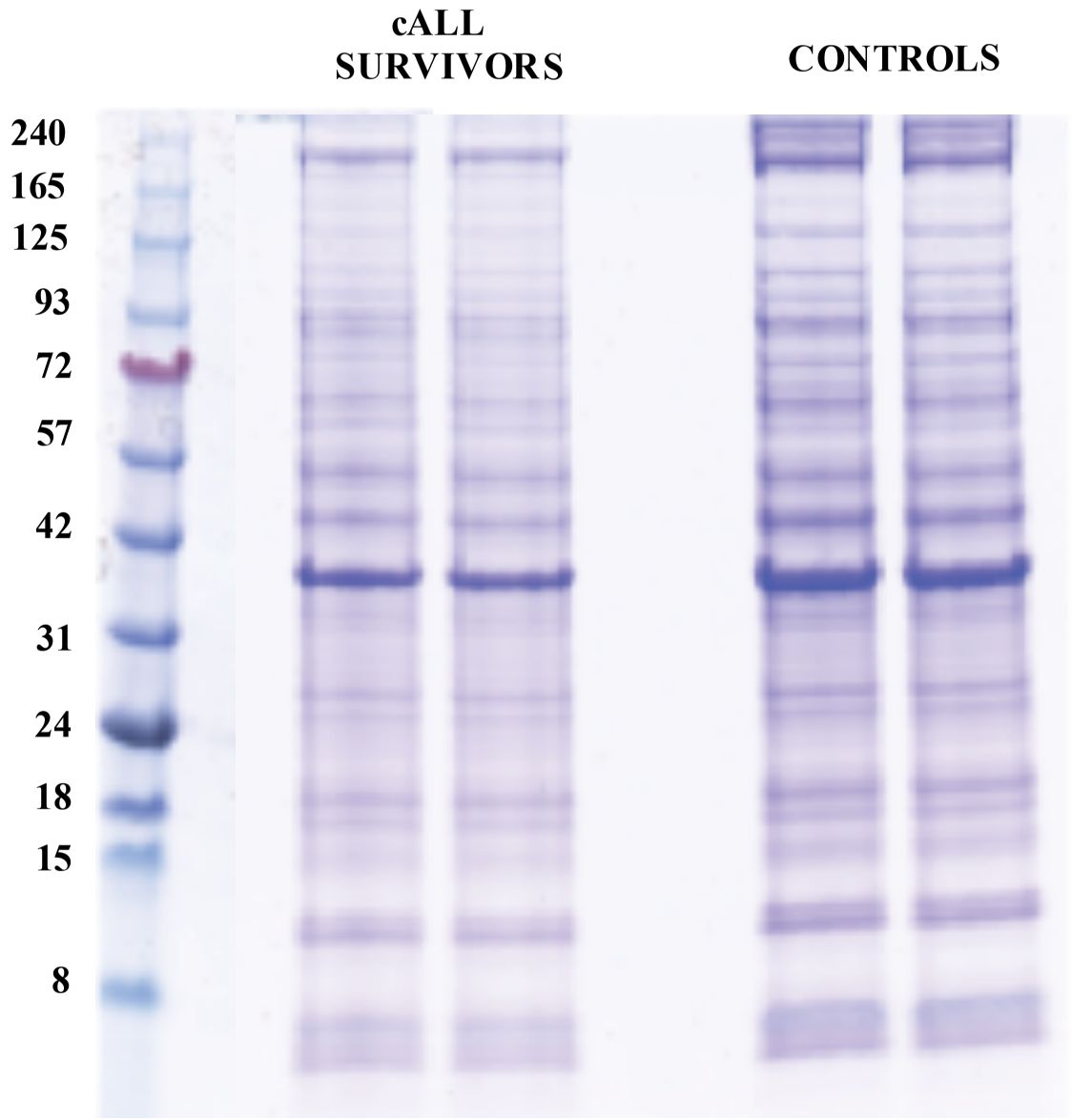

Figure 6

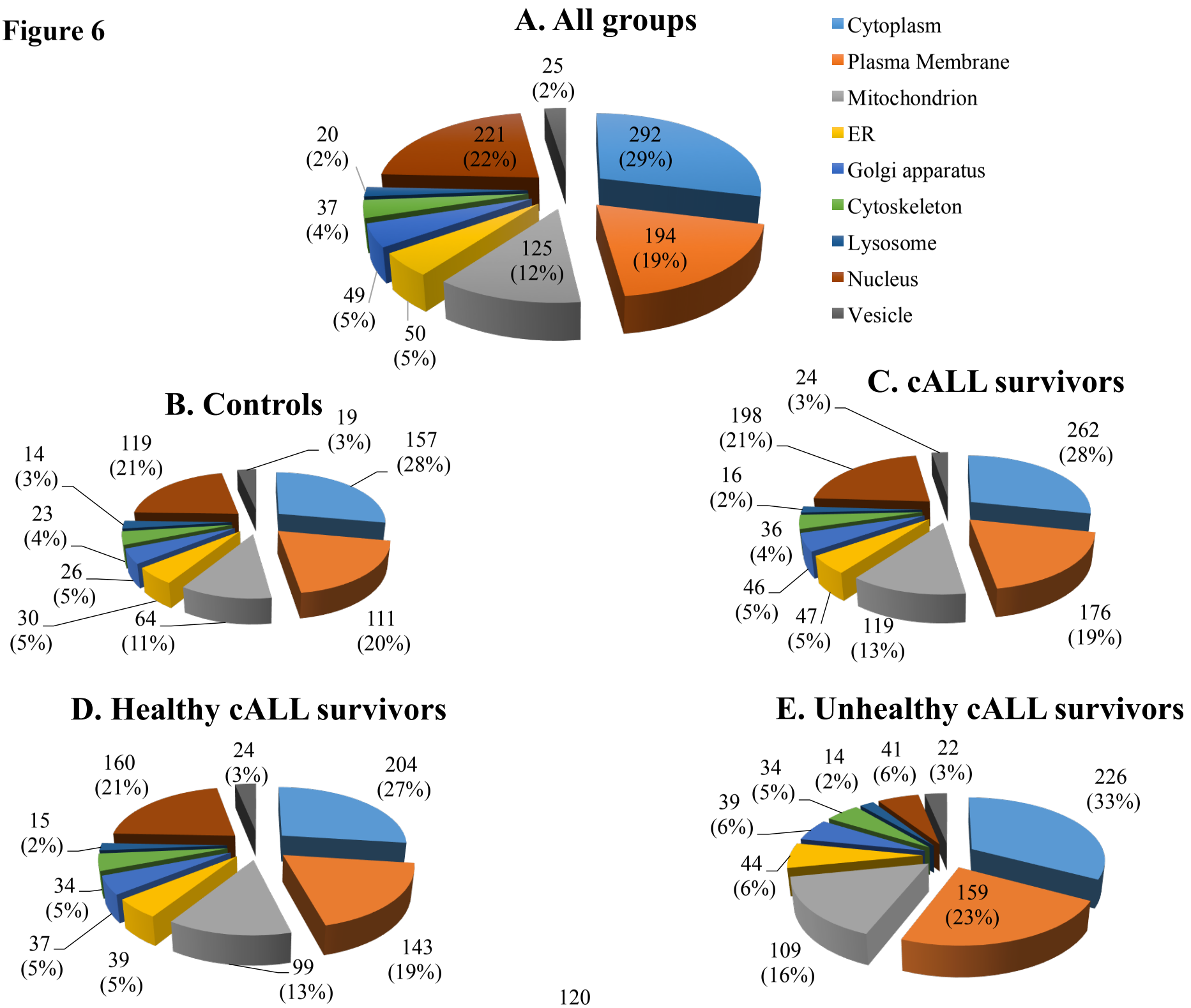
A. All groups
25 (2%)
292 (29%)
194 (19%)
125 (12%)
50 (5%)
49 (5%)
37 (4%)
20 (2%)
221 (22%)
Cytoplasm
Plasma Membrane
Mitochondrion
ER
Golgi apparatus
Cytoskeleton
Lysosome
Nucleus
Vesicle
B. Controls
19 (3%)
157 (28%)
111 (20%)
64 (11%)
30 (5%)
26 (5%)
23 (4%)
14 (3%)
119 (21%)
C. cALL survivors
24 (3%)
262 (28%)
176 (19%)
119 (13%)
47 (5%)
46 (5%)
36 (4%)
16 (2%)
198 (21%)
D. Healthy cALL survivors
24 (3%)
204 (27%)
143 (19%)
99 (13%)
39 (5%)
37 (5%)
34 (5%)
15 (2%)
160 (21%)
E. Unhealthy cALL survivors
22 (3%)
41 (6%)
14 (2%)
34 (5%)
39 (6%)
44 (6%)
226 (33%)
159 (23%)
109 (16%)

Figure 7

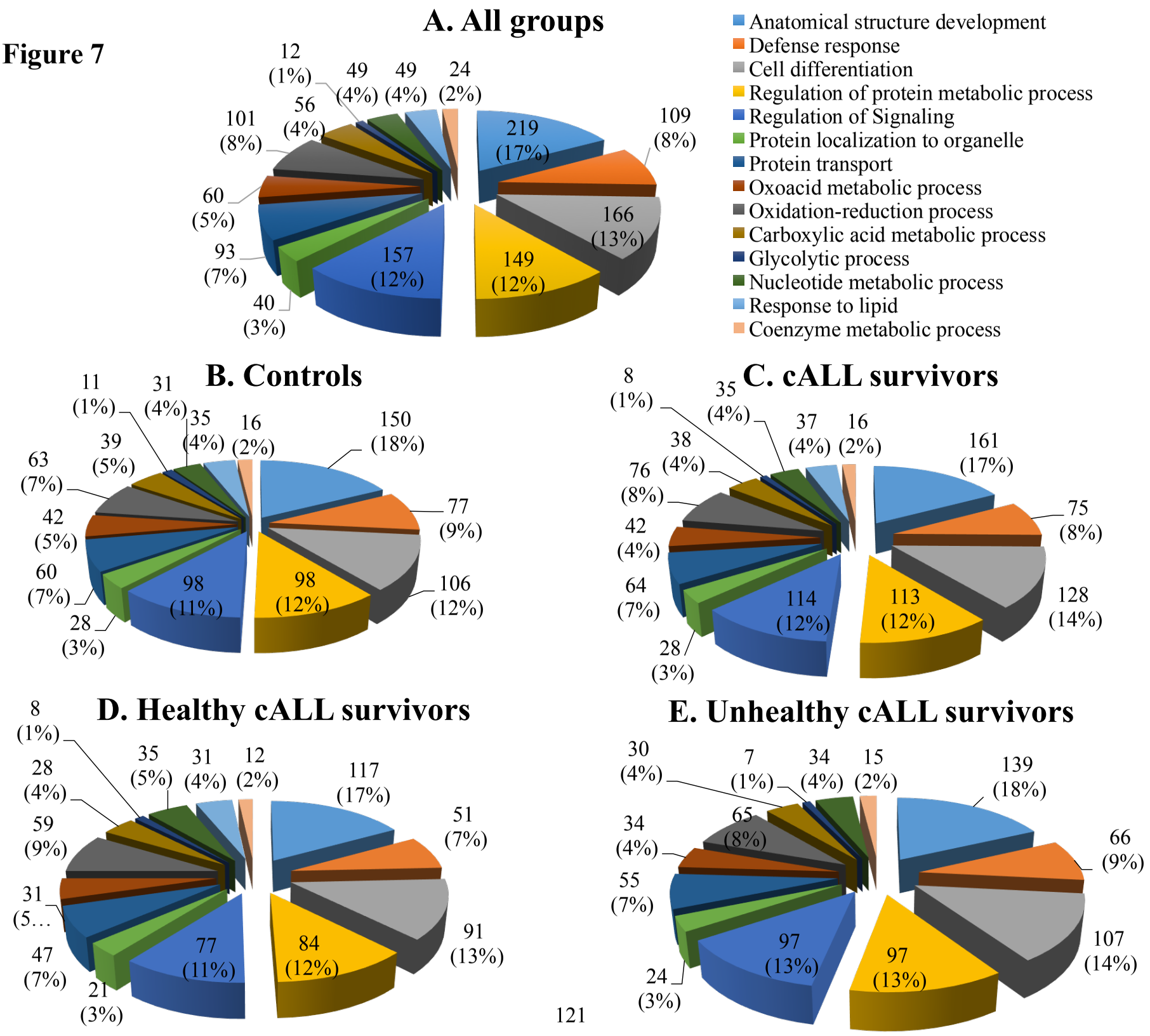
A. All groups
Anatomical structure development
Defense response
Cell differentiation
Regulation of protein metabolic process
Regulation of Signaling
Protein localization to organelle
Protein transport
Oxoacid metabolic process
Oxidation-reduction process
Carboxylic acid metabolic process
Glycolytic process
Nucleotide metabolic process
Response to lipid
Coenzyme metabolic process
219 (17%)
109 (8%)
166 (13%)
149 (12%)
157 (12%)
40 (3%)
93 (7%)
60 (5%)
101 (8%)
56 (4%)
49 (4%)
49 (4%)
24 (2%)
12 (1%)
B. Controls
150 (18%)
77 (9%)
106 (12%)
98 (12%)
98 (11%)
28 (3%)
60 (7%)
42 (5%)
63 (7%)
39 (5%)
35 (4%)
31 (4%)
16 (2%)
11 (1%)
C. cALL survivors
161 (17%)
75 (8%)
128 (14%)
113 (12%)
114 (12%)
28 (3%)
64 (7%)
42 (4%)
76 (8%)
38 (4%)
37 (4%)
35 (4%)
16 (2%)
8 (1%)
D. Healthy cALL survivors
117 (17%)
51 (7%)
91 (13%)
84 (12%)
77 (11%)
21 (3%)
47 (7%)
31 (5…
59 (9%)
28 (4%)
35 (5%)
31 (4%)
12 (2%)
8 (1%)
E. Unhealthy cALL survivors
139 (18%)
66 (9%)
107 (14%)
97 (13%)
97 (13%)
24 (3%)
55 (7%)
34 (4%)
65 (8%)
30 (4%)
7 (1%)
34 (4%)
15 (2%)

Figure 8

A

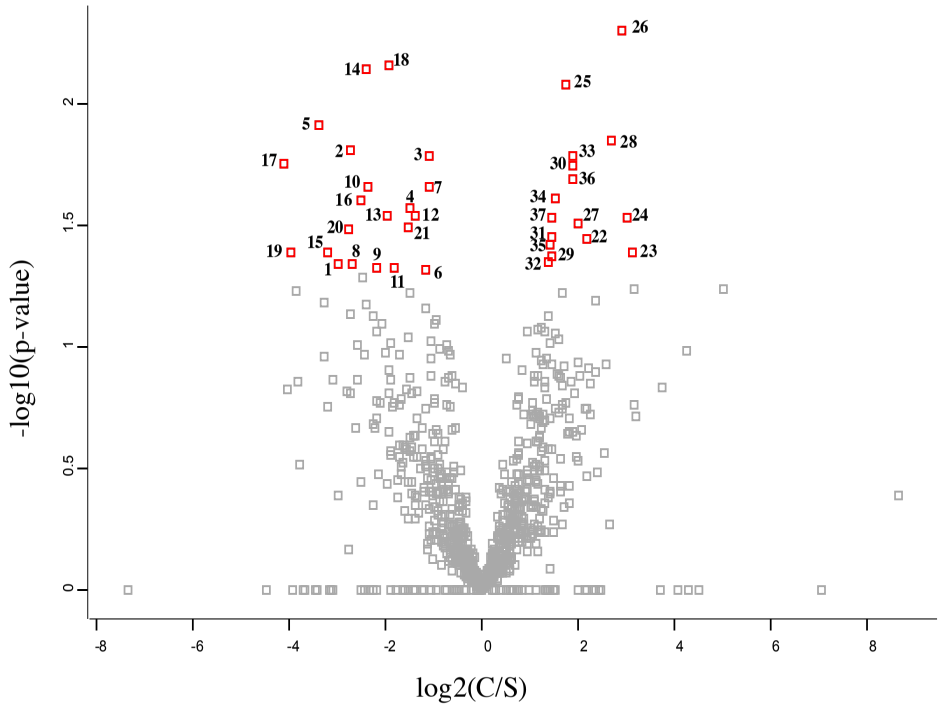

Function	#	Protein name	Accession number
Inflammation	25	Alpha-1-acid glycoprotein 1	P02763|A1AG1_HUMAN
	37	Neutrophil defensin 1	P59665|DEF1_HUMAN
Apoptosis & cell cycle	6	Isoform 5 of Unconventional myosin-XVIIIa	Q92614-5|MY18A_HUMAN
	8	Galectin-1	P09382|LEG1_HUMAN
	13	L-lactate dehydrogenase A chain	P00338|LDHA_HUMAN
	19	Isoform 2 of Putative ribosomal RNA methyltransferase NOP2	P46087-2|NOP2_HUMAN
	21	CDGSH iron-sulfur domain-containing protein 2	Q8N5K1|CISD2_HUMAN
	27	Isoform 2 of Prothymosin alpha	P06454-2|PTMA_HUMAN
	29	Serine/arginine-rich splicing factor 3	P84103|SRSF3_HUMAN
	30	Serine/threonine-protein kinase PAK 2	Q13177|PAK2_HUMAN
	31	Eukaryotic initiation factor 4A-I	P60842|IF4A1_HUMAN
ATP	22	ATP synthase subunit epsilon mitochondrial	P56381|ATP5E_HUMAN
	28	ATPase inhibitor mitochondrial	Q9UII2|ATIF1_HUMAN
REDOX	7	NADH-cytochrome b5 reductase 1	Q9UHQ9|NB5R1_HUMAN
	12	Stress-induced-phosphoprotein 1	P31948|STIP1_HUMAN
	14	Isoform 2 of Malate dehydrogenase cytoplasmic	P40925-2|MDHC_HUMAN
	17	GMP reductase 2	Q9P2T1|GMPR2_HUMAN
Antioxidant	1	Catalase	P04040|CATA_HUMAN
β-oxidation	2	Isoform 3 of Carnitine O-acetyltransferase	P43155-3|CACP_HUMAN
	23	Isoform 2 of Peroxisomal acyl-coenzyme A oxidase 1	Q15067-2|ACOX1_HUMAN
Protein transport & metabolism	9	Hsc70-interacting protein	P50502|F10A1_HUMAN
	10	Serotransferrin	P02787|TRFE_HUMAN
	11	F-actin-capping protein subunit alpha-1	P52907|CAZA1_HUMAN
	15	Rho GTPase-activating protein 1	Q07960|RHG01_HUMAN
	16	Isoform 1 of Gamma-adducin	Q9UEY8-2|ADDG_HUMAN
	18	60S ribosomal protein L10a	P62906|RL10A_HUMAN
	26	60S ribosomal protein L7	P18124|RL7_HUMAN
	32	V-type proton ATPase subunit G 1	O75348|VATG1_HUMAN
	33	Endonuclease domain-containing 1 protein	O94919|ENDD1_HUMAN
	34	60S acidic ribosomal protein P2	P05387|RLA2_HUMAN
Signalling	3	Isoform 2 of Sarcoplasmic/endoplasmic reticulum calcium ATPase 2	P16615-2|AT2A2_HUMAN
	4	Ras-related C3 botulinum toxin substrate 1	P63000|RAC1_HUMAN
	20	Isoform 2 of Minor histocompatibility protein HA-1	Q92619-2|HMHA1_HUMAN
	24	Protein S100-A11	P31949|S10AB_HUMAN
	35	Isoform 4 of Otoferlin	Q9HC10-4|OTOF_HUMAN
Other	5	Isoform C of Endothelin-converting enzyme 1	P42892-3|ECE1_HUMAN
	36	Ankyrin repeat domain-containing protein 13B	Q86YJ7|AN13B_HUMAN

Figure 8

B

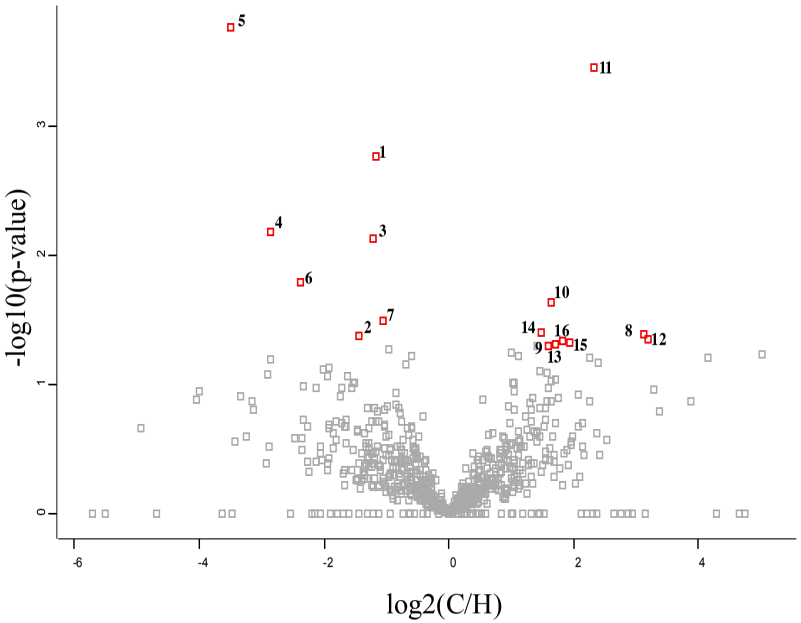

Function	#	Protein name	Accession number
Inflammation	9	Disintegrin and metalloproteinase domain-containing protein 10	O14672|ADA10_HUMAN
	11	Alpha-1-acid glycoprotein 1	P02763|A1AG1_HUMAN
	16	Neutrophil defensin 1	P59665|DEF1_HUMAN
Apoptosis & cell cycle	2	Isoform 5 of Unconventional myosin-XVIIIa	Q92614-5|MY18A_HUMAN
	3	Guanine nucleotide-binding protein G(i) subunit alpha-2	P04899|GNAI2_HUMAN
	7	Laminin subunit gamma-1	P11047|LAMC1_HUMAN
ATP	12	ATPase inhibitor mitochondrial	Q9UII2|ATIF1_HUMAN
REDOX	4	Isoform 2 of Malate dehydrogenase cytoplasmic	P40925-2|MDHC_HUMAN
	10	Glyoxylate reductase/hydroxypyruvate reductase	Q9UBQ7|GRHPR_HUMAN
β -oxidation	8	Isoform 2 of Peroxisomal acyl-coenzyme A oxidase 1	Q15067-2|ACOX1_HUMAN
Protein transport & metabolism	1	Isoform 2 of Filamin-A	P21333-2|FLNA_HUMAN
	5	Isoform 1 of Gamma-adducin	Q9UEY8-2|ADDG_HUMAN
	6	60S ribosomal protein L10a	P62906|RL10A_HUMAN
	13	Endonuclease domain-containing 1 protein	O94919|ENDD1_HUMAN
Signalling	14	Isoform 4 of Otoferlin	Q9HC10-4|OTOF_HUMAN
Other	15	Ankyrin repeat domain-containing protein 13B	Q86YJ7|AN13B_HUMAN

Figure 8

C

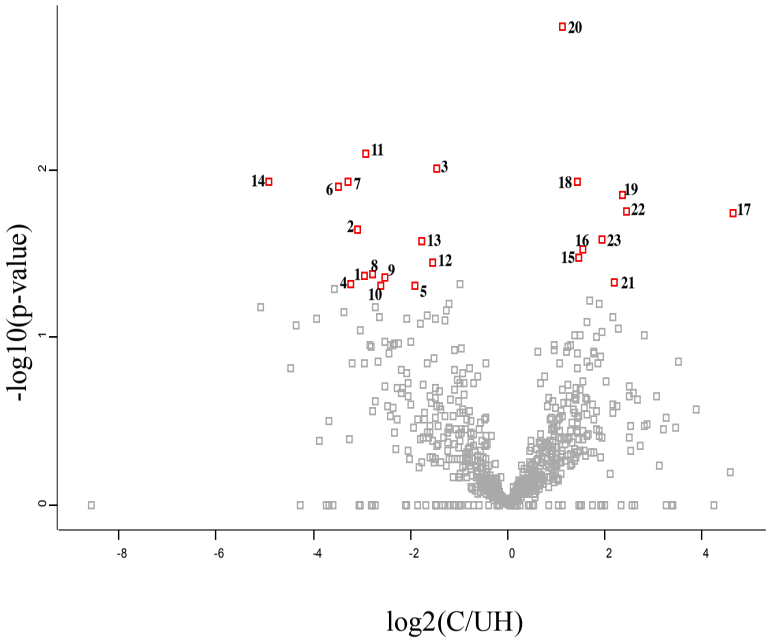

Function	#	Protein name	Accession number
Inflammation	18	Ig lambda-2 chain C regions	P0CG05|LAC2_HUMAN
	20	Alpha-1-acid glycoprotein 1	P02763|A1AG1_HUMAN
Apoptosis & cell cycle	6	Galectin-1	P09382|LEG1_HUMAN
	16	14-3-3 protein theta	P27348|1433T_HUMAN
	22	Serine/threonine-protein kinase PAK 2	Q13177|PAK2_HUMAN
ATP	15	ATP synthase subunit delta mitochondrial	P30049|ATPD_HUMAN
	21	ATPase inhibitor mitochondrial	Q9UII2|ATIF1_HUMAN
REDOX	11	Amine oxidase [flavin-containing] B	P27338|AOFB_HUMAN
	13	Isoform 2 of Malate dehydrogenase cytoplasmic	P40925-2|MDHC_HUMAN
	14	GMP reductase 2	Q9P2T1|GMPR2_HUMAN
β-oxidation	1	Medium-chain specific acyl-CoA dehydrogenase mitochondrial	P11310|ACADM_HUMAN
Protein transport & metabolism	3	Ras-related protein Rab-6A	P20340|RAB6A_HUMAN
	5	Dynactin subunit 1	Q14203|DCTN1_HUMAN
	7	Serotransferrin	P02787|TRFE_HUMAN
	8	Elongation factor 1-beta	P24534|EF1B_HUMAN
	9	Isoform 2 of Syntaxin-7	O15400-2|STX7_HUMAN
	12	Ras-related protein Rab-6B	Q9NRW1|RAB6B_HUMAN
	23	60S acidic ribosomal protein P2	P05387|RLA2_HUMAN
Signalling	17	Tyrosine-protein phosphatase non-receptor type 18	Q99952|PTN18_HUMAN
	19	Guanine nucleotide-binding protein G(q) subunit alpha	P50148|GNAQ_HUMAN
Other	2	Ribonuclease T2 O	O00584|RNT2_HUMAN
	4	Isoform 4 of Girdin	Q3V6T2-4|GRDN_HUMAN
	10	Coagulation factor V	P12259|FA5_HUMAN

Figure 8

D

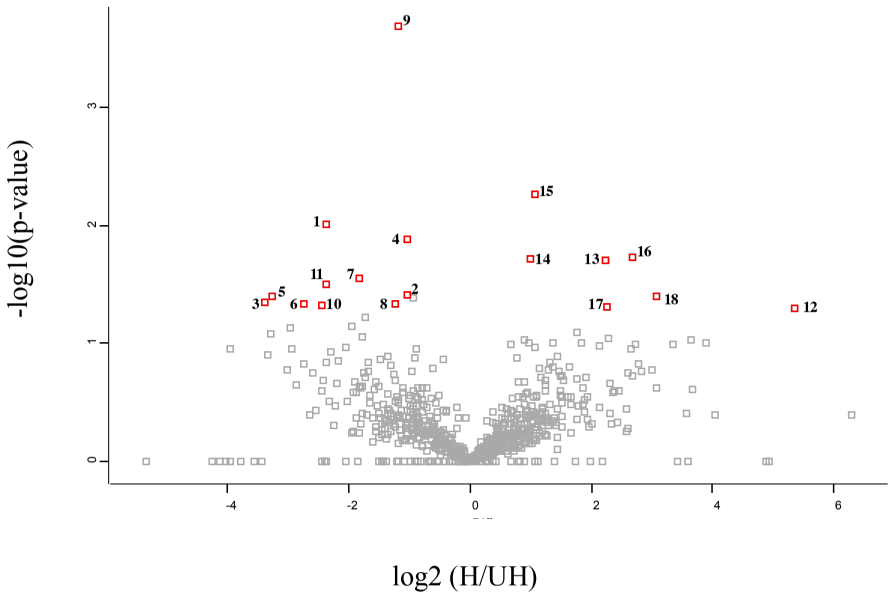

Function	#	Protein name	Accession number
Inflammation	2	Leukotriene A-4 hydrolase	P09960|LKHA4_HUMAN
	9	Alpha-1-acid glycoprotein 1	P02763|A1AG1_HUMAN
Apoptosis & cell cycle	1	14-3-3 protein eta	Q04917|1433F_HUMAN
	5	Isoform 1 of Four and a half LIM domains protein 1	Q13642-1|FHL1_HUMAN
	15	Guanine nucleotide-binding protein G(i) subunit alpha-2	P04899|GNAI2_HUMAN
	18	Vacuolar protein sorting-associated protein 35	Q96QK1|VPS35_HUMAN
ATP	13	ATP synthase subunit delta mitochondrial	P30049|ATPD_HUMAN
β-oxidation	11	Peroxisomal multifunctional enzyme type 2	P51659|DHB4_HUMAN
Protein transport & metabolism	4	Ras-related protein Rab-6A	P20340|RAB6A_HUMAN
	6	Dynactin subunit 1	Q14203|DCTN1_HUMAN
	7	Serotransferrin	P02787|TRFE_HUMAN
	8	Vesicle-associated membrane protein 3	Q15836|VAMP3_HUMAN
	10	60S ribosomal protein L12	P30050|RL12_HUMAN
	14	Alpha-actinin-4	O43707|ACTN4_HUMAN
	16	Isoform 1 of Gamma-adducin	Q9UEY8-2|ADDG_HUMAN
Signalling	17	Isoform 3 of 55 kDa erythrocyte membrane protein	Q00013-3|EM55_HUMAN
Other	3	Beta-hexosaminidase subunit alpha	P06865|HEXA_HUMAN
	12	Isoform 2 of Disheveled-associated activator of morphogenesis 1	Q9Y4D1-2|DAAM1_HUMAN

CHAPTER 3- DISCUSSION

Our study aimed at determining whether there was a presence of mitochondrial dysfunction in cALL survivors that could perhaps explain their increased risk of developing long term cardiometabolic complications. This study included 78 subjects comprising a healthy control group, and cALL survivors who were selected from phase 2 of the PETALE study and separated in 2 groups representing metabolically healthy or metabolically unhealthy survivors. The average age of the PETALE cohort is relatively young and our selected participants had an average age of 24.2 years, which was similar to the control group. Controls were metabolically healthy and had no past history nor family history of any metabolic complications or any other diseases or disorders.

To recapitulate, the metS is made up of a group of metabolic abnormalities which includes obesity, IR, dyslipidemia and HT [42]. The 4 components that make up the metS are interrelated risk factors that have been independently linked with a higher risk for atherosclerotic CV disease and mortality [42, 43], type 2 diabetes (T2D), and their resulting complications [44]. Although our young participants do not necessarily fit the complete metS profile, in agreement to previous studies concerning cALL survivors [12, 35, 36, 38-41] we identified components of the metS in a proportion of our participants. Unhealthy cALL survivors had significantly higher overweightness compared to controls and healthy cALL survivors. This was detected by the increased BMI (27.1 kg/m^2) and WC (94.2 cm). For women, WC even in healthy survivors was significantly higher than controls, although borderline of the normal range (80 cm). This is important because excess visceral fat in the abdominal area is associated with increased morbidity and mortality [41]. Furthermore, obesity, especially visceral obesity, is at the centre of the metS and is directly related to the prognosis of the metS [46, 47]. In addition, obesity is a risk factor for the other components of the metS (i.e. IR, HT, dyslipidemia) [45], hence its importance in the progression of metS. Interestingly, our metabolic characterization of cALL survivor participants also displays increased diastolic BP, a marker of HT, in unhealthy survivors compared to healthy survivors. Furthermore IR is present in unhealthy survivors marked by their increased insulin, HOMA-IR and HOMA-beta. Finally, unhealthy survivors display a dyslipidemic profile, in parallel to another study, which we

recently published (ANNEXE) [35]. Dyslipidemia was marked by increased TG, LDL-C and/or decreased HDL-C. Moreover, systemic OxS can increase the release of pro-inflammatory molecules, is closely connected to BMI [108] and is an early marker of the metS [105]. Correspondingly, CRP levels are increased in unhealthy survivors compared to healthy survivors, marking an increase in inflammation in this group. Overall we found that the unhealthy cALL survivor group in our cohort of the PETALE study were significantly more affected by metabolic risk factors than the control and healthy survivor groups. This is especially important considering the young age of our study group as this indicates that they are at risk of developing diabetes [44] and CV disease early on due to the presence of metabolic risk factors [42, 43]. Therefore it is crucial to determine intervention or prevention methods to evade the development of cardiometabolic complications in this population. However before determining intervention and prevention methods it is necessary to understand the mechanisms responsible for the high incidence of cardiometabolic complications among this population.

To our knowledge, our research is the first to examine mitochondrial dysfunction in a population of paediatric cancer survivors at risk of developing, or who have developed, cardiometabolic complications. Since the mitochondrion has been shown to be dysfunctional in cardiometabolic diseases [79, 86, 145] we were interested in studying and comparing several mitochondrial functions as well as mitochondria proteomic profile in cALL survivor groups and controls.

We assumed that unhealthy cALL survivors in our study would display mitochondrial dysfunction since they have an altered metabolic profile. However, in our functional experiments, we only reached significance for many of the measured mitochondrial proteins when we combined the 2 cALL survivor groups and compared to the control group. These results reveal significant differences in the expression of proteins involved in key mitochondrial pathways in cALL survivors including increased apoptosis (cytochrome c) and OxS (MDA), and decreased antioxidant production (SOD2) and mitochondrial biogenesis (PGC1-α). Unfortunately we were very limited in the number of experimentations we could achieve due to the material we were working with (i.e. human mitochondria from PBMCs). When isolated from PBMCs we obtained an average of 60µg of mitochondria to work with. Furthermore working with the homogenate (i.e. PBMCs) proved difficult and did not allow us to perform all

the experiments we had planned for. Thus we included a proteomic analysis to our study, which required a small amount of mitochondria allowing us to get a better in debt understanding of the differences in mitochondria function by analyzing their proteome between our groups.

Overall we identified a total of 957 proteins in our mitochondria samples which corresponds with the literature citing that there are approximately 1000 proteins in the mitochondrion [103] . Research also reports that this number varies based on cell type, cell state or during pathological conditions [86, 103]. Furthermore, we identified 69 proteins that were differentially expressed between groups. These alterations in the mitochondrial proteome between groups may cause alterations in mitochondrial functions. Importantly, many of the differentially expressed proteins are involved in key mitochondrial functions including apoptosis and cell cycle, ATP production, redox and antioxidant activity, fatty acid beta-oxidation, protein transport and metabolism, signalling and inflammation. Perhaps our most interesting finding was the discovery 4 down-regulated pro-apoptotic proteins (*Galectin-1, Isoform 5 of Unconventional myosin-XVIIIa, L-lactate dehydrogenase A chain, CDGSH iron-sulfur domain-containing protein 2*) and an up-regulated anti-apoptotic protein *(Serine/threonine-protein kinase PAK2)* in our controls compared to our cALL survivors. This demonstrates an increased apoptotic profile in cALL survivors compared to controls. To note specifically, we further discovered significantly increased pro-apoptotic protein expression (*Galectin*-1) and decreased anti-apoptotic protein expression (*Serine/threonine-protein kinase PAK2*) in unhealthy survivors compared to controls. These proteomic results support our functional finding indicating a significant increase in the pro-apoptotic protein cytochrome c among cALL survivors. Interestingly, the apoptosis machinery is implicated in the regulation of mitochondrial metabolism [146] and metabolic disorders [86] and has been involved in cancer studies [86, 147].

Another interesting finding was the identification of the up-regulation of 2 proteins (*ATPase inhibitor mitochondrial and ATP synthase subunit epsilon mitochondrial*) involved in ATP synthesis and metabolism in the control group compared to the cALL survivor group. Additionally *ATP synthase subunit delta mitochondrial* was upregulated in the control group and healthy survivor group compared to the unhealthy survivor group. Interestingly, other research similarly discovered alterations in ATP synthase subunits in groups displaying

cardiometabolic pathologies [145, 148, 149]. Thus these data demonstrate a decrease in expression of proteins involved in energy metabolism in cALL survivors, especially in unhealthy survivors, possibly participating in the development of metabolic complications since energy production pathways have demonstrated critical control over metabolic pathways [79] and have been shown to lead to the development of components of the metS [65].

Survivors of cALL, especially unhealthy survivors, demonstrated up-regulation of proteins involved in the stress response (*Stress-induced-phosphoprotein 1* and *Amine oxidase [flavin-containing] B*) compared to controls. Therefore the cALL survivor group had an increase in stress response proteins, which concurs our functional measures displaying an increase in a marker of OxS (MDA) in cALL survivors compared to controls. In view of the mitochondrion being the primary site of production of ROS [67], dysfunctional mitochondria may trigger pathological processes [150] by the overproduction of OxS. Furthermore, proteomic analysis identified the antioxidant protein *catalase* down-regulated in the control group compared to cALL survivors. One explanation for this could be that increased stress in cALL survivors, demonstrated by increased MDA and up-regulated stress related proteins, triggers antioxidant production as a response to this stress. Furthermore, the antioxidant system can become overwhelmed due to too much ROS, resulting in more OxS [89] and possibly advancing further to pathological conditions. Our functional experiments additionally exposed an alteration in the expression of the antioxidant protein SOD2, however this expression was decreased in cALL survivors. We must note that the antioxidant protein identified in our proteomic analysis was not the same one that was measured in our western blotting analysis, which may explain these confounding results.

The study of mitochondrial proteomics involving metabolic pathologies is relatively new and there is limited information on this topic making the interpretation of our proteomic results difficult. For example, some proteins may have multiple functions, do not have any identified function or have not been cited in literature. Furthermore, most studies have been performed on animals or cell cultures, making it difficult to compare our findings since the mitochondrial proteome can vary among different tissues and organisms. To our knowledge we are the first to research whether a population of paediatric cancer survivors displays alterations in their mitochondrial functions and proteomic profile, perhaps explaining their risk of development of

cardiometabolic complications. This makes our study unique but also challenging due to the lack of data on this matter.

Overall we discovered changes in the regulation and functional expression of certain proteins involved in major mitochondrial processes in cALL survivors compared to controls. Surprisingly, most of these differences were identified in the whole cALL group and not simply among the cALL group displaying metabolic anomalies. However our proteomic analysis did allow us to identify changes in the regulation of certain mitochondrial proteins in unhealthy cALL survivors compared to controls and healthy cALL survivors.

Question remains as to why some cALL survivors are affected by metabolic alterations while others have metabolically healthy profiles even though both groups have displayed alterations in the expression of certain mitochondrial proteins compared to a control group. Unfortunately we were not able to answer this question in our study. We must consider that our participants are young and perhaps the healthy survivors are not completely healthy even though their metabolic measurements were normal. It would be interesting to follow them as they age to determine if this is the case. Additionally, we must also consider that even though the metabolically healthy group has not yet acquired any metS components, alterations may still exist in their mitochondria compared to control subjects who have never had cancer or undergone its treatments. Mitochondrial dysfunction has been related to cardiometabolic complications as a cause or consequence of disease [57], yet since our metabolically healthy cALL group also displays several alterations in their mitochondrial proteome compared to controls, we could assume that this is a consequence of their cancer or their cancer treatment. Additionally, cancer development depends highly on modifications of mitochondria [84] and cancer treatments can target certain functions of mitochondria [125] which can lead to changes in this organelle possibly in all survivors.

Perhaps another theory is that participants in the metabolically healthy cALL survivor group have been protected by their genetics. The PETALE study has a group of researchers studying the genetics of this cohort, so it would be interesting to look at the genetics of our participants. Other elements to be explored include treatment type and lifestyle factors (e.g. nutrition, physical activity level, smoking habits, alcohol intake). It would also be important to

consider genetic factors inherited from parents as well as factors related to social and family environment which are strongly associated to obesity and to the treatments received. This may give us a better understanding of why some cALL survivors, at this time, seem protected of metabolic disturbances, which could help plan for preventative interventions of cardiometabolic development among this population. For example, if our cALL survivors who have been identified as having mitochondrial protein alterations however do not display any metabolic complications, consume a diet higher in antioxidants than the metabolically unhealthy group, then a dietary intervention may be interesting to consider.

Limits of this study include the small sample size making it difficult to obtain statistical significance in many of our experiments, especially when cALL groups were separated. Additionally, since we were working with human blood samples we were limited in the amount of experiments we could perform due to the small quantity of PBMCs and mitochondria that were isolated from each participant. Another issue considering the analysis on blood samples is that results obtained on PBMC mitochondria may not be representative of what happens in other tissues that undergo cellular renewal slower than blood cells (ex. muscular tissue, bone tissue, adipose tissue). Mitochondrial anomalies may be more important in survivors compared to controls when studied in other tissues. Additionally the composition of lymphocytes, notably the proportion of naïve T lymphocytes and memory T lymphocytes, correspond to different cell age and activation states. Cancer treatments using chemotherapy, radiotherapy and corticotherapy lead to the loss of naïve T lymphocytes while preserving mature T lymphocytes [151]. Therefore cancer survivors may comprise more mature T lymphocytes compared to controls, which could lead to biased results in mitochondrial analysis.

CONCLUSION

Our study demonstrates that a proportion of cALL survivors are affected by at least one component of the metS, thus highlighting the importance in determining the cause of this development in order to put together proper preventative interventions. Mitochondrial dysfunction has been implicated in several pathologies and our cALL survivors compared to controls display changes in the regulation and expression of several important mitochondrial proteins. Additionally, these proteins are essential in mitochondrial functions including metabolic pathways. This study contributes to increasing our understanding of the effects of cancer or cancer treatment in altering the mitochondrion, which could perhaps explain the high prevalence of cardiometabolic complications in this young population of paediatric cancer survivors. More studies are needed to confirm and extend our findings in order to determine mechanisms and to establish therapeutic strategies that target the mitochondrion. Identifying potential biomarkers could help indicate cALL survivors at risk of developing metabolic complications as a consequence of their cancer and/or its treatments.

BIBLIOGRAPHY

1. Baker, K.S., et al., *Impact of treatment exposures on cardiovascular risk and insulin resistance in childhood cancer survivors.* Cancer Epidemiol Biomarkers Prev, 2013. **22**(11): p. 1954-63.
2. NCI, *Leukemia- Childhood Acute Lymphoblastic Leukemia Treatment- Health Professional Version* 2017 US Department of Health Services USA.
3. Apostolidou, E., et al., *Treatment of acute lymphoblastic leukaemia : a new era.* Drugs, 2007. **67**(15): p. 2153-71.
4. Meacham, L.R., et al., *Cardiovascular risk factors in adult survivors of pediatric cancer--a report from the childhood cancer survivor study.* Cancer Epidemiol Biomarkers Prev, 2010. **19**(1): p. 170-81.
5. Mulrooney, D.A., et al., *Cardiac outcomes in a cohort of adult survivors of childhood and adolescent cancer: retrospective analysis of the Childhood Cancer Survivor Study cohort.* BMJ, 2009. **339**: p. b4606.
6. Aleman, B.M., et al., *Cardiovascular disease after cancer therapy.* EJC Suppl, 2014. **12**(1): p. 18-28.
7. Chandel, N.S., *Mitochondria as signaling organelles.* BMC Biol, 2014. **12**: p. 34.
8. Lyakhovich, A., et al., *Mitochondrial dysfunction in DDR-related cancer predisposition syndromes.* Biochim Biophys Acta, 2016. **1865**(2): p. 184-9.
9. Neustadt, J. and S.R. Pieczenik, *Medication-induced mitochondrial damage and disease.* Mol Nutr Food Res, 2008. **52**(7): p. 780-8.
10. Society, C.R. *Statistics and risk factors* 2017 [cited 2017 January]; Available from: https://www.crs-src.ca/page.aspx?pid=1759.
11. Canada, S., *The 10 leading causes of death, 2012*, C.V.S.D.d.a.S. Canada, Editor. 2015: Ottawa
12. de Haas, E.C., et al., *The metabolic syndrome in cancer survivors.* Lancet Oncol, 2010. **11**(2): p. 193-203.
13. Society, C.R. *Cancer survival rates* 2017 [cited 2017 January]; Available from: https://www.crs-src.ca/page.aspx?pid=1760.

14. Canada, S., *Canadian Cancer Statistics* 2016.
15. WHO. *Cancer Prevention* 2017 [cited 2017 March]; Available from: http://www.who.int/cancer/prevention/en/index.html.
16. WCRF/AICR. *Continuous Update Project Interim Report Summary. Food, Nutrition, Physical Activity, and the Prevention of Cancer: a Global Perspective.* . 2011 [cited 2017 Available from: http://www.aicr.org/assets/docs/pdf/reports/Second_Expert_Report.pdf.
17. WCRF/AICR. *Policy and Action for Cancer Prevention. Food, Nutrition and Physical Activity.* . 2010 [cited 2017 Available from: http://www.aicr.org/assets/docs/pdf/advocacypapers/WCRF_Policy_US_Summary_final.pdf.
18. Palumbo, M.O., et al., *Systemic cancer therapy: achievements and challenges that lie ahead.* Front Pharmacol, 2013. **4**: p. 57.
19. Joo, W.D., I. Visintin, and G. Mor, *Targeted cancer therapy--are the days of systemic chemotherapy numbered?* Maturitas, 2013. **76**(4): p. 308-14.
20. Society, C.R. *Cancer Treatments* 2017 2017]; Available from: https://www.crs-src.ca/cancer/treatments?
21. Kaatsch, P., *Epidemiology of childhood cancer.* Cancer Treat Rev, 2010. **36**(4): p. 277-85.
22. ACS, A.C.S., *Cancer in children and adolescents* 2017: p. 25.
23. Pui, C.H., L.L. Robison, and A.T. Look, *Acute lymphoblastic leukaemia.* Lancet, 2008. **371**(9617): p. 1030-43.
24. SJRH, S.J.C.s.R.H. *Acute Lymphoblastic Leukemia (ALL)* 2017 [cited 2017 Available from: https://www.stjude.org/disease/acute-lymphoblastic-leukemia-all.html.
25. ACS, A.C.S. *Signs and Symptoms of Acute Lymphocytic Leukemia* 2016 [cited 2017 Available from: https://www.cancer.org/cancer/acute-lymphocytic-leukemia/detection-diagnosis-staging/signs-symptoms.html - written_by.
26. O'Neill, K.A., et al., *Infant birthweight and risk of childhood cancer: international population-based case control studies of 40 000 cases.* Int J Epidemiol, 2015. **44**(1): p. 153-68.

27. Caughey, R.W. and K.B. Michels, *Birth weight and childhood leukemia: a meta-analysis and review of the current evidence.* Int J Cancer, 2009. **124**(11): p. 2658-70.
28. O'Neill, K.A., et al., *Immunophenotype and cytogenetic characteristics in the relationship between birth weight and childhood leukemia.* Pediatr Blood Cancer, 2012. **58**(1): p. 7-11.
29. Milne, E., et al., *Fetal growth and childhood acute lymphoblastic leukemia: findings from the childhood leukemia international consortium.* Int J Cancer, 2013. **133**(12): p. 2968-79.
30. CCS, C.C.S. *What is acute lymphoblastic leukemia?* 2017 Available from: http://www.cancer.ca/en/cancer-information/cancer-type/leukemia-acute-lymphocytic-all/acute-lymphocytic-leukemia/?region=on.
31. Ward, E., et al., *Childhood and adolescent cancer statistics, 2014.* CA Cancer J Clin, 2014. **64**(2): p. 83-103.
32. ACS, A.C.S. *What are the Key Statistics About Acute Lymphocytic Leukemia*. 2017 [cited 2017 Available from: https://www.cancer.org/cancer/acute-lymphocytic-leukemia/about/key-statistics.html.
33. Foa, R., *Acute lymphoblastic leukemia: age and biology.* Pediatr Rep, 2011. **3 Suppl 2**: p. e2.
34. Gibson, T.M. and L.L. Robison, *Impact of Cancer Therapy-Related Exposures on Late Mortality in Childhood Cancer Survivors.* Chem Res Toxicol, 2015. **28**(1): p. 31-7.
35. Morel, S., et al., *Lipid and lipoprotein abnormalities in acute lymphoblastic leukemia survivors.* J Lipid Res, 2017. **58**(5): p. 982-993.
36. Barnea, D., et al., *Obesity and Metabolic Disease After Childhood Cancer.* Oncology (Williston Park), 2015. **29**(11): p. 849-55.
37. Giordano, P., et al., *Endothelial dysfunction and cardiovascular risk factors in childhood acute lymphoblastic leukemia survivors.* Int J Cardiol, 2017. **228**: p. 621-627.
38. Nottage, K.A., et al., *Metabolic syndrome and cardiovascular risk among long-term survivors of acute lymphoblastic leukaemia - From the St. Jude Lifetime Cohort.* Br J Haematol, 2014. **165**(3): p. 364-74.

39. Malhotra, J., et al., *Atherogenic low density lipoprotein phenotype in long-term survivors of childhood acute lymphoblastic leukemia.* J Lipid Res, 2012. **53**(12): p. 2747-54.
40. Robison, L.L. and M.M. Hudson, *Survivors of childhood and adolescent cancer: life-long risks and responsibilities.* Nat Rev Cancer, 2014. **14**(1): p. 61-70.
41. Janiszewski, P.M., et al., *Abdominal obesity, liver fat, and muscle composition in survivors of childhood acute lymphoblastic leukemia.* J Clin Endocrinol Metab, 2007. **92**(10): p. 3816-21.
42. Talvensaari, K.K., et al., *Long-term survivors of childhood cancer have an increased risk of manifesting the metabolic syndrome.* J Clin Endocrinol Metab, 1996. **81**(8): p. 3051-5.
43. Huang, P.L., *A comprehensive definition for metabolic syndrome.* Dis Model Mech, 2009. **2**(5-6): p. 231-7.
44. Grundy, S.M., *Metabolic syndrome scientific statement by the American Heart Association and the National Heart, Lung, and Blood Institute.* Arterioscler Thromb Vasc Biol, 2005. **25**(11): p. 2243-4.
45. Despres, J.P. and I. Lemieux, *Abdominal obesity and metabolic syndrome.* Nature, 2006. **444**(7121): p. 881-7.
46. Weisberg, S.P., et al., *Obesity is associated with macrophage accumulation in adipose tissue.* J Clin Invest, 2003. **112**(12): p. 1796-808.
47. Shuster, A., et al., *The clinical importance of visceral adiposity: a critical review of methods for visceral adipose tissue analysis.* Br J Radiol, 2012. **85**(1009): p. 1-10.
48. Hutcheson, R. and P. Rocic, *The metabolic syndrome, oxidative stress, environment, and cardiovascular disease: the great exploration.* Exp Diabetes Res, 2012. **2012**: p. 271028.
49. Aguilera, C.M., et al., *Alterations in plasma and tissue lipids associated with obesity and metabolic syndrome.* Clin Sci (Lond), 2008. **114**(3): p. 183-93.
50. Carretero, O.A. and S. Oparil, *Essential hypertension. Part I: definition and etiology.* Circulation, 2000. **101**(3): p. 329-35.
51. Dharmashankar, K. and M.E. Widlansky, *Vascular endothelial function and hypertension: insights and directions.* Curr Hypertens Rep, 2010. **12**(6): p. 448-55.

52. Levy, E., et al., *The Epigenetic Machinery in Vascular Dysfunction and Hypertension.* Curr Hypertens Rep, 2017. **19**(6): p. 52.
53. Simon, P.H., et al., *Key Considerations and Methods in the Study of Gene-Environment Interactions.* Am J Hypertens, 2016. **29**(8): p. 891-9.
54. Byon, C.H., J.M. Heath, and Y. Chen, *Redox signaling in cardiovascular pathophysiology: A focus on hydrogen peroxide and vascular smooth muscle cells.* Redox Biol, 2016. **9**: p. 244-253.
55. Kim, G.J., K. Chandrasekaran, and W.F. Morgan, *Mitochondrial dysfunction, persistently elevated levels of reactive oxygen species and radiation-induced genomic instability: a review.* Mutagenesis, 2006. **21**(6): p. 361-7.
56. Vyas, S., E. Zaganjor, and M.C. Haigis, *Mitochondria and Cancer.* Cell, 2016. **166**(3): p. 555-66.
57. Aroor, A.R., et al., *Mitochondria and Oxidative Stress in the Cardiorenal Metabolic Syndrome.* Cardiorenal Medicine, 2012. **2**(2): p. 87-109.
58. Heath-Engel, H.M. and G.C. Shore, *Mitochondrial membrane dynamics, cristae remodelling and apoptosis.* Biochim Biophys Acta, 2006. **1763**(5-6): p. 549-60.
59. LadyofHats, M.R.V.o., *Animal mitochondrion diagram*. 2007, WIKIMEDIA COMMONS
60. Lee, H. and Y. Yoon, *Mitochondrial fission and fusion.* Biochem Soc Trans, 2016. **44**(6): p. 1725-1735.
61. Picard, M., et al., *Mitochondria: isolation, structure and function.* J Physiol, 2011. **589**(Pt 18): p. 4413-21.
62. Fleissner, G., et al., *A novel concept of Fe-mineral-based magnetoreception: histological and physicochemical data from the upper beak of homing pigeons.* Naturwissenschaften, 2007. **94**(8): p. 631-42.
63. Jornayvaz, F.R. and G.I. Shulman, *Regulation of mitochondrial biogenesis.* Essays Biochem, 2010. **47**: p. 69-84.
64. Pyle, A., et al., *Fall in circulating mononuclear cell mitochondrial DNA content in human sepsis.* Intensive Care Med, 2010. **36**(6): p. 956-62.
65. Yuzefovych, L.V., et al., *Mitochondrial DNA damage and dysfunction, and oxidative stress are associated with endoplasmic reticulum stress, protein degradation and*

apoptosis in high fat diet-induced insulin resistance mice. PLoS One, 2013. **8**(1): p. e54059.

66. Neupert, W. and J.M. Herrmann, *Translocation of proteins into mitochondria.* Annu Rev Biochem, 2007. **76**: p. 723-49.
67. Basak, N.P. and S. Banerjee, *Mitochondrial dependency in progression of acute myeloid leukemia.* Mitochondrion, 2015. **21**: p. 41-8.
68. Ning, X., et al., *Wnt3a regulates mitochondrial biogenesis through p38/CREB pathway.* Biochem Biophys Res Commun, 2016.
69. Scarpulla, R.C., *Transcriptional paradigms in mammalian mitochondrial biogenesis and function.* Physiol Rev, 2008. **88**(2): p. 611-38.
70. Fernandez-Marcos, P.J. and J. Auwerx, *Regulation of PGC-1alpha, a nodal regulator of mitochondrial biogenesis.* Am J Clin Nutr, 2011. **93**(4): p. 884S-90.
71. Villena, J.A. and A. Kralli, *ERRalpha: a metabolic function for the oldest orphan.* Trends Endocrinol Metab, 2008. **19**(8): p. 269-76.
72. GM, C., *The Cell: A molecular approach.* . 2nd ed. The Cell 2000, Sunderland (MA): Sinauer Associates.
73. Berg JM, T.J., Stryer L *Chapter 17, The Citric Acid cycle* 5th ed. Biochemistry. 5th edition. 2002, New York W H Freeman
74. Farge, G., et al., *The accessory subunit B of DNA polymerase gamma is required for mitochondrial replisome function.* Nucleic Acids Res, 2007. **35**(3): p. 902-11.
75. Jackson, S., et al., *Characterisation of a novel enzyme of human fatty acid beta-oxidation: a matrix-associated, mitochondrial 2-enoyl-CoA hydratase.* Biochem Biophys Res Commun, 1995. **214**(1): p. 247-53.
76. Fillmore, N., Alrob, O.A., Lopaschuk, G.D. *Fatty Acid beta-Oxidation*. 2017 [cited 2017 May 17]; Available from: http://lipidlibrary.aocs.org/Biochemistry/content.cfm?ItemNumber=39187.
77. Chiarugi, A., et al., *The NAD metabolome--a key determinant of cancer cell biology.* Nat Rev Cancer, 2012. **12**(11): p. 741-52.
78. Lodish H, B.A., Zipursky SL, et al. , *Molecular Cell Biology* 4th edition ed. 2000, New York W.H. Freeman

79. Liu, L., et al., *LRP130 protein remodels mitochondria and stimulates fatty acid oxidation.* J Biol Chem, 2011. **286**(48): p. 41253-64.

80. Correa, T., Jakob, SM., Takala, J. , *Mitochondrial Function in Sepsis.* . Critical Care Horizons 2015. **1**: p. 31-41.

81. Sohn, Y.B., et al., *The metabolic syndrome and body composition in childhood cancer survivors.* Korean J Pediatr, 2011. **54**(6): p. 253-9.

82. Brookes, P.S., et al., *Calcium, ATP, and ROS: a mitochondrial love-hate triangle.* Am J Physiol Cell Physiol, 2004. **287**(4): p. C817-33.

83. Elmore, S., *Apoptosis: a review of programmed cell death.* Toxicol Pathol, 2007. **35**(4): p. 495-516.

84. Bhat, T.A., et al., *Restoration of mitochondria function as a target for cancer therapy.* Drug Discov Today, 2015. **20**(5): p. 635-43.

85. Brookes, P.S., *Mitochondrial nitric oxide synthase.* Mitochondrion, 2004. **3**(4): p. 187-204.

86. Gregersen, N., J. Hansen, and J. Palmfeldt, *Mitochondrial proteomics--a tool for the study of metabolic disorders.* J Inherit Metab Dis, 2012. **35**(4): p. 715-26.

87. Tan, C.P., et al., *Metallomics insights into the programmed cell death induced by metal-based anticancer compounds.* Metallomics, 2014. **6**(5): p. 978-95.

88. Harrison, D.G. and M.C. Gongora, *Oxidative stress and hypertension.* Med Clin North Am, 2009. **93**(3): p. 621-35.

89. Matsuda, M. and I. Shimomura, *Increased oxidative stress in obesity: implications for metabolic syndrome, diabetes, hypertension, dyslipidemia, atherosclerosis, and cancer.* Obes Res Clin Pract, 2013. **7**(5): p. e330-41.

90. Reuter, S., et al., *Oxidative stress, inflammation, and cancer: how are they linked?* Free Radic Biol Med, 2010. **49**(11): p. 1603-16.

91. Jin, H.S., et al., *Mitochondrial Control of Innate Immunity and Inflammation.* Immune Netw, 2017. **17**(2): p. 77-88.

92. Conklin, K.A., *Chemotherapy-associated oxidative stress: impact on chemotherapeutic effectiveness.* Integr Cancer Ther, 2004. **3**(4): p. 294-300.

93. Schieber, M. and N.S. Chandel, *ROS function in redox signaling and oxidative stress.* Curr Biol, 2014. **24**(10): p. R453-62.

94. Lopez-Armada, M.J., et al., *Mitochondrial dysfunction and the inflammatory response.* Mitochondrion, 2013. **13**(2): p. 106-18.
95. Gilca, M., et al., *The oxidative hypothesis of senescence.* J Postgrad Med, 2007. **53**(3): p. 207-13.
96. Boilard, E. and P.R. Fortin, *Connective tissue diseases: Mitochondria drive NETosis and inflammation in SLE.* Nat Rev Rheumatol, 2016. **12**(4): p. 195-6.
97. Wajant, H., K. Pfizenmaier, and P. Scheurich, *Tumor necrosis factor signaling.* Cell Death Differ, 2003. **10**(1): p. 45-65.
98. Zhang, H., et al., *Role of TNF-alpha in vascular dysfunction.* Clin Sci (Lond), 2009. **116**(3): p. 219-30.
99. Madge, L.A. and J.S. Pober, *TNF signaling in vascular endothelial cells.* Exp Mol Pathol, 2001. **70**(3): p. 317-25.
100. Wullaert, A., K. Heyninck, and R. Beyaert, *Mechanisms of crosstalk between TNF-induced NF-kappaB and JNK activation in hepatocytes.* Biochem Pharmacol, 2006. **72**(9): p. 1090-101.
101. Ghosh, S. and M. Karin, *Missing pieces in the NF-kappaB puzzle.* Cell, 2002. **109 Suppl**: p. S81-96.
102. Schulze-Osthoff, K., et al., *Cytotoxic activity of tumor necrosis factor is mediated by early damage of mitochondrial functions. Evidence for the involvement of mitochondrial radical generation.* J Biol Chem, 1992. **267**(8): p. 5317-23.
103. Palmfeldt, J. and P. Bross, *Proteomics of human mitochondria.* Mitochondrion, 2016.
104. Brand, M.D. and D.G. Nicholls, *Assessing mitochondrial dysfunction in cells.* Biochem J, 2011. **435**(2): p. 297-312.
105. Hopps, E., et al., *A novel component of the metabolic syndrome: the oxidative stress.* Nutr Metab Cardiovasc Dis, 2010. **20**(1): p. 72-7.
106. Martinez-Hervas, S., et al., *Insulin resistance and oxidative stress in familial combined hyperlipidemia.* Atherosclerosis, 2008. **199**(2): p. 384-9.
107. Bhattacharyya, A., et al., *Oxidative stress: an essential factor in the pathogenesis of gastrointestinal mucosal diseases.* Physiol Rev, 2014. **94**(2): p. 329-54.
108. Furukawa, S., et al., *Increased oxidative stress in obesity and its impact on metabolic syndrome.* J Clin Invest, 2004. **114**(12): p. 1752-61.

109. Roberts, C.K. and K.K. Sindhu, *Oxidative stress and metabolic syndrome.* Life Sci, 2009. **84**(21-22): p. 705-12.

110. Marseglia, L., et al., *Oxidative stress in obesity: a critical component in human diseases.* Int J Mol Sci, 2014. **16**(1): p. 378-400.

111. Ando, K. and T. Fujita, *Metabolic syndrome and oxidative stress.* Free Radic Biol Med, 2009. **47**(3): p. 213-8.

112. Hotamisligil, G.S., *Endoplasmic reticulum stress and the inflammatory basis of metabolic disease.* Cell, 2010. **140**(6): p. 900-17.

113. Perticone, F., et al., *Obesity and body fat distribution induce endothelial dysfunction by oxidative stress: protective effect of vitamin C.* Diabetes, 2001. **50**(1): p. 159-65.

114. Silver, A.E., et al., *Overweight and obese humans demonstrate increased vascular endothelial NAD(P)H oxidase-p47(phox) expression and evidence of endothelial oxidative stress.* Circulation, 2007. **115**(5): p. 627-37.

115. Hotamisligil, G.S., N.S. Shargill, and B.M. Spiegelman, *Adipose expression of tumor necrosis factor-alpha: direct role in obesity-linked insulin resistance.* Science, 1993. **259**(5091): p. 87-91.

116. Xu, H., et al., *Chronic inflammation in fat plays a crucial role in the development of obesity-related insulin resistance.* J Clin Invest, 2003. **112**(12): p. 1821-30.

117. Behloul, N. and G. Wu, *Genistein: a promising therapeutic agent for obesity and diabetes treatment.* Eur J Pharmacol, 2013. **698**(1-3): p. 31-8.

118. Fabbri, E., et al., *Insulin Resistance Is Associated With Reduced Mitochondrial Oxidative Capacity Measured by 31P-Magnetic Resonance Spectroscopy in Participants Without Diabetes From the Baltimore Longitudinal Study of Aging.* Diabetes, 2017. **66**(1): p. 170-176.

119. Aguirre, V., et al., *The c-Jun NH(2)-terminal kinase promotes insulin resistance during association with insulin receptor substrate-1 and phosphorylation of Ser(307).* J Biol Chem, 2000. **275**(12): p. 9047-54.

120. Wieser, V., A.R. Moschen, and H. Tilg, *Inflammation, cytokines and insulin resistance: a clinical perspective.* Arch Immunol Ther Exp (Warsz), 2013. **61**(2): p. 119-25.

121. Benigni, A., P. Cassis, and G. Remuzzi, *Angiotensin II revisited: new roles in inflammation, immunology and aging.* EMBO Mol Med, 2010. **2**(7): p. 247-57.
122. Araujo, F.B., et al., *Evaluation of oxidative stress in patients with hyperlipidemia.* Atherosclerosis, 1995. **117**(1): p. 61-71.
123. Ferri, J., et al., *[8-oxo-7,8-dihydro-2'-deoxyguanosine as a marker of DNA oxidative stress in individuals with combined familiar hyperlipidemia].* Med Clin (Barc), 2008. **131**(1): p. 1-4.
124. Trimis, G., et al., *Early indicators of dysmetabolic syndrome in young survivors of acute lymphoblastic leukemia in childhood as a target for preventing disease.* J Pediatr Hematol Oncol, 2007. **29**(5): p. 309-14.
125. Rosen, G.P., H.T. Nguyen, and G.Q. Shaibi, *Metabolic syndrome in pediatric cancer survivors: a mechanistic review.* Pediatr Blood Cancer, 2013. **60**(12): p. 1922-8.
126. Kourti, M., et al., *Metabolic syndrome in children and adolescents with acute lymphoblastic leukemia after the completion of chemotherapy.* J Pediatr Hematol Oncol, 2005. **27**(9): p. 499-501.
127. Gurney, J.G., et al., *Metabolic syndrome and growth hormone deficiency in adult survivors of childhood acute lymphoblastic leukemia.* Cancer, 2006. **107**(6): p. 1303-12.
128. Mody, R., et al., *Twenty-five-year follow-up among survivors of childhood acute lymphoblastic leukemia: a report from the Childhood Cancer Survivor Study.* Blood, 2008. **111**(12): p. 5515-23.
129. Gibson, T.M., M.J. Ehrhardt, and K.K. Ness, *Obesity and Metabolic Syndrome Among Adult Survivors of Childhood Leukemia.* Curr Treat Options Oncol, 2016. **17**(4): p. 17.
130. Oeffinger, K.C., et al., *Insulin resistance and risk factors for cardiovascular disease in young adult survivors of childhood acute lymphoblastic leukemia.* J Clin Oncol, 2009. **27**(22): p. 3698-704.
131. Chow, E.J., et al., *Obesity and hypertension among children after treatment for acute lymphoblastic leukemia.* Cancer, 2007. **110**(10): p. 2313-20.
132. Armstrong, G.T., et al., *Late mortality among 5-year survivors of childhood cancer: a summary from the Childhood Cancer Survivor Study.* J Clin Oncol, 2009. **27**(14): p. 2328-38.

133. Ness, K.K., et al., *Adverse effects of treatment in childhood acute lymphoblastic leukemia: general overview and implications for long-term cardiac health.* Expert Rev Hematol, 2011. **4**(2): p. 185-97.
134. Montaigne, D., C. Hurt, and R. Neviere, *Mitochondria death/survival signaling pathways in cardiotoxicity induced by anthracyclines and anticancer-targeted therapies.* Biochem Res Int, 2012. **2012**: p. 951539.
135. Turner, S.D., et al., *Knowledge-driven multi-locus analysis reveals gene-gene interactions influencing HDL cholesterol level in two independent EMR-linked biobanks.* PLoS One, 2011. **6**(5): p. e19586.
136. Tan, Z., et al., *The Role of PGC1alpha in Cancer Metabolism and its Therapeutic Implications.* Mol Cancer Ther, 2016. **15**(5): p. 774-82.
137. Senft, D. and Z.A. Ronai, *Regulators of mitochondrial dynamics in cancer.* Curr Opin Cell Biol, 2016. **39**: p. 43-52.
138. Testa, U. and R. Riccioni, *Deregulation of apoptosis in acute myeloid leukemia.* Haematologica, 2007. **92**(1): p. 81-94.
139. Prasad, S., S.C. Gupta, and A.K. Tyagi, *Reactive oxygen species (ROS) and cancer: Role of antioxidative nutraceuticals.* Cancer Lett, 2017. **387**: p. 95-105.
140. Cruz-Bermudez, A., et al., *Spotlight on the relevance of mtDNA in cancer.* Clin Transl Oncol, 2016.
141. Scheffler, I.E., *Mitochondria, 2nd Edition* 2nd ed. 2007: John Wiley & Sons, Inc. .
142. Boultwood, J., et al., *Amplification of mitochondrial DNA in acute myeloid leukaemia.* Br J Haematol, 1996. **95**(2): p. 426-31.
143. Clayton, D.A. and J. Vinograd, *Circular dimer and catenate forms of mitochondrial DNA in human leukaemic leucocytes.* Nature, 1967. **216**(5116): p. 652-7.
144. Wardell, T.M., et al., *Changes in the human mitochondrial genome after treatment of malignant disease.* Mutation Research/Fundamental and Molecular Mechanisms of Mutagenesis, 2003. **525**(1-2): p. 19-27.
145. Essop, M.F., W.A. Chan, and S. Hattingh, *Proteomic analysis of mitochondrial proteins in a mouse model of type 2 diabetes.* Cardiovasc J Afr, 2011. **22**(4): p. 175-8.
146. Basak, N.P., A. Roy, and S. Banerjee, *Alteration of mitochondrial proteome due to activation of Notch1 signaling pathway.* J Biol Chem, 2014. **289**(11): p. 7320-34.

147. Jiang, Y. and X. Wang, *Comparative mitochondrial proteomics: perspective in human diseases.* J Hematol Oncol, 2012. **5**: p. 11.

148. Patti, M.E., et al., *Coordinated reduction of genes of oxidative metabolism in humans with insulin resistance and diabetes: Potential role of PGC1 and NRF1.* Proc Natl Acad Sci U S A, 2003. **100**(14): p. 8466-71.

149. Peinado, J.R., et al., *Mitochondria in metabolic disease: getting clues from proteomic studies.* Proteomics, 2014. **14**(4-5): p. 452-66.

150. Alston, C.L., et al., *The genetics and pathology of mitochondrial disease.* J Pathol, 2017. **241**(2): p. 236-250.

151. Haining, W.N., et al., *Antigen-specific T-cell memory is preserved in children treated for acute lymphoblastic leukemia.* Blood, 2005. **106**(5): p. 1749-54.

ANNEXE

patient-oriented and epidemiological research

Lipid and lipoprotein abnormalities in acute lymphoblastic leukemia survivors[S]

Sophia Morel,*,† Jade Leahy,*,† Maryse Fournier,*,† Benoit Lamarche,§ Carole Garofalo,* Guy Grimard, Floriane Poulain,* Edgard Delvin,* Caroline Laverdière,*,** Maja Krajinovic,*,** Simon Drouin,* Daniel Sinnett,*,** Valérie Marcil,*,† and Emile Levy[1],*,†,§**

Research Centre, Sainte-Justine University Hospital Health Center* and Departments of Nutrition† and Pediatrics,** Université de Montréal, Montreal, Quebec, Canada H3T 1C5; and Institute of Nutrition and Functional Foods,§ Laval University, Quebec, Quebec, Canada G1V 0A6

Abstract **Survivors of acute lymphoblastic leukemia (ALL), the most common cancer in children, are at increased risk of developing late cardiometabolic conditions. However, the mechanisms are not fully understood. This study aimed to characterize the plasma lipid profile, Apo distribution, and lipoprotein composition of 80 childhood ALL survivors compared with 22 healthy controls. Our results show that, despite their young age, 50% of the ALL survivors displayed dyslipidemia, characterized by increased plasma triglyceride (TG) and LDL-cholesterol, as well as decreased HDL-cholesterol. ALL survivors exhibited lower plasma Apo A-I and higher Apo B-100 and C-II levels, along with elevated Apo C-II/C-III and B-100/A-I ratios. VLDL fractions of dyslipidemic ALL survivors contained more TG, free cholesterol, and phospholipid moieties, but less protein. Differences in Apo content were found between ALL survivors and controls for all lipoprotein fractions except HDL_3. HDL_2, especially, showed reduced Apo A-I and raised Apo A-II, leading to a depressed Apo A-I/A-II ratio. Analysis of VLDL-Apo Cs disclosed a trend for higher Apo $C\text{-}III_1$ content in dyslipidemic ALL survivors.[JLR] In conclusion, this thorough investigation demonstrates a high prevalence of dyslipidemia in ALL survivors, while highlighting significant abnormalities in their plasma lipid profile and lipoprotein composition. Special attention must, therefore, be paid to these subjects given the atherosclerotic potency of lipid and lipoprotein disorders.—** Morel, S., J. Leahy, M. Fournier, B. Lamarche, C. Garofalo, G. Grimard, F. Poulain, E. Delvin, C. Laverdière, M. Krajinovic, S. Drouin, D. Sinnett, V. Marcil, and E. Levy. **Lipid and lipoprotein abnormalities in acute lymphoblastic leukemia survivors. *J. Lipid Res.* 2017.** 58: **982–993.**

Supplementary key words dyslipidemia • lipid and lipoprotein metabolism • apolipoproteins • atherosclerosis • cancer • clinical studies • cardiovascular diseases • metabolic syndrome

Acute lymphoblastic leukemia (ALL) accounts for 25% of all childhood malignancies and represents the most common form of leukemia in children. Cure rates for ALL now exceed 85%, allowing a growing number of childhood survivors to live into adulthood (1). However, survivors face severe, even life-threatening, long-term sequelae decades after the end of treatments (2, 3). Of interest, ALL survivors are at increased risk of developing cardiovascular conditions, including congestive heart failure, coronary artery disease, myocardial infarction, cardiac arrest, and cerebrovascular accidents (4–6). Studies on pediatric ALL survivors have reported a high prevalence of the typical components of the metabolic syndrome (MetS), such as obesity (7), hypertension (8), glucose tolerance (9), or dyslipidemia (10), and clustering of the three surrogates of MetS was also described (11). While chemo- and radiotherapy have often been associated with the development of these disorders in childhood cancer survivors (12–15), the precise etiology and the mechanisms of these late complications are not fully understood.

In view of the presence of metabolic disorders, lipid abnormalities were examined to appraise the cardiovascular risk in populations of long-term ALL survivors. Various research groups have focused on absolute LDL-cholesterol (LDL-C) and HDL-cholesterol (HDL-C) levels after treatment with cranial radiotherapy and chemotherapy. Compared with the general population, ALL survivors were found to be at higher risk of high LDL-C [relative risk (RR) = 1.25], elevated triglyceride (TG) (RR = 1.32), and low HDL-C (RR = 1.78) levels. These increased risks were particularly notable in those who were exposed to cranial

This work was supported by a grants from the Institute of Cancer Research of the Canadian Institutes of Health Research, in collaboration with C17 Council, Canadian Cancer Society, Cancer Research Society, Garron Family Cancer Centre at the Hospital for Sick Children, Ontario Institute for Cancer Research, and J.A. DeSeve Research Chair in Nutrition; the Fonds de Recherche du Québec – Santé; and the Cole Foundation.

Manuscript received 22 September 2016 and in revised form 6 February 2017.

Published, JLR Papers in Press, March 8, 2017
DOI https://doi.org/10.1194/jlr.M072207

Abbreviations: ALL, acute lymphoblastic leukemia; cALL, childhood acute lymphoblastic leukemia; EC, esterified cholesterol; FC, free cholesterol; HDL-C, HDL-cholesterol; HOMA-IR, homeostasis model assessment-insulin resistance; LDL-C, LDL-cholesterol; LDLR, LDL receptor; MetS, metabolic syndrome; PL, phospholipid; RR, relative risk; TC, total cholesterol; TG, triglyceride; TMU, tetramethylurea.

[1]To whom correspondence should be addressed.
e-mail: emile.levy@recherche-ste-justine.qc.ca

[S] The online version of this article (available at http://www.jlr.org) contains a supplement.

radiotherapy (11). Similarly, another smaller study found that childhood ALL (cALL) survivors treated with cranial radiotherapy and chemotherapy had higher LDL-C and lower HDL-C values than did controls (16). Other studies did not find differences between ALL survivors and non-cancer subjects (17, 18), apart from HDL-C, which was decreased in women exposed to cranial radiotherapy (18). In addition, despite LDL-C concentrations in the normal range, an atherogenic LDL profile was identified in young adult ALL survivors (10). LDL-C and HDL-C measurements are important, but clearly not sufficient, to identify cardiometabolic risk, as it appears that lipoprotein composition rather than concentration predicts atherosclerosis (19, 20). For example, HDL particles are highly heterogeneous and growing evidence suggests that their atheroprotective potential depends on their component composition and unique functional properties rather than their cholesterol concentrations (21–24). This was corroborated by studies that showed that higher levels of HDL-C are not associated with reduced risk of cardiovascular events in patients with advanced CVD (25, 26). In addition, a stronger correlation was found between CVD and small sized-LDL rather than with LDL-C concentrations (27). Accordingly, cholesterol of small sized-LDL was associated with an increased risk of subclinical atherosclerosis (28), CVDs (29), and future disadvantageous outcomes (30). Apo composition of lipoproteins is also considered a predictor of cardiovascular risk, as the Apo B-100/A-I ratio constitutes one of the strongest predictors of coronary heart disease (31).

The lipid disorders in the present study are reported for the first time in a French-Canadian population of cALL survivors, who are part of a unique population from the province of Quebec (Canada). Historically, this settler group expanded rapidly in relative isolation due to linguistic, religious, and geographic barriers, while reinforcing the strong genetic founder effect (32, 33). Although available literature generally reports an abnormal plasma lipid profile of ALL survivors, Apo distribution and lipoprotein core and surface composition have not been characterized in populations of childhood cancer survivors. Given the increased risk of CVDs suspected in these subjects, the present study was designed to examine these important issues in a cohort of dyslipidemic and normolipidemic pediatric ALL survivors compared with healthy controls.

MATERIALS AND METHODS

Study population

The 80 ALL survivors included in this study were recruited between January 2012 and September 2014 as part of the PETALE program at the Sainte-Justine University Hospital Center in Montreal. The study design was described elsewhere (34). Briefly, it aimed to characterize long-term effects in cALL survivors, namely, cardiotoxicity, cardiometabolic complications, neurocognitive problems, bone morbidity, quality of life issues, and genomic determinants. The PETALE cohort is comprised almost exclusively of cALL survivors of European-descent from the province of Québec. Participants enrolled in the PETALE study were unrelated, under age 19 at diagnosis, treated using Dana Farber Cancer Institute protocols (35), without hematopoietic stem cell transplantation, and more than 5 years event-free post diagnosis. For the present study, we included 40 adults and 40 adolescents (50% male) in order to create four groups: 20 men, 20 women, 20 boys, and 20 girls. Recruitment started with the first PETALE participant and ended when a total of 20 subjects had been reached for each group. The anthropometric and clinical features of the participants are outlined in **Table 1**. For comparison purposes, 22 unrelated age- and gender-matched healthy controls, who suffered from minor trauma (e.g., ankle sprains, mild strain injuries, broken leg), were recruited at the Orthopedics Clinic (adolescents) and within the Research Center (adults) of the Sainte-Justine Hospital. The exclusion criteria for their recruitment included an abnormal lipid profile, a chronic metabolic disease, and/or a chronic inflammatory disease. Adults were defined as being ⩾18 years of age and children <18 years old. The Institutional Review Board of Sainte-Justine Hospital approved the study and investigations were carried out in accordance with the principles of the Declaration of Helsinki. Written informed consent was obtained from study participants and/or parents/guardians.

Biochemical analyses and LDL particle size

Overnight fasting blood samples were collected in tubes containing 1 g/l EDTA and were kept on ice until centrifugation. Plasma was separated within 45 min of collection and stored at −80°C until analysis. Fasting insulin, glucose, total cholesterol (TC), TG, and HDL-C concentrations were measured as described previously (36). LDL-C was calculated using the Friedewald formula (37). Plasma Apos (A-I, A-IV, B-100, C-II, C-III,

TABLE 1. Clinical and biochemical characteristics of ALL survivors compared with age- and gender-matched controls

	Healthy Controls	ALL Survivors
Total	n = 22	n = 80
Age at visit (y)	21.23 ± 1.44	21.10 ± 0.83
Age at cancer diagnosis (y)	N/A	6.61 ± 0.53
Survival time (y)	N/A	12.38 ± 0.71
Gender (male, %)	50	50
Children (%)	45	50
BMI (kg/m^2)	22.53 ± 0.51	24.45 ± 0.64
Glucose (mmol/l)	5.11 ± 0.05	5.08 ± 0.06
Insulin (pmol/l)	55.32 ± 4.6	59.12 ± 4.34
HOMA-IR	1.82 ± 0.15	1.95 ± 0.15
Children	n = 10	n = 40
Age at visit (y)	15.60 ± 0.31	15.28 ± 0.31
Age at cancer diagnosis (y)	N/A	4.36 ± 0.39
Survival time (y)	N/A	8.74 ± 0.42
Gender (male, %)	50	50
BMI (kg/m^2)	22.32 ± 0.87	22.08 ± 0.60
Glucose (mmol/l)	5.14 ± 0.09	4.90 ± 0.07
Insulin (pmol/l)	71.51 ± 5.5	60.51 ± 4.47
HOMA-IR	2.34 ± 0.16	1.92 ± 0.15
Adults	n = 12	n = 40
Age at visit (y)	25.92 ± 1.66	26.92 ± 0.61
Age at cancer diagnosis (y)	N/A	8.87 ± 0.84
Survival time (y)	N/A	16.02 ± 1.08
Gender (male, %)	50	50
BMI (kg/m^2)	22.70 ± 0.61	26.82 ± 1.01[a]
Glucose (mmol/l)	5.08 ± 0.06	5.25 ± 0.08
Insulin (pmol/l)	41.83 ± 4.1	57.77 ± 7.44
HOMA-IR	1.36 ± 0.14	1.98 ± 0.27

Data are expressed as percentage or as mean ± SEM. Subjects were stratified according to age (adults: ⩾18 years old; children: <18 years old). HOMA-IR was calculated using the formula: [fasting insulin (mU/ml) × fasting glucose (mmol/l)]/22.5. N/A, not applicable.
[a] $P < 0.05$ versus healthy controls.

JOURNAL OF LIPID RESEARCH ASBMB JLR

and E) were determined by commercial ELISA kits. BMI was computed as weight in kilograms divided by height in square meters. The homeostasis model assessment-insulin resistance (HOMA-IR) index was calculated using the formula: [fasting insulin (mU/ml) × fasting glucose (mmol/l)]/22.5. Nondenaturing 2–16% PAGE was used to assess LDL particle size, as previously described (38, 39). LDL particle size was determined on the basis of the relative migration of plasma standards of known diameter and LDL peak particle size was computed as the estimated diameter for the major peak of each scan (38). An integrated (or mean) LDL size, corresponding to the weighed mean size of all LDL subclasses in each individual, was also assessed (40).

Lipoprotein isolation

Lipoprotein separation was carried out as previously described (41–43). Briefly, plasma was separated by low speed centrifugation (2,200 *g*, 20 min) at 4°C and the lipoprotein fractions were isolated by sequential ultracentrifugation with a Ti-50 rotor in a Beckman model LE-80 ultracentrifuge. After removal of chylomicrons by preliminary centrifugation (25,000 *g*, 30 min), VLDL (1.006 g/ml), IDL (1.019 g/ml), and LDL (1.063 g/ml) were isolated by centrifugation at 40,000 *g* for 18 h at 4°C. Isolation of HDL_2 (1.125 g/ml) and HDL_3 (1.21 g/ml) was carried out at 40,000 *g* for 48 h at 4°C.

Characterization of lipoprotein composition

The total protein content of each lipoprotein was determined by the Bradford method with BSA as a standard, whereas phospholipids (PLs) were measured using the Bartlett method (44). Commercial kits were used to quantify TG (Randox TRIGS, UK), TC, and free cholesterol (FC) (Wako Diagnostics) by enzymatic colorimetric methods. Esterified cholesterol (EC) was calculated as the difference between TC and FC. Lipoprotein composition was determined as the percentage of TG, EC, FC, PL, and total protein. The lipoprotein distribution of Apos was examined by electrophoresis on 4–20% gradient SDS-PAGE (41–43) and by tetramethylurea (TMU) gel electrophoresis (43). Electrophoretic analyses were performed in 22 controls and in 38 survivors selected according to their lipid profile (dyslipidemic and nondyslipidemic: n = 26 for SDS-PAGE and n = 12 for TMU). Apo densitometric distribution was assessed using the ChemiDoc MP and Imaging System (Bio-Rad) for band visualization followed by densitometric evaluation with the UN-SCAN-IT gel 6.1 software. Percent distribution of Apos was calculated as percent of total Apos.

Assessment of dyslipidemia

Dyslipidemia was determined by presenting at least one of three factors: high LDL-C, high TG, and/or low HDL-C. In adults, TG levels <1.3 mmol/l were classified as optimal, borderline (⩾1.3 and <1.7 mmol/l) (45) and high (⩾1.7 mmol/l) (46). Values of LDL-C <2.6 mmol/l were considered optimal, borderline between ⩾2.6 and <3.4 mmol/l, and elevated when ⩾3.4 mmol/l (46). Values of HDL-C <1.03 in men and <1.3 in women were considered low (46). In children, LDL-C, TG, and HDL-C values were compared with those of the National Heart, Lung, and Blood Institute guidelines according to gender and age group and were classified as optimal, borderline, or abnormal (45).

Whole-exome sequencing and analysis

APOE, LDL receptor (*LDLR*), and *LPL* gene variants were identified using whole-exome sequencing for the ALL survivor cohort. Sequencing data were obtained from the Sainte-Justine Hospital and Génome Québec Integrated Clinical Genomic Center using the SOLiD (Thermo Fisher Scientific) or Illumina HiSeq 2500 platforms and then aligned on the Hg19 reference genome. Rare and common variants with a predicted functional impact on protein were identified using the functional annotation from ANNOVAR (47). Only variants with a PolyPhen-2 score ⩾0.85 (48) or a SIFT score ⩽0.1 (49) were labeled as "potentially damaging" and used for further analyses. Following this analysis, two polymorphisms were identified (rs7412 in *APOE* and rs118204057 in *LPL*). For validation, these two SNPs were genotyped in the survivor and control cohorts, as described previously (50). Primers used were: rs7412, forward: GCCGATGACCTGCAGAAG, reverse: CTGCCCATCTCCTCCATC, allele specific probes: GCAGAAG**C**GCCTGGC, GCAGAAG**T**GCCTGGC; and rs118204057, forward: CGAGTCGTCTTTCTCCTGAT, reverse:

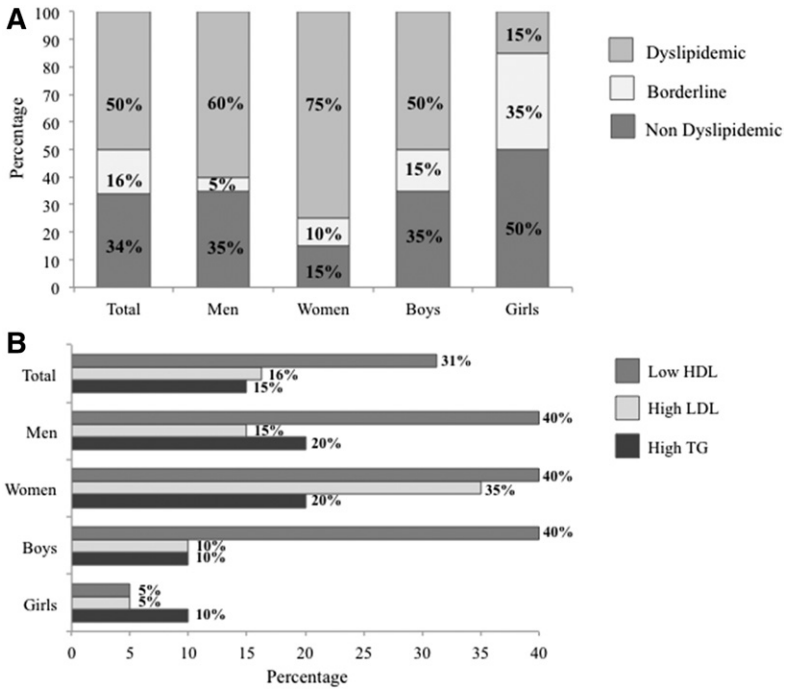

Fig. 1. Prevalence of dyslipidemia in n = 80 survivors of cALL. Data were analyzed in the entire cohort and stratified according to age (adults ⩾18 years old and children <18 years old) and gender (n = 20/group). Levels of LDL-C, TGs, and HDL-C were used to classify subjects according to their lipid profile, as described in the Materials and Methods. Subjects with at least one abnormal lipid value were defined as dyslipidemic; those with at least one borderline lipid value were defined as borderline; and subjects without abnormal and/or borderline values were classified as nondyslipidemic (A). The prevalence of high LDL-C, high TGs, and low HDL-C was assessed in the entire group and in men, women, boys, and girls (B). Data are expressed as a percentage. Prevalence of dyslipidemia in the control group is not represented due to the exclusion criteria described in the Materials and Methods.

CTGGCTGAAAAGTACCTCCA, allele specific probes: CCAGAG-**G**GTCCCCTG, CCAGAG**A**GTCCCCTG (specific allele is shown in bold). Potential genotyping errors were assessed using Chi-square tests to evaluate the deviation from the Hardy-Weinberg equilibrium.

Statistical analyses

ALL survivors were categorized according to their lipid status (dyslipidemic/nondyslipidemic). Differences in plasma lipids, lipoproteins, Apos, and in lipoprotein composition between groups were assessed using unpaired Student's *t*-tests or Mann-Whitney U tests depending on the normality of the distribution. Continuous variables are expressed as mean ± SEM unless otherwise specified. $P < 0.05$ was considered statistically significant. Statistical analyses were performed with GraphPad Prism version 6.0.

RESULTS

Anthropometric and clinical characteristics of participants

The clinical characteristics of ALL survivors and healthy controls are shown in Table 1. The mean age of ALL survivors was 21.2 years and 50% were male. The mean of their survival time was 12.4 years and age at diagnosis was 6.6 years. Analysis of the entire cohorts revealed no significant differences between ALL survivors and controls in terms of age, gender distribution, BMI, glucose, insulin, and HOMA-IR. Similarly, no differences between groups were noted after stratification by age (i.e., children vs. adults) with the exception of higher BMI in adult survivors compared with healthy adult controls.

Dyslipidemia in survivors of ALL

As outlined in **Fig. 1A**, analysis of the entire cohort of survivors revealed dyslipidemia in 50% of subjects. Stratification of data according to age and gender demonstrated a lower prevalence of dyslipidemia in girls (15%) than in boys (50%). This trend was reversed in adulthood with a predominance of dyslipidemia in women (75%) compared with men (60%). It should be pointed out that 35% of girls were characterized with borderline lipid levels, a condition that may deteriorate in adulthood. In contrast, a difference of only 10% was observed between boys and men.

Next, we scrutinized the types of disturbances that define dyslipidemia (Fig. 1B). Among ALL survivors, 15% had elevated TG, 16% disclosed high LDL-C, and 31% displayed low HDL-C levels. While the type of dyslipidemia varied among groups, the most frequent abnormalities observed were low HDL-C and high TG. Specifically, 20% of

TABLE 2. Plasma lipid and lipoprotein values in child and adult survivors of ALL and controls

		ALL Survivors		
	Healthy Controls	Entire Group	Subgroup without Dyslipidemia	Subgroup with Dyslipidemia
Total	n = 22	n = 80	n = 40	n = 40
TG (mmol/l)	0.91 ± 0.06	1.08 ± 0.07	0.75 ± 0.04[a]	1.42 ± 0.11[b,c]
TC (mmol/l)	4.23 ± 0.14	4.41 ± 0.08	N/A	N/A
LDL-C (mmol/l)	2.40 ± 0.12	2.63 ± 0.07	2.33 ± 0.08	2.92 ± 0.10[b,c]
HDL-C (mmol/l)	1.42 ± 0.05	1.29 ± 0.03[a]	1.40 ± 0.04	1.18 ± 0.05[c,d]
LDL mean diameter (Å)	254.4 ± 0.29	254.7 ± 0.18	254.8 ± 0.26	254.6 ± 0.25
Small dense LDL (%)	57.61 ± 2.65	53.60 ± 1.45	53.89 ± 2.29	53.30 ± 1.81
LDL/HDL-C	1.73 ± 0.10	2.17 ± 0.08[a]	1.74 ± 0.08	2.61 ± 0.11[c,d]
TC/HDL-C	3.03 ± 0.11	3.58 ± 0.10[b]	2.99 ± 0.09	4.18 ± 0.13[c,d]
Children	n = 10	n = 40	n = 27	n = 13
TG (mmol/l)	0.85 ± 0.07	0.94 ± 0.08	0.71 ± 0.05	1.42 ± 0.15[b,c]
TC (mmol/l)	3.96 ± 0.22	4.20 ± 0.09	N/A	N/A
LDL-C (mmol/l)	2.24 ± 0.17	2.49 ± 0.09	2.40 ± 0.10	2.70 ± 0.16
HDL-C (mmol/l)	1.34 ± 0.06	1.28 ± 0.04	1.394 ± 0.05	1.03 ± 0.05[c,d]
LDL mean diameter (Å)	254.2 ± 0.42	254.8 ± 0.25	254.9 ± 0.29	254.6 ± 0.48
Small dense LDL (%)	60.73 ± 3.36	53.16 ± 1.87	52.28 ± 2.30	54.99 ± 3.24
LDL/HDL-C	1.69 ± 0.14	2.08 ± 0.12	1.79 ± 0.10	2.70 ± 0.22[b,c]
TC/HDL-C	2.97 ± 0.15	3.45 ± 0.15	3.03 ± 0.11	4.33 ± 0.26[c,d]
Adults	n = 12	n = 40	n = 13	n = 27
TG (mmol/l)	0.95 ± 0.08	1.22 ± 0.11	0.82 ± 0.09	1.42 ± 0.14[e]
TC (mmol/l)	4.45 ± 0.15	4.61 ± 0.14	N/A	N/A
LDL-C (mmol/l)	2.53 ± 0.15	2.76 ± 0.11	2.20 ± 0.12	3.03 ± 0.12[a,c]
HDL-C (mmol/l)	1.49 ± 0.08	1.30 ± 0.05	1.40 ± 0.06	1.25 ± 0.07[a,f]
LDL mean diameter (Å)	254.6 ± 0.4	254.7 ± 0.25	254.5 ± 0.54	254.7 ± 0.28
Small dense LDL (%)	55.02 ± 3.93	54.03 ± 2.24	57.22 ± 5.21	52.49 ± 2.20
LDL/HDL	1.77 ± 0.16	2.27 ± 0.12[a]	1.64 ± 0.14	2.57 ± 0.13[c,d]
TC/HDL-C	3.06 ± 0.17	3.71 ± 0.14[a]	2.91 ± 0.14	4.10 ± 0.14[c,d]

Data are expressed as mean ± SEM. Dyslipidemia was defined when subjects presented at least one of three factors: high LDL-C, high TG, and/or low HDL-C. In adults, LDL-C <3.4 mmol/l was considered normal and ⩾3.4 mmol/l high. TGs <1.7 and ⩾1.7 mmol/l were classified as normal and high, respectively. HDL-C <1.03 mmol/l in men and <1.3 mmol/l in women were considered low. In children, cut-off values were defined according to the guidelines of the National Heart, Lung, and Blood Institute with consideration of gender and age (45). N/A, not applicable.

[a] $P < 0.05$ versus healthy controls.
[b] $P < 0.01$ versus healthy controls.
[c] $P < 0.001$ versus ALL survivors without dyslipidemia.
[d] $P < 0.001$ versus healthy controls.
[e] $P < 0.01$ versus ALL survivors without dyslipidemia.
[f] $P < 0.05$ versus ALL survivors without dyslipidemia.

JOURNAL OF LIPID RESEARCH ASBMB JLR

women and men had high TG and 40% of men, women, and boys presented with low HDL-C. High levels of LDL-C were mainly found in adults (15% of men and 35% of women).

We then compared fasting lipid values between the whole group of ALL survivors and age- and gender-matched healthy controls (**Table 2**). Results reveal a trend of increased LDL-C along with significantly decreased HDL-C values, which resulted in significantly higher ratios of LDL-C/HDL-C and TC/HDL-C than those of controls. Similarly, when we segregated the ALL survivor group according to their normal and abnormal lipid profile, the dyslipidemic ALL subgroup disclosed higher concentrations of TG and LDL-C, lower concentrations of HDL-C, as well as more elevated ratios of LDL-C/HDL-C and TC/HDL-C than did controls. The same significant trend was observed when ALL children were analyzed separately from ALL adults. Only TG levels were found to be significantly different between nondyslipidemic survivors and controls. In addition, neither the mean LDL-C diameter nor the proportions of small dense LDL-C (diameter <255 Å) showed any significant divergences among the groups (Table 2).

Plasma Apo profile

Several differences were observed between the plasma Apo profile of ALL survivors and that of healthy controls (**Table 3**). ALL survivors had significantly lower Apo A-I concentrations along with higher levels of Apo B-100 and Apo C-II. No significant divergences were seen in Apo A-IV, C-III, and E concentrations. Calculation of important ratios revealed higher Apo C-II/C-III and Apo B-100/A-I in the ALL survivor group. Stratification of the ALL survivor cohort according to age showed that both adults and children contributed to the observed differences (Table 3). Interestingly, Apos C-II and C-III were significantly higher in ALL survivors with hypertriglyceridemia (**Fig. 2**). Compared with healthy controls, differences in Apos A-I, B-100, and the Apo B100/A-I ratio were observed for ALL survivors with and without dyslipidemia (Table 3). However,

TABLE 3. Plasma Apo profile of ALL survivors and controls

	Healthy Controls	ALL Survivors		
		Entire Group	Subgroup without Dyslipidemia	Subgroup with Dyslipidemia
Total				
Apos				
A-I (g/l)	2.64 ± 0.09 (22)	2.28 ± 0.06 (79)[a]	2.35 ± 0.07 (40)[b]	2.22 ± 0.09 (39)[a]
A-IV (μg/ml)	1.22 ± 0.12 (22)	1.28 ± 0.06 (53)	1.22 ± 0.09 (27)	1.34 ± 0.08 (26)
B-100 (g/l)	0.69 ± 0.02 (22)	0.85 ± 0.02 (78)[c]	0.86 ± 0.03 (39)[c]	0.83 ± .03 (39)[a]
C-II (μg/ml)	111.6 ± 6.82 (21)	131.9 ± 4.26 (80)[b]	123.3 ± 5.27 (40)	140.2 ± 6.51 (40)[b,d]
C-III (μg/ml)	76.05 ± 3.47 (22)	86.22 ± 11.62 (79)	73.15 ± 11.60 (39)[b]	98.95 ± 19.93 (40)
E (μg/ml)	34.60 ± 0.91 (22)	31.70 ± 0.91 (80)	29.82 ± 0.98 (40)[a]	33.59 ± 1.48 (40)[d]
Ratios				
C-II/C-III	1.50 ± 0.83 (21)	2.53 ± 0.24 (79)[a]	2.81 ± 0.42 (39)[a]	2.25 ± 0.22 (40)[b]
B-100/TG	0.82 ± 0.06 (22)	0.99 ± 0.06 (78)	1.30 ± 0.10 (39)[c]	0.69 ± 0.05 (39)[b,e]
B-100/A-I	0.27 ± 0.01 (22)	0.38 ± 0.01 (78)[c]	0.37 ± 0.01 (39)[c]	0.39 ± 0.02 (39)[c]
Children				
Apos				
A-I (g/l)	2.41 ± 0.12 (10)	2.19 ± 0.07 (40)	2.26 ± 0.07 (27)	2.03 ± 0.14 (13)[b,d]
A-IV (μg/ml)	1.34 ± 0.24 (10)	1.22 ± 0.09 (27)	1.23 ± 0.12 (21)	1.15 ± 0.10 (6)
B-100 (g/l)	0.73 ± 0.03 (10)	0.85 ± 0.03 (40)[b]	0.84 ± 0.03 (27)	0.87 ± 0.05 (13)[b]
C-II (μg/ml)	109.3 ± 6.75 (9)	131.2 ± 5.55 (40)[b]	124.1 ± 6.84 (27)	146.1 ± 8.37 (13)[a]
C-III (μg/ml)	81.60 ± 3.67 (10)	78.03 ± 11.33 (39)	77.62 ± 16.43 (26)[b]	78.85 ± 9.73 (13)
E (μg/ml)	34.19 ± 1.14 (10)	29.79 ± 1.20 (40)	28.56 ± 1.22 (27)[b]	32.35 ± 2.62 (13)
Ratios				
C-II/C-III	1.36 ± 0.06 (9)	2.55 ± 0.36 (39)[a]	2.61 ± 0.49 (26)[a]	2.44 ± 0.47 (13)[b]
B-100/TG	0.91 ± 0.09 (10)	1.12 ± 0.10 (40)	1.34 ± 0.12 (27)[a]	0.67 ± 0.07 (13)[b]
B-100/A-I	0.31 ± 0.02 (10)	0.40 ± 0.02 (40)[b]	0.38 ± 0.02 (27)[b]	0.45 ± 0.04 (13)[a]
Adults				
Apos				
A-I (g/l)	2.84 ± 0.11 (12)	2.39 ± 0.09 (39)[b]	2.53 ± 0.13 (13)	2.32 ± 0.12 (26)[a]
A-IV (μg/ml)	1.13 ± 0.10 (12)	1.34 ± 0.09 (26)	1.21 ± 0.14 (2)	1.27 ± 0.13 (10)
B-100 (g/l)	0.65 ± 0.03 (12)	0.85 ± 0.03 (38)[a]	0.92 ± 0.04 (12)[c]	0.82 ± 0.04 (26)[b]
C-II (μg/ml)	113.3 ± 11.07 (12)	132.6 ± 6.54 (40)	122.5 ± 8.15 (13)	137.4 ± 8.81 (27)
C-III (μg/ml)	71.42 ± 5.12 (12)	94.20 ± 20.21 (40)	64.23 ± 12.01 (13)	108.6 ± 29.17 (27)
E (μg/ml)	34.94 ± 1.40 (12)	33.62 ± 1.31 (40)	32.44 ± 1.44 (13)	34.18 ± 1.81 (27)
Ratios				
C-II/C-III	1.61 ± 0.13 (12)	2.50 ± 0.31 (40)	3.22 ± 0.80 (13)	2.16 ± 0.23 (27)
B-100/TG	0.75 ± 0.07 (12)	0.88 ± 0.08 (38)	1.23 ± 0.14 (12)[a]	0.71 ± 0.07 (26)[f]
B-100/A-I	0.23 ± 0.02 (12)	0.37 ± 0.02 (38)[c]	0.38 ± 0.03 (12)[c]	0.37 ± 0.03 (26)[a]

Data are expressed as mean ± SEM (n).
[a] $P < 0.01$ versus healthy controls.
[b] $P < 0.05$ versus healthy controls.
[c] $P < 0.001$ versus healthy controls.
[d] $P < 0.05$ versus ALL survivors without dyslipidemia.
[e] $P < 0.001$ versus ALL survivors without dyslipidemia.
[f] $P < 0.01$ versus ALL survivors without dyslipidemia.

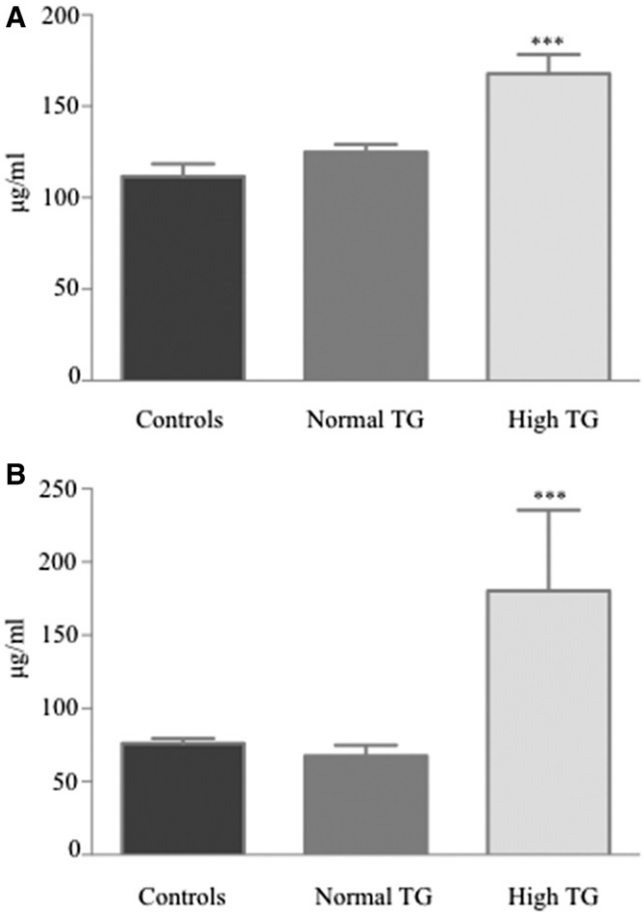

Fig. 2. Plasma levels of Apos (C-II and C-III) in controls and in ALL survivors with and without hypertriglyceridemia. Concentrations of Apo C-II (A) and Apo C-III (B) were measured by commercial ELISA kits in n = 22 healthy controls, n = 67 in ALL survivors with normal TGs, and n = 13 in ALL survivors with high TGs. ***$P <$ 0.001 versus controls.

compared with nondyslipidemic ALL survivors, those presenting abnormal lipid profiles had lower Apo A-I concentrations, as well as Apo C-II/C-III and Apo B-100/TG ratios, but a higher plasma content in Apos C-II, C-III, and E (Table 3). Similar trends were observed in the child and adult subgroups.

Composition of lipid moieties in lipoprotein classes

Appraising the composition of lipoproteins in lipids and total proteins did not reveal significant differences in the relative content of VLDL and LDL between the entire cohorts of ALL survivors and controls (**Table 4**). However, lower PL percentages were noticed in IDL, HDL_3, and HDL_2 for both dyslipidemic and nondyslipidemic survivors when compared with controls. Moreover, an increased proportion of FC characterized survivor HDL_2 particles. We calculated the weight ratio that estimates the size of lipoproteins by evaluating the mass ratio of core constituents (TG+EC) to surface constituents (FC+PR+PL), as lighter and larger particles are relatively enriched with TG and EC (41). Our results showed a significant increase in the weight ratio of HDL_2 in ALL survivors (both subgroups) when compared with controls. Comparing dyslipidemic with normolipidemic survivors revealed that the VLDL fraction of dyslipidemic subjects contained more TG, FC, and PL, but dramatically less protein (Table 4). These alterations led to a higher weight ratio, indicating larger VLDL particles. Moreover, IDL content in FC was higher in ALL survivors with dyslipidemia. While no differences were noted in LDL fraction composition among subgroups of ALL survivors and healthy controls, a higher content of TG in HDL_3 and of TG and FC in HDL_2 characterized dyslipidemic survivors.

Composition of Apo moieties in lipoprotein classes

Table 5 summarizes the Apo composition of VLDL, IDL, LDL, HDL_3, and HDL_2 in ALL survivors and controls. Representative gels are shown in **Fig. 3**. Differences in Apo distributions were detected between groups for all lipoprotein fractions. In contrast, with higher Apo B-100 plasma concentrations in ALL survivors compared with controls (Table 3), the proportion of Apo B-100 among groups was similar in VLDL and reduced in LDL (Table 5, Fig. 3). However, the percentage of Apo E was increased in the VLDL and IDL of both subgroups of ALL survivors compared with controls. While all the differences were not significant, a tendency for an elevated percentage of Apo Cs was noted in VLDL and IDL for both subgroups compared with controls and in the LDL of dyslipidemic survivors. Furthermore, the HDL_2 fraction showed reduced Apo A-I and augmented Apo A-II proportions, thereby resulting in a higher Apo A-I/A-II ratio in ALL survivors versus controls (Table 5). Similar to what was observed in VLDL fractions, Apo E was higher in the HDL_2 of dyslipidemic ALL survivors. No significant differences in the HDL_3 fraction were found between survivors and controls.

We further analyzed the distributions of Apo C isoforms in VLDL and HDL_2 fractions using TMU gels. Representative profiles are illustrated in **Fig. 4** and Apo distribution is presented in **Table 6**. The separation of VLDL-Apo Cs revealed a tendency for higher content in the Apo $C\text{-}III_1$ isoform in dyslipidemic ALL survivors compared with healthy controls and to nondyslipidemic ALL survivors. This trend was not observed in VLDL Apo $C\text{-}III_2$ or Apo C-II. Similar to what was observed on SDS-PAGE, no differences were noted in HDL_2 Apo content using the TMU gels.

APOE, *LDLR*, and *LPL* gene polymorphisms

To determine whether SNPs could account for the observed lipid alterations, we focused on the analysis of three major lipid-associated genes, *APOE*, *LDLR*, and *LPL*. The genetic characterization of the cohort revealed that rs7412 (*APOE*) minor allele frequency was not different between ALL survivors and controls (0.125 vs. 0.136, respectively; odds ratio: 0.905; 95% confidence interval: 0.338–2.425). In the ALL survivor cohort, we found 59 carriers of the *APOE* $\varepsilon3/\varepsilon3$ genotype (77.6%), 15 carriers (19.7%) of *APOE* $\varepsilon3/\varepsilon2$, and 2 carriers (2.6%) of *APOE* $\varepsilon2/\varepsilon2$ (supplemental Table S1). In the control group, 16 participants (72.7%) were *APOE* $\varepsilon3/\varepsilon3$ carriers, six (27.3%) had *APOE* $\varepsilon3/\varepsilon2$, and none had the *APOE* $\varepsilon2/\varepsilon2$ genotype. In the

TABLE 4. Lipoprotein composition of ALL survivors compared with age- and gender-matched controls

Lipoprotein	Composition					Weight Ratio [(TG+EC):(FC+PL+PR)]
	TG	FC	EC	PL	PR	
	Percentage of total content					
VLDL (1.006 g/ml)						
Controls	41.69 ± 2.05	4.65 ± 0.34	6.36 ± 0.67	18.53 ± 0.80	28.77 ± 2.79	1.00 ± 0.08
ALL survivors	44.90 ± 1.27	5.14 ± 0.17	5.66 ± 0.25	16.74 ± 0.39	27.56 ± 1.76	1.13 ± 0.05
No dyslipidemia	40.27 ± 1.89	4.68 ± 0.28	5.21 ± 0.40	15.36 ± 0.61[a]	34.48 ± 2.62	0.93 ± 0.07
Dyslipidemia	49.53 ± 1.36[a,b]	5.60 ± 0.19[a,c]	6.11 ± 0.31	18.13 ± 0.38[b]	20.63 ± 1.78[a,b]	1.33 ± 0.06[a,b]
Hypertriglyceridemia	55.04 ± 1.44[d]	5.63 ± 0.37[e]	6.01 ± 0.62	18.73 ± 0.54	14.59 ± 1.55[a]	1.60 ± 0.08[d]
IDL (1.019 g/ml)						
Controls	27.65 ± 1.83	6.93 ± 0.32	13.94 ± 0.98	29.13 ± 1.94	22.35 ± 2.02	0,75 ± 0.05
ALL survivors	27.68 ± 0.83	7.92 ± 0.27	14.46 ± 0.72	24.02 ± 0.64[a]	25.93 ± 1.55	0.78 ± 0.03
No dyslipidemia	27.66 ± 1.21	7.44 ± 0.40	12.58 ± 0.99	23.27 ± 1.02[a]	29.06 ± 2.22[e]	0.73 ± 0.05
Dyslipidemia	27.69 ± 1.17	8.40 ± 0.36[a]	16.34 ± 0.97[b]	24.76 ± 0.78[e]	22.80 ± 2.07[c]	0.84 ± 0.04
LDL (1.063 g/ml)						
Controls	6.51 ± 0.45	11.02 ± 0.31	40.32 ± 1.09	27.73 ± 1.06	14.43 ± 0.50	0.89 ± 0.04
ALL survivors	7.15 ± 0.30	10.76 ± 0.20	40.64 ± 0.71	27.33 ± 0.41	14.11 ± 0.53	0.93 ± 0.02
No dyslipidemia	7.19 ± 0.45	10.62 ± 0.25	40.59 ± 0.91	27.28 ± 0.51	14.31 ± 0.59	0.91 ± 0.03
Dyslipidemia	7.11 ± 0.38	10.90 ± 0.30	40.70 ± 1.10	27.39 ± 0.64	13.91 ± 0.88	0.94 ± 0.03
HDL3 (1.210 g/ml)						
Controls	2.24 ± 0.22	2.06 ± 0.09	15.49 ± 0.76	31.89 ± 3.00	49.58 ± 2.53	0.20 ± 0.01
ALL survivors	2.17 ± 0.09	2.26 ± .07	16.35 ± 0.38	25.41 ± 0.48[a]	53.77 ± 0.69	0.23 ± 0.005
No dyslipidemia	1.92 ± 0.12	2.32 ± 0.08	16.66 ± 0.58	25.15 ± 0.74[a]	53.96 ± 1.00	0.23 ± 0.008
Dyslipidemia	2.41 ± 0.13[b,c]	2.21 ± 0.11	16.05 ± 0.51	25.67 ± 0.60[e]	53.52 ± 0.96	0.23 ± 0.007
HDL_2 (1.125 g/ml)						
Controls	3.14 ± 0.27	5.09 ± 0.23	20.14 ± 1.02	35.04 ± 1.28	36.60 ± 1.63	0.31 ± 0.02
ALL survivors	3.70 ± 0.16	6.29 ± 0.23[e]	22.36 ± 0.61	32.30 ± 0.40[e]	35.35 ± 0.64	0.36 ± 0.01[e]
No dyslipidemia	3.24 ± 0.20	5.93 ± 0.24[e]	22.56 ± 0.82	32.56 ± 0.43[e]	35.71 ± 0.86	0.36 ± 0.02[e]
Dyslipidemia	4.16 ± 0.24[a,c]	6.66 ± 0.39[e]	22.16 ± 0.91	32.04 ± 0.67[e]	34.98 ± 0.97	0.37 ± 0.02[e]
Low HDL-C	4.01 ± 0.24[e]	6.91 ± 0.53[e]	21.91 ± 1.24	31.33 ± 0.72[a]	35.79 ± 1.32	0.36 ± 0.02

Data are expressed as percentage of total lipoprotein content ± SEM. VLDL, IDL LDL, HDL_3, and HDL_2 of n = 80 ALL survivors and n = 22 gender- and age-matched healthy controls were characterized as described in the Materials and Methods. ALL survivors were stratified in two groups according to their dyslipidemia status, as described in the Materials and Methods (n = 40/group). Two additional subgroups were stratified among dyslipidemic survivors: hypertriglyceridemic ALL survivors (n = 12) and ALL survivors with low HDL (n = 25). PR, protein.

[a] $P < 0.01$ versus healthy controls.

[b] $P < 0.001$ versus ALL survivors without dyslipidemia.

[c] $P < 0.01$ versus ALL survivors without dyslipidemia.

[d] $P < 0.001$ versus healthy controls.

[e] $P < 0.05$ versus healthy controls.

LPL gene, rs118204057 was identified in one survivor (1.3%) and none in healthy controls, while no SNP was identified in the *LDLR* gene in ALL survivors. Moreover, our analyses revealed that the metabolic and lipid profiles were not different between survivor and control carriers of the same genotype. However, in both groups, *APOE* ε3/ε2 carriers had reduced LDL-C compared with *APOE* ε3/ε3 (supplemental Table S1).

DISCUSSION

The aim of this study was to scrutinize the lipid, Apo, and lipoprotein abnormalities in pediatric ALL survivors in order to better understand their late cardiovascular risks. Our study focused on the PETALE cohort, which is unique due to its origin and its established genetic founder effect (51, 52). The homogenous ethnic background of the participants provided us with a significant advantage for association studies by reducing the number of confounding variables (51, 52). Overall, this study has identified important alterations in lipid and lipoprotein profiles. In particular, dyslipidemia was highly prevalent in ALL survivors of both genders and age groups. Of note, the proportion of women ALL survivors presenting with high TG (20%) was twice that of the one reported in the general Canadian population of women between 18 and 39 years old (53). Low HDL-C affected 40% of men in our cohort, while a general prevalence of 29% was reported for the same Canadian age group (53). Using the same Canadian Health Measure Survey, MacPherson, de Groh, and Loukine (54) reported that 19.1% of boys had low HDL-C compared with 40% in our cohort. In both studies, cut-off values to classify dyslipidemia were identical to ours.

Our study also revealed differences in plasma Apo concentrations between ALL survivors with and without dyslipidemia compared with healthy controls. Predominantly, plasma Apo B-100 levels were significantly elevated, while Apo A-I concentrations were decreased, leading to an increase in the Apo B-100/A-I ratio in ALL survivors with and without dyslipidemia. This unbalanced ratio between potentially atherogenic Apo B-100 and anti-atherogenic Apo A-I particles is a predictor of cardiovascular risk (20, 31). It is noticeable that, for both plasma Apo A-I and B-100, similar alterations were observed in dyslipidemic and nondyslipidemic survivors. To a lesser extent, alterations in plasma Apo Cs were identified in ALL subjects with dyslipidemia.

TABLE 5. Composition of Apo moieties in lipoproteins of ALL survivors compared with age- and gender-matched controls using SDS-PAGE

Lipoprotein	Composition in Apos						Ratio (A-I/A-II)
	B-100	A-IV	E	A-I	Cs	A-II	
	Percentage of total content						
VLDL (1.006 g/ml)							
Controls	49.55 ± 3.12	16.41 ± 1.91	10.09 ± 1.16	10.82 ± 1.59	13.23 ± 1.61	—	—
ALL survivors	42.88 ± 1.92	13.88 ± 1.11	14.46 ± 0.83[a]	11.65 ± 1.00	17.00 ± 1.33	—	—
No dyslipidemia	44.08 ± 2.51	14.77 ± 1.07	13.69 ± 1.25	11.00 ± 1.21	16.38 ± 1.71	—	—
Dyslipidemia	41.69 ± 2.98	13.00 ± 1.97	15.23 ± 1.09[a]	12.31 ± 1.61	17.62 ± 2.09	—	—
IDL (1.019 g/ml)							
Controls	79.18 ± 2.30	4.68 ± 0.51	4.75 ± 0.60	4.69 ± 0.82	6.54 ± 0.86	—	—
ALL survivors	57.81 ± 3.68[b]	9.96 ± 0.68[b]	8.35 ± 0.59[b]	8.15 ± 0.94[c]	15.81 ± 2.25[a]	—	—
No dyslipidemia	59.08 ± 4.41[b]	10.69 ± 0.92[b]	8.00 ± 0.88[a]	6.85 ± 1.08	15.31 ± 3.26	—	—
Dyslipidemia	56.54 ± 6.07[b]	9.23 ± 0.99[b]	8.69 ± 0.83[b]	9.46 ± 1.49[c]	16.31 ± 3.22[a]	—	—
LDL (1.063 g/ml)							
Controls	65.77 ± 1.53	3.27 ± 0.21	4.32 ± 0.31	23.23 ± 1.64	3.55 ± 0.30	—	—
ALL survivors	68.73 ± 2.26	3.88 ± 0.36	4.50 ± 0.26	19.08 ± 2.13	3.89 ± 0.49	—	—
No dyslipidemia	67.69 ± 2.97	3.46 ± 0.51	4.23 ± 0.23	23.69 ± 2.79	2.85 ± 0.52	—	—
Dyslipidemia	71.62 ± 2.94[c]	4.31 ± 0.49	4.77 ± 0.47	14.46 ± 2.74[a,d]	4.92 ± 0.75[e]	—	—
HDL3 (1.210 g/ml)							
Controls	—	1.10 ± 0.07	1.58 ± 0.10	83.29 ± 0.81	4.67 ± 0.35	9.52 ± 0.82	10.10 ± 0.76
ALL survivors	—	1.26 ± 0.09	1.78 ± 0.09	83.04 ± 0.63	5.54 ± 0.43	8.58 ± 0.49	10.58 ± 0.63
No dyslipidemia	—	1.44 ± 0.14[c]	1.78 ± 0.16	83.15 ± 0.84	5.31 ± 0.63	8.39 ± 0.63	10.54 ± 0.77
Dyslipidemia	—	1.09 ± 0.09[e]	1.79 ± 0.10	82.92 ± 0.96	5.77 ± 0.59	8.77 ± 0.78	10.62 ± 1.03
HDL_2 (1.125 g/ml)							
Controls	—	1.27 ± 0.14	3.33 ± 0.33	72.23 ± 0.97	13.09 ± 0.92	10.14 ± 0.85	7.31 ± 0.65
ALL survivors	—	0.89 ± 0.033[a]	3.85 ± 0.41	68.50 ± 1.11[c]	11.88 ± 0.74	14.54 ± 1.21[c]	5.59 ± 0.47[a]
No dyslipidemia	—	0.80 ± 0.04	2.64 ± 0.24	69.31 ± 1.76	10.46 ± 0.67	16.31 ± 1.88[a]	4.99 ± 0.63[a]
Dyslipidemia	—	0.97 ± 0.04[d]	4.73 ± 0.59[c,d]	67.69 ± 1.40[c]	13.31 ± 1.22	12.77 ± 1.44	6.19 ± 0.67

Data are expressed as percentage of total Apo content ± SEM. Composition in Apos was assessed in VLDL, IDL, LDL, HDL_3, and HDL_2 of n = 26 ALL survivors and n = 22 gender- and age-matched controls. ALL survivors were stratified in two groups according to their dyslipidemia status as described in the Materials and Methods (n = 13/group). Apo distribution was analyzed using SDS-PAGE (4–20% gradient).

[a] $P < 0.01$ versus controls.

[b] $P < 0.001$ versus controls.

[c] $P < 0.05$ versus controls.

[d] $P < 0.01$ versus ALL survivors without dyslipidemia.

[e] $P < 0.05$ versus ALL survivors without dyslipidemia.

Dyslipidemia is a significant component of the MetS definition, as stated by the National Cholesterol Education Program-Adult Treatment Panel III and the International Diabetes Federation (55). The alterations in TG and HDL-C levels found in our study correspond to risk factors that define dyslipidemia in MetS. Because the presence of MetS increases the risk for type 2 diabetes and CVD in the general population (56), it is reasonable to include lipid profile analysis in the long-term follow-up of ALL survivors. In line with our results, a high prevalence of dyslipidemia was reported in a cohort from the St. Jude Lifetime Cohort Study composed of older ALL survivors (median age of 31.7 years) (11).

To our knowledge, prior to our study, no information was available on lipid and Apo composition of lipoproteins in the survivorship context. Our findings disclose variations in the content of various lipoproteins. In subjects with dyslipidemia and particularly with hypertriglyceridemia, we found VLDL with a reduced protein moiety and an increased TG and FC content that resulted in a higher weight ratio and that reflected a larger particle size. Although the precise mechanism leading to hypertriglyceridemia in our population is unclear, it may indicate increased production of large-sized VLDL rather than an enhanced biogenesis of the number of VLDL particles by the liver, as reflected by the lower ratio of Apo B-100/TG in dyslipidemic ALL survivors. Derangements in VLDL-TG degradation are also possible in view of the concomitantly high Apo C-II and C-III concentrations noted in the plasma and also observed using SDS-PAGE. In addition, the tendency of increased Apo $C\text{-}III_1$ in VLDL observed by TMU gels might impact on VLDL-TG degradation (57). If Apo C-II at moderate concentrations represents an activator of LPL for VLDL lipolysis, its excess (as we observed in ALL survivors) may impede LPL activity and VLDL clearance, thereby leading to hypertriglyceridemia (58). Moreover, because Apo C-III is a well-known inhibitor of LPL, higher levels suggest a delay in TG-rich lipoprotein clearance from circulation (59, 60). Altogether, these alterations in VLDL composition may affect VLDL catabolism and explain hypertriglyceridemia in ALL survivors.

Polymorphisms in *APOE*, *LPL*, or *LDLR* could impact lipoprotein composition and lipid and Apo profile and, thus, contribute to CVD risk (61–64). The frequencies of *APOE* $\varepsilon3/\varepsilon2$ and $\varepsilon2/\varepsilon2$ genotypes found in our ALL survivor cohort were slightly higher than those reported in adult Caucasian populations (65). This is in line with the previously reported higher $\varepsilon2$ allele frequency in the French-Canadian population of Quebec than in other Caucasian populations (66). It was found that the $\varepsilon2$ allele

JOURNAL OF LIPID RESEARCH ASBMB JLR

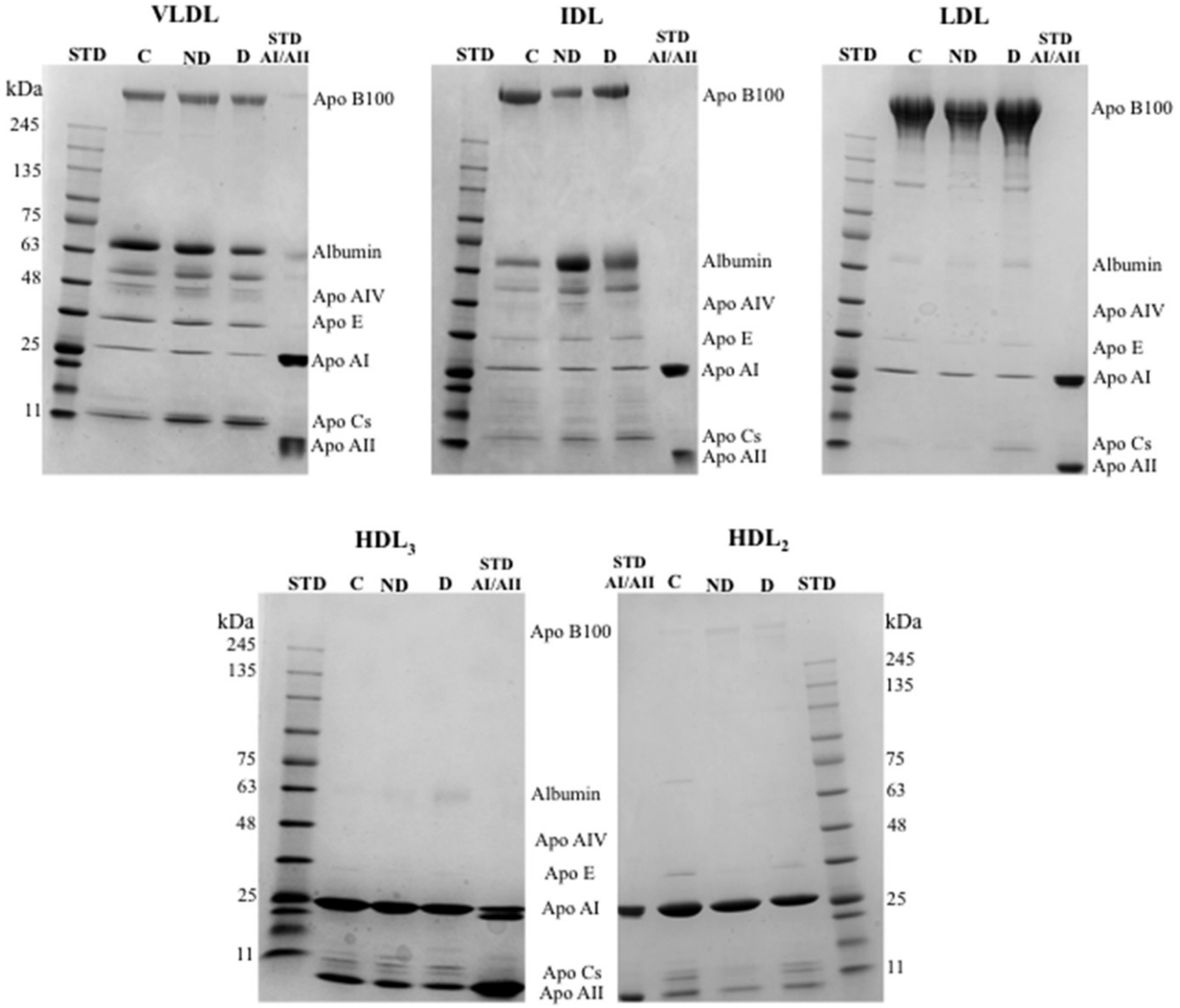

Fig. 3. VLDL, LDL, IDL, HDL_3, and HDL_2 composition in Apos. Content of each lipoprotein fraction was examined in n = 22 controls and n = 26 ALL survivors with or without dyslipidemia, gradient SDS-PAGE (4–20%). A molecular mass marker and Apo A-I and A-II standards were used to identify Apos. A representative blot is shown. STD, molecular mass marker standard; STD AI/AII, Apos A-I and A-II standard; C, controls; ND, nondyslipidemic ALL survivors; D, dyslipidemic ALL survivors.

potentially has a nil effect on CVD risk: while it may reduce LDL-C levels, it may also increase the accumulation of large VLDL and remnant TG-rich lipoproteins and, accordingly, we found lower LDL-C in *APOE* ε2/ε2 carriers (61). However *APOE* genotypes did not appear to impact the differences observed between the two cohorts.

Furthermore, *LPL* G188E (rs118204057) is one of three missense mutations that account for >97% of complete LPL deficiency in the homozygous French-Canadian population (62). It could result in a very important increase of plasma TG levels (63). However, due to the complexity of interactions between genetic and environmental factors, G188E heterozygote carriers may develop hypertriglyceridemia generally later in adulthood (62, 67). In our cohort, the detection of only one heterozygote carrier of this allele prevented us from going further. Note that in the French-Canadian population of Quebec, the carrier frequency for familial LPL deficiency disorder is 1:40 (68), which is above the general population average (one per million) (69) and is attributed to a founder effect (68). To our knowledge, none of the study participants showed symptoms of this disorder, which usually manifests in childhood and includes abdominal pain, failure to thrive, hepatosplenomegaly, lipemia retinalis, or eruptive xanthomas (70). Apparently, the increased plasma TG levels and proportions in VLDL fractions observed in our study are, therefore, not related to LPL deficiency, but this assumption should be confirmed with the determination of LPL activity in view of the association of specific variants with mild hypertriglyceridemia (71).

Our data also documented important alterations in HDL_2 composition and Apo distribution and size in dyslipidemic and nondyslipidemic ALL survivors. The HDL_2 subfraction

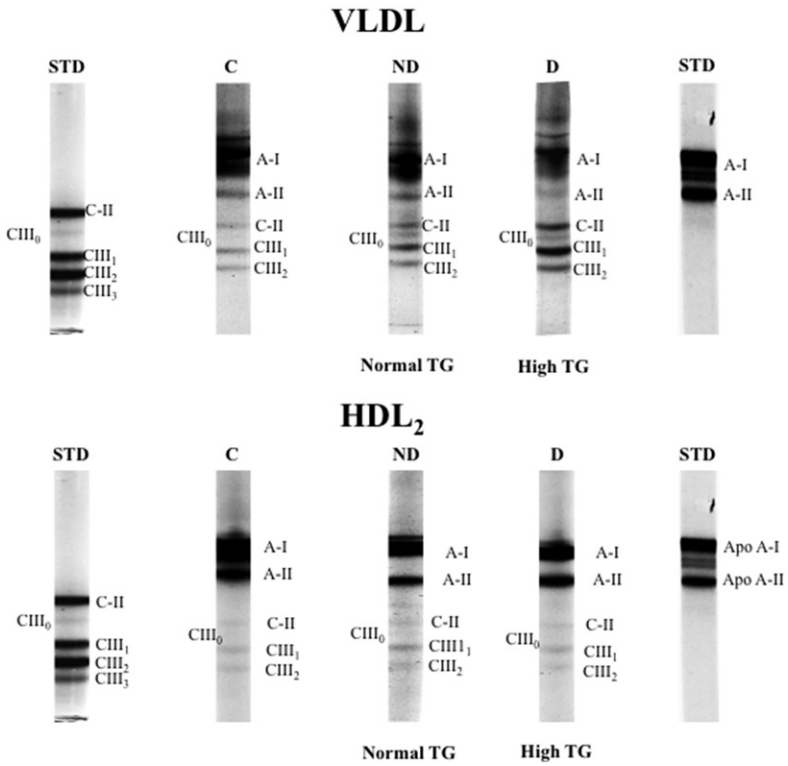

Fig. 4. VLDL and HDL_2 composition in Apos (A-I, A-II, C-II, $CIII_0$, $CIII_1$, and $CIII_2$). Lipoprotein composition examined in n = 6 controls and n = 12 ALL survivors with or without dyslipidemia using 12.5% polyacrylamide gels containing TMU. Human purified Apos C-II and C-III and purified Apos A-I and A-II were used as standards to identify Apos. A representative blot is shown. STD, standard; C, controls; ND, nondyslipidemic ALL survivors; D, dyslipidemic ALL survivors.

was enriched in TG and poorer in PL, indicators of increased particle size. The Apo A-I/A-II ratio was significantly reduced (given the high proportion of Apo A-II), but only a rising trend was noted in the Apo C-II/C-III ratio. All these modifications may strongly compromise the protective role of HDL against CVD. Higher Apo A-II levels displayed pro-atherogenic potentials (72) and predicted the incidence of MetS and type 2 diabetes (73). In support of these assertions, some investigators stressed the opposite functions of Apos A-I and A-II: the former was more effective in enhancing reverse cholesterol transport and activating LCAT, whereas the latter exhibited its pernicious inhibitory effects (74–76).

In conclusion, this biochemical investigation highlights significant abnormalities in the plasma concentration and composition of lipids, Apos, and lipoproteins of ALL survivors. Several of these alterations were more prominent in survivors defined as dyslipidemic, although they were observed in nondyslipidemic survivors as well. Therefore, special attention must be paid to these subjects, given the atherosclerotic potency of lipid and lipoprotein disorders.

The authors thank Mrs. Schohraya Spahis and Anita Franco for their technical assistance.

TABLE 6. Distribution of Apos A-I, A-II, C-II, C-III and Apo C-III isoforms ($C\text{-}III_1$, $C\text{-}III_2$) in VLDL and HDL_2 of ALL survivors compared with age- and gender-matched controls using TMU gels

Lipoprotein	Composition in Apos						Ratio (C-II/CIII)
	A-I	A-II	C-II	C-III	$C\text{-}III_1$	$C\text{-}III_2$	
	Percentage of total content						
VLDL (1.006 g/ml)							
Controls	57.48 ± 7.36	12.89 ± 2.74	6.92 ± 1.24	22.40 ± 4.31	12.02 ± 2.30	10.42 ± 2.13	0.32 ± 0.04
ALL survivors	67.56 ± 7.47	3.66 ± 0.97[a]	7.80 ± 1.86	22.05 ± 4.94	13.81 ± 3.17	8.08 ± 1.88	0.35 ± 0.04
No dyslipidemia	78.95 ± 9.30	4.08 ± 1.78	5.24 ± 1.97	13.10 ± 5.84	7.54 ± 3.48	5.54 ± 2.53	0.39 ± 0.07
Dyslipidemia	56.18 ± 10.36	3.24 ± 0.93[b]	9.93 ± 2.84	29.52 ± 6.50	19.03 ± 4.11	10.20 ± 2.60	0.31 ± 0.04
HDL_2 (1.125 g/ml)							
Controls	78.97 ± 2.65	17.05 ± 2.34	0.67 ± 0.15	3.30 ± 0.62	1.97 ± 0.41	1.35 ± 0.30	0.20 ± 0.02
ALL survivors	76.13 ± 2.32	18.80 ± 2.12	1.08 ± 0.15	4.03 ± 0.47	2.40 ± 0.42	1.62 ± 0.18	0.32 ± 0.07
No dyslipidemia	80.02 ± 1.75	15.20 ± 1.77	1.00 ± 0.13	3.82 ± 0.35	2.02 ± 0.31	1.80 ± 0.22	0.25 ± 0.02
Dyslipidemia	72.23 ± 3.82	22.40 ± 3.39	1.15 ± 0.27	4.23 ± 0.91	2.78 ± 0.79	1.43 ± 0.28	0.38 ± 0.15

Data are expressed as percentage of total Apo content ± SEM. VLDL, IDL, LDL, HDL_3, and HDL_2 relative composition in Apos was characterized using polyacrylamide gels containing TMU in n = 12 survivors of ALL and n = 6 gender- and age-matched controls. ALL survivors were stratified in two groups according to their dyslipidemia status as described in the Materials and Methods (n = 6/group).

[a] $P < 0.05$ versus controls.

[b] $P < 0.01$ versus controls.

JOURNAL OF LIPID RESEARCH ASBMB JLR

REFERENCES

1. Pui, C. H., C. G. Mullighan, W. E. Evans, and M. V. Relling. 2012. Pediatric acute lymphoblastic leukemia: where are we going and how do we get there? *Blood.* **120:** 1165–1174.
2. Essig, S., Q. Li, Y. Chen, J. Hitzler, W. Leisenring, M. Greenberg, C. Sklar, M. M. Hudson, G. T. Armstrong, K. R. Krull, et al. 2014. Risk of late effects of treatment in children newly diagnosed with standard-risk acute lymphoblastic leukaemia: a report from the Childhood Cancer Survivor Study cohort. *Lancet Oncol.* **15:** 841–851.
3. Mody, R., S. Li, D. C. Dover, S. Sallan, W. Leisenring, K. C. Oeffinger, Y. Yasui, L. L. Robison, and J. P. Neglia. 2008. Twenty-five-year follow-up among survivors of childhood acute lymphoblastic leukemia: a report from the Childhood Cancer Survivor Study. *Blood.* **111:** 5515–5523.
4. Chen, M. H., S. D. Colan, and L. Diller. 2011. Cardiovascular disease: cause of morbidity and mortality in adult survivors of childhood cancers. *Circ. Res.* **108:** 619–628.
5. Gurney, J. G., R. P. Ojha, K. K. Ness, S. Huang, S. Sharma, L. L. Robison, M. M. Hudson, and S. C. Kaste. 2012. Abdominal aortic calcification in young adult survivors of childhood acute lymphoblastic leukemia: results from the St. Jude Lifetime Cohort Study. *Pediatr. Blood Cancer.* **59:** 1307–1309.
6. Mertens, A. C., Q. Liu, J. P. Neglia, K. Wasilewski, W. Leisenring, G. T. Armstrong, L. L. Robison, and Y. Yasui. 2008. Cause-specific late mortality among 5-year survivors of childhood cancer: the Childhood Cancer Survivor Study. *J. Natl. Cancer Inst.* **100:** 1368–1379.
7. Janiszewski, P. M., K. C. Oeffinger, T. S. Church, A. L. Dunn, D. A. Eshelman, R. G. Victor, S. Brooks, A. J. Turoff, E. Sinclair, J. C. Murray, et al. 2007. Abdominal obesity, liver fat, and muscle composition in survivors of childhood acute lymphoblastic leukemia. *J. Clin. Endocrinol. Metab.* **92:** 3816–3821.
8. Chow, E. J., C. Pihoker, K. Hunt, K. Wilkinson, and D. L. Friedman. 2007. Obesity and hypertension among children after treatment for acute lymphoblastic leukemia. *Cancer.* **110:** 2313–2320.
9. Neville, K. A., R. J. Cohn, K. S. Steinbeck, K. Johnston, and J. L. Walker. 2006. Hyperinsulinemia, impaired glucose tolerance, and diabetes mellitus in survivors of childhood cancer: prevalence and risk factors. *J. Clin. Endocrinol. Metab.* **91:** 4401–4407.
10. Malhotra, J., E. S. Tonorezos, M. Rozenberg, G. L. Vega, C. A. Sklar, J. Chou, C. S. Moskowitz, D. A. Eshelman-Kent, P. Janiszewski, R. Ross, et al. 2012. Atherogenic low density lipoprotein phenotype in long-term survivors of childhood acute lymphoblastic leukemia. *J. Lipid Res.* **53:** 2747–2754.
11. Nottage, K. A., K. K. Ness, C. Li, D. Srivastava, L. L. Robison, and M. M. Hudson. 2014. Metabolic syndrome and cardiovascular risk among long-term survivors of acute lymphoblastic leukaemia - from the St. Jude Lifetime Cohort. *Br. J. Haematol.* **165:** 364–374.
12. Armenian, S. H., S. K. Gelehrter, and E. J. Chow. 2012. Strategies to prevent anthracycline-related congestive heart failure in survivors of childhood cancer. *Cardiol. Res. Pract.* **2012:** 713294.
13. Harake, D., V. I. Franco, J. M. Henkel, T. L. Miller, and S. E. Lipshultz. 2012. Cardiotoxicity in childhood cancer survivors: strategies for prevention and management. *Future Cardiol.* **8:** 647–670.
14. Lipshultz, S. E., S. R. Lipsitz, S. M. Mone, A. M. Goorin, S. E. Sallan, S. P. Sanders, E. J. Orav, R. D. Gelber, and S. D. Colan. 1995. Female sex and drug dose as risk factors for late cardiotoxic effects of doxorubicin therapy for childhood cancer. *N. Engl. J. Med.* **332:** 1738–1743.
15. Silverman, L. B. 2014. Balancing cure and long-term risks in acute lymphoblastic leukemia. *Hematology Am. Soc. Hematol. Educ. Program.* **2014:** 190–197.
16. Link, K., C. Moell, S. Garwicz, E. Cavallin-Stahl, J. Bjork, U. Thilen, B. Ahren, and E. M. Erfurth. 2004. Growth hormone deficiency predicts cardiovascular risk in young adults treated for acute lymphoblastic leukemia in childhood. *J. Clin. Endocrinol. Metab.* **89:** 5003–5012.
17. Geenen, M. M., P. J. M. Bakker, L. C. M. Kremer, J. J. P. Kastelein, and F. E. van Leeuwen. 2010. Increased prevalence of risk factors for cardiovascular disease in long-term survivors of acute lymphoblastic leukemia and Wilms tumor treated with radiotherapy. *Pediatr. Blood Cancer.* **55:** 690–697.
18. Oeffinger, K. C., B. Adams-Huet, R. G. Victor, T. S. Church, P. G. Snell, A. L. Dunn, D. A. Eshelman-Kent, R. Ross, P. M. Janiszewski, A. J. Turoff, et al. 2009. Insulin resistance and risk factors for cardiovascular disease in young adult survivors of childhood acute lymphoblastic leukemia. *J. Clin. Oncol.* **27:** 3698–3704.
19. Parish, S., R. Peto, A. Palmer, R. Clarke, S. Lewington, A. Offer, G. Whitlock, S. Clark, L. Youngman, P. Sleight, et al. 2009. The joint effects of apolipoprotein B, apolipoprotein A1, LDL cholesterol, and HDL cholesterol on risk: 3510 cases of acute myocardial infarction and 9805 controls. *Eur. Heart J.* **30:** 2137–2146.
20. Walldius, G., and I. Jungner. 2004. Apolipoprotein B and apolipoprotein A-I: risk indicators of coronary heart disease and targets for lipid-modifying therapy. *J. Intern. Med.* **255:** 188–205.
21. Maranhão, R. C., and F. R. Freitas. 2014. HDL metabolism and atheroprotection: predictive value of lipid transfers. *Adv. Clin. Chem.* **65:** 1–41.
22. Schwendeman, A., D. O. Sviridov, W. Yuan, Y. Guo, E. E. Morin, Y. Yuan, J. Stonik, L. Freeman, A. Ossoli, S. Thacker, et al. 2015. The effect of phospholipid composition of reconstituted HDL on its cholesterol efflux and anti-inflammatory properties. *J. Lipid Res.* **56:** 1727–1737.
23. Gursky, O. 2015. Structural stability and functional remodeling of high-density lipoproteins. *FEBS Lett.* **589:** 2627–2639.
24. Guha, M., X. Gao, S. Jayaraman, and O. Gursky. 2008. Correlation of structural stability with functional remodeling of high-density lipoproteins: the importance of being disordered. *Biochemistry.* **47:** 11393–11397.
25. Angeloni, E., F. Paneni, U. Landmesser, U. Benedetto, G. Melina, T. F. Lüscher, M. Volpe, R. Sinatra, and F. Cosentino. 2013. Lack of protective role of HDL-C in patients with coronary artery disease undergoing elective coronary artery bypass grafting. *Eur. Heart J.* **34:** 3557–3562.
26. Heinecke, J. 2011. HDL and cardiovascular-disease risk–time for a new approach? *N. Engl. J. Med.* **364:** 170–171.
27. Koba, S., Y. Yokota, T. Hirano, Y. Ito, Y. Ban, F. Tsunoda, T. Sato, M. Shoji, H. Suzuki, E. Geshi, et al. 2008. Small LDL-cholesterol is superior to LDL-cholesterol for determining severe coronary atherosclerosis. *J. Atheroscler. Thromb.* **15:** 250–260.
28. Aoki, T., H. Yagi, H. Sumino, K. Tsunekawa, O. Araki, T. Kimura, M. Nara, T. Ogiwara, K. Nakajima, and M. Murakami. 2015. Relationship between carotid artery intima-media thickness and small dense low-density lipoprotein cholesterol concentrations measured by homogenous assay in Japanese subjects. *Clin. Chim. Acta.* **442:** 110–114.
29. Hoogeveen, R. C., J. W. Gaubatz, W. Sun, R. C. Dodge, J. R. Crosby, J. Jiang, D. Couper, S. S. Virani, S. Kathiresan, E. Boerwinkle, et al. 2014. Small dense low-density lipoprotein-cholesterol concentrations predict risk for coronary heart disease: the Atherosclerosis Risk in Communities (ARIC) study. *Arterioscler. Thromb. Vasc. Biol.* **34:** 1069–1077.
30. Arsenault, B. J., I. Lemieux, J. P. Despres, N. J. Wareham, R. Luben, J. J. Kastelein, K. T. Khaw, and S. M. Boekholdt. 2007. Cholesterol levels in small LDL particles predict the risk of coronary heart disease in the EPIC-Norfolk prospective population study. *Eur. Heart J.* **28:** 2770–2777.
31. Walldius, G., I. Jungner, I. Holme, A. H. Aastveit, W. Kolar, and E. Steiner. 2001. High apolipoprotein B, low apolipoprotein A-I, and improvement in the prediction of fatal myocardial infarction (AMORIS study): a prospective study. *Lancet.* **358:** 2026–2033.
32. Bherer, C., D. Labuda, M. H. Roy-Gagnon, L. Houde, M. Tremblay, and H. Vezina. 2011. Admixed ancestry and stratification of Quebec regional populations. *Am. J. Phys. Anthropol.* **144:** 432–441.
33. Heyer, E., M. Tremblay, and B. Desjardins. 1997. Seventeenth-century European origins of hereditary diseases in the Saguenay population (Quebec, Canada). *Hum. Biol.* **69:** 209–225.
34. Marcoux, S., S. Drouin, C. Laverdiere, N. Alos, G. U. Andelfinger, L. Bertout, D. Curnier, M. G. Friedrich, E. A. Kritikou, G. Lefebvre, et al. The PETALE study: late adverse effects and biomarkers in childhood acute lymphoblastic leukemia survivors. *Pediatr. Blood Cancer.* Epub ahead of print. December 4, 2016; doi:10.1002/pbc.26361.
35. Vrooman, L. M., D. S. Neuberg, K. E. Stevenson, B. L. Asselin, U. H. Athale, L. Clavell, P. D. Cole, K. M. Kelly, E. C. Larsen, C. Laverdiere, et al. 2011. The low incidence of secondary acute myelogenous leukaemia in children and adolescents treated with dexrazoxane for acute lymphoblastic leukaemia: a report from the Dana-Farber Cancer Institute ALL Consortium. *Eur. J. Cancer.* **47:** 1373–1379.
36. Lambert, M., G. Paradis, J. O'Loughlin, E. E. Delvin, J. A. Hanley, and E. Levy. 2004. Insulin resistance syndrome in a representative sample of children and adolescents from Quebec, Canada. *Int. J. Obes. Relat. Metab. Disord.* **28:** 833–841.

37. Friedewald, W. T., R. I. Levy, and D. S. Fredickson. 1972. Estimation of the concentration of low-density lipoprotein cholesterol in plasma, without use of the preparative ultracentrifuge. *Clin. Chem.* **18:** 499–502.
38. St-Pierre, A. C., I. L. Ruel, B. Cantin, G. R. Dagenais, P-M. Bernard, J-P. Després, and B. Lamarche. 2001. Comparison of various electrophoretic charateristics of LDL particles and their relationship to the risk of ischemic heart disease. *Circulation.* **104:** 2295–2299.
39. Stan, S., E. Levy, E. E. Delvin, J. A. Hanley, B. Lamarche, J. O'Loughlin, G. Paradis, and M. Lambert. 2005. Distribution of LDL particle size in a population-based sample of children and adolescents and relationship with other cardiovascular risk factors. *Clin. Chem.* **51:** 1192–1200.
40. Tchernof, A., B. Lamarche, D. Prud'Homme, A. Nadeau, S. Moorjani, F. Labrie, P. J. Lupien, and J. P. Després. 1996. The dense LDL phenotype. Association with plasma lipoprotein levels, visceral obesity, and hyperinsulinemia in men. *Diabetes Care.* **19:** 629–637.
41. Levy, E., G. Lepage, M. Bendayan, N. Ronco, L. Thibault, N. Galéano, L. Smith, and C. C. Roy. 1989. Relationship of decreased hepatic lipase activity and lipoprotein abnormalities to essential fatty acid deficiency in cystic fibrosis patients. *J. Lipid Res.* **30:** 1197–1209.
42. Levy, E., C. C. Roy, L. Thibault, A. Bonin, P. Brochu, and E. G. Seidman. 1994. Variable expression of familial heterozygous hypobetalipoproteinemia: transient malabsorption during infancy. *J. Lipid Res.* **35:** 2170–2177.
43. Levy, E., A. Thibault, C. C. Roy, M. Bendayan, G. Lepage, and J. Letarte. 1988. Circulation lipids and lipoproteins in glycogen storage disease type I with nocturnal intragastric feeding. *J. Lipid Res.* **29:** 215–226.
44. Bartlett, G. R. 1959. Phosphorus assay in column chromatography. *J. Biol. Chem.* **234:** 466–468.
45. Expert Panel on Integrated Guidelines for Cardiovascular Health and Risk Reduction in Children and Adolescents and National Heart, Lung, and Blood Institute. 2011. Expert panel on integrated guidelines for cardiovascular health and risk reduction in children and adolescents: summary report. *Pediatrics.* **128(Suppl 5):** S213–S256.
46. Genest, J., R. McPherson, J. Frohlich, T. Anderson, N. Campbell, A. Carpentier, P. Couture, R. Dufour, G. Fodor, and G. A. Francis. 2009. 2009 Canadian Cardiovascular Society/Canadian guidelines for the diagnosis and treatment of dyslipidemia and prevention of cardiovascular disease in the adult - 2009 recommendations. *Can. J. Cardiol.* **25:** 567–579.
47. Wang, K., M. Li, and H. Hakonarson. 2010. ANNOVAR: functional annotation of genetic variants from high-throughput sequencing data. *Nucleic Acids Res.* **38:** e164.
48. Adzhubei, I. A., S. Schmidt, L. Peshkin, V. E. Ramensky, A. Gerasimova, P. Bork, A. S. Kondrashov, and S. R. Sunyaev. 2010. A method and server for predicting damaging missense mutations. *Nat. Methods.* **7:** 248–249.
49. Ng, P. C., and S. Henikoff. 2003. SIFT: predicting amino acid changes that affect protein function. *Nucleic Acids Res.* **31:** 3812–3814.
50. Ansari, M., G. Sauty, M. Labuda, V. Gagne, J. Rousseau, A. Moghrabi, C. Laverdiere, D. Sinnett, and M. Krajinovic. 2012. Polymorphism in multidrug resistance-associated protein gene 3 is associated with outcomes in childhood acute lymphoblastic leukemia. *Pharmacogenomics J.* **12:** 386–394.
51. Krajinovic, M., D. Labuda, C. Richer, S. Karimi, and D. Sinnett. 1999. Susceptibility to childhood acute lymphoblastic leukemia: influence of CYP1A1, CYP2D6, GSTM1, and GSTT1 genetic polymorphisms. *Blood.* **93:** 1496–1501.
52. Sinnett, D., M. Krajinovic, and D. Labuda. 2000. Genetic susceptibility to childhood acute lymphoblastic leukemia. *Leuk. Lymphoma.* **38:** 447–462.
53. Riediger, N. D., and I. Clara. 2011. Prevalence of metabolic syndrome in the Canadian adult population. *CMAJ.* **183:** E1127–E1134.
54. MacPherson, M., M. de Groh, L. Loukine, D. Prud'homme, and L. Dubois. 2016. Prevalence of metabolic syndrome and its risk factors in Canadian children and adolescents: Canadian Health Measures Survey Cycle 1 (2007-2009) and Cycle 2 (2009-2011). *Health Promot. Chronic Dis. Prev. Can.* **36:** 32–40. [Erratum. 2016. *Health Promot. Chronic Dis. Prev. Can.*]
55. Lorenzo, C., K. Williams, K. J. Hunt, and S. M. Haffner. 2007. The National Cholesterol Education Program - Adult Treatment Panel III, International Diabetes Federation, and World Health Organization definitions of the metabolic syndrome as predictors of incident cardiovascular disease and diabetes. *Diabetes Care.* **30:** 8–13.
56. Grundy, S. M., J. I. Cleeman, S. R. Daniels, K. A. Donato, R. H. Eckel, B. A. Franklin, D. J. Gordon, R. M. Krauss, P. J. Savage, S. C. Smith, Jr., et al. 2005. Diagnosis and management of the metabolic syndrome: an American Heart Association/National Heart, Lung, and Blood Institute scientific statement. *Circulation.* **112:** 2735–2752. [Erratum. 2005. *Circulation.* 112: e297–e298.]
57. Mauger, J. F., P. Couture, N. Bergeron, and B. Lamarche. 2006. Apolipoprotein C-III isoforms: kinetics and relative implication in lipid metabolism. *J. Lipid Res.* **47:** 1212–1218.
58. Kei, A. A., T. D. Filippatos, V. Tsimihodimos, and M. S. Elisaf. 2012. A review of the role of apolipoprotein C–II in lipoprotein metabolism and cardiovascular disease. *Metabolism.* **61:** 906–921.
59. Ito, Y., N. Asrolan, A. O'Connell, A. Walsh, and J. L. Breslow. 1990. Hypertriglyceridemia as a result of human apo CIII gene expression in transgenic mice. *Science.* **249:** 790–793.
60. Bobik, A. 2008. Apolipoprotein CIII and atherosclerosis: beyond effects on lipid metabolism. *Circulation.* **118:** 702–704.
61. Song, Y., M. J. Stampfer, and S. Liu. 2004. Meta-analysis: apolipoprotein E genotypes and risk for coronary heart disease. *Ann. Intern. Med.* **141:** 137–147.
62. Minnich, A., A. Kessling, M. Roy, C. Giry, G. DeLangavant, J. Lavigne, S. Lussier-Cacan, and J. Davignon. 1995. Prevalence of alleles encoding defective lipoprotein lipase in hypertriglyceridemic patients of French Canadian descent. *J. Lipid Res.* **36:** 117–124.
63. Merkel, M. 2002. Lipoprotein lipase: genetics, lipid uptake, and regulation. *J. Lipid Res.* **43:** 1997–2006.
64. Franceschini, N., H. Muallem, K. M. Rose, E. Boerwinkle, and N. Maeda. 2009. Low density lipoprotein receptor polymorphisms and the risk of coronary heart disease: the Atherosclerosis Risk in Communities study. *J. Thromb. Haemost.* **7:** 496–498.
65. Eichner, J. E., S. T. Dunn, G. Perveen, D. M. Thompson, K. E. Stewart, and C. Stroehla. 2002. Apolipoprotein E polymorphism and cardiovascular disease: a HuGE review. *Am. J. Epidemiol.* **155:** 487–495.
66. Robitaille, N., G. Cormier, R. Couture, D. Bouthillier, J. Davignon, and L. Perusse. 1996. Apolipoprotein E polymorphism in a French Canadian population of northeastern Quebec: allele frequencies and effects on blood lipid and lipoprotein levels. *Hum. Biol.* **68:** 357–370.
67. Wilson, D. E., M. Emi, P. H. Iverius, A. Hat, L. L. Wu, E. Hillas, R. R. Williams, and J. M. Lalouel. 1990. Phenotypic expression of heterozygous lipoprotein lipase deficiency in the extended pedigree of a proband homozygous for a missense mutation. *J. Clin. Invest.* **86:** 735–750.
68. Gagné, C., L. D. Brun, P. Julien, S. Moorjani, and P. J. Lupien. 1989. Primary lipoprotein-lipase-activity deficiency: clinical investigation of a French Canadian population. *CMAJ.* **140:** 405–411.
69. Rahalkar, A. R., F. Giffen, B. Har, J. Ho, K. M. Morrison, J. Hill, J. Wang, R. A. Hegele, and T. Joy. 2009. Novel LPL mutations associated with lipoprotein lipase deficiency: two case reports and a literature review. *Can. J. Physiol. Pharmacol.* **87:** 151–160.
70. Kolářová, H., M. Tesařová, Š. Švecová, V. Stránecký, A. Přistoupilová, T. Zima, J. Uhrová, S. Y. Volgina, J. Zeman, and T. Honzík. 2014. Lipoprotein lipase deficiency: clinical, biochemical and molecular characteristics in three patients with novel mutations in the LPL gene. *Folia Biol. (Praha).* **60:** 235–243.
71. Hegele, R. A. 2016. Multidimensional regulation of lipoprotein lipase: impact on biochemical and cardiovascular phenotypes. *J. Lipid Res.* **57:** 1601–1607.
72. Alaupovic, P., W. J. Mack, C. Knight-Gibson, and H. N. Hodis. 1997. The role of triglyceride-rich lipoprotein families in the progression of atherosclerotic lesions as determined by sequential coronary angiography from a controlled clinical trial. *Arterioscler. Thromb. Vasc. Biol.* **17:** 715–722.
73. Onat, A., G. Hergenc, E. Ayhan, M. Ugur, and G. Can. 2009. Impaired anti-inflammatory function of apolipoprotein A-II concentrations predicts metabolic syndrome and diabetes at 4 years follow-up in elderly Turks. *Clin. Chem. Lab. Med.* **47:** 1389–1394.
74. Barbaras, R., P. Puchois, J. C. Fruchart, and G. Ailhaud. 1987. Cholesterol efflux from cultured adipose cells is mediated by LpAI particles but not by LpAI:AII particles. *Biochem. Biophys. Res. Commun.* **142:** 63–69.
75. Durbin, D. M., and A. Jonas. 1999. Lipid-free apolipoproteins A-I and A-II promote remodeling of reconstituted high density lipoproteins and alter their reactivity with lecithin:cholesterol acyltransferase. *J. Lipid Res.* **40:** 2293–2302.
76. Lagrost, L., C. Dengremont, A. Athias, C. de Geitere, J. C. Fruchart, C. Lallemant, P. Gambert, and G. Castro. 1995. Modulation of cholesterol efflux from Fu5AH hepatoma cells by the apolipoprotein content of high density lipoprotein particles. Particles containing various proportions of apolipoproteins A-I and A-II. *J. Biol. Chem.* **270:** 13004–13009.